Shaken Not Stirred: Unleashing the Potential of Mechanochemical Synthesis

William I. Nicholson

This thesis is submitted for the degree of Doctor of Philosophy (PhD) at Cardiff University

August 2021

Summary

Within this thesis is described a series of studies into performing organic synthesis under mechanochemical conditions during which new procedures were developed and advantages into using these methods discussed.

Initial investigations focused on establishing a procedure for a mechanochemical Buchwald-Hartwig amination under ball milling conditions finding that the use of grinding auxiliaries was key for efficient mass transfer and high yields. Furthermore, the established procedure was applied to a range of aryl halide and amine substrates including the synthesis of an API. It was also investigated how the newly established conditions were found to be tolerant to air and moisture under ball milling conditions.

During the substrate scope of the first investigation the direct amidation of simple esters was observed. This transformation was then investigated finding that the potassium *tert*-butoxide present in the Buchwald-Hartwig conditions was enabling this transformation. This method was then optimised and applied to a broad scope of esters and amines including the synthesis of five biologically active compounds. The developed conditions were then compared to solution and neat stirring conditions that had previously been established.

Previously in the group the dimerization of benzylidene malonates had been discovered while investigating the formation of organomanganese halides mechanochemically. This reaction was studied in detail uncovering the possibility of ball milling enhancing the reactivity of manganese metal.

Following, the generation of organomanganese halides directly from manganese metal and benzyl halides was investigated with promising initial results. This work was initially guided by some previous results obtained within the group that had uncovered some reactivity.

Finally, included in an appendix, a reference to a manuscript discussing the investigations of the first examples of NHC catalysed reaction under ball milling conditions is presented. This discusses the application of ball milling to both the Benzoin and Stetter reactions catalysed by NHC's and the application of asymmetric catalysts to these reactions for the induction of chiral information to the products.

Related Publications

Publications resulting from work carried out during the completion of this PhD.

1. **Robust Buchwald–Hartwig Amination Enabled by Ball-Milling**

    Qun Cao, William I. Nicholson, Andrew C. Jones and Duncan L. Browne, *Org. Biomol. Chem.*, 2019, **17**, 1722–1726.

2. **A Robust Pd-Catalyzed C−S Cross-Coupling Process Enabled by Ball-Milling**

    Andrew C. Jones, William I. Nicholson, Harry R. Smallman, and Duncan L. Browne, *Org. Lett.*, 2020, **22**, 7433−7438.

3. **Direct Amidation of Esters *via* Ball Milling**

    William I. Nicholson, Fabien Barreteau, Jamie A. Leitch, Riley Payne, Ian Priestley, Edouard Godineau, Claudio Battilocchio and Duncan L. Browne, *Angew. Chem. Int. Ed.*, 2021, 10.1002/anie.202106412, Also available from ChemRxiv: 10.26434/chemrxiv.14556153.v2.

4. **Ball Milling Enabled Reactivity of Manganese Metal**

    William I. Nicholson, Joseph L. Howard, Giuseppina Magri, Alex C. Seastram, Adam Khan, Louis C. Morrill, Emma Richards and Duncan L. Browne, *Angew. Chem. Int. Ed.*, 2021, 10.1002/anie.202108752, Also available from ChemRxiv: 10.33774/chemrxiv-2021-s7r6b.

5. **N-Heterocyclic Carbene Acyl Anion Organocatalysis by Ball-Milling**

    William I. Nicholson, Alex C. Seastram, Saqib A. Iqbal, Benjamin G. Reed-Berendt, Louis C. Morrill, and Duncan L. Browne, *ChemSusChem,* 2020, **13**, 131–135.

6. **A Ball Milling Enabled Cross-Electrophile Coupling**

    Andrew C. Jones, William I. Nicholson, Jamie A. Leitch and Duncan L. Browne, *Org. Lett.* 2021, 10.1021/acs.orglett.1c02096.

Acknowledgments

The work presented in this thesis would not have been possible without significant support from many individuals, whom a great deal of thanks is owed, and I will be forever grateful for their support.

Firstly, Dr Duncan L. Browne my PhD supervisor, MChem supervisor, and personal tutor, you have supported and guided me for the past six years of my academic life without which I could not have accomplished much of what I have now attained. You have pushed me to become not only a better chemist but a well-rounded scientist.

Many talented members of the Browne group have helped me over the last five years and deserve a mention here. Joey was the unfortunate member to supervise me as a MChem student in the group where on my first day I broke a Schlenk line, but through Joey's persistence I was able learn a lot from him and we became close friends. Roddy was always there for great advice about how to run the most beautiful TLC and his fun-loving nature produced a great atmosphere in the lab and made it a pleasure to work in. Tom and I have worked in the group since we both joined as MChem students, it has been a long road to get to the end and his ability to listen and offer a new perspective on anything has helped me a countless number of times. Andy and Alex, an inseparable pair with a huge knowledge of chemistry and great fun in the lab or while playing football.

Numerous other members in the group have assisted me in and we have all become friends during our time in Cardiff; Chrissi, Saqib, Yerbol, Qun, Matt, Renan, Harry, Jamie, Adam, Calum, and Tom LW.

Several people have directly contributed to some of the results presented in this thesis either through collaboration or while working with my supervision. These are, Qun Cao (postdoc), Andrew C. Jones (then MChem), Joseph L. Howard (PhD), Giuseppina Magri (PhD), and Alex C. Seastram (PhD). I would also like to thank the people whose results are not presented in this thesis, but I was fortunate enough to work with, Saqib A. Iqbal, Benjamin G. Reed-Berendt, Jamie A. Leitch, Harry Smallman, Adam Khan and Riley Payne.

I should also thank Dr Louis C. Morrill and members of the Morrill group whom we shared a lab and group meetings with where there was always a welcoming environment.

Finally, an enormous thanks is owed to my friends and family for their ongoing support. Especially to my girlfriend Victoria Tozer, my brother Samuel Nicholson, and my parents Diana and Gerald Nicholson, without them none of this would have been possible.

Abbreviations

1,5-cod	1,5-Cyclooctadiene
ACS	American Chemical Society
API	Active Pharmaceutical Ingredient
atm	Atmosphere
BODIPY	4,4-difluoro-4-bora-3a,4a-diaza-s-indacene
cat.	Catalyst
d.e.	Diastereotopic excess
d.r.	Diastereomeric ratio
DABCO	1,4-Diazabicyclo[2.2.2]octane
DBU	1,8-Diazabicyclo[5.4.0]undec-7-ene
DCM	Dichloromethane
DDQ	2,3-Dichloro-5,6-dicyano-1,4-benzoquinone
DMA	N,N-Dimethylacetamide
DME	1,2-Dimethoxyethane
DMF	N,N-Dimethylformamide
DMSO	Dimethyl sulfoxide
EDC	1-Ethyl-3-(3-dimethylaminopropyl)carbodiimide
equiv.	Equivalent
ESI-MS	Electrospray Ionisation Mass Spectrometry
etc	*Et cetera*
GC	Gas Chromatography
GDCh	Gesellschaft Deutscher Chemiker (German Chemical Society)
h	Hours
HPGDS	Hematopoietic prostaglandin D synthase
IUPAC	International Union of Pure and Applied Chemistry
LAG	Liquid assisted grinding
LHMDS	Lithium bis(trimethylsilyl)amide
MCRs	Multi-component reactions
min	Minutes
MOFs	Metal organic frameworks
NHC	*n*-Heterocyclic Carbene
NMP	N-Methyl-2-pyrrolidone
NMR	Nuclear magnetic resonance

PEPPSI	Pyridine enhanced precatalyst preparation stabilisation and initiation
PFA	Paraformaldehyde
PXRD	Powder x-ray diffraction
rpm	Revolutions per minute
RSC	Royal Society of Chemistry
SEM	Scanning electron microscopy
SET	Single electron transfer
S_NAr	Nucleophilic aromatic substitution
TBAB	Tetrabutylammonium bromide
TEM	Transmission electron microscopy
TEMPO	2,2,6,6-Tetramethyl-1-piperidinyloxy, free radical
THF	Tetrahydrofuran
TSE	Twin screw extrusion

Table of Contents

1   Introduction to Mechanochemical Synthesis

1.01 What is mechanochemistry?

The IUPAC gold book definition of a mechanochemical reaction is 'A chemical reaction that is induced by the direct adsorption of mechanical energy.'[1] This definition is applicable to a range of techniques which may be found in a synthetic research laboratory including sonication; atomic force microscopy; manual grinding; ball milling; and twin-screw extrusion (TSE).[2] Each of these techniques is able to apply a unique combination of mechanical forces in a variety of reaction environments allowing for their use to be directed towards specific challenges. Interest is growing in the use of mechanochemistry causing a modern renaissance of the techniques.[3] The resurgence of mechanochemistry has facilitated the display of a range of benefits using these techniques within a broad spectrum of chemical reactivity.[4] These methods can be used to significantly increase reaction rate, reduce the waste produced, and demonstrate alternate reactivity.[4o] Examples include sonication and atomic force microscopy being used to alter the products of pericyclic reactions which are well understood by the application of the Woodward-Hoffman rules for thermo- and photo- chemistry.[5]

1.02 Equipment for Ball Milling and Process Intensification

The development of automated milling equipment and their application to mechanochemistry has allowed the implementation of easily reproducible synthetic methods. Prior to the use of automated devices hand grinding with a mortar and pestle was the most common method to carry out a mechanochemical transformation.[6] Intrinsic human error can lead to difficulties in reproducing results as the application of force and the stamina required for a long reaction will vary greatly from between human operators.

Among the variety of milling equipment available the most popular devices for synthetic transformations are ball mills with the most common styles of being mixer mills and planetary mills.[7] Each of these devices utilize the same basic principle that the application of kinetic energy to one or more balls within a sealed vessel can produce collisions to supply mechanical energy to a reaction.

Mixer mills, such as the Retsch MM400 (Scheme 1.01), employ a horizontally mounted jar, oscillating from side to side to provide the kinetic energy key to produce collisions of the ball(s) with the reaction mixture. The frequency of the oscillations and time for the reaction can be set on the device allowing for easily reproduced conditions. The most

common energy transfer event in a mixer mill is a direct impact of the ball with the material at the ends of the jar, although due to the stochastic nature of the motion of the ball shearing or glancing collisions along the sides of the jar are also possible.[8]
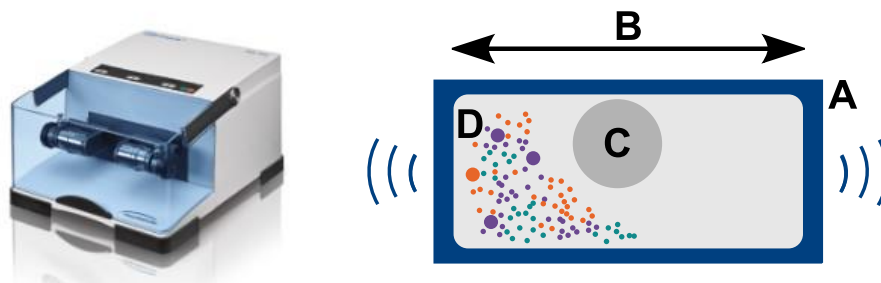
Scheme 1.01 Retsch MM400 mixer mill alongside schematics explaining their motion. **A** milling vessel, **B** motion of the jar, **C** milling ball, **D** reaction mixture.

Planetary mills, for example the Fritsch Pulverisette 7 (Scheme 1.02), differs from the mixer mill by mounting the jars vertically on a rotating plate upon which the jars counter rotate on their central axis. For example, the plate may spin clockwise relative to the device while the jars spin anticlockwise relative to the plate. This complex motion produces a large amount of shearing forces, which provide the greatest contribution to the type of energy applied to the sample, while direct collisions provide the remainder of the mechanical energy.[9]
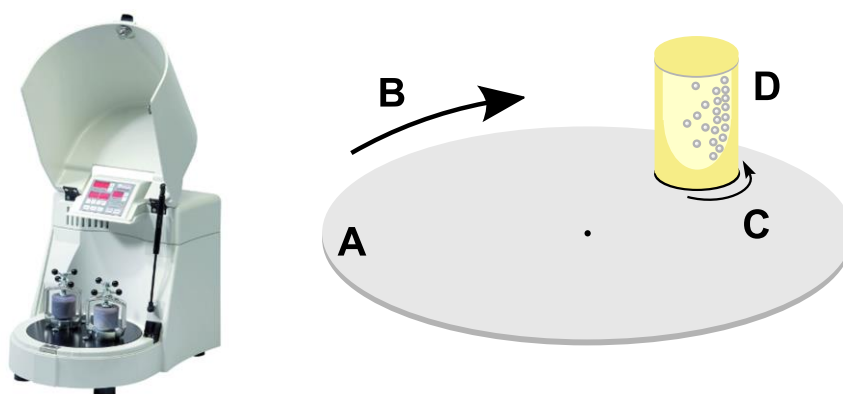
**Scheme 1.02** Fritsch Pulverisette 7 classic line planetary mill alongside schematics explaining their motion. **A** central rotating plate, **B** rotation direction of central plate, **C** rotation direction of jar, **D** jar with cutaway showing balls.

These devices are very useful for research scale activities up to a couple of grams, with the largest planetary mills accommodating close to a hundred grams.[10] The scale up to

quantities required for industrial applications would require alternate mechanochemical techniques.[11] For example, in drug discovery chemistry where typically milligrams of material can be initially prepared for candidate selection the use of mixer or planetary mills could be readily implemented. As the scale is increased for further testing such as preclinical trials where hundreds of grams may be required alternatives mills will be required such as mixed media mills which have been demonstrated for the scale up of the Knoevenagel condensation by Stolle *et al.*[12] But further increase in scale becomes more challenging without rethinking the entire approach of the methodology from batch to a continuous method.[11] Twin screw extrusion (TSE), which is already used in drug manufacturing for formulation, has been shown to be a powerful method for the scale up of mechanochemical reactions.[4r]

The application of TSE to the synthesis of molecular organic frameworks (MOFs) has unlocked the potential of these materials.[13] Prior to the use of TSE, the synthesis of MOFs could not be carried out in a cost-effective method due to the large amounts of solvents necessary for their synthesis and purification.[14] TSE has significantly decreased the manufacturing cost of MOFs such that it is viable to produce them commercially, where James and coworkers at MOF Technologies have been among those key in the development of these highly tuneable porous materials.[15]

Within the extruder barrel shearing and compression forces are applied to the reactive material to provide the mechanical energy but often the design of the extruder allows for accurate control of the temperature of the barrel, blurring the lines between mechano- and thermo- chemistry (Scheme1.03). The design of the screws may also be altered to optimize the mechanical forces applied utilizing kneading and reverse screw configurations to apply additional shearing and compressive forces.
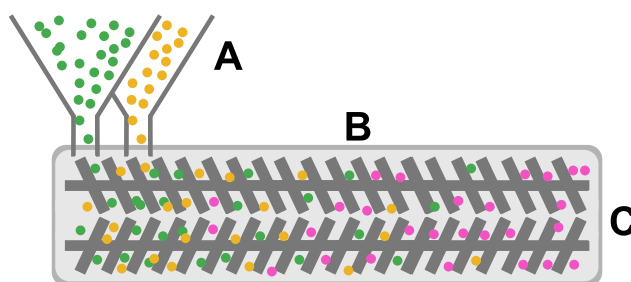
Scheme 1.03 TSE barrel revealing screw configuration alongside schematic. **A** reagent hopper, **B** counter rotating screws, **C** barrel with controllable temperature.

1.03 Optimization of a ball milling reaction

For the optimization of any chemical reaction understanding the variables and how to control them are key to successfully optimization. Within any ball milling reaction, the most important facets of the optimization are the energy per collision, the efficiency of the absorption of the energy by the material, and the rate of collisions of sufficient energy for the reaction to proceed. Unfortunately for the optimization of a ball milled reaction many of the directly controllable variables will alter multiple of these facets. The directly controlled variables of a mechanochemical reaction are the milling frequency, the number and size of the balls, the size of the milling vessel, the material the ball or jar are made from, grinding auxiliaries, and liquid additives.[16] This is in addition to the chemical variables such as reagent stoichiometries.

Altering the frequency of the ball mill can be compared to controlling the temperature of a solution reaction, with increasing frequency similar to that of increasing temperature. As frequency increases the kinetic energy of the ball(s) also increases creating higher energy collisions.[17] Furthermore, the higher frequency will increase the rate of collisions leading to a faster reaction.[18] With increased kinetic energy an increase in friction within the jar can also be expected to produce a greater temperature change. All of these aspects may lead to an improved yield or faster reaction, but as with solution chemistry more energy available may also lead to unwanted side reactions or degradation of the product or starting materials.

The number and size of ball(s) can be used to control the rate and kinetic energy of collisions. Also, optimization often varies greatly depending on the specific mill being used. As general rules set out by Stolle *et al*, a mixer mill is more suited to one ball of the largest size possible that allows for efficient mixing, alternatively a planetary mill often achieves optimal conditions with the greatest number of the smallest ball(s) that produces collisions of sufficient energy and allow for efficient mixing.[4d] These rules come about due to the different mechanisms used to apply the mechanical forces. Within a mixer mill, collisions at the ends of the jar are responsible for much of the energy provided. With one ball of maximal size the collisions provide the largest amount of kinetic energy per collision and the greatest area for each collision thus providing energy to more material. Within the planetary mill the shearing of the balls along the vertical walls of the container provides the greatest proportion of the energy input. In this scenario the greatest number of the smallest ball that provides collisions of sufficient energy for the reaction to take place. This allows for the greatest number of effective

collisions over the largest area. The only similarity with the optimization of these techniques is to not use a ball of such size or in such numbers that prevent the efficient mass transfer of reagents within the milling vessel.

Modifying the size of the milling vessel will vary the free space within the vessel which will alter the rate of collisions. With a larger vessel the rate of collisions will decrease but the energy of each collision will increase due to a lower number of glancing blows. Vice versa a smaller jar will increase the number of collisions and lower their energy.[10b] This leads to two possible scenarios; a reaction that is limited by the energy of collision may perform superiorly in a larger jar whereas a reaction limited by the number of collisions could increase in yield in a smaller jar. Also, by altering the volume of the vessel the ratio between the space required by the ball(s), the reagents, and free space, will change. There have been a number of reports, including manufacturers guidance, concerning the optimal ratio of these variables.[19] This has led to a 'rule of thirds' where each element should be contained in, close to, a third of the jar to allow for efficient mixing and energy transfer.[20] Often the use of a larger jar, alongside a larger ball, could be required for the increase in scale of a reaction. This has been successfully applied on several examples without considerable difficulty.[21] Though complications can arise due to altering rates of collisions and energy per collision not scaling perfectly.[11]

Chemical compatibility is of the utmost importance when considering the choice of material for the jar and ball(s). Second to this a jar and ball(s) of the same materials should be paired to prevent unnecessary wear on the components, though if this is not possible a softer material for the ball(s) will be preferred as these will then wear more quickly and are cheaper to replace.[22] With these considerations made the likely choice for the optimal material for a reaction will be the hardest and densest material. A harder material will provide more efficient energy transfer and a denser material will be heavier and produce higher energy collisions. Exceptions are possible to this rule, work from Boldyreva and coworkers has shown that the use of polymer balls can produce faster reactions than that of denser and harder materials, though this is explained by the deformation of more elastic materials which provide a significant increase of the internal temperature.[8] As previously mentioned, chemical compatibility of the chosen materials is key to ensure the lifetime of the equipment, but this does not prevent a jar or ball(s) being involved in the reaction. There is growing interest in the field of mechanocatalysis where metals such as Pd, Cu, or Ni present in the jar or ball can be used for the catalysis of a reaction.[4f, 23]

6

Grinding auxiliaries are often employed in synthetic organic reactions undertaken in a ball mill.[24] These solid additives are used to disperse liquid reagents or intermediate states to assist in mass transfer during a reaction and prevent the mixture from becoming overly viscous or sticky which can prevent efficient mixing and energy transfer into the reaction mixture. Often inorganic salts are used for this role such as sodium chloride shown by Friščić and coworkers through work on a mechanochemical ruthenium catalysed olefin metathesis.[25] The reaction proceeded sluggishly due to aggregation of the sticky reaction mixture on the ball (Scheme 1.04a and b), but addition of sodium chloride to the reaction mixture produced a free-flowing powder (Scheme 1.04c) allowing more efficient mass and energy transfer. These solid additions do not necessarily have to be chemically inert to the reaction environment and indeed compounds can be used that fulfil a role in the reaction, such as molecular sieves as a desiccant or use of super-stoichiometric quantities of bases such as potassium carbonate.[26]
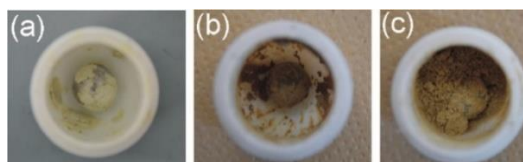
Scheme 1.04 Reaction mixture with and without a solid auxiliary (a) after 15 min, (b) after 5 h, and (c) after 2 h of milling with sodium chloride.[i]

The use of liquid additives in ball milling, a technique often referred to as liquid assisted grinding (LAG), utilizes a small quantity of liquid (predominantly common organic solvents) during the milling reaction.[4g, 27] This inclusion of a small amount of solvent places this technique within the spectrum of solvent requirement which ranges from neat grinding with no solvent to solution reactions where all components are completely solvated (Scheme 1.05). The amount of solvent present in a ball milling process is often reported as η, which is the ratio between the volume of liquid added and the total mass of all reagents (Scheme 1.05). LAG is then defined as a reaction with a value of η greater than zero but less than one.

$$\eta = \frac{\text{Volume of liquid } (\mu L)}{\text{Total mass of all reagents (mg)}}$$
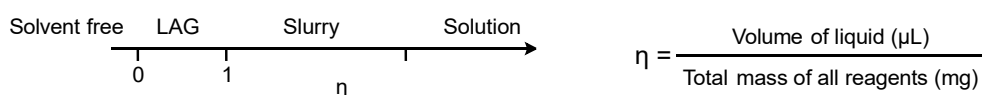
Scheme 1.05 Scale visualizing solvent requirement for LAG, slurry, and solution. The formula for calculating η.

---

[i] Scheme reproduced from ref. 25 with permission from the ACS. Further permissions for reproduction of this scheme should be directed to the ACS.
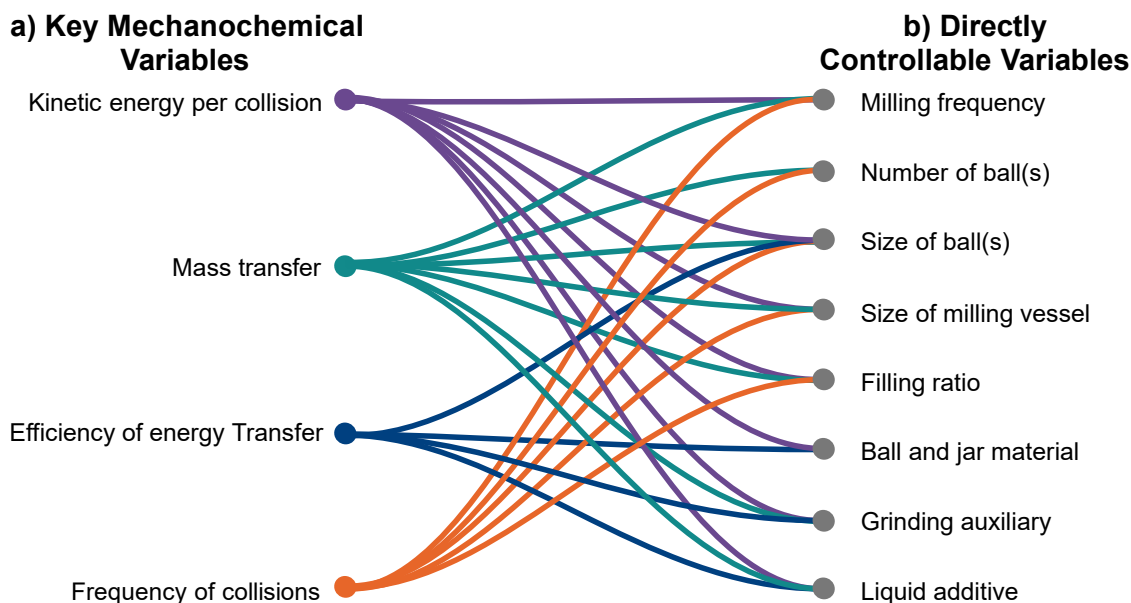
The use of liquid additives was initially developed for the construction of cocrystals and MOFs as it was shown to increase the rate and selectivity of cocrystal formation as well as templating the MOFs during their construction.[28] Similar results have also been achieved in organic reactions with improved rates and selectivity's by the employment of liquid additives.[4g] Through tailoring the quantity and polarity of the liquid additive used different polymorphs of various cocrystals can be formed.[27a] Emmerling and coworkers demonstrated altering between kinetic and thermodynamic cocrystal polymorphs with the use of nonpolar (or neat grinding) and polar liquid additives respectively (Scheme 1.06a).[28b] Furthermore, Browne and coworkers demonstrated a similar switch in chemoselectivity for the synthesis of difluorinated thioethers with the desired product being observed under conditions using DMSO as a polar liquid additive (Scheme 1.06b).[29] Alternatively, under nonpolar liquid additive or neat grinding conditions the kinetic product would be observed.
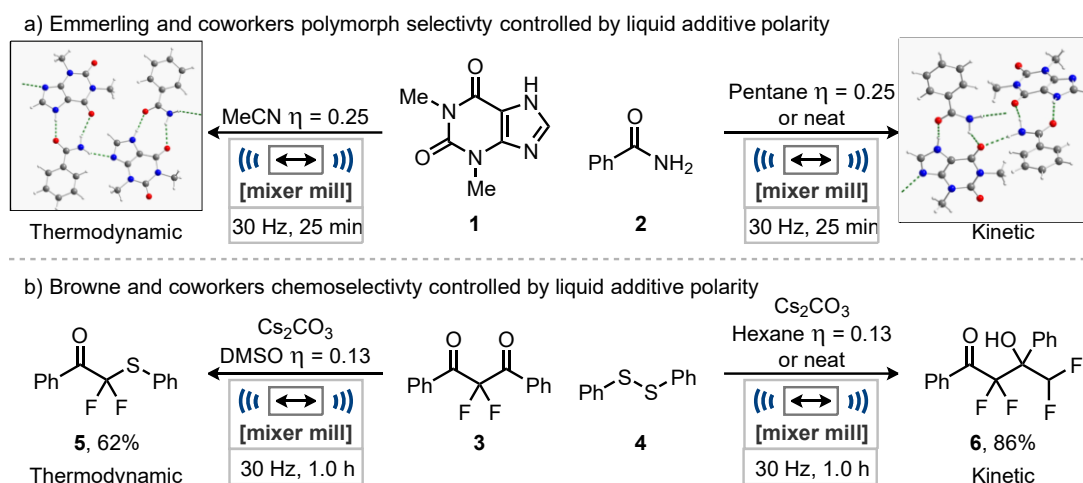
Scheme 1.06 Observation of alternate products controlled by the polarity or presence of a liquid additive. Crystal structures were reproduced with permission.[ii]

The interconnected nature of the controllable variables (Scheme 1.07b) Directly Controllable Variables with those which are key to control reaction outcomes (Scheme 1.07a) Key Mechanochemical Variables are visualized in Scheme 1.07. This clearly highlights the complexity of interlinked effects by altering these variables and the challenge of optimizing ball milling reactions. This is without also taking into consideration the chemical variables for any transformation.

[ii] Crystal structures reproduced from ref. 28b with permission from the ACS. Further permissions for reproduction of this scheme should be directed to the ACS.

a) Key Mechanochemical Variables

Kinetic energy per collision

Mass transfer

Efficiency of energy Transfer

Frequency of collisions

b) Directly Controllable Variables

Milling frequency

Number of ball(s)

Size of ball(s)

Size of milling vessel

Filling ratio

Ball and jar material

Grinding auxiliary

Liquid additive

Scheme 1.07 Visualization of Mechanochemical variables linked with those that are directly controllable in a ball milling reaction.

To gain further insight into the effects of these variables across a number of ball milling devices, the Knoevenagel reaction of vanillin **7** and barbituric acid **8** has been used as a control reaction (Scheme 1.08). Where throughout these reports the systematic review of each variable has been established across multiple devices and on a variety of scales.[4r, 10-12, 30] With these thorough investigations combined, alternating observations of the mechanism of the ball milled Knoevenagel condensation have been observed. James and coworkers established that the reaction could occur via a eutectic state intermediate surrounding the ball (Scheme 1.08a).[30b] This eutectic intermediate coating the ball was then able to react incredibly quickly due to each collision providing energy to a large portion of the reaction mixture. This caused the reaction to display a sigmoidal rate of reaction similar to that of self-catalysed reactions. More recently, Užarević and coworkers demonstrated that the same reaction underwent the formation of a cocrystal intermediate of such structure that the reacting molecules were orientated to undergo the reaction (Scheme 1.08 b).[30e] Analysis showed cocrystals poised to undergo the reaction, with reacting centres only 3.74 Å apart, which also led to significant rate enhancement. For both reports a mixer mill was utilized and the most significant difference was the James report used one ball whereas the Užarević report used two balls. It has been suggested that the use of 2 balls prevented the eutectic intermediate from forming by collisions between the balls cleaning it from the surface.[30d]
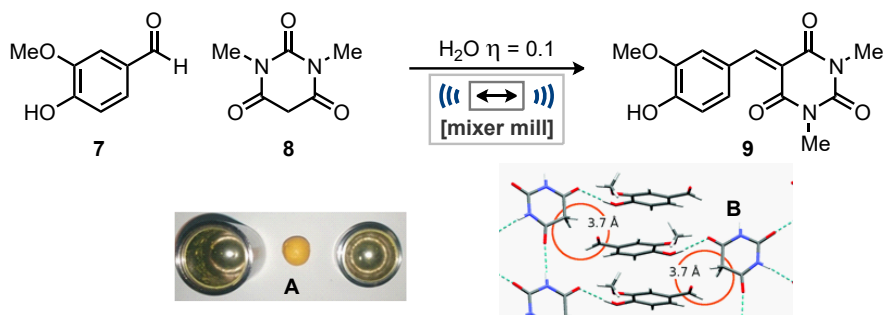
Scheme 1.08 The Knoevenagel condensation of barbituric acid **8** and vanillin **7**. **A** The eutectic intermediate state reported by James and coworkers. [iii] **B** Cocrystal intermediate from Užarević and coworkers. [iv]

1.04 Why Use Ball Milling?

Recently ball milling was named alongside twin screw extrusion as one of the top ten chemical innovations that could change the world. [31] These methods were chosen for this accolade in part for their ability to run chemical reactions as a solvent free (or minimized) process. The reduction in the use of solvents is one of the key challenges for the implementation of green chemistry across the chemical industry as set out by the ACS Green Chemistry Pharmaceutical Round Table. [32] The development of these greener methods is an active area of research within mechanochemistry. [4v]

Enabling solvent free reactions is very attractive but is not the only reason mechanochemical reactions should be developed. These transformations often produce several other benefits such as shorter reaction times, reduced catalyst loadings, improved selectivity's and the potential discovery of new transformations. [4a] The application of liquid additives as previously discussed has been shown to allow for the discovery of new products in cocrystallizations or covalent intermolecular reactions. [28b, 29, 33] These new products may be inaccessible by other methods currently limiting their synthesis to only mechanochemical methods.

[iii] Scheme reproduced from ref. 30b with permission from the GDCh. Further permissions for reproduction of this scheme should be directed to the GDCh.
[iv] Scheme reproduced from ref. 30e with permission from the ACS. Further permissions for reproduction of this scheme should be directed to the ACS.

1.05 *In situ* Spectroscopy and Reaction Monitoring

To gain a detailed understanding on how these reactions proceed the ability to carry out *in situ* reaction monitoring is key. Without these methods being developed all analysis must be carried out *ex situ* which requires each data point to come from an individual reaction. Sampling an ongoing reaction by stopping the milling and opening the jar may allow volatiles to escape along with the cooling of the jar altering the reaction conditions.[34] Furthermore, removing material from within the jar will alter the filling ratio of the reagents with the ball and free space potentially leading to increased energy of collisions. Fortunately, the development of a range of *in situ* monitoring techniques for ball milling reactions is ongoing thus allowing for detailed mechanistic study.[35] Although these techniques are not yet widespread within the mechanochemistry community.

The three most common forms of *in situ* reaction monitoring employed during mechanochemical reactions are PXRD, Raman spectroscopy, and thermography.[36] Emmerling and coworkers combined these three analytical techniques for the analysis of a cocrystal formation, a manganese-phosphonate formation, and the synthesis of C-C bonds through a Knoevenagel condensation.[30c] This analysis allows information to be correlated with chemical changes within the reaction as well as detection and delineation of possible intermediate states, such as co-crystal, eutectic, or liquid intermediates.

Halasz and coworkers also combined the use of *in situ* PXRD with Raman spectroscopy. in which they demonstrated the rapid whole molecule exchange of benzoic acid **10** and **11** using isotope labelling studies (Scheme 1.09a).[37] Fast atom exchange could also be monitored utilizing labile deuterium atoms through cocrystal formation of benzoic acid **10** and 2-pyridone **13** (Scheme 1.09b) or between D_2O and benzoic acid. These experiments demonstrated that ball milling is able to overcome the slow solid-solid diffusion of typical solid-state reactions through particle refinement and growth during a reaction.
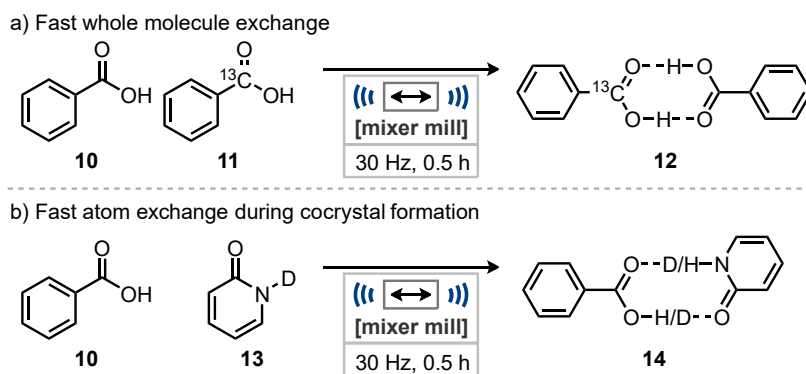
Scheme 1.09 Whole molecule and atom exchange observed through ball milling.

Through the analysis of PXRD combined with temperature monitoring and Raman spectroscopy, Hernández and coworkers could visualize the exact moment of the phenyl migration during a benzil-benzillic acid rearrangement (Scheme 1.10).[38] The rapid structural change of the starting material **15** to product **16** was not preceded by the formation of any intermediate states. Through this study the feasibility of mechanochemically induced migration reactions was demonstrated along with reinforcing the ability to gain a deeper understanding of the mechanism of a mechanochemical reaction through *in situ* monitoring.
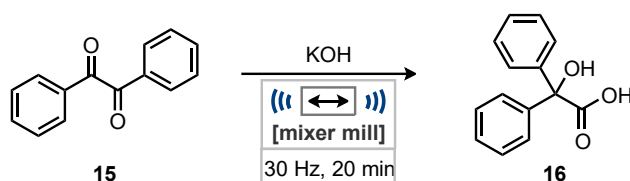

Scheme 1.10 The benzil-benzillic acid rearrangement.

With the use of *in situ* techniques growing, it can be expected that a greater understanding of unusual reactivity or advantages observed by ball milling will be achieved. This enhanced insight into the internal workings of some of these reactions may allow application to other transformations, as to improve reaction conditions or possibly for alternate mechanistic outcomes, although the challenge of identifying transformations which may benefit from mechanochemical treatment is currently carried out through trial and error.

1.06 Temperature Control

As previously mentioned for TSE it is often possible for the control of the temperature of the barrel during the reaction due to the design of the equipment. However, the ability to control reaction temperature is still in its infancy for ball milling methods. Commercial availability of devices that are able to control milling temperature is limited to devices such as the Cryomill from Retsch which is restricted to milling samples at cryogenic temperatures.[39] Researchers have undertaken the construction of their own devices able to control the temperature of the milling vessel. These range in complexity from electrical heating belts,[30d] recirculating liquid,[16e, 40] or simply use of a heat gun.[41]

Utilizing temperature control through a heating belt wrapped around the jar, Užarević and coworkers were able to further accelerate milling reactions and achieve selectivity not previously observed for conventional milling or solution reaction conditions.[30d] These

benefits were demonstrated through a range of transformations including MOF construction, condensation reactions, and reactivity of acyl azides (Scheme 1.11). Through careful reagent choice and reaction optimization it was possible to selectively synthesize the intermediate amide **20** from one of two acyl azides **18** and **19** in reaction with the diamine **17**. Upon formation of the intermediate **20**, milling could be stopped and using their heating belt the internal jar temperature could be raised to 90 ˚C inducing the Curtius rearrangement of **19**. Milling could then be restarted, and the isocyanate generated from **19** could then react with **20** forming the final amide and urea containing product **21** in excellent yield and selectivity. Such a one pot procedure had not previously been developed under any reaction conditions with comparable selectivity.
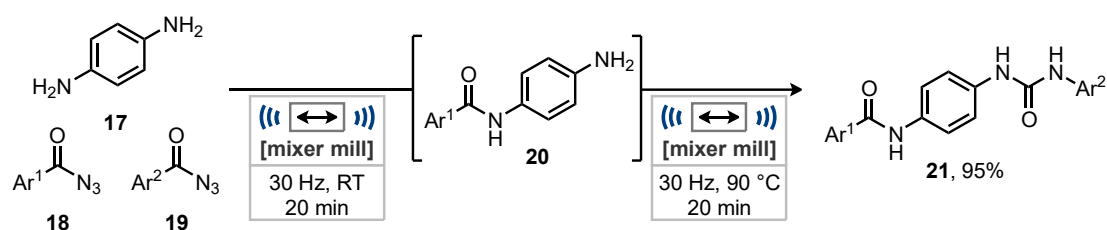
Scheme 1.11 Synthesis of amide and urea containing diamine. Ar^1 4-nitrobenzene, Ar^2 4-methoxybenzene.

Mack and Coworkers modified a SPEX 8000M mixer mill to allow a recirculating chiller to pump temperature-controlled liquid around the jar allowing for precise reaction temperature control.[40] Using the reduction of 4-*tert*butyl cyclohexanone **22** with sodium borohydride as a control reaction, they were able explore the effects on diastereoselectivity with temperature during a ball milled reaction (Scheme 1.12). Comparisons could then also be made with the same reaction carried out in solution. At the lowest temperatures investigated (-10 ˚C and 5 ˚C) there was a significant increase in the diastereomeric excess (*d.e.*) observed under ball milling conditions than that of solution reactions. As temperature increased, the *d.e.* decreased following a similar trend under ball milling and solution conditions. The values generated for each technique finally converged as temperature reached 25 ˚C. The relationship between *d.e.* and milling frequency was also explored at a range of temperatures. It was observed that milling frequency had some effect on the *d.e.* with higher frequencies leading to a decrease in *d.e.* but that the temperature of the reaction vessel had a much greater influence on the selectivity. It was found that milling frequency greatly impacted on the conversion of the reaction, with low milling frequencies providing minimal conversion. This investigation demonstrated the ability to control reaction selectivity and conversion

through control of both temperature and milling frequency. This potentially allows for faster reactions with greater selectivity utilizing their method.
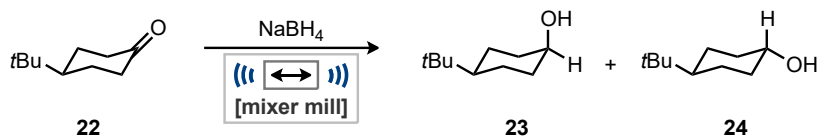

Scheme 1.12 Reduction of 4-(*tert*butyl)-cyclohexanone with sodium borohydride.

Temperature controlled ball milling reactions, similarly to *in situ* spectroscopic methods, is a technique that is currently in its infancy largely due to lack of commercially available ball mills with requisite temperature control. Through these examples it has been shown that temperature control can provide benefits to ball milling transformation by increasing accessible reactivity. Additionally, temperature control can allow for greater understanding of the variables in mechanochemical reaction and their effects on reaction outcomes.

1.07   Well Suited Reactions

There are a broad range of reactions well suited to be undertaken by ball milling conditions, taking advantage of the solvent free reaction medium. Products or reagents that are often poorly soluble in solution synthesis are prime candidates for use within ball mills. To this end Borchardt and coworkers have synthesized a range of nanographenes under ball milling conditions. In the initial work a Scholl reaction was applied to benchmark nanographenes, hexa-*peri*-hexabenzocoronene **25**, the triangular shaped C_{60} **26**, and further expanded to C_{222} **27**, forging up to 54 new C-C bonds in a single step (Scheme 1.13).[42] Expanding on this synthesis the group successfully implemented a dehydrogenative catalytic synthesis of nanographenes with the aid of an elemental copper catalyst which avoided the production of hydrochloric acid as a byproduct.[43] These nanographenes and their precursors are poorly soluble in typical organic solvents which necessitates the use of large quantities of solvent at high temperatures for their synthesis which often result poor yields (typically 40 – 60%) and long reaction times.[44] The solvent free mechanochemical processes provided a fast and high yielding reaction (up to 99%) to access these materials.
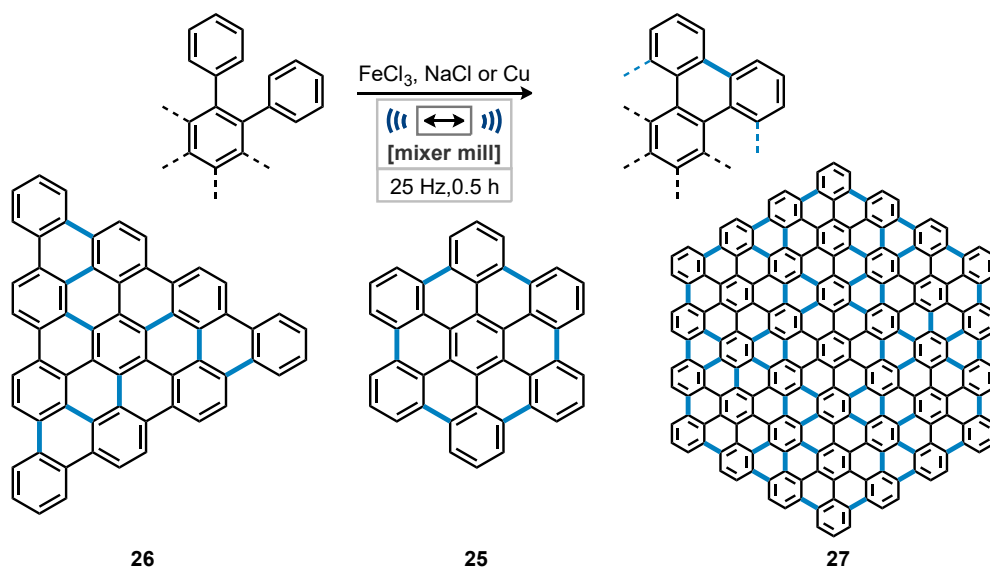
**Scheme 1.13** Synthesis of nanographene's from Borchardt and coworkers.

Ito and coworkers have taken advantage of the solvent free nature of ball milling for the development of a solid-state Suzuki-Miyaura cross-coupling reaction (Scheme 1.14).[41, 45] Utilizing compounds with poor solubility in organic solvents such as pigment violet 23 **28** (solubility in PhMe <2 x 10^{-5} M) which had not previously been able to undergo derivatization through cross-coupling procedures. Through this new protocol they have been able to prepare new luminescent organic materials from Pigment Violet 23 **28** including **29** which has a strong red emission. This cross-coupling could therefore facilitate the derivatization of insoluble aryl halides for the discovery of new photoactive materials such as **29**, only currently accessible through ball milling.
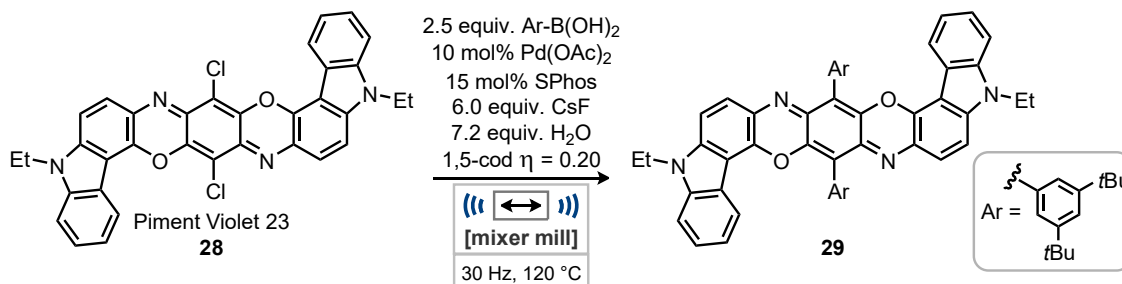
Scheme 1.14 Solid-state Suzuki-Miyaura cross-coupling enabled by ball milling.

The ability to carry out truly solvent free reactions that require no solvent during the reaction, work up and purification is very challenging. Most examples of ball milling reactions still require the use of some solvents through work up and purification requirements, however there are a number of examples that do achieve this impressive feat of a solvent free reaction that has no solvent requirement for work up or purification.[46] Simple condensation reactions are often so effective under mechanochemical conditions

in which several examples exist producing a range of products with minimal solvent contribution, such as liquid additives or a water wash for purification.[30a, f, 46] Some of these condensation reactions can be used to produce valuable compounds, such as salen ligands. James and coworkers have taken these condensation reactions a step further for the synthesis of salen ligands from salicylaldehyde **30** and ethylenediamine **31** by including their coordination to a number of metals via either a one-pot or two-step one-pot approach (Scheme 1.15a).[47] In these examples they have produced several salen complexes, including **32**, requiring no solvent for the synthesis or purification. Finally, utilizing their expertise in transferring reactions from ball milling to TSE they have established a procedure for the synthesis of a zinc salen complex from salicylaldehyde **30**, a 1,2-diamine **33** and zinc acetate dihydrate (Scheme 1.15b).[48] This continuous process would provide the product **34** analytically pure by ^{1}H NMR spectroscopy albeit allowing for the presence of the remaining sodium carbonate.
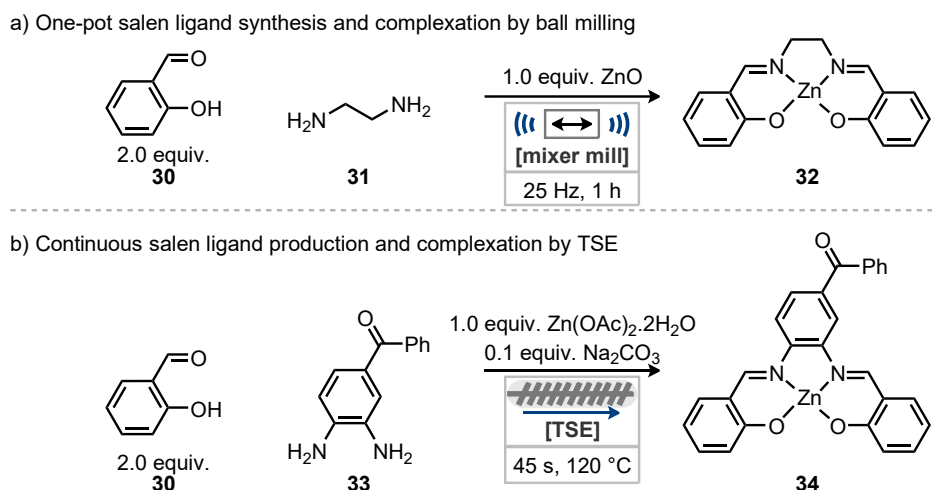

Scheme 1.15 Synthesis of salen ligands and their complexes using ball milling and TSE.

It's clear from these examples that ball milling is able to access reactivity in compounds that would often be very challenging in solution due to their poor solubility with ease. Also, simple condensation reactions are often high yielding under ball milling conditions and can be used to provide valuable products. The simplicity of their conditions also allows them to be combined with other reactions for further elaboration of the products.

1.08   Increased Rate of Reaction

The lack of large quantities of solvents from mechanochemical reactions often significantly increases the rate of reactions due to the increase in reagent concentration.
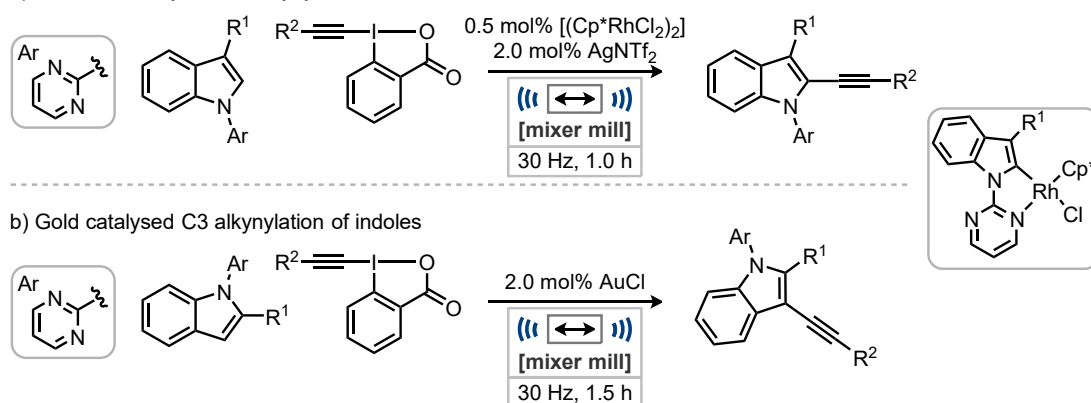
Furthermore, the removal of solvent also removes the thermodynamic barrier of desolvation which can hinder some reactivity in solution.[4j] Such benefits are observed by Su and coworkers for the cross dehydrogenative coupling of tetrahydroisoquinoline **35** derivatives with terminal alkynes **36** (Scheme 1.16b).[49] Similar procedures developed in solution required two days in refluxing decane (Scheme 1.16a), but this approach produced similar or higher yields and enantioselectivities in only one hour.[50] Also, the catalyst could be replaced by copper balls making the removal and recycling of the catalyst simple for this procedure while still achieving good enantioselectivities.
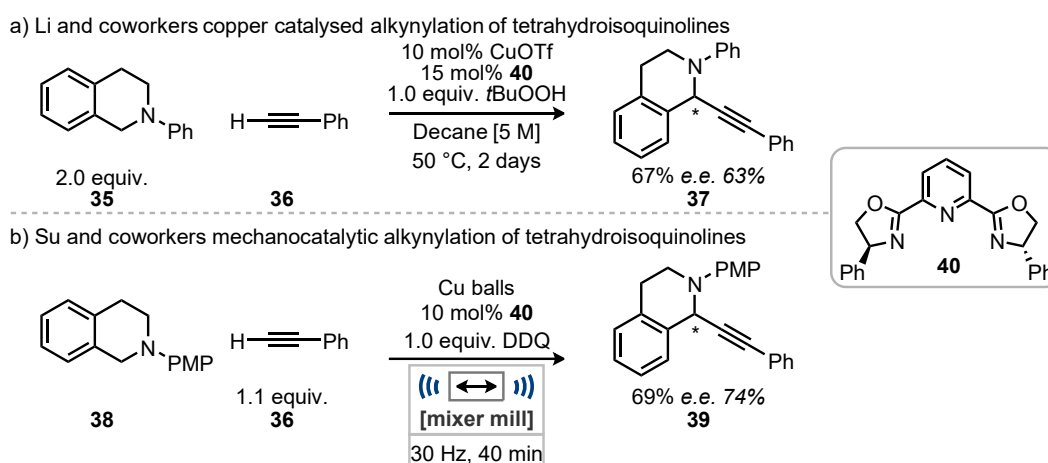
Scheme 1.16 Copper catalysed alkynylation of tetrahydroisoquinoline.

Bolm and coworkers expanded on the range of alkynylation reactions possible under ball milling conditions with rhodium (Scheme 1.17a) and gold (Scheme 1.17b) catalysed C-H activation for the synthesis of C2 and C3 alkynylated indoles.[51] In the developed transformations lower catalysts loadings than that of solution counterparts were capable of producing the products in higher yields and shorter reaction times (12 – 24 h in solution). Preliminary mechanistic studies allowed for the isolation of an intermediate rhodacycle via stoichiometric reaction with the indole, this intermediate was then confirmed as an active catalyst for the C-H functionalization.
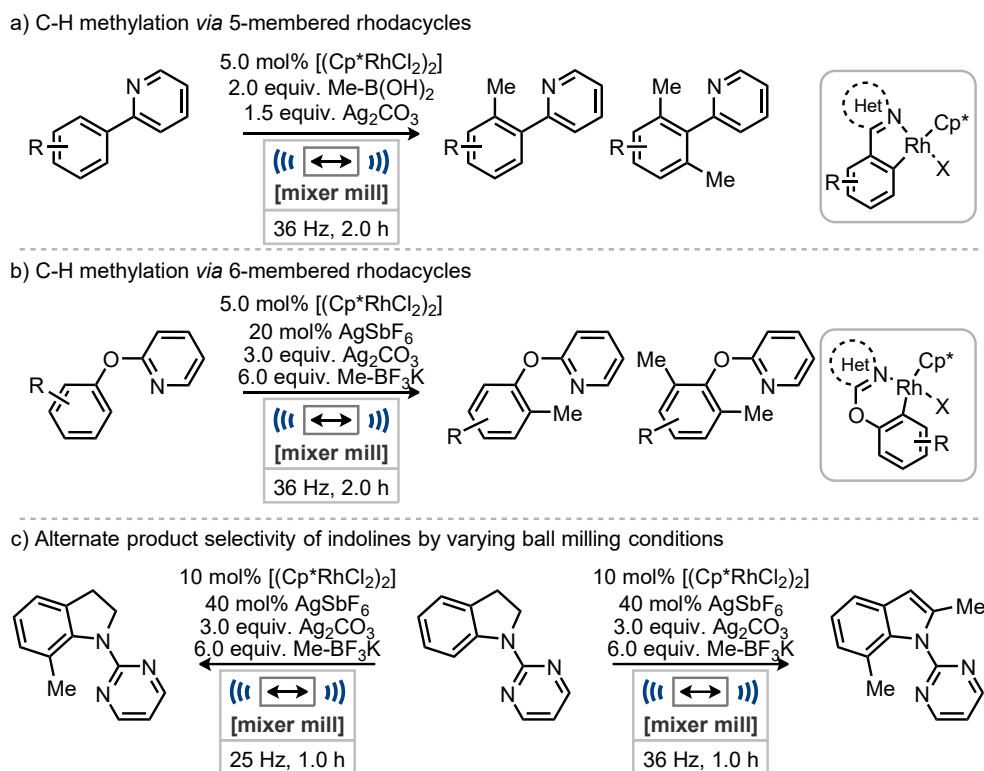
Scheme 1.17. Alkynylation of indoles through Rh and Au catalysis.

The late stage introduction of methyl groups into bioactive molecules can improve their potency by improving lipophilicity, binding interactions, metabolic stability and more.[52] These collective benefits have been referred to as the 'magic methyl effect' and have garnered significant recent efforts into new C-H methylation strategies.[53] Pilarski and coworkers have developed ruthenium catalysed methylation strategies for a range of aromatic and heteroaromatic substrates under ball milling conditions (Scheme 1.18).[54] They achieved selectivity's currently unattainable for solution variants for the mono-methylation of phenyl pyridines (Scheme 1.18a) and phenoxypyridines (Scheme 1.18b) both often suffer with dimethylation. Furthermore, in the C7 methylation of indolines (Scheme 1.18c) the C2,7-dimethylated indole product was identified as a byproduct in initial work. This led to further investigation the formation of this dimethylated product, which could be produced selectively by increasing the milling speed from 25 Hz to 36 Hz. This dimethylation requires a catalytic dehydrogenative aromatization which generally require high temperatures in solution and had not previously been achieved under mechanochemical conditions. During their mechanistic investigations into these transformations, the researchers carried out the synthesis of a range of rhodacycle intermediates through stoichiometric reactions of the catalyst and substrates under mechanochemical conditions. They successfully synthesiszed both 5 and 6 membered rhodacycles in higher yields and shorter reaction times than for previous solution synthesis. The expedient synthesis of these compounds provided a much more convenient method for their production than prior methods. Finally, they applied their methylation strategies to a range of biologically active compounds including pharmaceuticals and natural products.

a) C-H methylation *via* 5-membered rhodacycles

b) C-H methylation *via* 6-membered rhodacycles

c) Alternate product selectivity of indolines by varying ball milling conditions

Scheme 1.18 Rh catalysed C-H methylation.

The advantage of faster reactions is not only possible for metal catalysed processes, but MCRs under ball milling conditions.[4q] Ugi and Passerini reaction methods have shown significant rate enhancement via the application of ball milling in work carried out by Juaristi and coworkers (Scheme 1.19a).[55] These MCRs undergo a cascade of elementary chemical reactions all controlled by individual equilibria that must align to produce the desired products. Often, optimization of MCRs requires careful balance of reaction conditions to provide the most successful pathway to the desired product avoiding unwanted side products. The implementation of ball milling on these MCRs has provided a synthesis of these complex products in a single step in good to excellent yields in only 45 – 180 minutes, with comparative solution reactions requiring 16 hours to 3 days at elevated temperatures.[56] El-Remaily and coworkers have successfully carried out the Ugi reaction using TSE which achieved this MCR with a retention time of only 15 minutes demonstrating a notable increase in the rate of this transformation utilizing this continuous method (Scheme 1.19b).[57] This significant increase in the reaction rate from the ball milling variant could be achieved due to the elevated reaction temperature possible using TSE.

a) Ball milling Ugi and Passerini reaction from Juaristi and coworkers
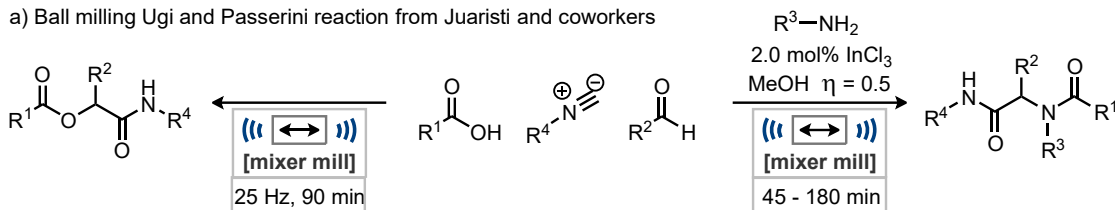
b) TSE Ugi reaction from El-Remaily and coworkers
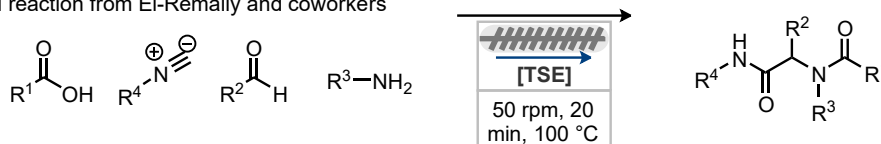
Scheme 1.19 Ugi and Passerini reaction.

Rapid access to metal organic materials has been demonstrated by Lamaty and coworkers in their efforts for the production for copper NHC complexes, whereby imidazolium salts were coordinated to copper(I) following the oxidation of the elemental copper by oxygen present in the jar, thus simplifying the procedure and the purification of the final product (Scheme 1.20).[58] The straightforward reaction conditions with minimal solvent requirement and reduced reaction time, compared to solution,[59] provides a convenient method for the synthesis of these complexes. With their established method, the synthesis of five novel complexes could be achieved indicating the potential of mechanochemistry for the synthesis of new metal complexes with potential value as catalysts.[60]
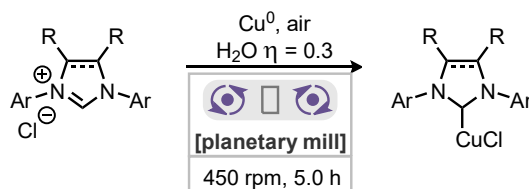

Scheme 1.20 Synthesis of copper NHC complexes from copper metal.

These selected examples highlight that the lack of bulk solvent in ball milling reactions can allow for significant rate enhancement for a broad spectrum of reactivity. It also can provide simplified reaction work up and product isolation further increasing the ease of access to the products.

1.09   Improving Sustainability

Discovery of sustainable methods of synthesis is becoming increasingly important to synthetic chemistry.[61] The ACS Green Chemistry Institute Roundtable provide numerous valuable objectives for the implementation of sustainable practices in industrial and research settings that do not yet exist.[32] The reduction in the use of chlorinated and polar a-protic solvents are the most commonly associated aims with ball milling but these are not the only benefits to more sustainable synthesis that ball milling can provide.[4v, 46, 62]

Through the synthesis of PZ-1361 **48**, Lamaty and coworkers demonstrated the possible benefits of a multistep solvent free synthesis employing ball milling (Scheme 1.21).[63] In comparison to the solution method the total reaction time could be reduced from 60 hours to 5 hours and improved the overall yield from 34% to 64%.[64] Furthermore, the excess of epichlorohydrin **42** was reduced from 3.0 equiv. to 1.2 equiv. for the synthesis of **43** and the subsequent Boc deprotection was carried out using HCl gas in quantitative yield. Throughout their synthesis a variety of fragments were applied at each stage of the synthesis for a diversification of the final product. Finally, the ball milling procedures established were high yielding enough such that column chromatography could be completely avoided during the synthesis of PZ-1361 and many of its derivatives.
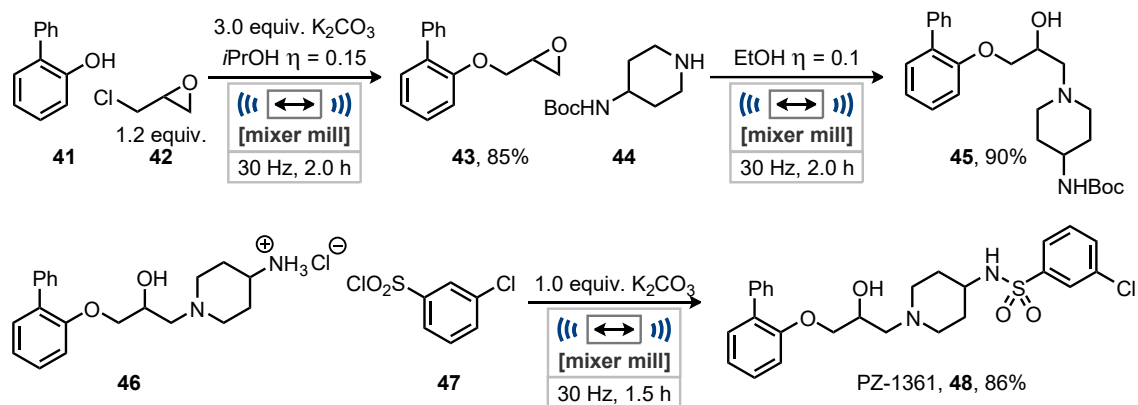
**Scheme 1.21** Ball milling synthesis of PZ-1361.

However, the practical synthesis of pharmaceutical compounds on an industrial scale requires material to be produced in much larger quantities than what is possible to achieve through most ball milling devices, other mechanochemical techniques could be applied to their synthesis.[11] Colacino and coworkers performed the condensation of aryl aldehydes with 1-aminohydantoin **49** for the synthesis of hydrazone containing APIs, Nitrofurantoin **50** and Dantrolene **51**, via TSE (Scheme 1.22).[65] This continuous method could produce analytically pure APIs without the need for any purification. Additionally,

the space time yield of the TSE method is 68000 kgm^{-3}day^{-1}, versus the solution method 430 kgm^{-3}day^{-1} thus highlighting the significant reduction in space and time required for this process by the application of mechanochemistry.[66] The application also simplifies the procedure avoiding the requirement of pH adjustments, cooling and heating the entire batch, and the use of concentrated mineral acids and bases required in the solution synthesis. This highly streamlined process simplified the synthesis of these compounds and significantly improved the sustainability of the product.
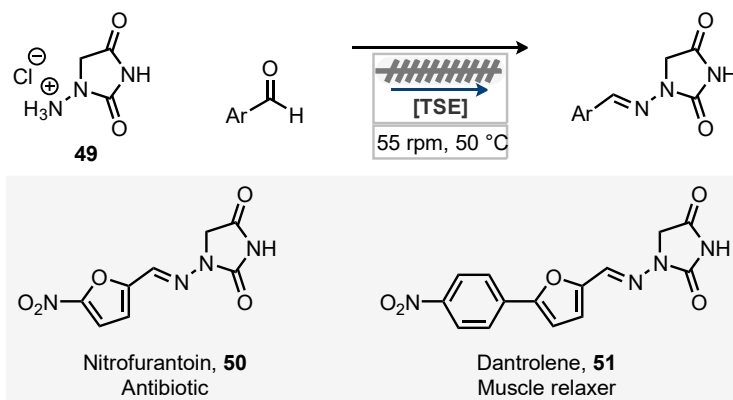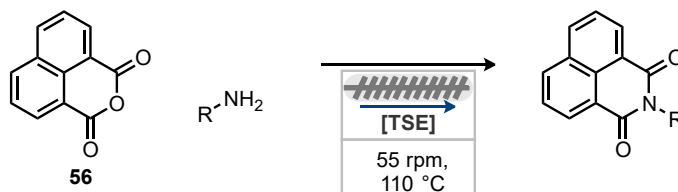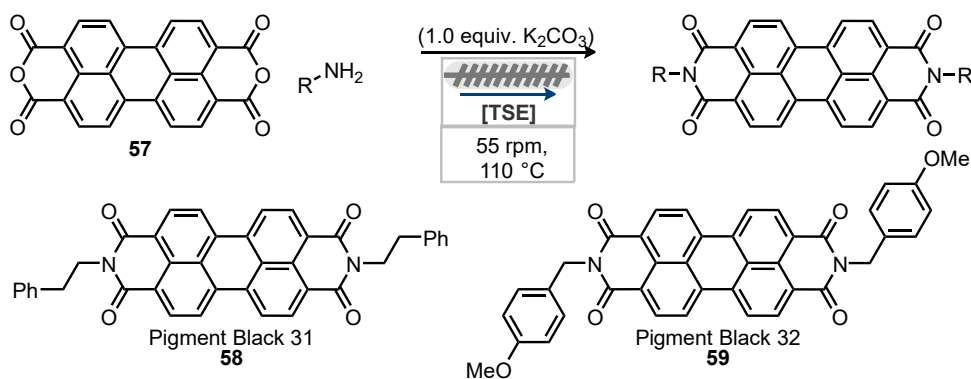

Scheme 1.22 TSE synthesis of Nitrofurantoin and Dantrolene.

C-H activation preventing the necessity of prior synthesis of more activated starting materials has been studied by Zhong and coworkers through a rhodium catalysed C-H amination process (Scheme 1.23).[67] Under their reaction conditions they have been able to remove the use of solvent and reduce the loading of the catalyst compared to solution methods economizing the reaction. Within this work the increased stability of the catalyst under ball milling compared to solution which was studied using ^{19}F NMR spectroscopy to measure the catalyst decay profile. This revealed the remarkable advantages of ball milling to this process alleviating one electron oxidation of the rhodium dimer and circumventing solvent oxidation side reactions.[68] This allowed for lower catalyst requirements for this C-H amination reaction increasing the sustainability and reducing the cost for the catalyst required in the reaction.
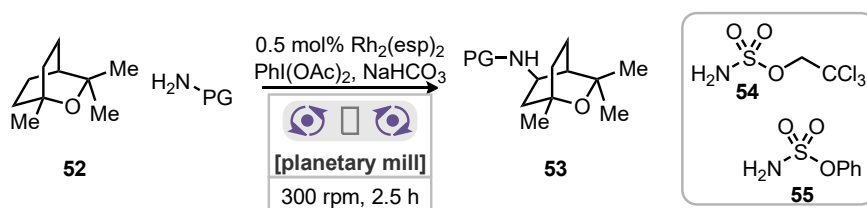
Scheme 1.23 Direct C-H amination.

During the manufacture and application of dyes the strongly coloured waste effluents can result in significant environmental contamination.[69] The quantity of waste can be significantly reduced through the application of alternate manufacturing practices. James and coworkers applied TSE technology to the synthesis of a number of commercial pigments in a solvent free manner (Scheme 1.24).[70] The synthesis of naphthalic imides could be achieved in quantitative yields with water as the only byproduct without the need for any solvent during the reaction or purification (Scheme 1.24a). The reaction method could be expanded to synthesize perylene diimides in good to excellent yields (Scheme 1.24b). When less nucleophilic amines were used potassium carbonate could be added to facilitate the reaction. Using automated synthesis methods, they successfully applied TSE to the synthesis of Pigments Black 31 **58** and 32 **59** with a throughput rate of ~1500 gday^{-1} with a corresponding space time yield of 30 x 10^3 kgm^{-3}day^{-1} which is 1-2 orders of magnitude greater than for solvent batch methods. The application of TSE provides substantial waste reduction and improved efficiency of these compounds. Similar benefits have also been found for the synthesis and elaboration of other dyes under mechanochemical techniques such as BODIPY and azo-dyes.[71]

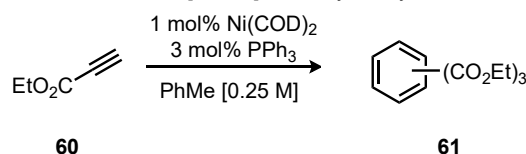**Scheme 1.24** TSE synthesis of naphthalic imides and perylene diimides.

Through these examples it has been demonstrated that mechanochemistry can significantly improve sustainability of organic synthesis through waste reduction. This can be in the form of significant quantities of solvent in the reaction and purification but also through reducing the stoichiometry of reagents or catalyst loading in the reaction.
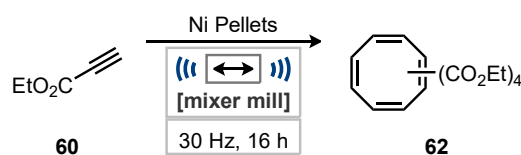
1.10 Alternate Products and Reactivity

Increasing the rate and sustainability of a transformation are attractive benefits, boosting interest in mechanochemistry.[4v] That being the case the distinct reaction environment of mechanochemical techniques could be pave the way for the discovery of alternate reactivity, producing new products than that of solution counterparts.[4c] The ability to discover new chemical reactivity is fundamental to any area of chemical research, and there have been numerous examples which have been mechanochemically facilitated.

The [2+2+2] cyclotrimerization of alkynes such as **60** for the synthesis of benzene derivatives **61** with nickel(0) catalysts has been observed in solution with moderate regioselectivity by Guan and coworkers (Scheme 1.25a).[72] When Mack and coworkers attempted this mechanocatalytic transformation utilizing nickel pellets under mixer mill conditions the expected trimer products were not observed as the major product. [2+2+2+2] cyclotetramization products **62** were observed as the major products, albeit as a mixture of regioisomers (Scheme 1.25b).[73] The optimized process demonstrated the activity of nickel metal as an active catalyst for a process that would usually require glove box or Schlenk line manipulation to facilitate the use of a nickel(0) catalyst.

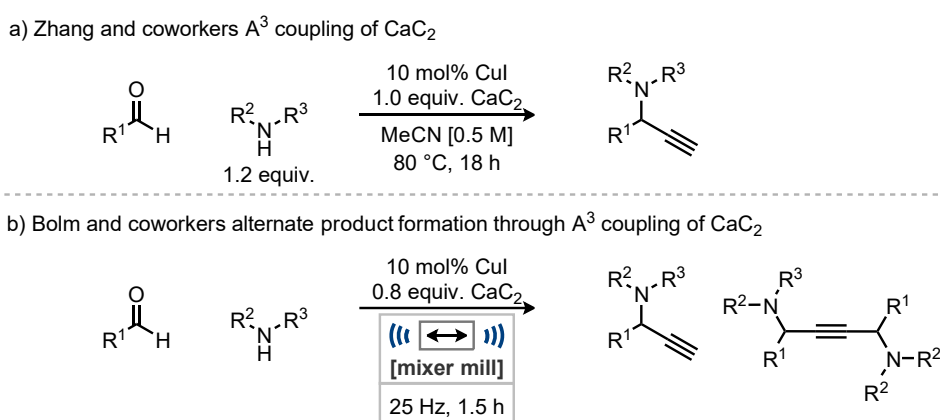a) Guan and coworkers [2+2+2] Ni catalysed cyclotrimerization

$$EtO_2C \quad \xrightarrow[\text{PhMe [0.25 M]}]{\substack{1 \text{ mol\% Ni(COD)}_2 \\ 3 \text{ mol\% PPh}_3}} \quad (CO_2Et)_3$$

60   **61**

b) Mack and coworkers [2+2+2+2] Ni catalysed cyclotetramization

$$EtO_2C \quad \xrightarrow[\substack{\text{[mixer mill]} \\ 30 \text{ Hz, 16 h}}]{\text{Ni Pellets}} \quad (CO_2Et)_4$$

60   **62**

Scheme 1.25 Alternating the product of Ni catalysed cyclisation of alkynes

Flammable gases such as acetylene can be challenging to handle under any conditions requiring either use in large excess or under high pressures to force the compound into solution. Although the use of alternate surrogates to these gaseous reagents can simplify their use. Calcium carbide (CaC$_2$) has been demonstrated as a suitable candidate as a solid replacement for acetylene although not without issue due to its poor solubility in organic solvents. Bolm and coworkers have recently explored the use of CaC$_2$ as a

nucleophile under ball milling conditions (Scheme 1.26 and 1.27).[74] Initial work focused on the synthesis of propargyl amines under ball milling conditions expanding on previous work from Su and coworkers on the formation of this synthetically valuable compound.[75] Although to their surprise the desired A[3] coupling product was not observed and in its place was the 1,4-diamino-2-butyne (Scheme 1.26b).[74a] This reactivity was contradictory to previously reported A[3] couplings with CaC$_2$ by Zhang and coworkers, where the reactive species is likely an acetylide nucleophile where the carbide has been singularly protonated by water as they specify the use of undried acetonitrile in their methodology (Scheme 1.26a).[76] The alternate reactivity observed mechanochemically is postulated to be due to the carbide remaining di-anionic during the reaction in the mill.

a) Zhang and coworkers A[3] coupling of CaC$_2$

b) Bolm and coworkers alternate product formation through A[3] coupling of CaC$_2$

Scheme 1.26 A[3] coupling of CaC$_2$.

Mechanochemical synthesis and functionalization of two- and three- dimensional carbon-based materials had already been well established, although one-dimensional structures had yet to be explored.[4l, 77] Bolm and coworkers applied their experience using CaC$_2$ to the synthesis of odd-numbered tetraaryl[n]cumulenes (Scheme 1.27).[74b] Due to their practical accessibility, cumulenes are often used as model substrates to predict the physio- and chemical properties of carbyne.[78] These structures are typically synthesized from Li or Mg acetylide addition to carbonyl compounds followed by reductive elimination of the 1,4-butyndiols with tin(II) chloride and a strong acid.[78] Under ball milling conditions the addition of CaC$_2$ to benzophenone **63** and its derivatives produced the necessary 1,4-butyndiols **64** intermediates. These could then be reduced with SnCl$_2$·2H2O without the need for an acid, improving the functional group tolerance to include acid labile functional groups for the synthesis of cumulenes. This two-step approach yielded tetraaryl[3]cumulenes **65** in good yields in relatively short reaction times (Scheme 1.27a). They also then went on to develop a synthesis of tetraaryl[5]cumulenes **68** from propargyl alcohols **65** through an oxidative dimerization reaction followed by reductive elimination (Scheme 1.27b). This initial concept realization could be applied in the future

in the synthesis of other carbon-based materials from CaC_2 such as polycyclic hydrocarbons or cumulenes from poorly soluble precursors.
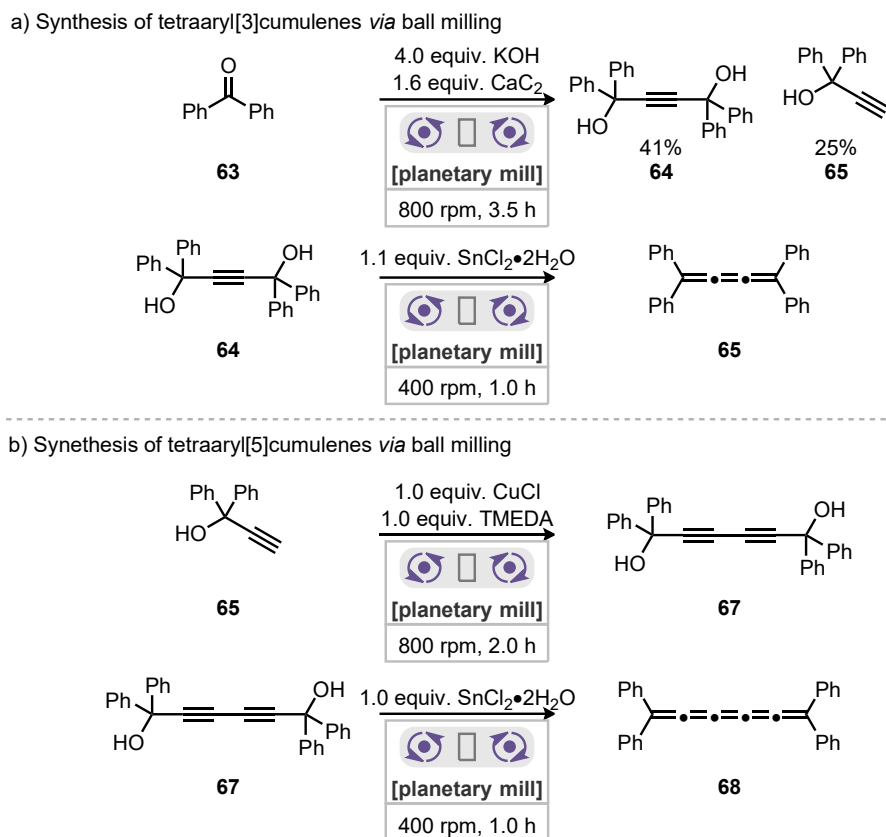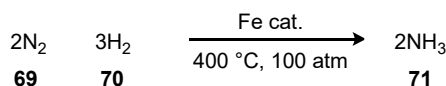

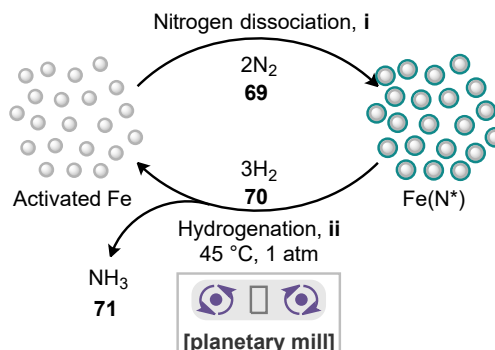**Scheme 1.27** Synthesis of odd numbered tetraaryl[n]cumulenes from CaC_2.

Ammonia **71** is one of the top 10 most fundamental feedstock chemicals for the synthesis of herbicides, plastics and other chemicals.[79] Global production of ammonia is greater than 100 million tonnes per year, and currently it is synthesized on an industrial scale via the Haber-Bosch process at pressures over 100 bar and between 400-500 °C (Scheme 1.28a). [80] Work from Baek and coworkers demonstrated the effect of ball milling on the synthesis of ammonia **71** using an iron catalyst under mild conditions (1 bar and 45 °C) which produced **71** at a higher final concentration (82.5 vol%) than the current state of the art industrial synthesis (25 vol%, 450 °C and 200 bar)(Scheme 1.28b).[81] Although this current mechanochemical production is limited to batch synthesis with the catalyst surface being loaded with nitrogen prior to milling **i**, it demonstrates the potential of this technique still in its infancy. Application of mechanochemistry to this transformation could reduce the energy requirement for this reaction which currently uses 1% of global energy production.[82]

a) The Haber-Bosch reaction

$$2N_2 \quad 3H_2 \xrightarrow[\text{400 °C, 100 atm}]{\text{Fe cat.}} 2NH_3$$

69   **70**   **71**

b) Step wise Haber-Bosch by ball milling under milled conditions

Nitrogen dissociation, **i**

$2N_2$ **69**

Activated Fe $3H_2$ **70**   Fe(N*)

Hydrogenation, **ii**
45 °C, 1 atm

NH_3 **71**

[planetary mill]

Scheme 1.28 Haber-Bosch process.

The solid-state generation of phosphorous ylides and their application to a Wittig reaction from Balema and coworkers demonstrated surprisingly mild synthesis of phosphonium ylides (Scheme 1.29).[83] In solution the generation of phosphorous ylides from triphenyl phosphine **72** and alkyl halides often requires a strong base such as the pyrophoric *n*-butyl lithium, but under ball milling conditions this can be achieved with potassium carbonate.[84] These phosphorous ylides are then shown to still react effectively with ketones or aldehydes for the synthesis of alkenes (Scheme 1.27).[85] This discovery revealed the ability to use weaker bases under ball milling conditions when compared to solution chemistry which could improve the functional group tolerance of a transformation, simplify and improve the safety of the reaction. Mack and coworkers have since expanded on the understanding of the ball milling Wittig reaction elucidating the effects of liquid additives and ion pairing towards conversion and diastereoselectivity.[27c] Their findings suggested significant rate enhancement using liquid additives with high dielectric constants and that with Cs^+/Br^- ion pair excellent diastereoselectivity could be achieved in the synthesis of E-stilbenes.

Ar–X PPh_3 [mixer mill]   30 Hz, 1.0 h $Ar\overset{\oplus}{PPh_3}\overset{\ominus}{X}$ K_2CO_3 [mixer mill]   30 Hz, 3.0 h $[Ar{=}PPh_3]$ $R^1{-}C({=}O){-}R^2$ $Ar\overset{R^2}{\underset{R^1}{=}}$

72
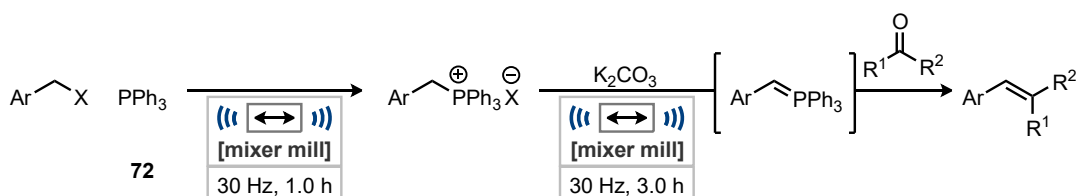
**Scheme 1.29** Ball milled synthesis of phosphonium ylides and their use in a Wittig reaction.

Clearly from these examples presented that previously unobserved reactivity has been enabled by the implementation of ball milling. This alternate reactivity can be in the form of new products or through significant alteration in the activity of known reagents. Although, it is currently impossible to predict where this new reactivity could be unveiled, with increasing understanding of the mechanics that produce these new transformations such deductions may be possible in the future.

1.11 Ball Milling Enabled Reactivity

The use of ball milling has enabled a range of reactivities that would be very challenging under solution conditions. This is through the implementation of reagents that are poorly soluble in common organic solvents or the need for direct mechanical activation of the reagents.

Metal ores require significant processing and purification to extract the desired metal components.[86] This is a time and energy consuming process that can be avoided if the metal ores can be used directly in synthesis. Two examples from Bolm and coworkers exploit ball milling for copper catalysed atom transfer radical cyclisation (Scheme 1.30a) and a vanadium catalysed oxidative coupling of 2-napthol **74** and derivatives using metal ores (Scheme 1.30b).[87] The ores used, covallite (copper) and vanadinite (vanadium), have very poor solubility in common reaction solvents making them very challenging to use under solution conditions. This results in poor uptake in the use of these and other minerals as catalysts for organic transformations. While under ball milling conditions readily available organic ligands Me_6TREN **73** and DPA **76** were used to harness these metals ores for the catalytic activity of the metals.

a) Covalite catalysed atom transfer radical cyclisation

b) Vanadinate catalysed oxidative coupling of 2-napthols
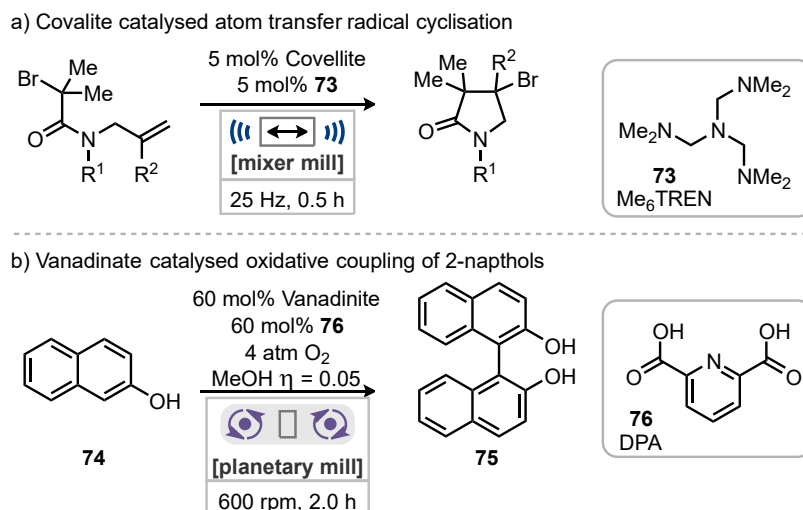
Scheme 1.30 Metal ore catalysed atom transfer cyclisation and oxidative coupling of 2-napthol derivatives.

Prebiotic chemistry may have relied on mechanical activation of compounds during, weathering, tectonic activity, or asteroid impact, for the synthesis of the molecules required for life.[39c, 88] Hernández and coworkers activated iron cyano complexes in an envisaged prebiotic scenario for the synthesis of amino acids (Scheme 1.31).[89] In this MCR benzyl amine **78** was condensed with benzaldehyde **77** and the resultant imine could be attacked by a cyanide anion liberated by the mechanical activation of the iron cyano complexes (Scheme 1.31a). The resulting α-aminonitriles **79** could then be hydrolysed in the ball mill also under pseudoprebiotic conditions with sodium hydroxide monohydrate to furnish the amino amide **80** (Scheme 1.31b).

a) Prebiotic α-aminonitriles synthesis

b) Pseudoprebiotic hydrolysis of α-aminonitriles
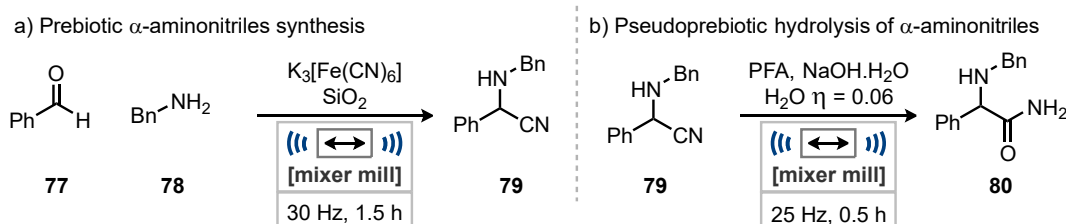
**Scheme 1.31** Iron cyano complexes activated by ball milling.

Mechanoredox reactions are a new class of reactivity initially discovered by Ito and coworkers for the borylation or arylation of diazonium salts **81** (Scheme 1.32a).[90] In a process that mirrors photoredox catalysis where a catalyst enters an excited state once excited by a photon of sufficient energy in mechanoredox chemistry a piezoelectric material enters an excited state when compressed during a collision.[91] This excited state is in the form of a temporary highly polarized particle which is then able to reduce a substrate via a SET. Ito and coworkers expanded the mechanoredox field with a radical

trifluoromethylation of electron rich arenes and heteroarenes (Scheme 1.32b).[92] Finally, Bolm and coworkers employed mechanoredox for the reduction of a copper(II) pre-catalyst to the active copper(I) required for an atom transfer radical cyclisation (Scheme 1.32c) previously established utilizing covalite a copper(I) containing mineral (Schemes 1.30).[87, 93]
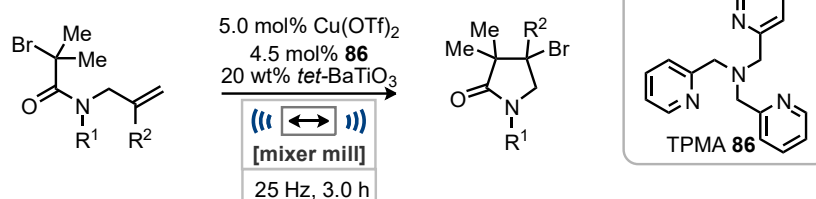
a) Mechanoredox arylation and borylation from Ito and coworkers
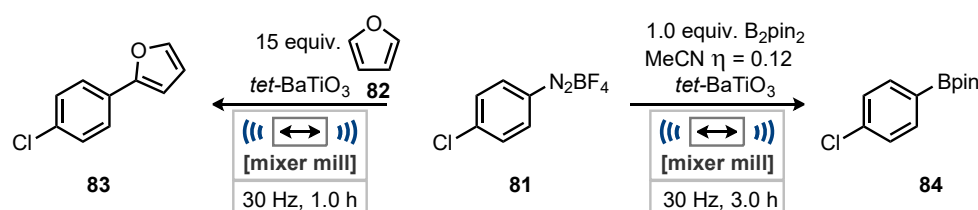
b) Mechanoredox trifluoro methylation from Ito and coworkers
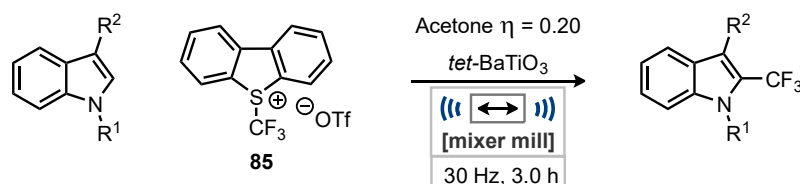
c) Mechanoredox copper catalysed atom transfer radical cyclisation from Bolm and coworkers

**Scheme 1.32** Examples of mechanoredox reactions.

The generation of hydrogen gas typically uses methane as the hydrogen source generating large amounts of carbon dioxide as a by-product.[94] With limited resources of fossil fuels an alternate source is necessary. One such method is the dehydrogenation of simple alkanes to produce molecular hydrogen which can be achieved with a range of metal catalysts. Sajiki and coworkers have discovered a method for the production of hydrogen from diethyl ether **88** and applied it to the reduction of aromatic compounds **87** for the synthesis of cyclohexane **89** derivative as a one pot procedure (Scheme 1.33).[95] This method utilized hardened steel balls and jars (SUS304) typically used for ball milling reactions, which enabled oxidation of diethyl ether releasing hydrogen gas, which can then be used for the reduction of aromatic compounds. They proposed that one or more of the metals present in the stainless-steel jar was responsible for this transfer hydrogenation process. Their mechanistic investigation of the reaction utilized a zirconia jar and balls and isolating each metal component of the stainless steel allowing for its activity in the transfer hydrogenation reaction to be individually evaluated. This study

found that nickel was the most reactive component of the stainless-steel jar and likely responsible for the observed reactivity.
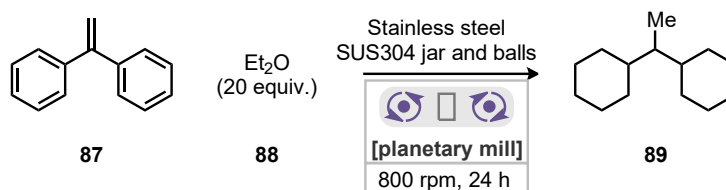
**Scheme 1.33** Reduction of 1,1-diphenylethylene via transfer hydrogenation from diethyl ether.

The solvent free and minimized reaction environment in ball mills has produced a number of surprising observations. Belenguer and coworkers discovered a dynamic covalent reaction of disulfides **90** and **91** that under ball milling conditions had incredibly high selectivity for the formation of the mixed disulfide **92** (Scheme 1.34).[96] Whereas, in solution it would proceed a statistical mixture of the mixed disulfide along with both starting disulfides in a 1:1:2 ratio (**90**:**91**:**92**). Due to the solvent free or minimized environment the lattice enthalpy of the mixed disulfide **92** could act as the thermodynamic driving force to selectively lead to the mixed disulfide **92** as the only product. Furthermore, the final polymorph of this mixed disulfide **92** was altered dependent on either neat or the chosen liquid additive applied. This selectivity can only be achieved in solvent free or minimized reaction environments and could potentially be applied to other transformations.
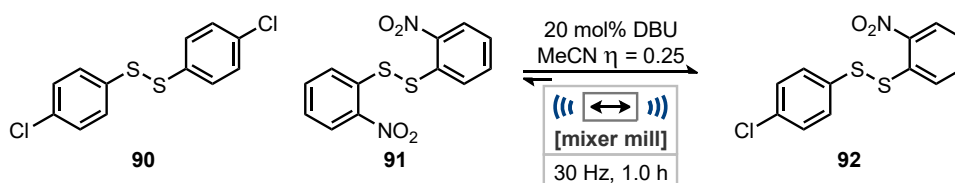
**Scheme 1.34** Disulfide metathesis under ball milling.

Observations of new products from well understood chemistry is unusual, such as the palladium catalysed Heck reaction.[97] Su and coworkers while optimizing a ball milling Heck coupling of indoles **93** with acrylates **94** discovered a previously unobserved product **96** (Scheme 1.35).[98] The desired 3-vinyl indoles **95** were synthesized in good yields with palladium acetate and acetic acid as a liquid additive but when the catalyst was exchanged for a palladium halide, salt β,β-diindolyl propionates **96** were observed as the major product. Removal of acetic acid as liquid additive during reaction optimization improved the selectivity of the new product. Through control reactions, it was determined that the 3-vinyl indoles **95** did not participate as an intermediate in the

production of β,β-diindolyl propionates **96**. ESI-MS was employed to probe the mechanism, delineating **97** and **98** as possible intermediates. With these results plausible mechanisms were suggested, where the rate of addition of the olefin to a dimeric palladium species may determine the product. Furthermore, a solvent-labile dimeric palladium intermediate could be responsible for the differing reactivity in the ball mill versus in dimethylformamide due to the decreased rate of chain walking in solution.
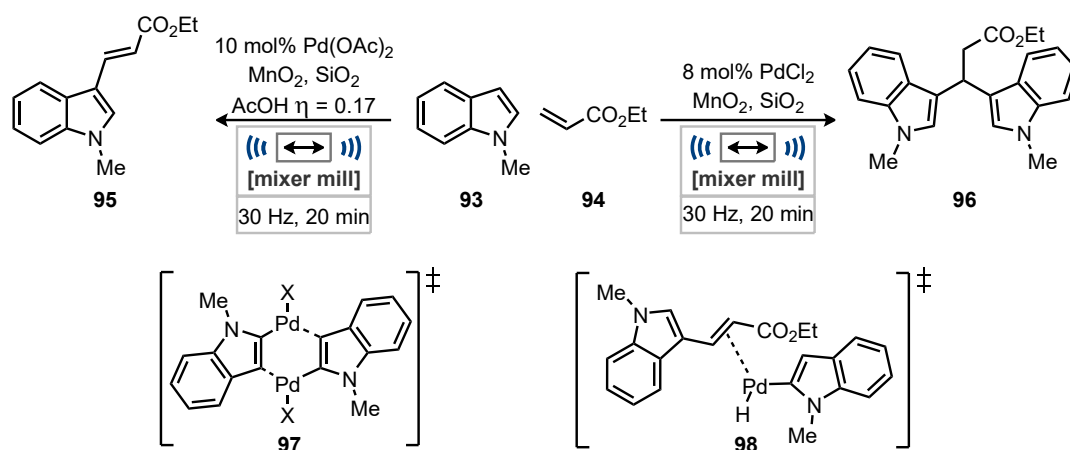
Scheme 1.35 Synthesis of 3-vinyl indoles and β,β-diindolyl propionates.

Ball milling can also be used to successfully combine reactions that are currently not possible under solution conditions due to differing solvent needs.[99] While working on alkyne cyclopropenation Mack and coworkers successfully coupled two previously incompatible reactions (Scheme 1.36).[100] The cyclopropenation of alkynes with diazoacetates through copper or silver catalysis was successfully coupled with a palladium catalysed Sonogoshira reaction. This multi component reaction could then be applied to the synthesis of a library of cyclopropene derivatives *via* the intermediate Sonogashira product. The coupling of these reactions could significantly expand the scope of available internal alkynes due to their limited commercial availability. Finally, these reactions have not previously been reported as a one pot procedure under any other conditions and would require the isolation of the intermediate internal alkyne.
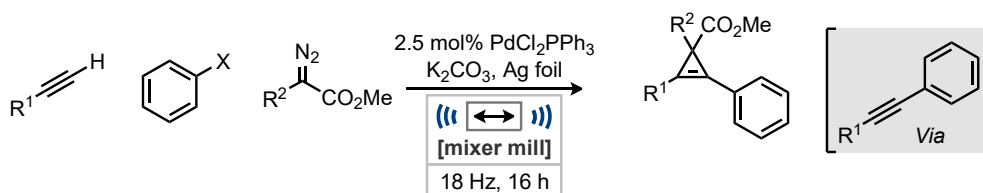
Scheme 1.36 Multi component synthesis of cyclopropene's.

Enabling new reactivity through the application of mechanical force in the case of mechanoredox reactions demonstrates the ability to open up a new area of chemistry using ball milling. Mechanochemistry has also enabled several other transformations, presented in the previous examples due to its unique reaction environment. This can simplify multistep processes and allow access to new products from well understood chemistry.

1.12 Conclusion and Outlook

The application of mechanochemistry through ball milling has demonstrated a broad variety of benefits to organic synthesis. These advantages include shorter reaction times, improving the safety of a process, and the ability to telescope reactions for multistep reactions not possible in solution, among many others. It has also been highlighted by IUPAC and in several publications that the application of mechanochemistry can produce a more sustainable reaction generating less waste. This greener approach to synthesis has attracted the attention of the wider chemical industry but this alone may not be enough for its application in an industrial setting.

The discovery of novel reactions and new products is the one of most fundamental areas of chemical research and the ability to do this using mechanochemistry has been well established. The capacity to discover new reactivity that is not currently possible in solution may produce a necessity for industrial applications of mechanochemical techniques, such as the use of TSE in the synthesis of MOFs which would not be financially viable without the use of mechanochemistry. Although, it is not currently possible to predict when this new reactivity will be observed, the breadth of transformations that have currently been improved by mechanochemistry makes it likely that many transformations could still be improved upon.

The ability to probe reaction mechanisms by *in situ* spectroscopy and reaction monitoring is a growing area of interest that is able to reveal in greater detail the mechanisms that these mechanochemical processes undertake. This expanding area of research may be able to investigate what mechanical attributes leads to new reactivity. It may be possible in the future to use this mechanistic data to manipulate reactions to produce new products or alternate reactivity.

Notwithstanding the level of progress made in ball milling for organic synthesis there is still clear potential for further application to more transformations. This could establish

what transformations are possible under mechanochemical conditions and improve on the understanding and predictability of the transformations while using these methods.

1.13 Aims and Objectives

The aims of this thesis are to investigate further applications of ball milling to organic synthesis to improve on known transformations and potentially in the discovery of new reactivity. This will be achieved by altering conditions of reactions from solution to apply them to ball milling. By probing their reactivity in depth, it may be possible to discover new reactivity or selectivity to that of solution. Comparisons of the ball milling reactions to solution will be necessary to contextualize any reactivity differences. These solution reactions can be either from previous reports of the transformations or reactions utilizing the optimal conditions for ball milling but transferred back to solution.

If any new reactivity which has not been previously established in solution is discovered, it may also be necessary to attempt to reproduce these transformations in solution to explain why this new reactivity is observed. Furthermore, significant mechanistic studies will be necessary to establish the mechanism of these new transformations.

Initial study into the application of ball milling onto known reactions will be carried out using the palladium catalysed Buchwald-Hartwig amination for the synthesis of aryl C-N bonds. This reaction was chosen for study due to its importance in industrial synthesis which was hoped to garner further interest in mechanochemical techniques within industry.[101] Furthermore, this reaction had yet to see any development under mechanochemical methods at the onset of this investigation.

1.14 Bibliography

1.   a) G. Book, *International Union of Pure and Applied Chemistry*, 2014, **528**; b) K. Horie, M. Barón, R. B. Fox, J. He, M. Hess, J. Kahovec, T. Kitayama, P. Kubisa, E. Maréchal, W. Mormann, R. F. T. Stepto, D. Tabak, J. Vohlídal, E. S. Wilks and W. J. Work, *Pure Appl. Chem.*, 2004, **76**, 889-906.
2.   a) D. E. Crawford, *Beilstein J. Org. Chem.*, 2017, **13**, 65-75; b) R. Nixon and G. De Bo, *J. Am. Chem. Soc.*, 2021, **143**, 3033-3036; c) C. L. Brown, B. H. Bowser, J. Meisner, T. B. Kouznetsova, S. Seritan, T. J. Martinez and S. L. Craig, *J. Am. Chem. Soc.*, 2021, **143**, 3846-3855; d) N. N. Gharat and V. K. Rathod, in *Green Sustainable Process for Chemical and Environmental Engineering and Science*, 2020, DOI: 10.1016/b978-0-12-819540-6.00001-2, pp. 1-41.
3.   G. W. Wang, *Chem. Soc. Rev.*, 2013, **42**, 7668-7700.
4.   a) J. L. Howard, Q. Cao and D. L. Browne, *Chem. Sci.*, 2018, **9**, 3080-3094; b) D. Tan and T. Friščić, *Eur. J. Org. Chem.*, 2018, **2018**, 18-33; c) J. G. Hernández and C. Bolm, *J. Org. Chem.*, 2017, **82**, 4007-4019; d) A. Stolle, T. Szuppa, S. E. Leonhardt and B. Ondruschka, *Chem. Soc. Rev.*, 2011, **40**, 2317-2329; e) J. Yu, Z. Hong, X. Yang, Y. Jiang, Z. Jiang and W. Su, *Beilstein J. Org. Chem.*, 2018, **14**, 786-795; f) W. Pickhardt, S. Gratz and L. Borchardt, *Chem. Eur. J.*, 2020, **26**, 12903-12911; g) P. Ying, J. Yu and W. Su, *Adv. Synth. Catal.*, 2021, **363**, 1246-1271; h) X. Zhu, J. Liu, T. Chen and W. Su, *Appl. Organomet. Chem.*, 2012, **26**, 145-147; i) K. Kubota and H. Ito, *Trends Chem.*, 2020, **2**, 1066-1081; j) J. Andersen and J. Mack, *Green Chem.*, 2018, **20**, 1435-1443; k) T. Friscic, C. Mottillo and H. M. Titi, *Angew. Chem. Int. Ed.*, 2020, **59**, 1018-1029; l) S.-E. Zhu, F. Li and G.-W. Wang, *Chem. Soc. Rev.*, 2013, **42**, 7535; m) C. Bolm and J. G. Hernández, *Angew. Chem. Int. Ed.*, 2019, **58**, 3285-3299; n) J. L. Do and T. Friscic, *ACS Cent. Sci.*, 2017, **3**, 13-19; o) S. L. James, C. J. Adams, C. Bolm, D. Braga, P. Collier, T. Friscic, F. Grepioni, K. D. Harris, G. Hyett, W. Jones, A. Krebs, J. Mack, L. Maini, A. G. Orpen, I. P. Parkin, W. C. Shearouse, J. W. Steed and D. C. Waddell, *Chem. Soc. Rev.*, 2012, **41**, 413-447; p) J. G. Hernández and T. Friščić, *Tetrahedron Lett.*, 2015, **56**, 4253-4265; q) M. Leonardi, M. Villacampa and J. C. Menendez, *Chem. Sci.*, 2018, **9**, 2042-2064; r) D. E. Crawford, C. K. G. Miskimmin, A. B. Albadarin, G. Walker and S. L. James, *Green Chem.*, 2017, **19**, 1507-1518; s) A. Bruckmann, A. Krebs and C. Bolm, *Green Chem.*, 2008, **10**; t) V. Declerck, E. Colacino, X. Bantreil, J. Martinez and F. Lamaty, *Chem. Commun.*, 2012, **48**, 11778-11780; u) B. Rodríguez, A. Bruckmann, T. Rantanen and C. Bolm, *Adv. Synth. Catal.*, 2007, **349**, 2213-2233; v) K. J. Ardila-Fierro and J. G. Hernandez, *ChemSusChem*, 2021, DOI: 10.1002/cssc.202100478; w) R. T. O'Neill and R. Boulatov, *Nat. Rev. Chem.*, 2021, **5**, 148-167; x) A. Porcheddu, E. Colacino, L. De Luca and F. Delogu, *ACS Catal.*, 2020, **10**, 8344-8394.
5.   a) C. R. Hickenboth, J. S. Moore, S. R. White, N. R. Sottos, J. Baudry and S. R. Wilson, *Nature*, 2007, **446**, 423-427; b) R. Hoffmann and R. B. Woodward, *Acc. Chem. Res.*, 1968, **1**, 17-22; c) M. Wollenhaupt, M. Krupicka and D. Marx, *Chemphyschem*, 2015, **16**, 1593-1597; d) R. B. Woodward and R. Hoffmann, *J. Am. Chem. Soc.*, 1965, **87**, 395-397.
6.   D. Tan and F. García, *Chem. Soc. Rev.*, 2019, **48**, 2274-2292.
7.   D. Margetic and V. Strukil, *Mechanochemical Organic Synthesis*, Elsevier Science, 2016.
8.   A. A. L. Michalchuk, I. A. Tumanov and E. V. Boldyreva, *CrystEngComm*, 2019, **21**, 2174-2179.
9.   G. R. Kumar, K. Jayasankar, S. K. Das, T. Dash, A. Dash, B. K. Jena and B. K. Mishra, *RSC Adv.*, 2016, **6**, 20067-20073.

10. a) C. F. Burmeister, A. Stolle, R. Schmidt, K. Jacob, S. Breitung-Faes and A. Kwade, *Chem. Eng. Technol.*, 2014, **37**, 857-864; b) R. Schmidt, C. F. Burmeister, M. Baláž, A. Kwade and A. Stolle, *Org. Process Res. Dev.*, 2015, **19**, 427-436.

11. A. Stolle, R. Schmidt and K. Jacob, *Faraday Discuss.*, 2014, **170**, 267-286.

12. C. F. Burmeister, R. Schmidt, K. Jacob, S. Breitung-Faes, A. Stolle and A. Kwade, *Chem. Eng. J.*, 2020, **396**.

13. D. Crawford, J. Casaban, R. Haydon, N. Giri, T. McNally and S. L. James, *Chem. Sci.*, 2015, **6**, 1645-1649.

14. a) B. D. Egleston, M. C. Brand, F. Greenwell, M. E. Briggs, S. L. James, A. I. Cooper, D. E. Crawford and R. L. Greenaway, *Chem. Sci.*, 2020, **11**, 6582-6589; b) S. S. Chui, *Science*, 1999, **283**, 1148-1150.

15. J. Casaban, Y. Zhang, R. Pacheco, C. Coney, C. Holmes, E. Sutherland, C. Hamill, J. Breen, S. James, D. Tufano, D. Wong, E. Stavrakakis, H. Annath and A. Moore, *Faraday Discuss.*, 2021, DOI: 10.1039/d1fd00025j.

16. a) T. Szuppa, A. Stolle, B. Ondruschka and W. Hopfe, *ChemSusChem*, 2010, **3**, 1181-1191; b) K. S. McKissic, J. T. Caruso, R. G. Blair and J. Mack, *Green Chem.*, 2014, **16**; c) F. Fischer, N. Fendel, S. Greiser, K. Rademann and F. Emmerling, *Org. Process Res. Dev.*, 2017, **21**, 655-659; d) Y. Huang, L. Zhou, W. Yang, Y. Li, Y. Yang, Z. Zhang, C. Wang, X. Zhang and Q. Yin, *Crystals*, 2019, **9**; e) F. Fischer, K.-J. Wenzel, K. Rademann and F. Emmerling, *PCCP*, 2016, **18**, 23320-23325.

17. J. M. Andersen and J. Mack, *Chem. Sci.*, 2017, **8**, 5447-5453.

18. T. Szuppa, A. Stolle, B. Ondruschka and W. Hopfe, *Green Chem.*, 2010, **12**.

19. R. Thorwirth, F. Bernhardt, A. Stolle, B. Ondruschka and J. Asghari, *Chem. Eur. J.*, 2010, **16**, 13236-13242.

20. H. Kulla, F. Fischer, S. Benemann, K. Rademann and F. Emmerling, *CrystEngComm*, 2017, **19**, 3902-3907.

21. a) P. R. Patil and K. P. Ravindranathan Kartha, *J. Carbohydr. Chem.*, 2008, **27**, 279-293; b) M. T. J. Williams, L. C. Morrill and D. L. Browne, *ACS Sustain Chem Eng*, 2020, **8**, 17876-17881; c) Y. Wang, H. Wang, Y. Jiang, C. Zhang, J. Shao and D. Xu, *Green Chem.*, 2017, **19**, 1674-1677; d) E. Tullberg, D. Peters and T. Frejd, *J. Organomet. Chem.*, 2004, **689**, 3778-3781; e) H. Cheng, J. G. Hernández and C. Bolm, *Adv. Synth. Catal.*, 2018, **360**, 1800-1804; f) P. Staleva, J. G. Hernandez and C. Bolm, *Chem. Eur. J.*, 2019, **25**, 9202-9205; g) L. Jicsinszky, F. Calsolaro, K. Martina, F. Bucciol, M. Manzoli and G. Cravotto, *Beilstein J. Org. Chem.*, 2019, **15**, 1448-1459; h) F. Schneider, A. Stolle, B. Ondruschka and H. Hopf, *Org. Process Res. Dev.*, 2009, **13**, 44-48.

22. A. A. L. Michalchuk, I. A. Tumanov and E. V. Boldyreva, *J. Mater. Sci.*, 2018, **53**, 13380-13389.

23. C. G. Vogt, S. Gratz, S. Lukin, I. Halasz, M. Etter, J. D. Evans and L. Borchardt, *Angew. Chem. Int. Ed.*, 2019, **58**, 18942-18947.

24. F. Schneider, T. Szuppa, A. Stolle, B. Ondruschka and H. Hopf, *Green Chem.*, 2009, **11**.

25. J. L. Do, C. Mottillo, D. Tan, V. Strukil and T. Friscic, *J. Am. Chem. Soc.*, 2015, **137**, 2476-2479.

26. a) M. Jörres, J. L. Aceña, V. A. Soloshonok and C. Bolm, *ChemCatChem*, 2015, **7**, 1265-1269; b) J. L. Howard, Y. Sagatov, L. Repusseau, C. Schotten and D. L. Browne, *Green Chem.*, 2017, **19**, 2798-2802; c) J. Bonnamour, T.-X. Métro, J. Martinez and F. Lamaty, *Green Chem.*, 2013, **15**, 1116.

27. a) D. Hasa, G. S. Rauber, D. Voinovich and W. Jones, *Angew. Chem. Int. Ed.*, 2015, **54**, 7371-7375; b) T. Stolar, L. Batzdorf, S. Lukin, D. Zilic, C. Motillo, T. Friscic, F. Emmerling, I. Halasz and K. Uzarevic, *Inorg. Chem.*, 2017, **56**, 6599-

6608; c) K. L. Denlinger, L. Ortiz-Trankina, P. Carr, K. Benson, D. C. Waddell and J. Mack, *Beilstein J. Org. Chem.*, 2018, **14**, 688-696.

28.   a) T. Friscic, D. G. Reid, I. Halasz, R. S. Stein, R. E. Dinnebier and M. J. Duer, *Angew. Chem. Int. Ed.*, 2010, **49**, 712-715; b) F. Fischer, A. Heidrich, S. Greiser, S. Benemann, K. Rademann and F. Emmerling, *Cryst. Growth Des.*, 2016, **16**, 1701-1707.

29.   J. L. Howard, M. C. Brand and D. L. Browne, *Angew. Chem. Int. Ed.*, 2018, **57**, 16104-16108.

30.   a) O. H. Qareaghaj, S. Mashkouri, M. R. Naimi-Jamal and G. Kaupp, *RSC Adv.*, 2014, **4**, 48191-48201; b) B. P. Hutchings, D. E. Crawford, L. Gao, P. Hu and S. L. James, *Angew. Chem. Int. Ed.*, 2017, **56**, 15252-15256; c) H. Kulla, S. Haferkamp, I. Akhmetova, M. Rollig, C. Maierhofer, K. Rademann and F. Emmerling, *Angew. Chem. Int. Ed.*, 2018, **57**, 5930-5933; d) N. Cindro, M. Tireli, B. Karadeniz, T. Mrla and K. Užarević, *ACS Sustain. Chem. Eng.*, 2019, **7**, 16301-16309; e) S. Lukin, M. Tireli, I. Loncaric, D. Barisic, P. Sket, D. Vrsaljko, M. di Michiel, J. Plavec, U. Z. K and I. Halasz, *Chem. Commun.*, 2018, **54**, 13216-13219; f) S. Mashkouri and M. R. Naimi-Jamal, *Molecules*, 2009, **14**, 474-479.

31.   F. Gomollón-Bel, *Chemistry International*, 2019, **41**, 12-17.

32.   a) M. C. Bryan, P. J. Dunn, D. Entwistle, F. Gallou, S. G. Koenig, J. D. Hayler, M. R. Hickey, S. Hughes, M. E. Kopach, G. Moine, P. Richardson, F. Roschangar, A. Steven and F. J. Weiberth, *Green Chem.*, 2018, **20**, 5082-5103; b) D. J. C. Constable, P. J. Dunn, J. D. Hayler, G. R. Humphrey, J. J. L. Leazer, R. J. Linderman, K. Lorenz, J. Manley, B. A. Pearlman, A. Wells, A. Zaks and T. Y. Zhang, *Green Chem.*, 2007, **9**, 411-420.

33.   L. Chen, M. Regan and J. Mack, *ACS Catal.*, 2016, **6**, 868-872.

34.   I. A. Tumanov, A. A. L. Michalchuk, A. A. Politov, E. V. Boldyreva and V. V. Boldyrev, *Doklady Chemistry*, 2017, **472**, 17-19.

35.   a) I. Halasz, T. Friscic, S. A. Kimber, K. Uzarevic, A. Puskaric, C. Mottillo, P. Julien, V. Strukil, V. Honkimaki and R. E. Dinnebier, *Faraday Discuss.*, 2014, **170**, 203-221; b) A. D. Katsenis, A. Puskaric, V. Strukil, C. Mottillo, P. A. Julien, K. Uzarevic, M. H. Pham, T. O. Do, S. A. Kimber, P. Lazic, O. Magdysyuk, R. E. Dinnebier, I. Halasz and T. Friscic, *Nat. Commun.*, 2015, **6**, 6662.

36.   H. Kulla, M. Wilke, F. Fischer, M. Rollig, C. Maierhofer and F. Emmerling, *Chem. Commun.*, 2017, **53**, 1664-1667.

37.   S. Lukin, M. Tireli, T. Stolar, D. Barisic, M. V. Blanco, M. di Michiel, K. Uzarevic and I. Halasz, *J. Am. Chem. Soc.*, 2019, **141**, 1212-1216.

38.   K. J. Ardila-Fierro, S. Lukin, M. Etter, K. Uzarevic, I. Halasz, C. Bolm and J. G. Hernandez, *Angew. Chem. Int. Ed.*, 2020, **59**, 13458-13462.

39.   a) I. Solala, U. Henniges, K. F. Pirker, T. Rosenau, A. Potthast and T. Vuorinen, *Cellulose*, 2015, **22**, 3217-3224; b) T. Shanmugasundaram, J. Guyon, J. P. Monchoux, A. Hazotte and E. Bouzy, *Intermetallics*, 2015, **66**, 141-148; c) M. Haas, S. Lamour, S. B. Christ and O. Trapp, *Communications Chemistry*, 2020, **3**.

40.   J. Andersen and J. Mack, *Angew. Chem. Int. Ed.*, 2018, **57**, 13062-13065.

41.   T. Seo, N. Toyoshima, K. Kubota and H. Ito, *J. Am. Chem. Soc.*, 2021, **143**, 6165-6175.

42.   S. Gratz, D. Beyer, V. Tkachova, S. Hellmann, R. Berger, X. Feng and L. Borchardt, *Chem. Commun.*, 2018, **54**, 5307-5310.

43.   S. Grätz, M. Oltermann, C. G. Vogt and L. Borchardt, *ACS Sustain. Chem. Eng.*, 2020, **8**, 7569-7573.

44.   a) M. Grzybowski, K. Skonieczny, H. Butenschon and D. T. Gryko, *Angew. Chem. Int. Ed.*, 2013, **52**, 9900-9930; b) A. Narita, X. Y. Wang, X. Feng and K. Mullen, *Chem. Soc. Rev.*, 2015, **44**, 6616-6643.

45.   T. Seo, T. Ishiyama, K. Kubota and H. Ito, *Chem. Sci.*, 2019, **10**, 8202-8210.

46. A. Stolle and B. Ranu, *Ball Milling Towards Green Synthesis: Applications, Projects, Challenges*, Royal Society of Chemistry, 2014.

47. M. Ferguson, N. Giri, X. Huang, D. Apperley and S. L. James, *Green Chem.*, 2014, **16**, 1374-1382.

48. D. E. Crawford, C. K. Miskimmin, J. Cahir and S. L. James, *Chem. Commun.*, 2017, **53**, 13067-13070.

49. J. Yu, Z. Li, K. Jia, Z. Jiang, M. Liu and W. Su, *Tetrahedron Lett.*, 2013, **54**, 2006-2009.

50. Z. Li, P. D. MacLeod and C.-J. Li, *Tetrahedron: Asymmetry*, 2006, **17**, 590-597.

51. G. N. Hermann, M. T. Unruh, S. H. Jung, M. Krings and C. Bolm, *Angew. Chem. Int. Ed.*, 2018, **57**, 10723-10727.

52. a) E. J. Barreiro, A. E. KüMmerle and C. A. M. Fraga, *Chem. Rev.*, 2011, **111**, 5215-5246; b) H. Schönherr and T. Cernak, *Angew. Chem. Int. Ed.*, 2013, **52**, 12256-12267.

53. D. Aynetdinova, M. C. Callens, H. B. Hicks, C. Y. X. Poh, B. D. A. Shennan, A. M. Boyd, Z. H. Lim, J. A. Leitch and D. J. Dixon, *Chem. Soc. Rev.*, 2021, **50**, 5517-5563.

54. S. Ni, M. Hribersek, S. K. Baddigam, F. J. L. Ingner, A. Orthaber, P. J. Gates and L. T. Pilarski, *Angew. Chem. Int. Ed.*, 2021, **60**, 6660-6666.

55. L. A. Polindara-García and E. Juaristi, *Eur. J. Org. Chem.*, 2016, **2016**, 1095-1102.

56. a) L. El Kaim, M. Gizolme and L. Grimaud, *Synlett*, 2007, **2007**, 0227-0230; b) P. Pramitha and D. Bahulayan, *Bioorg. Med. Chem. Lett.*, 2012, **22**, 2598-2603.

57. M. Ali El-Remaily, A. M. M. Soliman and O. M. Elhady, *ACS Omega*, 2020, **5**, 6194-6198.

58. A. Beillard, T. X. Metro, X. Bantreil, J. Martinez and F. Lamaty, *Chem. Sci.*, 2017, **8**, 1086-1089.

59. B. Liu, Q. Xia and W. Chen, *Angew. Chem. Int. Ed.*, 2009, **48**, 5513-5516.

60. F. Lazreg, F. Nahra and C. S. J. Cazin, *Coord. Chem. Rev.*, 2015, **293-294**, 48-79.

61. a) C. J. Li and B. M. Trost, *PNAS*, 2008, **105**, 13197-13202; b) W. Zhang and B. W. Cue, *Green Techniques for Organic Synthesis and Medicinal Chemistry*, Wiley, 2012.

62. C. Espro and D. Rodríguez-Padrón, *Curr. Opin. Green Sustain. Chem.*, 2021, **30**, 100478.

63. V. Canale, V. Frisi, X. Bantreil, F. Lamaty and P. Zajdel, *J. Org. Chem.*, 2020, **85**, 10958-10965.

64. a) P. Zajdel, V. Canale, A. Partyka, K. Marciniec, R. Kurczab, G. Satała, A. Siwek, M. Jastrzębska-Więsek, A. Wesołowska, T. Kos, P. Popik and A. J. Bojarski, *Med. Chem. Comm.*, 2015, **6**, 1272-1277; b) V. Canale, R. Kurczab, A. Partyka, G. Satała, K. Słoczyńska, T. Kos, M. Jastrzębska-Więsek, A. Siwek, E. Pękala, A. J. Bojarski, A. Wesołowska, P. Popik and P. Zajdel, *Biorg. Med. Chem.*, 2016, **24**, 130-139.

65. D. E. Crawford, A. Porcheddu, A. S. McCalmont, F. Delogu, S. L. James and E. Colacino, *ACS Sustain. Chem. Eng.*, 2020, **8**, 12230-12238.

66. M. Baumann, T. S. Moody, M. Smyth and S. Wharry, *Org. Process Res. Dev.*, 2020, **24**, 1802-1813.

67. X. Lu, Y. Bai, J. Qin, N. Wang, Y. Wu and F. Zhong, *ACS Sustain. Chem. Eng.*, 2021, **9**, 1684-1691.

68. a) G. Li, A. K. Dilger, P. T. Cheng, W. R. Ewing and J. T. Groves, *Angew. Chem. Int. Ed.*, 2018, **57**, 1251-1255; b) D. Ravelli, M. Fagnoni, T. Fukuyama, T. Nishikawa and I. Ryu, *ACS Catal.*, 2018, **8**, 701-713.

69. A. Malik and E. Grohmann, *Environmental Protection Strategies for Sustainable Development*, Springer Netherlands, 2011.

70.   Q. Cao, D. E. Crawford, C. Shi and S. L. James, *Angew. Chem. Int. Ed.*, 2020, **59**, 4478-4483.

71.   a) F. M. Eissa and N. Salah-Eldeen Mohamed, *Journal of Chemical Engineering & Process Technology*, 2018, **09**; b) B. M. Sharma, R. S. Atapalkar and A. A. Kulkarni, *Green Chem.*, 2019, **21**, 5639-5646; c) L. P. Jameson and S. V. Dzyuba, *Beilstein J. Org. Chem.*, 2013, **9**, 786-790; d) M. Pérez-Venegas, T. Arbeloa, J. Bañuelos, I. López-Arbeloa, N. E. Lozoya-Pérez, B. Franco, H. M. Mora-Montes, J. L. Belmonte-Vázquez, C. I. Bautista-Hernández, E. Peña-Cabrera and E. Juaristi, *Eur. J. Org. Chem.*, 2021, **2021**, 253-265.

72.   S. K. Rodrigo, I. V. Powell, M. G. Coleman, J. A. Krause and H. Guan, *Org. Biomol. Chem.*, 2013, **11**, 7653.

73.   R. A. Haley, A. R. Zellner, J. A. Krause, H. Guan and J. Mack, *ACS Sustain. Chem. Eng.*, 2016, **4**, 2464-2469.

74.   a) M. Turberg, K. J. Ardila-Fierro, C. Bolm and J. G. Hernandez, *Angew. Chem. Int. Ed.*, 2018, **57**, 10718-10722; b) K. J. Ardila-Fierro, C. Bolm and J. G. Hernandez, *Angew. Chem. Int. Ed.*, 2019, **58**, 12945-12949.

75.   a) Z. Li, Z. Jiang and W. Su, *Green Chem.*, 2015, **17**, 2330-2334; b) B. M. Trost and C. J. Li, *Modern Alkyne Chemistry: Catalytic and Atom-Economic Transformations*, Wiley, 2015; c) V. A. Peshkov, O. P. Pereshivko and E. V. Van Der Eycken, *Chem. Soc. Rev.*, 2012, **41**, 3790.

76.   Z. Lin, D. Yu, Y. N. Sum and Y. Zhang, *ChemSusChem*, 2012, **5**, 625-628.

77.   a) J. M. González-Domínguez, V. León, M. I. Lucío, M. Prato and E. Vázquez, *Nat. Protoc.*, 2018, **13**, 495-506; b) V. J. González, A. M. Rodríguez, V. León, J. Frontiñán-Rubio, J. L. G. Fierro, M. Durán-Prado, A. B. Muñoz-García, M. Pavone and E. Vázquez, *Green Chem.*, 2018, **20**, 3581-3592; c) G.-W. Wang, K. Komatsu, Y. Murata and M. Shiro, *Nature*, 1997, **387**, 583-586.

78.   a) D. Wendinger and R. R. Tykwinski, *Acc. Chem. Res.*, 2017, **50**, 1468-1479; b) J. A. Januszewski and R. R. Tykwinski, *Chem. Soc. Rev.*, 2014, **43**, 3184-3203; c) L. Leroyer, V. Maraval and R. Chauvin, *Chem. Rev.*, 2012, **112**, 1310-1343.

79.   a) J. G. Chen, R. M. Crooks, L. C. Seefeldt, K. L. Bren, R. M. Bullock, M. Y. Darensbourg, P. L. Holland, B. Hoffman, M. J. Janik, A. K. Jones, M. G. Kanatzidis, P. King, K. M. Lancaster, S. V. Lymar, P. Pfromm, W. F. Schneider and R. R. Schrock, *Science*, 2018, **360**, eaar6611; b) R. L. Myers, *The 100 Most Important Chemical Compounds: A Reference Guide*, Greenwood Press, 2007.

80.   a) L. E. Apodaca, NITROGEN (FIXED)—AMMONIA, https://prd-wret.s3-us-west-2.amazonaws.com/assets/palladium/production/atoms/files/mcs-2019-nitro.pdf, (accessed 20/05/2021, 2021); b) M. Appl, *Ammonia: Principles and Industrial Practice*, Wiley, 2020; c) S. L. Foster, S. I. P. Bakovic, R. D. Duda, S. Maheshwari, R. D. Milton, S. D. Minteer, M. J. Janik, J. N. Renner and L. F. Greenlee, *Nat. Catal.*, 2018, **1**, 490-500; d) Y. Gong, J. Wu, M. Kitano, J. Wang, T.-N. Ye, J. Li, Y. Kobayashi, K. Kishida, H. Abe, Y. Niwa, H. Yang, T. Tada and H. Hosono, *Nat. Catal.*, 2018, **1**, 178-185.

81.   G. F. Han, F. Li, Z. W. Chen, C. Coppex, S. J. Kim, H. J. Noh, Z. Fu, Y. Lu, C. V. Singh, S. Siahrostami, Q. Jiang and J. B. Baek, *Nat. Nanotechnol.*, 2021, **16**, 325-330.

82.   M. Capdevila-Cortada, *Nat. Catal.*, 2019, **2**, 1055-1055.

83.   V. P. Balema, J. W. Wiench, M. Pruski and V. K. Pecharsky, *J. Am. Chem. Soc.*, 2002, **124**, 6244-6245.

84.   a) in *Phosphorus Ylides*, 1999, DOI: https://doi.org/10.1002/9783527613908.ch01, pp. 1-8; b) A. W. Johnson, W. C. Kaska, K. A. O. Starzewski, D. A. Dixon, J. Wiley and Sons, *Ylides and Imines of Phosphorus*, Wiley, 1993.

85.   a) G. Wittig and U. Schöllkopf, *Chem. Ber.*, 1954, **87**, 1318-1330; b) in *Phosphorus Ylides*, 1999, DOI: https://doi.org/10.1002/9783527613908.ch06, pp. 359-538.

86. K.-H. Gaudry, D. Charro and A. Shaban, *Data in Brief*, 2020, **31**, 106019.
87. F. Puccetti, C. Schumacher, H. Wotruba, J. G. Hernández and C. Bolm, *ACS Sustain. Chem. Eng.*, 2020, **8**, 7262-7266.
88. a) V. P. McCaffrey, N. E. B. Zellner, C. M. Waun, E. R. Bennett and E. K. Earl, *Orig. Life. Evol. Biosph.*, 2014, **44**, 29-42; b) Y. Furukawa, Y. Chikaraishi, N. Ohkouchi, N. O. Ogawa, D. P. Glavin, J. P. Dworkin, C. Abe and T. Nakamura, *PNAS*, 2019, **116**, 24440-24445.
89. C. Bolm, R. Mocci, C. Schumacher, M. Turberg, F. Puccetti and J. G. Hernandez, *Angew. Chem. Int. Ed.*, 2018, **57**, 2423-2426.
90. K. Kubota, Y. Pang, A. Miura and H. Ito, *Science*, 2019, **366**, 1500-1504.
91. D. L. Browne and J. A. Leitch, *Chem. Eur. J.*, 2021, DOI: 10.1002/chem.202100348.
92. Y. Pang, J. W. Lee, K. Kubota and H. Ito, *Angew. Chem. Int. Ed.*, 2020, **59**, 22570-22576.
93. C. Schumacher, J. G. Hernandez and C. Bolm, *Angew. Chem. Int. Ed.*, 2020, **59**, 16357-16360.
94. S. Durr, M. Muller, H. Jorschick, M. Helmin, A. Bosmann, R. Palkovits and P. Wasserscheid, *ChemSusChem*, 2017, **10**, 42-47.
95. Y. Sawama, N. Yasukawa, K. Ban, R. Goto, M. Niikawa, Y. Monguchi, M. Itoh and H. Sajiki, *Org. Lett.*, 2018, **20**, 2892-2896.
96. a) A. M. Belenguer, G. I. Lampronti, D. J. Wales and J. K. Sanders, *J. Am. Chem. Soc.*, 2014, **136**, 16156-16166; b) A. M. Belenguer, A. A. L. Michalchuk, G. I. Lampronti and J. K. M. Sanders, *Beilstein J. Org. Chem.*, 2019, **15**, 1226-1235.
97. I. P. Beletskaya and A. V. Cheprakov, *Chem. Rev.*, 2000, **100**, 3009-3066.
98. K. Y. Jia, J. B. Yu, Z. J. Jiang and W. K. Su, *J. Org. Chem.*, 2016, **81**, 6049-6055.
99. a) J. F. Briones and H. M. L. Davies, *Org. Lett.*, 2011, **13**, 3984-3987; b) R. Chinchilla and C. Nájera, *Chem. Rev.*, 2007, **107**, 874-922.
100. L. Chen, D. Leslie, M. G. Coleman and J. Mack, *Chem. Sci.*, 2018, **9**, 4650-4661.
101. R. Dorel, C. P. Grugel and A. M. Haydl, *Angew. Chem. Int. Ed.*, 2019, **58**, 17118-17129.

2   Robust Buchwald-Hartwig Amination *via* Ball Milling

2.1 Introduction to C(sp^2)-N Bond Formation

During the last 25 years the Buchwald-Hartwig amination has become a core method for the formation of C(sp^2)-N bonds.[1] The effectiveness of this and other transformations has led to heteroatom alkylation and arylation reactions making up 23% of all steps in the production of pharmaceuticals. Furthermore, the formation of C(sp^2)-N bonds make up 27% of these reactions.[2] This makes the formation of aryl C-N bonds among the most common steps in drug discovery.[3] The synthesis of C(sp^2)-N bonds is also commonplace for the synthesis of natural products, agrochemicals, and compounds studied in material science (Scheme 2.01).[4] The ubiquity of this transformation has prompted development of improved catalyst systems and advancement of reaction conditions.
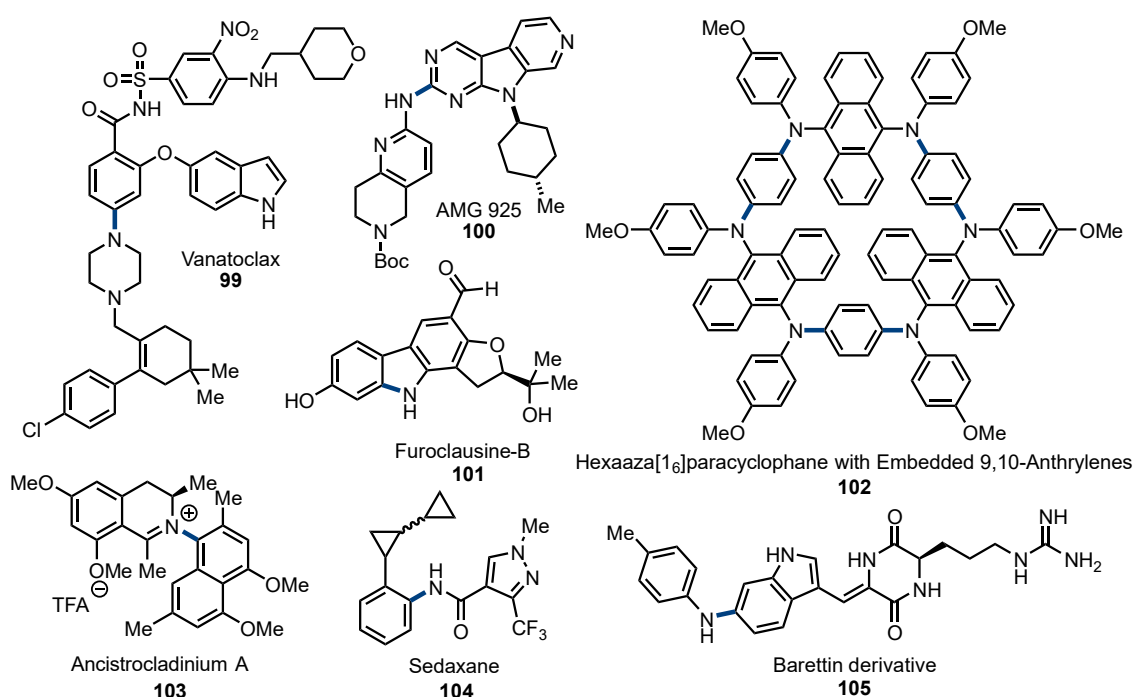
Scheme 2.01 Examples of pharmaceuticals, natural products, and aromatic macrocycles synthesized using the Buchwald-Hartwig reaction.

2.1.1 Synthesis of Aryl C-N Bonds

Some of the most common methods for the synthesis of C(sp^2)-N bonds include S$_N$Ar reactions (Scheme 2.2a), nitration followed by reduction (Scheme 2.2b), and cross-coupling reactions (Scheme 2.2c). Even though S$_N$Ar reactions are a powerful transformation they often require activated starting materials such as electron deficient aromatic systems. This necessity for activated starting materials reduces the scope of

this transformation.[5] Nitration reactions can be highly exothermic requiring the need for precise temperature control to prevent over-reaction. Furthermore, they can suffer from poor regioselectivity, and minimal functional group tolerance.[6] The desired product then requires further reduction for the synthesis of aryl amine derivatives. This multi-step process and challenging conditions often resulting in poor yields can prevent its successful implementation in target synthesis. The use of coupling reactions between aryl halides or boronic acids and amines with transition metal catalysts can provide a high yielding alternative synthesis method. The most common coupling reactions used to achieve $C(sp^2)$-N bond formation are the Ullman, the Chan-Evans-Lam and the Buchwald-Hartwig couplings. The Ullman reaction is unfortunately often limited to aryl iodides and the requirement for high copper catalyst loading limiting its applications, though significant efforts have been made to improve on these drawbacks.[7] The Chan-Evans-Lam coupling can either be carried out with stoichiometric copper(II) or catalytic copper(II) with the addition of a primary oxidant, or using oxygen from the air.[8] Exploring the mechanism of this transformation has allowed for an expanded range of application of this coupling reaction although it still suffers from similar drawbacks as the Ullman coupling. Whereas the palladium catalysed Buchwald-Hartwig coupling has been found to be highly selective with superior functional group tolerance and is regularly carried out with low catalyst loadings on a range of halides and pseudo-halides.[1a]
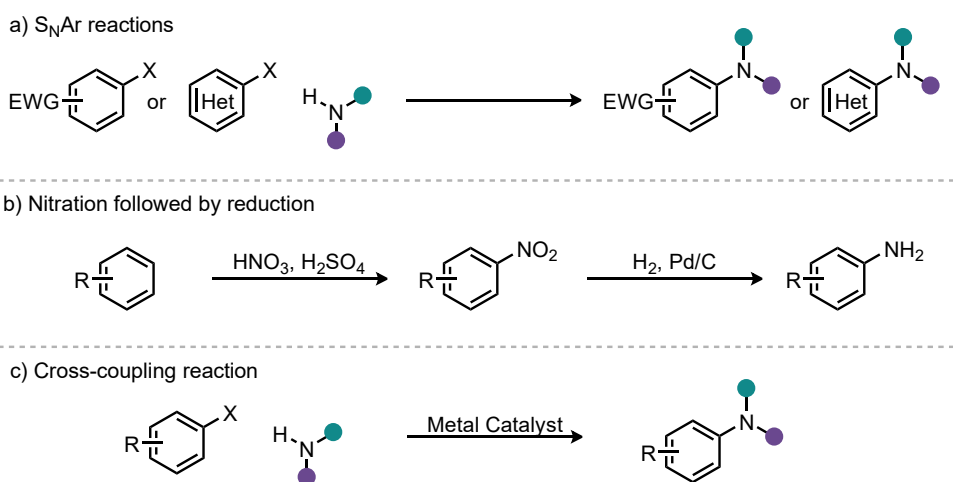
Scheme 2.02 Common methods for the synthesis of $C(sp^2)$-N bonds.

2.1.2 The Buchwald-Hartwig Reaction

Migita and coworkers discovered the first palladium catalysed C-N bond formation utilizing aminostannane **106** and bromobenzene **107** in a reaction that resembles a Stille coupling (Scheme 2.03).[9] This initial report was minimal in scope (10 examples) but represents the starting point for the development of this now widely utilized transformation.
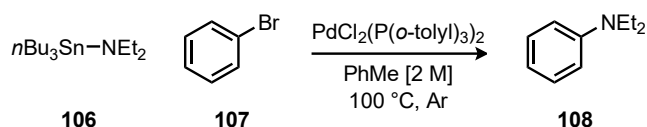
Scheme 2.03 Initial conditions discovered by Migita and coworkers.

The work of Buchwald and coworkers on the development of palladium catalysed amination reactions focused on the rational development of new phosphine-based ligand systems that initially allowed the tin amides to be substituted for free amines.[10] Their continued research programme has allowed for a broad scope of applicable substrates expanding the utility of the reaction. This included expanding the range of halides which could be successfully coupled from iodides and bromides to include chlorides and sulfonates. The series of catalyst systems developed have also been applied to other cross-coupling reactions and the use of Buchwald ligands is still commonplace in transformations reported in the literature.

Simultaneously Hartwig and coworkers have also made significant efforts into the development and understanding of this reaction, developing extensive mechanistic insight of the transformation.[11] This was achieved through isolation of [Pd^0(P(o-tolyl)$_3$)$_2$] which was could then be used in stoichiometric studies with aryl bromides for the isolation of catalytic intermediates. This work has produced the now accepted mechanism similar to that of other palladium catalysed cross-coupling reactions (Scheme 2.04). Initially a low valent palladium(0) (**i**) species undergoes oxidative addition of an aryl halide producing the palladium(II) intermediate (**ii**) which can then be attacked by the amine. The initial amido palladiu(II) complex (**iii**) can be deprotonated by the base present followed by de-coordination of the halide. The final palladium(II) amido complex (**iv**) can then reductively eliminate the aryl amine product and return the catalyst to its initial palladium(0) oxidation state.
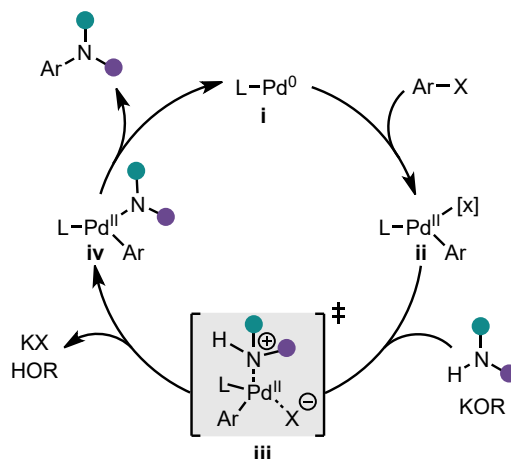
Scheme 2.04 Buchwald-Hartwig catalytic cycle.

Research into the improvement of cross-coupling reactions to lower catalyst loadings and expand the range of applicable substrates is ongoing.[12] Such developments include alternate ligands such as NHCs.[12b] Initially work in this area was under the assumption that the NHC ligands could simply be used as phosphine mimics due to their similar bonding interactions with palladium.[13] Both phosphine and NHC ligands are neutral 2 electron σ-donors creating electron rich palladium catalysts. This strong σ-donation produces much stronger bonds between the palladium and the NHC ligand than that of even the most electron rich phosphine ligands.[14] Furthermore, NHC ligands are able to increase their bond strength through π-backbonding from the metal and π-donation to the metal, with these π-interactions contributing to between 15 – 20% of the total bonding interaction.[15] However, the extent of these π-interactions for NHC ligands has been disputed.[16]

The steric properties of phosphine ligands have been well defined by their cone angle; it is widely understood that altering the size of substituents impacts the cone angle and in turn can impact the number of ligands coordination mode and catalyst activity.[17] Studies into the geometry of NHC ligands suggest that the flanking substituents can create a pocket of flexible steric bulk around the metal centre.[18] Thus the amine substituents can be tuned to tailor the size of the ligand without significant alteration to the electronics of the ligand.[19] Whereas for monodentate phosphine ligands the steric and electronic properties cannot be so easily separated as the basicity of the ligand is directly determined by its substituents.[12a]

The most common heterocycle found in NHC ligands is the imidazolium species due to its ease of synthesis and modular design permitting for a range of augmentations for the tailoring of the ligand for specific transformations, although a broad range of other

heterocycles have been explored (Scheme 2.05).[12b, 20] Organ and coworkers have reported a number of palladium NHC pre-catalysts in their PEPPSI (Pyridine Enhanced Pre-catalyst Preparation Stabilization and Initiation) series and demonstrated their use in a range of cross-coupling reactions.[12a, 21] The pre-catalysts, as the acronym suggests, contain a pyridine ligand which assists in the isolation of the palladium NHC complex. Furthermore, the labile nature of the pyridine produces a low valent species in solution enhancing the rate of initiation of the palladium(II) pre-catalyst to the active palladium(0) oxidation state.[19b, 21b] The variation to the ligand system includes the level of saturation of the imidazole ring and its substitution (X = H, Cl, NR_2…) allowing for fine control of the electronics of the system.[12a, 21a] The size of the flanking aryl rings substitution (R = Me, *i*Pr, *i*Pent…) can vary the sterics of the ligand and further substitution of electron rich groups on these rings allow for finer control of the electronics of the system.
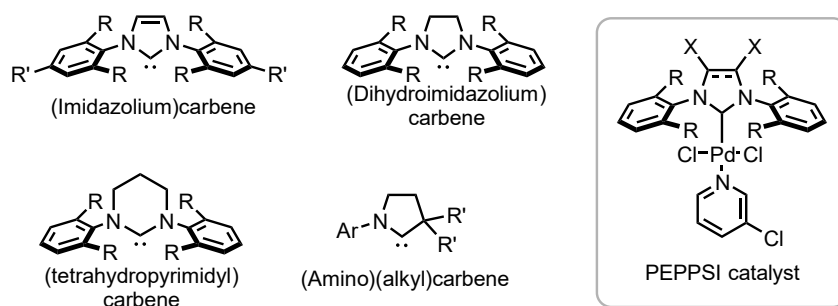
Scheme 2.05 Pd-PEPPSI catalyst developed by Organ and coworkers.

2.2 Development of Cross-Coupling Reactions in Mechanochemistry

The alternate chemical space that can be accessed using mechanochemistry has been applied to a number of cross-coupling reactions. This has enabled a range of possible benefits to these well-known transformations. The Nobel prize winning Suzuki-Miyaura coupling was the first palladium catalysed cross-coupling to be reported with the use of ball milling by Peters and coworkers in 2000 reporting similar yields and slightly reduced reaction times compared to solution (Scheme 2.06a).[22] This versatile and powerful C-C bond forming reaction which is widely used in both academic and industrial settings has since been explored numerous times under ball milling conditions.[23] Proceeding reports of the Suzuki-Miyaura cross-coupling under ball milling conditions improved on the scope of applicable substrates including heteroaromatic chlorides and reduced the catalyst loading.[24] The inclusion of a liquid additive from Su and coworkers produced a profound increase on the rate of the reaction with a small quantity of methanol (Scheme 2.06b). In this work the Suzuki-Miyuara reaction of aryl chlorides and boronic acids could be achieved in only 99 mins whereas in solution this transformation would require up to 16 hours at elevated temperatures.[25] All of these reports were largely limited to liquid aryl halides with only a small number of solid substrates reported throughout. Ito and coworkers contributed to the development of this transformation in 2019 with a procedure for the selective monoarylation of dibromoarenes.[26] The monoarylated product was proposed to undergo an *in situ* crystallization preventing further reaction, producing a highly selective reaction for monoarylation of dibromoarenes which could then be further derivatized in one-pot two-step methodology (Scheme 2.06c).[26] This selective crystallization provided intermediates of reduced reactivity in the solvent free environment providing a selectivity unachievable in solution. Ito and coworkers then expanded on this work, reporting a solid state cross-coupling procedure which could access these solid aryl halides.[27] This new solid-state procedure provided a method for which Stuparu and coworkers could synthesize corannulene-based curved nanographenes **113**, which is challenging in solution due to the product and intermediates poor solubility (Scheme 2.06d).[28] Ball milling in this case allowed facile access to these materials. Finally, Ito and coworkers returned to their developed solid state Suzuki-Miyaura cross-coupling for the functionalization of typically insoluable aryl halides such as nanographenes or pigments, such as the functionalization of Pigment Violet 23 **29** (Scheme 2.06d).[29]
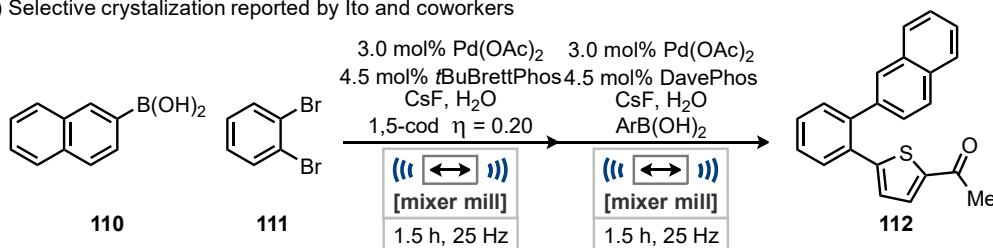
Scheme 2.06 Suzuki-Miyaura cross-coupling development under ball milling conditions.

Other cross-coupling reactions have undergone development under ball milling conditions such as the Mizoroki-Heck reaction. The stereoselective synthesis is of multi-substituted alkenes can often be achieved using this reaction in high yields. Frejd and coworkers initially presented the Mizoroki-Heck reaction under ball milling conditions with protected amino acrylates (Scheme 2.07a) and later expanded the transformation under similar conditions to include unprotected amino acrylates providing direct access to unprotected dehydrophenylalanines.[30] Lamaty and coworkers utilized polyethylene glycol as a grinding additive for the polymer supported Mizoroki-Heck reaction, where the oxygen atoms in the polymer coordinate to the palladium catalyst removing the need for ligands. Nevertheless, this reaction was limited to aryl iodides and a small number of styrene derivatives with most leading to poor yields.[31] Su and coworkers developed a method for a ball milled Mizoroki-Heck reaction where TBAB was used as an additive preventing proto-deholgenation of the starting material **114** (Scheme 2.07b).[32] This

method was successfully applied to the synthesis of E-stilbene derivatives and expanded to 3-bromoindazoles **114** which could be coupled with acrylates.[33] This transformation provided an efficient route to the synthesis of axitinib, a tyrosine kinase inhibitor.[32] Finally, the same group has continued their work in this area towards an oxidative Mizoroki-Heck reaction for the synthesis of alkenylbenzenes from activated and unactivated alkenes **117** and boronic acids (Scheme 2.07c).[34]
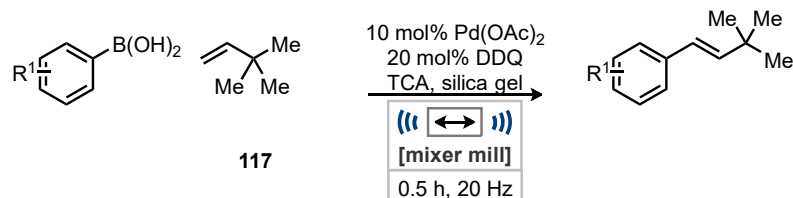
a) Initial report by Frejd and coworkers 2004
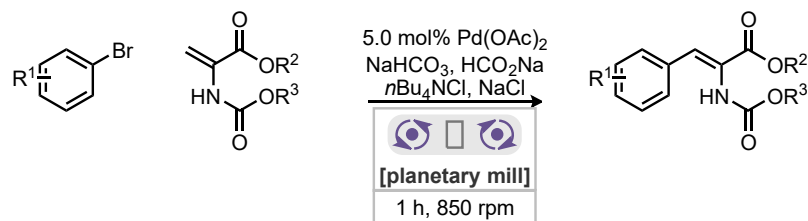
b) Mizoroki-Heck reaction towards the synthesis of axitinib from Su and coworkers 2018
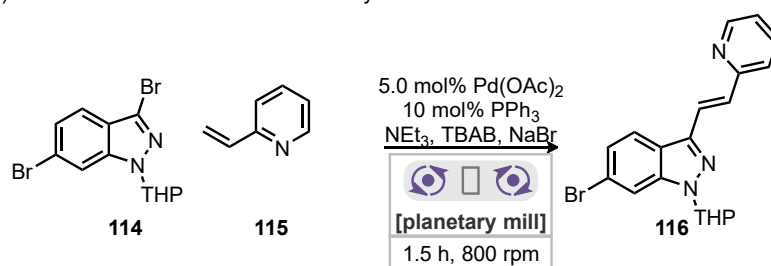
c) Oxidative Mizoroki-Heck reaction

Scheme 2.07 Mizoroki-Heck reaction development under ball milling conditions.

The Sonogashira cross-coupling of terminal alkynes and aryl halides has also been explored under ball milling conditions with a number of advantages over solution reactions presented. Mack and coworkers established the first example of this palladium and copper co-catalysed reaction transferring conditions from solution in 2009 (Scheme 2.08a).[35] The use of copper balls in place of the copper co-catalyst expanded on this transformation in an early example of mechanocatalysis from the Mack group. Soon after, in 2010, Stolle and coworkers introduced a copper and ligand free Sonogoshira reaction under ball milling conditions with DABCO as a base (Scheme 2.08b).[36] Kulkarni and coworkers using the previously established conditions from Stolle and coworkers have developed the first palladium catalysed transformation under continuous extrusion

conditions.[37] With residence times of only 65 to 180 seconds this continuous method for the solvent, ligand, and copper free Sonogashira reaction is extremely fast.

a) Solvent free Sonogashira reaction from Mack and coworkers in 2009

b) Solvent, ligand, and copper free Sonogashira reaction from Stolle and coworkers in 2010
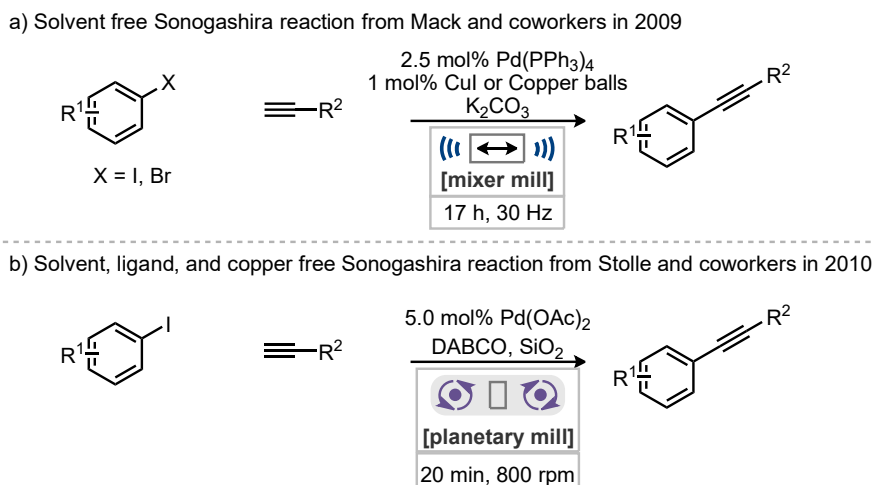
Scheme 2.08 Sonogoshira reaction development under ball milling conditions.

Previous work within the Browne group on mechanochemical cross-coupling reactions focused on the Negishi cross-coupling (Scheme 2.09).[38] In this work, a two-step one-pot approach was applied to the generation of organozinc reagents, followed by palladium catalysed cross-coupling under ball milling conditions without the need for an inert atmosphere (Scheme 2.09a). Furthermore, it was possible to carry out the transformation as a one pot procedure where all reagents for organozinc generation and cross-coupling are present from the start (Scheme 2.09b), which had not been reported prior to this work in solution. This methodology provided a simple procedure for this often-challenging cross-coupling reaction.[39]

a) Two-step one-pot procedure for the mechonchemical Negishi cross-coupling

b) One-pot procedure for the mechonchemical Negishi cross-coupling
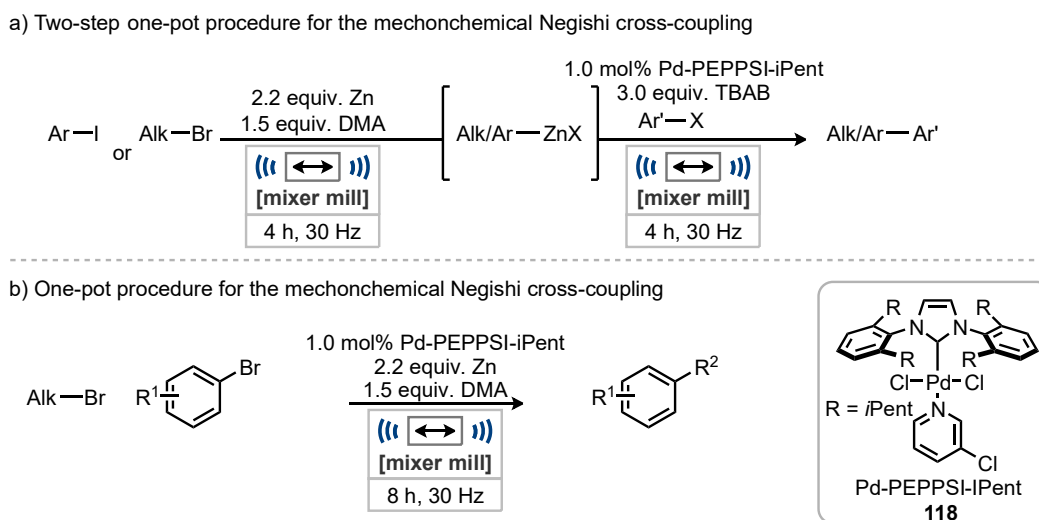
Scheme 2.09 Negishi cross-coupling under ball milling conditions.

2.2.1 Summary, Outlook, and Aims & Objectives

Ball milling has been an effective method for simplifying cross-coupling procedures which often require dry and inert reaction environments free from air and moisture in solution. Often these examples have significantly enhanced reaction rates and reduced catalyst loadings. These benefits potentially provide more convenient procedures to synthesize C-C bonds that are also more sustainable with reduced solvent and catalyst requirements or more easily recycled catalysts. However, cross-coupling procedures generating carbon heteroatom bonds, such as the Buchwald-Hartwig reaction, have yet to be explored under ball milling conditions.

2.3 Buchwald-Hartwig Amination - Results and discussion

This work was carried out as a collaboration between Dr Qun Cao, Andrew C. Jones, and myself. My major contributions focused on the supervision of Andrew C. Jones, an MChem student at the time, and carrying out the various aryl halide examples in the substrate scope. All results obtained by Dr Qun Cao and Andrew C. Jones are clearly indicated in the captions.

Initial investigations into the mechanochemical Buchwald-Hartwig reaction used chlorobenzene **119** and morpholine **120**, as model substrates on a 1 mmol scale with a slight excess of the amine coupling partner, mimicking reported solution reaction conditions.[21c] Potassium *tert*-butoxide was used as the base due to it being amongst the most common bases for solution methods. All ball milling reactions were carried out under an air atmosphere with no efforts made for the exclusion of air or moisture. Finally, two Pd-PEPPSI catalysts developed by Organ and coworkers, which are commercially available, were probed for their activity under ball milling for this reaction.

2.3.1 Initial results
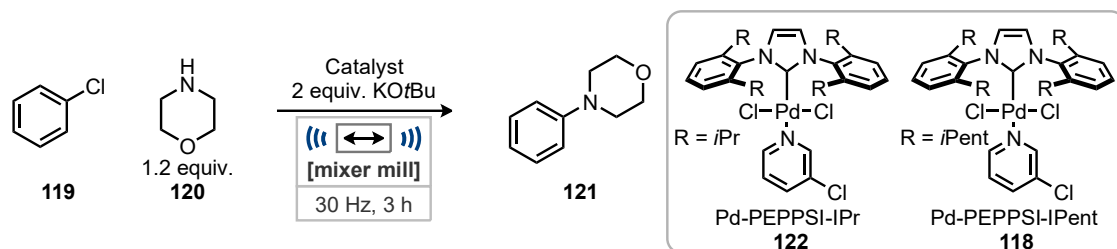
| Entry	Pd-PEPPSI Catalyst	Catalyst loading / mol%	Yield of 121[a] / %
1	IPr **122**	2.0	43
2	IPr **122**	1.0	8
3	IPent **118**	2.0	56
4	IPent **118**	1.0	28

[a] Determined by GC.

Table 2.01 Initial results. Results obtained by Dr Qun Cao.

These initial results for the mechanochemical Buchwald-Hartwig reaction were promising achieving moderate yields of **121** (Table 2.01). The catalyst bearing the larger of the ligands (Table 2.01, entries 3 and 4), IPent, led to greater activity in the reaction likely due to increasing the rate of the reductive elimination step which is often the rate limiting step of cross-coupling reactions.[19b, 40] This catalyst system was carried forward with a loading of 2 mol% due to the good activity observed yielding 56% (Table 2.01, entries 3).

2.3.2 Optimization

With initial conditions showing moderate activity for the reaction, which had been derived from previous reports using solvent, the optimization began for the ball milling variant. The application of different grinding auxiliaries were screened due to the reaction mixture being viscous during the initial results possibly leading to poor mass transfer during the reaction.
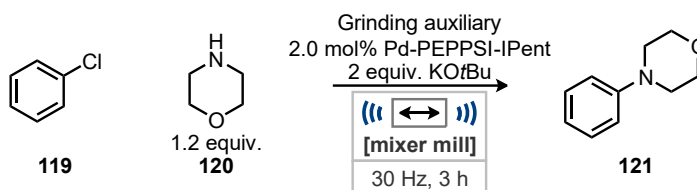
Entry	Grinding auxiliary	Mass equiv.	Yield of **121**[a] / %
1	-	NA	56[b]
2	Silica	3	11
3	MgSO$_4$	3	10
4	NaCl	3	24
5	Celite	3	67
6	Sand	3	82 (75)[c]
7	Sand	0.5	28
8	Sand	1	34
9	Sand	2	59
10	Sand	4	81

[a] Determined by ^{1}H NMR spectroscopy using mesitylene as an internal standard. [b] Determined by GC. [c] Yield of isolated product.

Table 2.02 Grinding auxiliary optimization. Results obtained by Dr Qun Cao and Andrew C. Jones.

Silica and magnesium sulphate both performed very poorly as grinding auxiliary's likely due to both being highly absorbent preventing a free-flowing reaction mixture, in both cases the majority of the reaction mixture was localized on the surface of the ball (Table 2.02, entries 2 and 3). Sodium chloride also performed poorly but did lead to more even distribution of material around the jar (Table 2.02, entry 4). All three of these grinding auxiliaries resulted in decreases in yield than without any present (Table 2.02, entry 1). Fortunately, both celite and sand increased the yield (Table 2.02, entries 5 and 6) from the initial results where a grinding auxiliary was not present (Table 2.02, entry 1). These two additives led to even distribution of the material within the jar and likely the most efficient mass transfer. As sand performed significantly better than celite the optimization continued by changing the quantity of sand added to the reaction.

Varying the amount of sand used caused a profound change in the reaction outcome, which is likely attributable to altering mass transfers in the reaction (Table 2.02, entries 7-9). With low loadings of sand, the reaction mixture became stickier under these conditions, which then led to inferior energy transfer and mixing. Increasing the amount of sand present to 4 mass equivalents had little effect on the yield of the reaction (Table

2.02, entry 10) and as a lower quantity of material in the jar leads to more powerful collisions 3 mass equivalents was caried ahead as optimal.

A range of alternate Pd-PEPPSI catalysts were screened to test their activity.[19b, 21a, c] As under the current conditions Pd-PEPPSI-IPent was achieving a good yield of 82% (Table 2.02, entry 3) the loading of the catalysts was decreased to 1 mol% for the catalyst screen as this lower loading should provide greater discrepancy in catalyst activity.
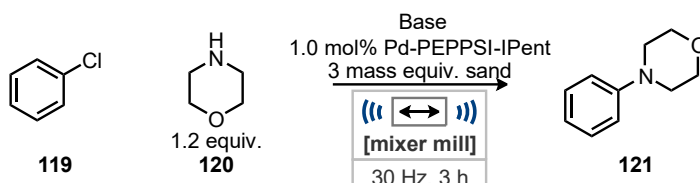
Scheme 2.10 Catalyst screen. Results obtained by Dr Qun Cao and Andrew C. Jones.
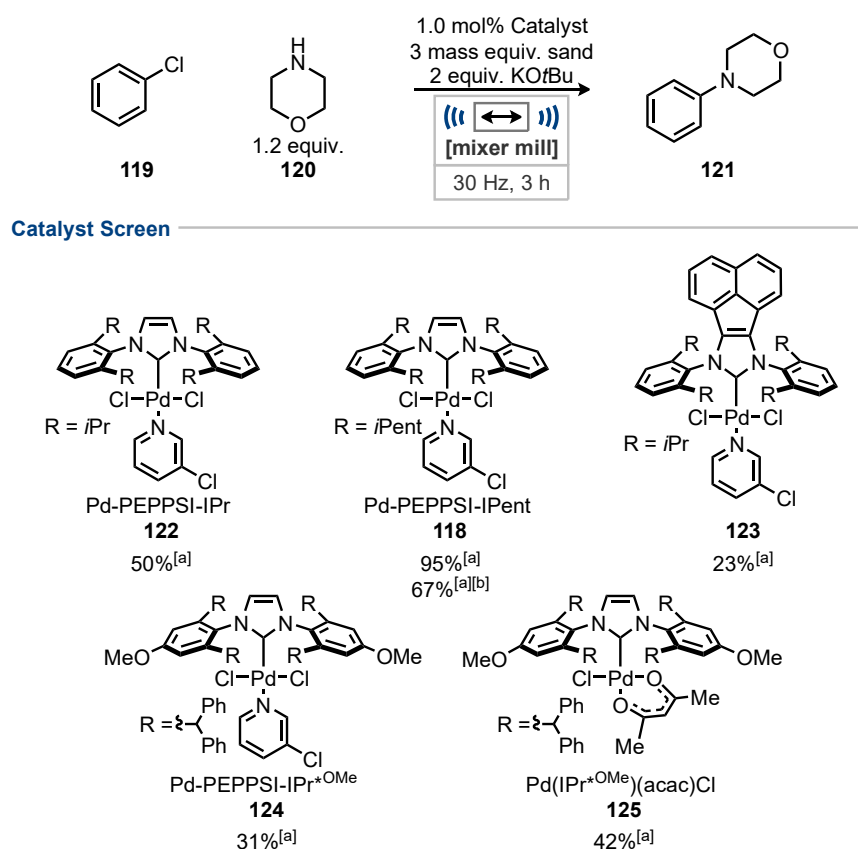
[a] Determined by ^{1}H NMR spectroscopy using mesitylene as an internal standard.
[b] 0.5 mol% catalyst loading.

All the catalysts examined showed some activity for the reaction with a large range of yields achieved. Surprisingly, the decreased loading of Pd-PEPPSI IPent **118** led to a higher yield of 95% (Scheme 2.10) than previously at 2 mol% catalyst loading (82%, Table 2.02, entry 3). The less sterically hindered Ipr **122** was still highly active in the reaction but only lead to a 50% yield showing the benefit of more steric hinderance from the ligand likely aiding the reductive elimination. The more electron rich variant of the Ipr catalyst **123** showed a decrease in activity by more than half which may be due to a slower reductive elimination step. Ipr*^{Ome} **124** which not only being more electron rich with its methoxy substituents but also increased sterics with the biphenyl side groups

also showed lower activity than either the Ipr **122** or Ipent **118** catalysts. The very large size of this ligand it may be inhibiting the oxidative addition step preventing the reaction from taking place. When the labile pyridine ligand and a chloride were replaced with acetylacetate Ipr*[Ome](acac)Cl **125** the catalyst increased in activity possibly due to being more readily activated. It would be possible to make the same adjustment to the Ipent catalyst **118** but due to the system already being a highly active it was continued to be used without modification. When the catalyst loading was further decreased to 0.5 mol% for Pd-PEPPSI-Ipent **118** the yield of the reaction dropped to 67% so this catalyst using 1 mol% was decided as the optimal choice for both catalyst and loading.

The next stage in the optimization was to ensure the optimal base was being used in the reaction. Both the strength and stoichiometry of the base was varied to find the optimal conditions.

Entry	Base (equiv.)	Solution pKa[41]	Yield of **121**[a] / %
1	KO*t*Bu (2.0)	17	95
2	NaO*t*Bu (2.0)	17	52
3	K$_3$PO$_4$ (2.0)	12	8
4	Cs$_2$CO$_3$ (2.0)	10	15
5	K$_2$CO$_3$ (2.0)	10	5
6	KOH (2.0)	15.7	14
7	KO*t*Bu (0.5)	17	17
8	KO*t*Bu (1.0)	17	76
9	KO*t*Bu (3.0)	17	32

[a] Determined by ^{1}H NMR spectroscopy using mesitylene as an internal standard. **Table 2.03** Base optimization. Results obtained by Andrew C. Jones.

Potassium *tert*-butoxide, which is among the most common bases reported for this reaction in solution, was the best performing base for the reaction in the ball mill (Table 2.03, entry 1). The sodium equivalent was also applicable but led to only a moderate yield of 52% (Table 2.03, entry 2). This lower yield may be due to a stronger Na-O ionic bond as sodium is a harder cation. Without the benefit of solvation, the separation of these atoms to release the active base may be more difficult to overcome under the solvent free conditions in a ball milling reaction, whereas in solution these

bases can be more readily exchanged. Weaker bases performed quite poorly in the reaction because of difficulty to deprotonate the amine after coordination to the palladium catalyst preventing the coupling reaction (Table 2.03, entries 3-6). Altering the equivalents of potassium *tert*-butoxide did not improve upon the yield using 2 equivalents (Table 2.03, entries 7 – 9).

Finally, the reaction time was varied to identify if 3 hours were in fact optimal.

Entry	Time / h	Yield of 121[a] / %
1	1	42
2	2	57
3	3	95 (91)[b]
4	4	91

[a] Determined by ^{1}H NMR spectroscopy using mesitylene as an internal standard. [b] Yield of isolated product.

Table 2.04 Reaction time optimization. Results obtained by Andrew C. Jones.

The shortest reaction time of 1 h (Table 2.04, entry 1) showed a rapid onset of the reaction achieving 42%, the rate then slowed reaching only 57% after 2 hours (Table 2.04, entry 2). A further hour of milling again led to a rapid increase in yield jumping to 91% (Table 2.04, entry 3). It is unclear precisely what leads to the variation in rate but unusual sigmoidal rates have been observed previously under ball milling which have been caused by variation in the rheological properties of the reaction mixture.[42] Increasing the reaction time to 4 hours led to a slight decrease in the product yield and with these results 3 hours was taken forward as the optimum reaction time.

2.3.3 Substrate Scope

The conditions optimized thus far for morpholine **120** and chlorobenzene **119** were then taken forward for the substrate scope. Initial variation focused on the aryl halide coupling partner changing the electronics and sterics of the coupling partner as well as the halide leaving group.

1.0 mol% Pd-PEPPSI-IPent
2 equiv. KO*t*Bu
3 mass equiv. sand

[mixer mill]
30 Hz, 3 h

121; 91% X = Cl
75% X = Br
84% X = I

126; 40% X = Cl

127; 70% X = Br

128; 83% X = Br

129; 59% X = Br

130; 65% X = Cl

131; 60% X = Br

132; 32% X = Cl

133; 72% X = Br

134; 52% X = Br

135; 42% X = Br

136; 51% X = Cl
46% X = Br
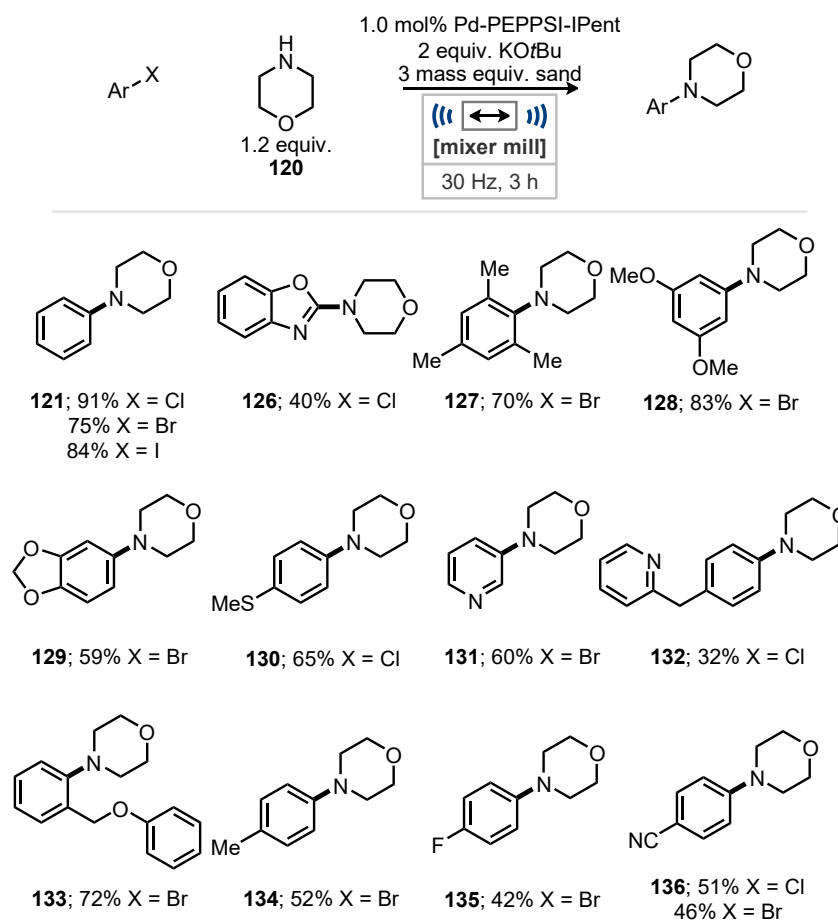
Heteroaryl halides were used as received without purification.

Scheme 2.11 Aryl halide substrate scope.

From the substrate scope of aryl halides (Scheme 2.11) it was shown that chlorides, bromides, and iodides were successful coupling partners for the synthesis of **121**. Especially pleasing was the ability to couple often challenging ortho substituted aryl halides producing **133** and the di-ortho substituted **127** which can be a particularly demanding coupling. Electron rich substrates generally performed well with 1-bromo-3,5-dimethoxybenzene giving a good yield of **128** and 5-bromobenzo[1,3]dioxole gave a moderate yield of **129** likely due to the oxygen atom being para substituted making the carbon which was coupled very electron rich which can slow the rate of oxidative addition.[23b] Electron poor substrates were less successful with both **135** and **136** providing poor yields, although electron deficient heteroaromatics still achieved good yields. This is surprising as generally electron poor substrates perform well in palladium catalysed cross-coupling reactions due to increased rate of oxidative addition with palladium(0). Heterocycles were coupled successfully in the reaction including 2-chloro benzoxazole and 3-bromopyridine which is often a challenging substrate for metal

catalysed reactions due to coordination with the active palladium catalyst leading to suppression of the reaction.

As the product arising from the coupling of 2-chloro benzoxazole **137** may be forged through an S$_N$Ar reaction this substrate was also attempted with Pd-PEPPSI-IPent omitted.
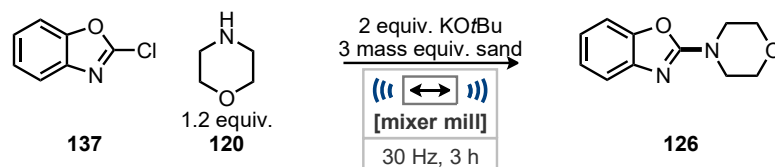
Scheme 2.12 Investigating possible S$_N$Ar mechanism in the formation of **126**.

This control reaction only provided a trace of the product **126** in the reaction mixture confirming that there is very little background S$_N$Ar reaction occurring (Scheme 2.12).

With a range of aryl substituents and electronic factors varied the scope of the reaction was investigated regarding other secondary amines including cyclic and acyclic substrates.

1.0 mol% Pd-PEPPSI-IPent
2 equiv. KO*t*Bu
3 mass equiv. sand

[mixer mill]

30 Hz, 3 h

119   1.2 equiv.

121; 91%   **138**; 81%   **139**; 88%

140; 77%   **141**; 78%   **142**; 72%   **35**; 72%

143; 80%   **144**; 80%   **145**; 68%   **146**; 71%

147; 61%   **148**; 72%   **149**; 60%
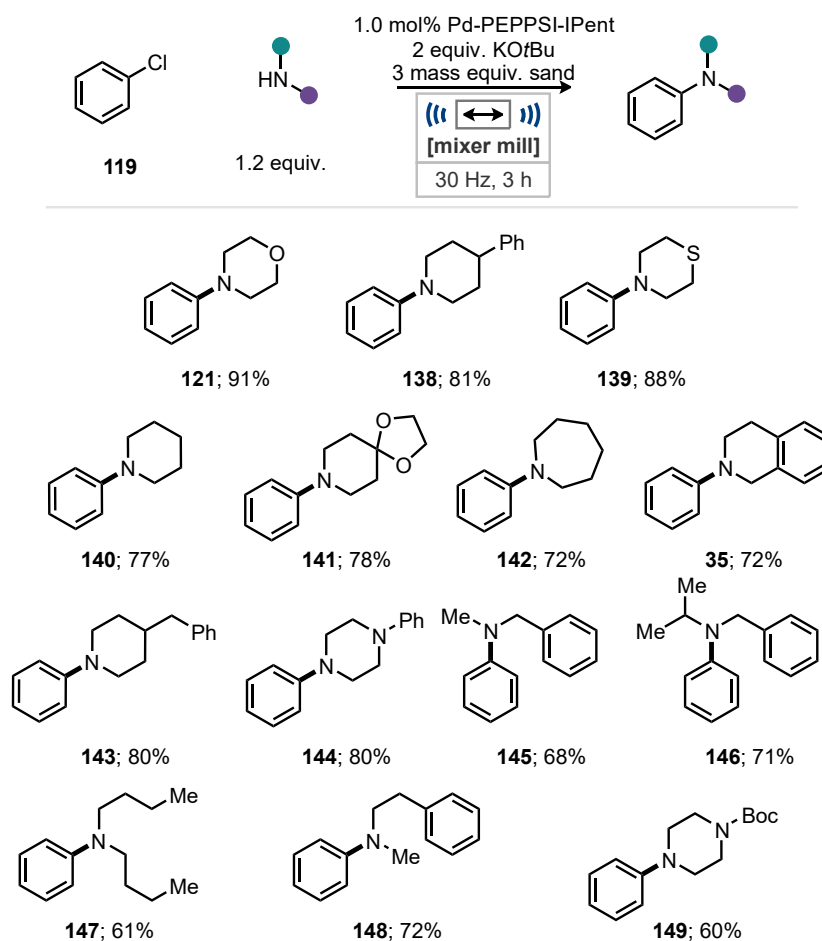
Scheme 2.13 Amine substrate scope. Results obtained by Andrew C. Jones.

The scope of secondary amines (Scheme 2.13) all using chlorobenzene as the coupling partner gave good to excellent yields. Acyclic amines gave marginally lower yields than the cyclic counter parts due to the increased mobility of the side chains which can hinder the nucleophilicity. A range of protecting groups including, Boc, benzyl, and ketal, were tolerated and remained in place during the reaction which paved the way for development of multistep synthesis using this procedure.
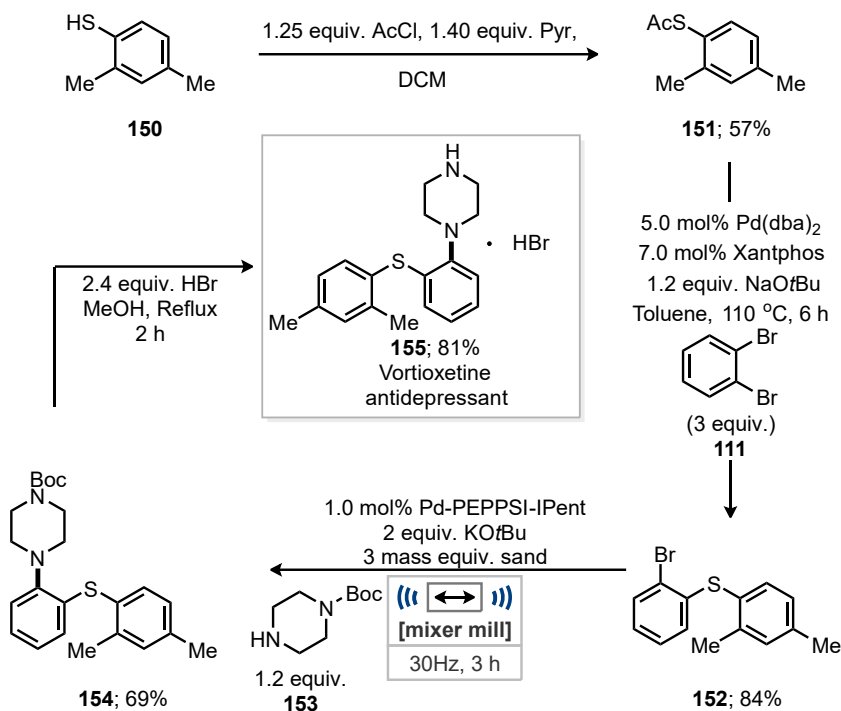
Scheme 2.14 Vortioxetine synthesis. Thanks to Dr Qun Cao for the synthesis of **152**.

With both coupling partners being varied in substrate scopes the conditions that had been developed were applied to the synthesis of Votioxetine **155**, an antidepressant (Scheme 2.13). The initial C-S bond coupling was achieved using a palladium catalysed coupling of thioacetate **151** and 1,2-dibromobenzene **111** in good yield. This was followed with the key C-N coupling step with 1-Boc piperazine **153** which was achieved in good yield to produce Boc protected Vortioxetine **154**. This material was then deprotected using hydrobromic acid to form the active API **155** in good yield.

2.3.4 Investigation of Catalyst Stability Towards Moisture and Air

With the successful application of the reaction to a range of substrates, the focus shifted to understanding why the reaction seemed to be so tolerant to air and moisture. As often when these reactions are performed in solution, dry and even degassed solvent under strictly inert atmospheres are required.[1] The possible reason for this apparent increased tolerance could be due to altering either the rate of the reaction or the rate of catalyst deactivation. Also, it may be possible that the catalyst system is in fact tolerant to air under any conditions, but this had yet to be established. To investigate these possibilities some experiments were carried out using the catalyst under solution conditions in solvents that are common for Buchwald-Hartwig reactions but without the usual protection from air and moisture.

60
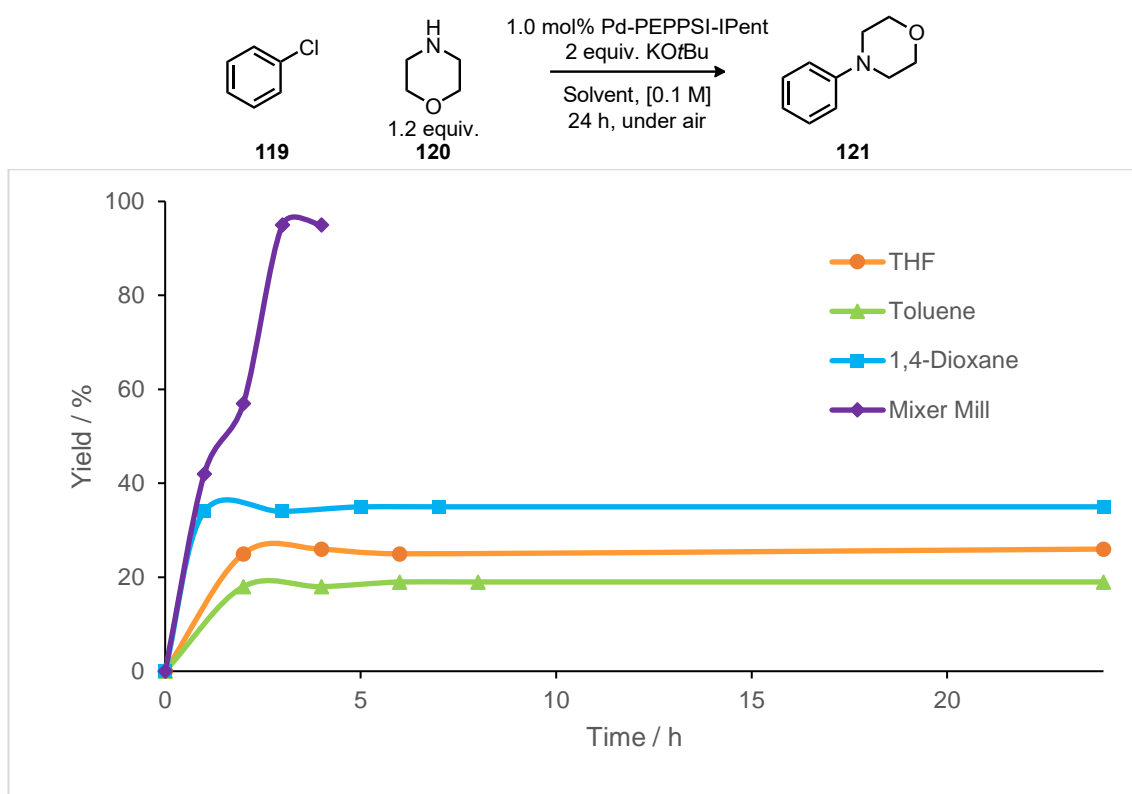
Figure 2.01 Solution comparison under aerobic conditions. Results obtained by Andrew C. Jones.

Under these aerobic conditions the catalyst seemed to completely deactivate in the first 2 hours of the reactions run in solution (Figure 2.01). The more coordinating solvents led to a more active catalyst system but were not able to prevent the catalyst deactivation. While in mechanochemical conditions the reaction is compete soon after the catalyst has deactivated in solution conditions. To further investigate the stability of the catalyst under mechanochemical conditions the loading of the reaction was decreased to 0.2 mol% and the reaction time was increased to 8 hours.
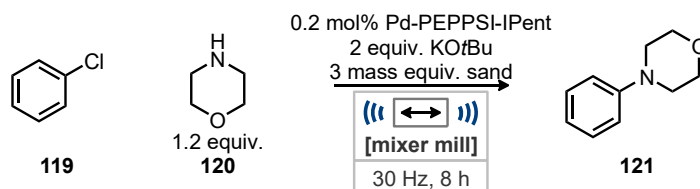
Scheme 2.15 Catalyst stability under mechanochemical conditions testing. Results obtained by Andrew C. Jones.

Under these altered conditions the reaction still achieved a good yield of 80% (Scheme 2.15). This shows the increased stability of the catalyst to moisture and air within the neat ball milling conditions versus solution conditions. If the catalyst were

deactivating under these conditions the reaction would have been expected to produce a significantly lower yield with the reduced catalyst loading and longer reaction times.

2.4   Conclusion of the Buchwald-Hartwig Reaction

Ball milling was successfully applied for the palladium catalysed Buchwald-Hartwig reaction. During optimization the liquid starting materials being used provided a viscous reaction mixture with poor mixing but through the implementation of grinding auxiliaries, mass and energy transfer could be improved. Through further reaction optimization the catalyst loading could be lowered to only 1 mol% with further investigations into the base and its stoichiometry or reaction times providing no additional benefits.

The developed procedure was then applied to a range of substrates. Aryl halides including chlorides, bromides, and iodides could all be effectively coupled in good yields including heteroaromatic examples. Furthermore, electron rich and poor examples produced moderate to good yields as well as sterically demanding examples. Secondary and cyclic amines were also studied in the coupling with chlorobenzene producing good to excellent yields across the board. The reaction was next applied to the synthesis of Vortioxetine the antidepressant providing the Boc protected precursor in good yield.

With the substrate scope established the stability of the catalyst under aerobic ball milling was probed due to the necessity of a protective atmosphere under solution conditions. Solution comparisons showed rapid catalyst deactivation without an inert atmosphere and reduced catalyst loading with prolonged reaction time still provided a high yield for the developed ball milling method showcasing the stability of the catalyst system.

During the substrate scope of aryl halides ethyl 4-chlorobenzoate **156** did not produce the desired coupling product **157** (Scheme 2.16a), although the substrate has previously been reported to be amenable in solution by Organ and coworkers (Scheme 2.16c).[40a] The only product of this reaction was found to be the formation of an amide **158** in moderate yield (Scheme 2.16a). This direct amidation of esters has the potential to be a powerful transformation due to the prevalence of amides in compounds of commercial interest.[43] Previously Szostak and coworkers have demonstrated the amidation of phenyl esters using Pd-PEPPSI-IPr **118** as a catalyst (Scheme 2.16d).[40b] This led to an initial investigation of the amidation reaction without the Pd-PEPPSI-IPent **118** to evaluate if the catalyst was required for the transformation (Scheme 2.16b). This reaction provided

the amide product **158** in almost identical yield to the initial observation. Further investigation into the direct amidation of esters is presented in chapter 3.
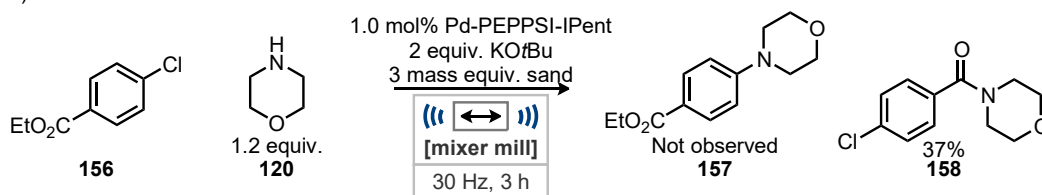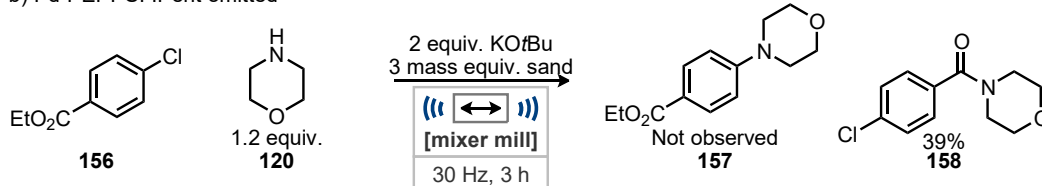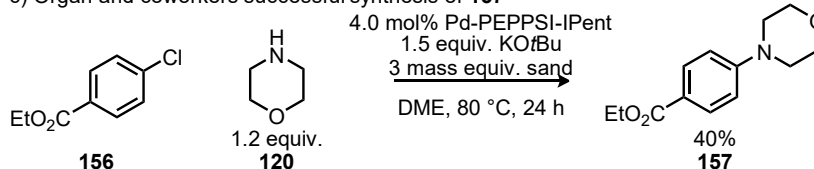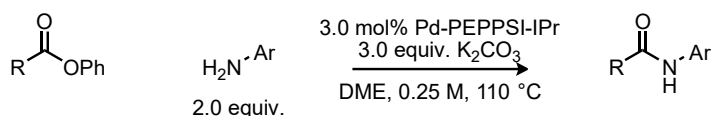

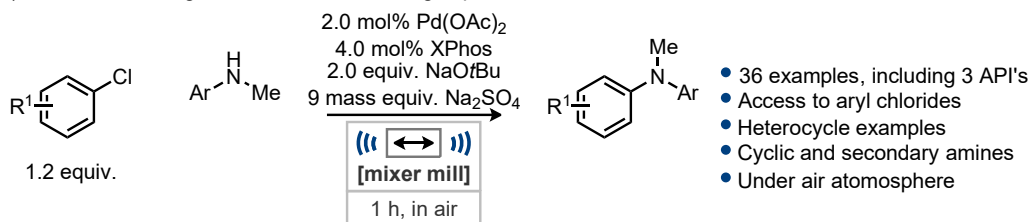**Scheme 2.16** Direct amidation of esters observation.

2.5   Comparison to Other Methods and Further Developments

Shortly prior and following the publication of this work, examples of Buchwald-Hartwig reactions were published using ball milling.[44] The first example of this reaction under ball milling conditions was published by Su and coworkers in 2018 finding similar benefits to the results presented in this thesis forgoing the need for a protective atmosphere and significant rate acceleration (Scheme 2.17a).[45] The developed conditions utilized twice the loading of palladium and employed a phosphine-based ligand, XPhos. They also found significant benefit from the application of a grinding agent finding sodium sulfate as the best choice which also acted as a desiccant reducing the water content of the reaction. As both their substate scope and ours focused on the use of liquid substrates the implementation of the grinding agent provided improved mass and energy transfer

to the reaction mixture. Whereas, Ito and coworkers developed a solid-state Buchwald-Hartwig reaction using ball milling, but required the addition of reagents to the milling jars to be carried out in a glove box (Scheme 2.17c).[46] Furthermore, this coupling required five times the palladium loading than the method developed in this work. Ito and coworkers also opted for a phosphine-based ligand using tri-*tert*-butyl phosphine. It is likely that the glove box was required to prevent the oxidation of this highly electron rich phosphine to the phosphonium oxide in the air preventing it from coordinating to palladium. The scope of the work from Ito and coworkers was restricted to solid starting materials such as poly aromatic bromides and secondary amines bearing multiple aromatic rings. During this work the group also discovered significant rate enhancement with the use of 1,5-cod, as a liquid additive. Using transmission electron microscopy (TEM) the olefin additive was shown to act as a molecular dispersant of the palladium catalyst preventing the formation of nanoparticles in the reaction. The group then went on to further develop this transformation so that the solid-state Buchwald Hartwig reaction could be carried out without the need for the inert atmosphere (Scheme 2.17d).[47] They found by simply exchanging the ligand for the much bulkier tri(1-adamantyl)phosphine, which is known to be air stable, the reaction could be carried out under an air atmosphere. Although the high catalyst loadings are still required for this air tolerant reaction.

a) Buchwald-Hartwig reaction free from inert gas protection from Su and coworkers 2018

2.0 mol% Pd(OAc)$_2$
4.0 mol% XPhos
2.0 equiv. NaO*t*Bu
9 mass equiv. Na$_2$SO$_4$

[mixer mill]

1 h, in air

1.2 equiv.

- 36 examples, including 3 API's
- Access to aryl chlorides
- Heterocycle examples
- Cyclic and secondary amines
- Under air atomosphere

b) This work

1.0 mol% Pd-PEPPSI-IPent
2 equiv. KO*t*Bu
3 mass equiv. sand

[mixer mill]

3 h, in air

X = Cl, Br, I   1.2 equiv.

- 30 examples, including 1 API
- Access to aryl chlorides
- Heterocycle examples
- Cyclic and secondary amines
- Under air atomosphere
- Investigation into air tolerance
- Catalyst loading of only 0.2 mol% possible

c) Olefin accelerated solid state Buchwald-Hartwig reaction from Ito and coworkers 2019

5.0 mol% Pd(OAc)$_2$
5.0 mol% P*t*Bu$_3$
1.5 equiv. NaO*t*Bu
1,5-cod η = 0.20

[mixer mill]

under N$_2$

Ar^1-Br Ar^2-N(H)-Ar^3 Ar^1-N(Ar^2)-Ar^3

- 30 examples, scale up to >2.5 g
- Solid state reaction
- Limited to polyaromatic aryl bromides and amines
- Under N$_2$ atomosphere
- SEM and TEM imaging
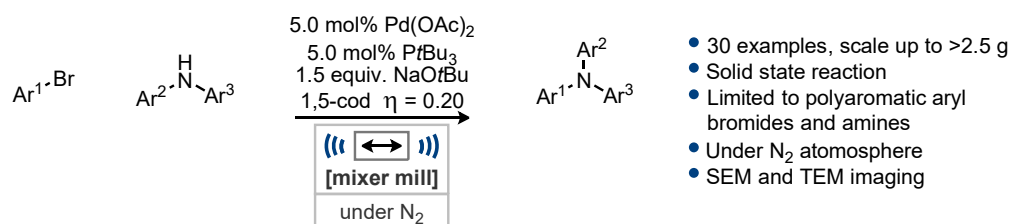
d) Inert atmosphere free solid state Buchwald-Hartwig reaction from Ito and coworkers 2020

5.0 mol% Pd(OAc)$_2$
5.0 mol% PAd$_3$
1.5 equiv. NaO*t*Bu
1,5-cod η = 0.20

[mixer mill]

1.5 h, in air

Ar^1-Br Ar^2-N(H)-Ar^3 Ar^1-N(Ar^2)-Ar^3

- 19 examples, scale up to >1.0 g
- Solid state reaction
- Heterocycle examples
- Limited to polyaromatic aryl bromides and amines
- Under air atomosphere
- Thermography and SEM imaging
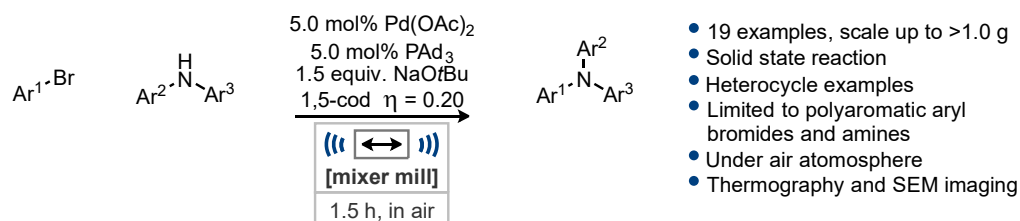
Scheme 2.17 Mechanochemical Buchwald-Hartwig developments.

All of the currently reported methods for the mechanochemical Buchwald-Hartwig reaction have poor yielding or no primary amine examples within their substrate scopes. It may be possible to include these poorer nucleophiles with extended reaction times or by increasing the energy of collisions by the use of a heavier ball.

Possible future developments of this transformation include the application of alternate nucleophiles such as thiols for the synthesis of thioethers. Initial application of the conditions developed for the Buchwald-Hartwig reaction with thiophenol has shown a moderate yield of the thioether product though significant further development is still required (Scheme 2.18).[48]
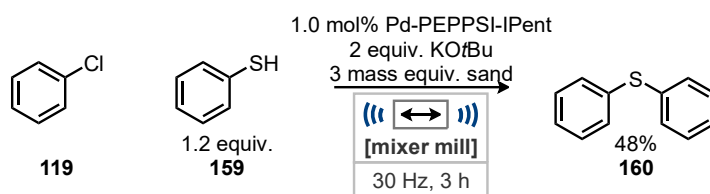
Scheme 2.18 Initial results on mechanochemical Migita cross-coupling.

2.6   Bibliography

1. a) R. Dorel, C. P. Grugel and A. M. Haydl, *Angew. Chem. Int. Ed.*, 2019, **58**, 17118-17129; b) M. M. Heravi, Z. Kheilkordi, V. Zadsirjan, M. Heydari and M. Malmir, *J. Organomet. Chem.*, 2018, **861**, 17-104.
2. S. D. Roughley and A. M. Jordan, *J. Med. Chem.*, 2011, **54**, 3451-3479.
3. a) P. Yaseneva, P. Hodgson, J. Zakrzewski, S. Falß, R. E. Meadows and A. A. Lapkin, *React. Chem. Eng.*, 2016, **1**, 229-238; b) T. W. Cooper, I. B. Campbell and S. J. Macdonald, *Angew. Chem. Int. Ed.*, 2010, **49**, 8082-8091.
4. a) H. Walter, H. Tobler, D. Gribkov and C. Corsi, *CHIMIA International Journal for Chemistry*, 2015, **69**, 425-434; b) Y.-Y. Ku, V. S. Chan, A. Christesen, T. Grieme, M. Mulhern, Y.-M. Pu and M. D. Wendt, *J. Org. Chem.*, 2019, **84**, 4814-4829; c) C. Affouard, R. D. Crockett, K. Diker, R. P. Farrell, G. Gorins, J. R. Huckins and S. Caille, *Org. Process Res. Dev.*, 2015, **19**, 476-485; d) B. Spindler, O. Kataeva and H.-J. Knölker, *J. Org. Chem.*, 2018, **83**, 15136-15143; e) R. Kurata, D. Sakamaki, M. Uebe, M. Kinoshita, T. Iwanaga, T. Matsumoto and A. Ito, *Org. Lett.*, 2017, **19**, 4371-4374; f) Y. J. G. Renault, R. Lynch, E. Marelli, S. V. Sharma, C. Pubill-Ulldemolins, J. A. Sharp, C. Cartmell, P. Cárdenas and R. J. M. Goss, *Chem. Commun.*, 2019, **55**, 13653-13656; g) G. Bringmann, T. Gulder, B. Hertlein, Y. Hemberger and F. Meyer, *J. Am. Chem. Soc.*, 2010, **132**, 1151-1158.
5. S. Rohrbach, A. J. Smith, J. H. Pang, D. L. Poole, T. Tuttle, S. Chiba and J. A. Murphy, *Angew. Chem. Int. Ed.*, 2019, **58**, 16368-16388.
6. B. P. Fors and S. L. Buchwald, *J. Am. Chem. Soc.*, 2009, **131**, 12898-12899.
7. a) F. Monnier and M. Taillefer, *Angew. Chem. Int. Ed.*, 2009, **48**, 6954-6971; b) C. Sambiagio, S. P. Marsden, A. J. Blacker and P. C. McGowan, *Chem. Soc. Rev.*, 2014, **43**, 3525-3550; c) G. Evano, N. Blanchard and M. Toumi, *Chem. Rev.*, 2008, **108**, 3054-3131.
8. M. J. West, J. W. B. Fyfe, J. C. Vantourout and A. J. B. Watson, *Chem. Rev.*, 2019, **119**, 12491-12523.
9. K. Masanori, K. Masayuki and M. Toshihiko, *Chem. Lett.*, 1983, **12**, 927-928.
10. a) A. S. Guram and S. L. Buchwald, *J. Am. Chem. Soc.*, 1994, **116**, 7901-7902; b) J. P. Wolfe and S. L. Buchwald, *Angew. Chem. Int. Ed.*, 1999, **38**, 2413-2416; c) J. P. Wolfe, S. Wagaw, J.-F. Marcoux and S. L. Buchwald, *Acc. Chem. Res.*, 1998, **31**, 805-818.
11. a) J. Hartwig, *Synlett*, 1997, **1997**, 329-340; b) F. Paul, J. Patt and J. F. Hartwig, *J. Am. Chem. Soc.*, 1994, **116**, 5969-5970.
12. a) E. A. Kantchev, C. J. O'Brien and M. G. Organ, *Angew. Chem. Int. Ed.*, 2007, **46**, 2768-2813; b) G. C. Fortman and S. P. Nolan, *Chem. Soc. Rev.*, 2011, **40**, 5151-5169.
13. a) R. H. Crabtree, *J. Organomet. Chem.*, 2005, **690**, 5451-5457; b) N. M. Scott and S. P. Nolan, *Eur. J. Inorg. Chem.*, 2005, **2005**, 1815-1828.
14. a) R. Dorta, E. D. Stevens, N. M. Scott, C. Costabile, L. Cavallo, C. D. Hoff and S. P. Nolan, *J. Am. Chem. Soc.*, 2005, **127**, 2485-2495; b) A. R. Chianese, X. Li, M. C. Janzen, J. W. Faller and R. H. Crabtree, *Organometallics*, 2003, **22**, 1663-1667.
15. H. Jacobsen, A. Correa, A. Poater, C. Costabile and L. Cavallo, *Coord. Chem. Rev.*, 2009, **253**, 687-703.
16. a) J. C. Green, R. G. Scurr, P. L. Arnold and F. Geoffrey N. Cloke, *Chem. Commun.*, 1997, **1997**, 1963-1964; b) J. C. Green and B. J. Herbert, *Dalton Trans.*, 2005, **2005**, 1214-1220.
17. C. A. Tolman, *Chem. Rev.*, 1977, **77**, 313-348.

18. a) A. Gómez-Suárez, D. J. Nelson and S. P. Nolan, *Chem. Commun.*, 2017, **53**, 2650-2660; b) Z. Jin, L.-L. Qiu, Y.-Q. Li, H.-B. Song and J.-X. Fang, *Organometallics*, 2010, **29**, 6578-6586.

19. a) W. A. Herrmann, J. Schütz, G. D. Frey and E. Herdtweck, *Organometallics*, 2006, **25**, 2437-2448; b) C. Valente, S. Calimsiz, K. H. Hoi, D. Mallik, M. Sayah and M. G. Organ, *Angew. Chem. Int. Ed.*, 2012, **51**, 3314-3332.

20. a) O. Schuster, L. Yang, H. G. Raubenheimer and M. Albrecht, *Chem. Rev.*, 2009, **109**, 3445-3478; b) S. K. Schneider, W. A. Herrmann and E. Herdtweck, *J. Mol. Catal. A: Chem.*, 2006, **245**, 248-254.

21. a) K. H. Hoi, J. A. Coggan and M. G. Organ, *Chem. Eur. J.*, 2013, **19**, 843-845; b) C. J. O'Brien, E. A. Kantchev, C. Valente, N. Hadei, G. A. Chass, A. Lough, A. C. Hopkinson and M. G. Organ, *Chem. Eur. J.*, 2006, **12**, 4743-4748; c) M. G. Organ, M. Abdel-Hadi, S. Avola, I. Dubovyk, N. Hadei, E. A. B. Kantchev, C. J. O'Brien, M. Sayah and C. Valente, *Chem. Eur. J.*, 2008, **14**, 2443-2452.

22. S. F. Nielsen, D. Peters and O. Axelsson, *Synth. Commun.*, 2000, **30**, 3501-3509.

23. a) Á. Molnár, *Palladium-Catalyzed Coupling Reactions: Practical Aspects and Future Developments*, Wiley, 2013; b) N. Miyaura and A. Suzuki, *Chem. Rev.*, 1995, **95**, 2457-2483; c) C. C. Johansson Seechurn, M. O. Kitching, T. J. Colacot and V. Snieckus, *Angew. Chem. Int. Ed.*, 2012, **51**, 5062-5085.

24. a) F. Schneider, T. Szuppa, A. Stolle, B. Ondruschka and H. Hopf, *Green Chem.*, 2009, **11**; b) L. M. Klingensmith and N. E. Leadbeater, *Tetrahedron Lett.*, 2003, **44**, 765-768; c) F. Schneider and B. Ondruschka, *ChemSusChem*, 2008, **1**, 622-625; d) G. Cravotto, D. Garella, S. Tagliapietra, A. Stolle, S. Schüßler, S. E. S. Leonhardt and B. Ondruschka, *New J. Chem.*, 2012, **36**; e) F. Schneider, A. Stolle, B. Ondruschka and H. Hopf, *Org. Process Res. Dev.*, 2009, **13**, 44-48.

25. Z. J. Jiang, Z. H. Li, J. B. Yu and W. K. Su, *J. Org. Chem.*, 2016, **81**, 10049-10055.

26. T. Seo, K. Kubota and H. Ito, *J. Am. Chem. Soc.*, 2020, **142**, 9884-9889.

27. T. Seo, T. Ishiyama, K. Kubota and H. Ito, *Chem. Sci.*, 2019, **10**, 8202-8210.

28. G. Bati, D. Csokas, T. Yong, S. M. Tam, R. R. S. Shi, R. D. Webster, I. Papai, F. Garcia and M. C. Stuparu, *Angew. Chem. Int. Ed.*, 2020, **59**, 21620-21626.

29. T. Seo, N. Toyoshima, K. Kubota and H. Ito, *J. Am. Chem. Soc.*, 2021, **143**, 6165-6175.

30. a) E. Tullberg, D. Peters and T. Frejd, *J. Organomet. Chem.*, 2004, **689**, 3778-3781; b) T. Frejd, E. Tullberg, F. Schacher and D. Peters, *Synthesis*, 2006, **2006**, 1183-1189.

31. V. Declerck, E. Colacino, X. Bantreil, J. Martinez and F. Lamaty, *Chem. Commun.*, 2012, **48**, 11778.

32. J. Yu, Z. Hong, X. Yang, Y. Jiang, Z. Jiang and W. Su, *Beilstein J. Org. Chem.*, 2018, **14**, 786-795.

33. X. Zhu, J. Liu, T. Chen and W. Su, *Appl. Organomet. Chem.*, 2012, **26**, 145-147.

34. J. Yu, H. Shou, W. Yu, H. Chen and W. Su, *Adv. Synth. Catal.*, 2019, **361**, 5133-5139.

35. D. A. Fulmer, W. C. Shearouse, S. T. Medonza and J. Mack, *Green Chem.*, 2009, **11**.

36. R. Thorwirth, A. Stolle and B. Ondruschka, *Green Chem.*, 2010, **12**.

37. B. M. Sharma, R. S. Atapalkar and A. A. Kulkarni, *Green Chem.*, 2019, **21**, 5639-5646.

38. Q. Cao, J. L. Howard, E. Wheatley and D. L. Browne, *Angew. Chem. Int. Ed.*, 2018, **57**, 11339-11343.

39. J. Del Pozo, G. Salas, R. Álvarez, J. A. Casares and P. Espinet, *Organometallics*, 2016, **35**, 3604-3611.

40. a) C. Valente, M. Pompeo, M. Sayah and M. G. Organ, *Org. Process Res. Dev.*, 2014, **18**, 180-190; b) S. Shi and M. Szostak, *Chem. Commun.*, 2017, **53**, 10584-10587.

68

41.   D.   H.   Ripin   and   D.   A.   Evans, https://organicchemistrydata.org/hansreich/resources/pka/pka_data/evans_pKa _table.pdf, (accessed 16/06/2021, 2021).

42.   B. P. Hutchings, D. E. Crawford, L. Gao, P. Hu and S. L. James, *Angew. Chem. Int. Ed.*, 2017, **56**, 15252-15256.

43.   D. G. Brown and J. Boström, *J. Med. Chem.*, 2016, **59**, 4443-4458.

44.   Q. Cao, W. I. Nicholson, A. C. Jones and D. L. Browne, *Org. Biomol. Chem.*, 2019, **17**, 1722-1726.

45.   Q.-L. Shao, Z.-J. Jiang and W.-K. Su, *Tetrahedron Lett.*, 2018, **59**, 2277-2280.

46.   K. Kubota, T. Seo, K. Koide, Y. Hasegawa and H. Ito, *Nat. Commun.*, 2019, **10**.

47.   K. Kubota, R. Takahashi, M. Uesugi and H. Ito, *ACS Sustain. Chem. Eng.*, 2020, **8**, 16577-16582.

48.   A. C. Jones, W. I. Nicholson, H. R. Smallman and D. L. Browne, *Org. Lett.*, 2020, **22**, 7433-7438.

3 Direct Amidation of Esters Enabled by Ball Milling

3.1   Introduction to the Synthesis of Amides

The synthesis of amide bonds is an often-overlooked synthetic challenge, unsurprisingly due to their prevalence in pharmaceuticals, agrochemicals, materials, and natural products.[1] This was highlighted by a study from Brown and coworkers that 50% of all medicinal chemistry routes contain one or more amide formation steps.[2] The vast majority of these amides are synthesized by the coupling of an amine with a carboxylic acid employing an activating reagent such as, oxayl chloride **161**, DIC **162**, HBTU **163**, etc. (Scheme 3.01).[3] These reagents often allow for facile scale up of amidation reactions for the commercial synthesis of a broad range of products.[4] Although the use of these reagents is not without downsides. These reagents generate stoichiometric amounts of often toxic biproducts in the process of activating the acid. This has led to the ACS Green Chemistry Roundtable in 2007, and again in 2018, including the formation of amides avoiding poor atom economy reagents in the list of reactions where an alternative is needed.[5] Furthermore some of these reagents have been shown to be possibly thermally unstable leading to safety concerns about their large scale use.[6] Those reagents derived from hydroxybenzotriazole **170** are of particular concern as this biproduct of the reaction is known to be thermally unstable and shock sensitive, leading to Pfizer taking the stance to no longer develop processes employing those reagents.[7]
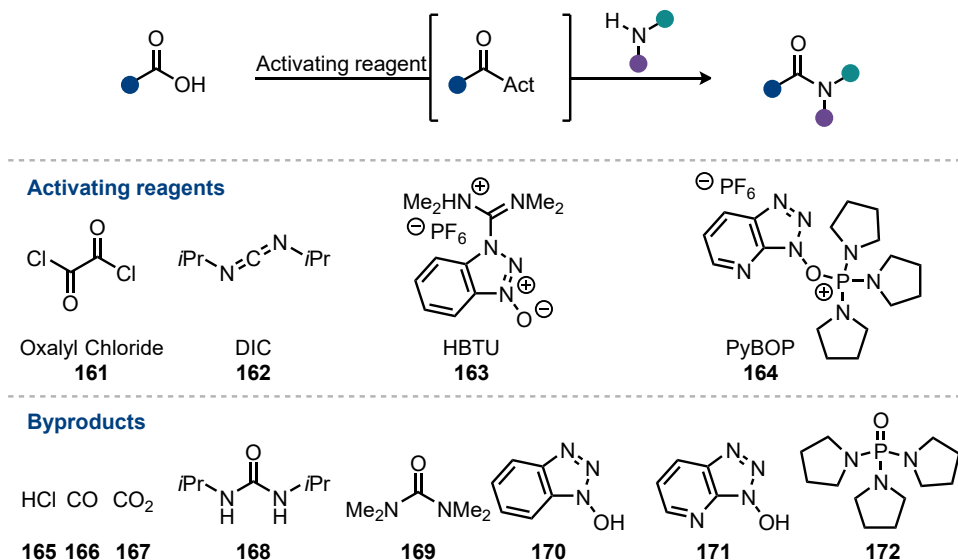
Scheme 3.01 Synthesis of amides through activated carboxylic acids.

Improvements in the synthesis of amides is an active area of research with a broad range of methods being explored.[8] Following is a selection of some of the key areas in which

improvements have been made including seminal works and successful application of these methods in industrial stetting's.

3.1.1 Catalytic Methods for the Direct Amidation of Carboxylic Acids

The simple condensation of an amine with a carboxylic acid often requires forcing conditions such as high temperature (>200 ˚C). These conditions can be detrimental to the reagents being used limiting the scope of this reaction significantly.[9] Although there has been significant advancement of catalytic amidation reactions of carboxylic acids.[10]

Metal catalysed reactions for the synthesis of amides from carboxylic acids often focus of the use of the oxophilic group IV metals.[11] The seminal works in this area from the groups of Williams and Adolfsson focused on the use of zirconium(IV) based catalysts, these methods were developed simultaneously. In the example from Williams and coworkers refluxing toluene was used to azeotropically remove water from the reaction at elevated temperatures with a low catalyst loading (Scheme 3.02a).[12] Adolfsson and coworkers achieved similar catalyst loading in their reaction although exchanging the use of refluxing toluene for THF at 70 ˚C and using 4 Å molecular sieves as a desiccant (Scheme 3.02b).[13] They also successfully applied the transformation to the derivatization of Indomethacin, a nonsteroidal anti-inflammatory. Adolfsson and coworkers later went on to investigate a range of early transition metal alkoxides activity in the amidation of carboxylic acids finding titanium(IV) *iso*-propoxide as an efficient catalyst that was easier to handle than some of the zirconium derivatives (Scheme 3.02c).[14]

a) Williams and coworkers direct amide formation catalysed by zirconium
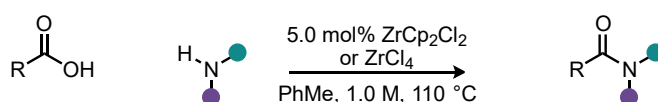
5.0 mol% ZrCp₂Cl₂ or ZrCl₄
PhMe, 1.0 M, 110 °C

b) Adolfsson and coworkers direct amide formation catalysed by zirconium

2.0 - 10 mol% ZrCl₄
4 Å MS
THF, 0.4 M, 70 °C
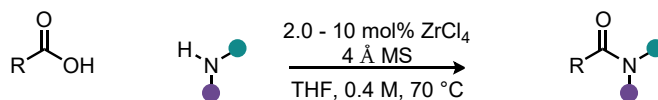
c) Adolfsson and coworkers amidation mediated by Ti(O*i*Pr)₄

10 mol% Ti(O*i*Pr)₄
4 Å MS
THF, 0.4 M, 70 °C

1.2 equiv.
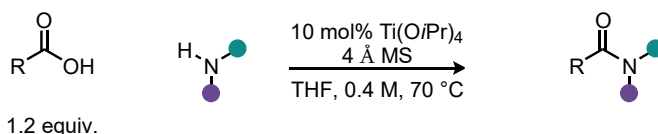
Scheme 3.02 Catalytic amidation of carboxylic acids with group(IV) transition metals.

The use of boronic acid catalysts for the activation of hydroxy functional groups such as alcohols and carboxylic acids has recently been explored for a number of

transformations.[15] This has included the synthesis of amides which was first demonstrated by Yamamoto and coworkers in 1996 (Scheme 3.03a).[16] They discovered the catalytic activity of a range of boronic acids in the condensation of 4-phenylbutyric acid **173** and 3,5-dimethylpiperidine **174**, finding 3,4,5-trifluorophenylboronic acid **176** to be optimal. These initial conditions utilized azeotropic removal of water with refluxing toluene and only 1 mol% of the catalyst **176** to forge the amide bonds. They also proposed a catalytic cycle via a boroxine intermediate which was still considered correct until recent detailed study of the mechanism by Whiting and coworkers in 2018.[17] The boronic acid catalysts have continued to develop including bi-functional catalysts containing a pendant tertiary amine to assist in catalyst stability and acting as a base **177** (Scheme 3.03b).[18] The key developments of the catalyst system came from Hall and coworkers in 2008 (Scheme 3.03c).[19] Their discovery of the enhanced activity of *ortho*-iodophenylboronic acid **180** allowed for much milder reaction conditions. However, with reactions being carried out at room temperature 4 Å molecular sieves were required to remove water. The Hall group went on to further develop this catalyst system finding that 5-methoxy-2-iodophenylboronic acid (MIBA) **181** was kinetically more active providing higher yields in shorter reaction times. Hall and coworkers went on to develop a multigram procedure with improved sustainability than the initially established method using MIBA **181** (Scheme 3.03d). The mild conditions that the MIBA catalyst operates under has allowed it to successfully be used for the synthesis of dipeptides without epimerization of protected α-amino acids.[20] Although due to the inhibitive nature of Boc protected α-amino acids either phthalimide protection of the use of α-azido acids must be used. Whiting and coworkers had previously found the synthesis of dipeptides to be similarly challenging requiring a binary catalytic system of *o*-tolyl- **188** and *o*-nitrophenyl-boronic acid **189** in refluxing fluorobenzene provided the least epimerization (Scheme 3.03e).

a) Yamamoto and coworkers initial discovery of boronic acid catalysed amide synthesis
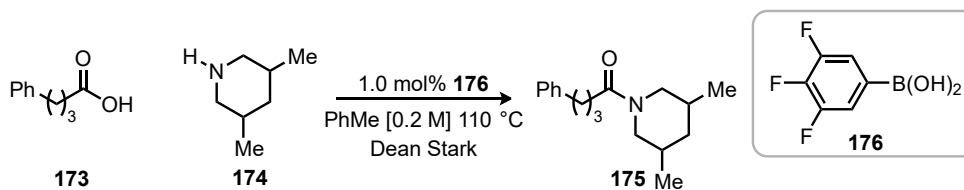
b) Whiting and coworkers development of bifunctional catalysts
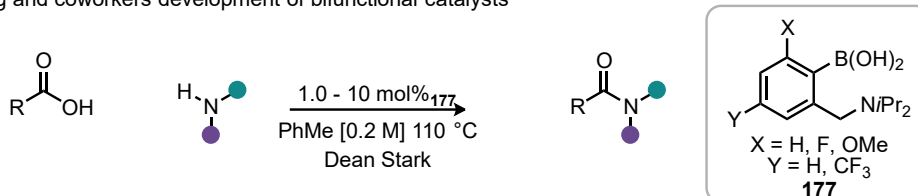
c) Hall and coworkers discovery and development of the *ortho*-iodo activation of the boronic acid catalyst
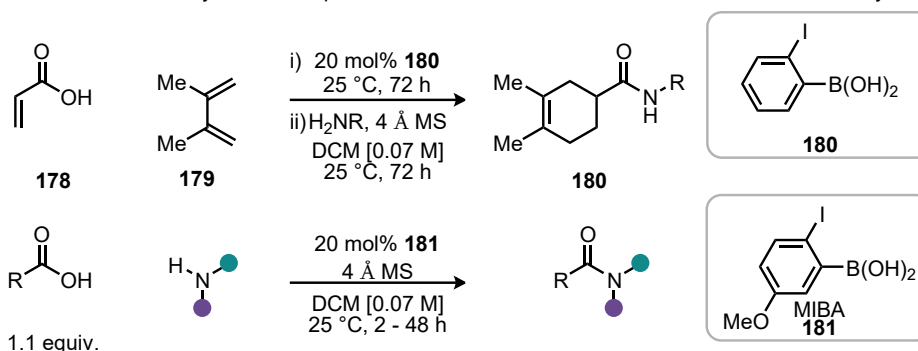
d) Hall and coworkers multigram improved sustainability method usign the MIBA catalyst
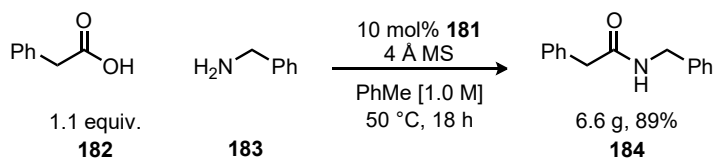
e) Whiting and coworkers binary catalyst system for dipeptide synthesis
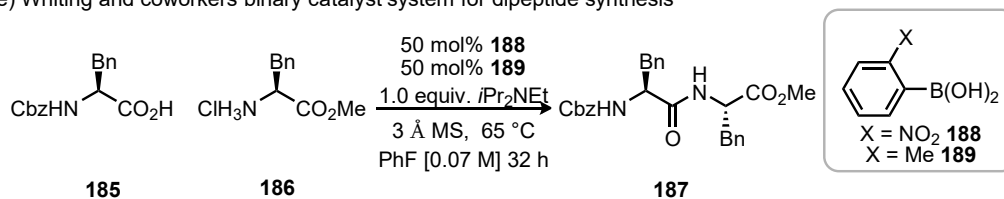
. **Scheme 3.03** Boronic acid catalysed amidation of carboxylic acids.

The catalytic synthesis of amides from carboxylic acids has seen significant development, especially since the additional focus brought about by the ACS Green Chemistry Roundtable in 2007 and again in 2018.[5a, 21] Although these new methods are yet to be adopted in industry for the large scale preparation of amides. This shows that there is still improvement needed in this area.[10] One of the key challenges is a general catalyst which can be used in peptide coupling chemistry in conjugation with solid phase

peptide synthesis.[3b] If this goal is reached it could remove the necessity for the use of wasteful peptide coupling reagents.

3.1.2 Advancements in the Amidation of Inactivated Esters

The amidation of simple esters has been well explored. These methods can benefit multistep synthesis in which carboxylic acids may have to be protected as the methyl or ethyl esters. Therefore, methods which can access amides from these functional groups could lead to improved step economy in multistep synthesis. In this section the amidation of simple inactivated substrates will be explored using the definition set out by El-Faham and Albericio.[3b]

"The activated species may or may not be isolable but will immediately undergo aminolysis."[3b]

Metal catalysed processes for the amidation of esters have recently garnered some attention. In 2017, Hu and coworkers demonstrated a nickel catalysed coupling of nitro arenes with alkyl or aryl esters (Scheme 3.04).[22] The reaction required stoichiometric quantities of zinc and TMSCl for the *in situ* reduction of the nitro group which could then undergo the coupling reaction. The reaction could be applied to the synthesis of several biologically active molecules such as natural products and pharmaceuticals.
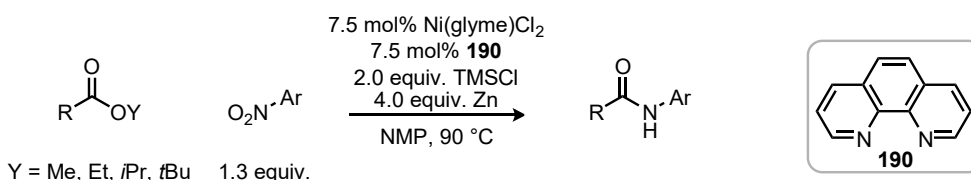
Scheme 3.04 Hu and coworkers nickel catalysed amidation of esters with nitroarenes.

The palladium catalysed Buchwald-Hartwig amination has provided a powerful method for the coupling of aryl halides with amines. Recently the groups of Newman and Szostak both produced similar procedures for a palladium catalysed amidation of ester inspired by the well-known cross-coupling (Scheme 3.05). Each of their methods utilized NHC ligands to produce an electron rich palladium catalyst capable of oxidatively inserting into the C-O bond of the phenyl esters. Newman and coworkers initial demonstration could be applied to both alkyl and benzoate esters including those derived from amino acids without significant epimerization (Scheme 3.05b).[23] Szostak and coworkers compiled a similarly broad scope of ester derivatives for the synthesis of amides (Scheme 3.05a).[24] Furthermore, the coupling could be expanded to include the of the coupling to twisted amides, a group of compounds well explored by the Szostak group.[25]

a) Newman and coworkers palladium catalysed amidation of phenyl esters
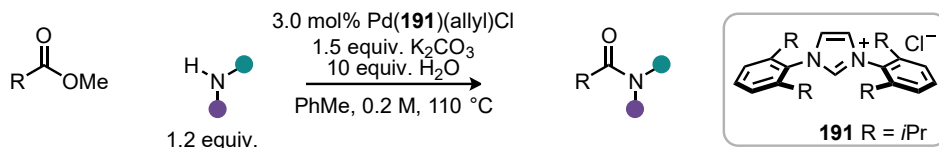
b) Szostak and coworkers palladium catalysed amidation of phenyl esters
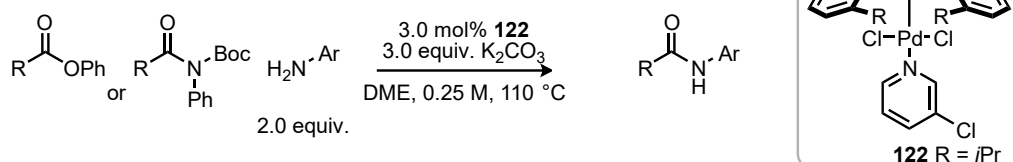
Scheme 3.05 Direct amidation of esters using palladium catalysis.

Garg and coworkers later improved on the Hu amide synthesis using Nickel catalysis, enabling the coupling with free amines (Scheme 3.06a).[26] Unfortunately, in this initial work the reaction was limited to napthyl or anthracyl derived methyl esters such as **192** with benzoate or alkyl esters being unreactive under their conditions. They also found the use of aluminium(III) *tert*-butoxide was required in stoichiometric quantity to act as a Lewis acid activating the esters. Newman and coworkers have since advanced this method removing the need for the Lewis acid additive and have accessed benzoate and alkyl ester examples (Scheme 3.06b).[27] Additionally, the Newman nickel catalysed approach could couple proline derivatives without any epimerization.

a) Garg and coworkers nickel catalyzed amidation of esters mediated by Al(O*t*Bu)$_3$
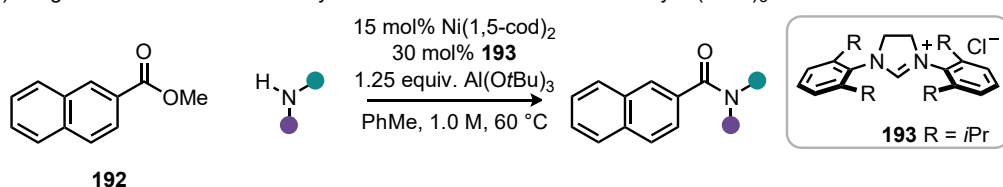
b) Newman and coworkers nickel catalyzed amidation of esters
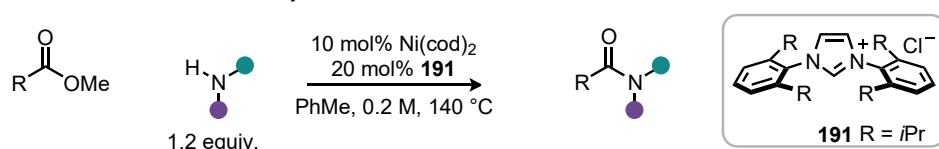
Scheme 3.06 Direct amidation of esters using nickel catalysis.

Alongside the development of metal catalysed approaches to amidation of esters organocatalytic methods have also been developed. NHCs have been shown to be effective catalysts for the amidation of methyl esters by Movassaghi and coworkers (Scheme 3.07a).[28] Under their conditions the esters could be amidated at room temperature although the scope was limited to amino alcohol compounds and for more

challenging esters lithium chloride was required as a co-catalyst. Du and coworkers expanded the range of amines which could be amidated using NHC catalysis but required the use of vinyl esters (Scheme 3.07b). This would produce acetaldehyde as the biproduct which would be removed under the elevated reaction temperature preventing the reverse reaction and any unwanted condensation reactions. This NHC catalysed procedure was also carried out on a multigram scale for the acylation of *p*-anisidine **195**.

a) Movassghi and coworkers NHC catalysed amidation of esters with aminoalcohols
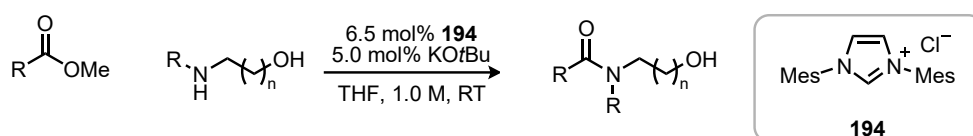
b) Du and coworkers NHC catalysed amidation of vinyl esters
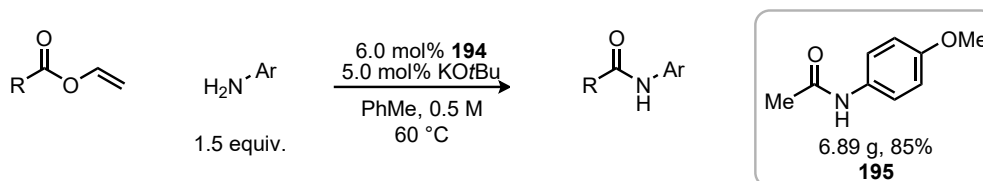
Scheme 3.07. NHC catalysed amidation of esters.

Other Lewis base organocataysts such as 1,8-diazabicyclo[5.4.0]undec-7-ene (DBU) have also been successfully employed by the groups of Birman (Scheme 3.08a) and Vaidyanathan (Scheme 3.08b) for the amidation of esters. Initially reported by Birman and coworkers using a co-catalytic system of DBU and 1,2,4-triazole for the amidation of benzyl and alkyl amines under solvent free conditions.[29] Although the scope of the amines was limited a variety of esters including aryl and alkyl examples, some of which were sterically challenging, participated in the reaction. Vaidyanathan and coworkers subsequently reported an amidation of cyanoactates under mild conditions using DBU.[30] Addition of DBU was found to accelerate the rate of the reaction significantly allowing the reaction to be complete in under 1 hour, whereas without its presence reactions required greater than 24 hours to reach completion. Through this amidation they also showed significant simplification of the synthesis of CP-690,550-10 **196** by forgoing the generation of the mixed anhydride which was required in previous synthesis. Another Lewis base which has seen some development for the amidation of ester is triazabicyclo[4.4.0]dec-5-ene (TBD) **197**. Mioskowski and coworkers established a solvent free amidation using TBD as the catalyst with many examples undergoing the transformation at room temperature (Scheme 3.08c).[31] Although some of the more challenging substrates such as α-substituted amines required increased reaction

temperature of 75 °C to reach complete conversion. Weiberth and coworkers at Sanofi realized the utility of TBD **197** as an amidating reagent in the multi-kilo synthesis of the HPGDS inhibitor **200** in excellent yields (Scheme 3.08d). Furthermore, they could greatly improve the sustainability of the transformation which previously required the deprotection of the methyl ester **198** followed by amidation of the carboxylic acid with an activating reagent.
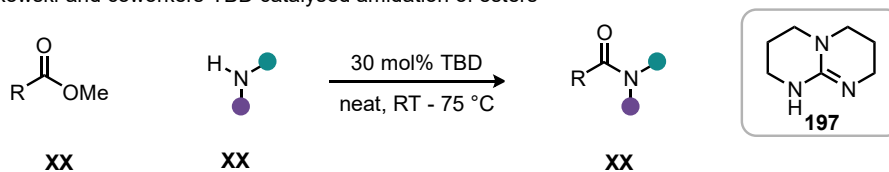

Scheme 3.08 Organocatalytic amidation of esters.

The use of Brønsted bases to induce the amidation of simple esters is well known but often still allows for efficient synthesis of a variety of substrates. Alcázar and coworkers described a rapid amidation of esters using a flow microreactor in 2014 (Scheme 3.09a i).[32] Lithium bis(trimethylsilyl)amide (LHMDS) was used in super stoichiometric quantity to facilitate the use of poorly nucleophilic amine containing heterocycles, such as amino pyridines. In 2018, Szostak and coworkers developed a room temperature amidation of esters and twisted amides also using LHMDS which could be successfully applied to a broad range of esters and amines (Scheme 3.09a ii).[33] During this work they produced a range of pharmaceutical and functionalized natural

products using their method including amino acid derivates without epimerization. Furthermore, they continued to investigate the transamidation method to further understand the selectivity of the transamidation on a variety of amine and amide partners.[34] Through this study they have suggested the ability to predict the transamidation ability of various amines and amide partners. Alkoxide bases have also been shown to be very effective for the synthesis of amides from esters (Scheme 3.09a iv and v).[35] Most recently Qin and coworkers developed a practical and sustainable direct amidation procedure using sodium *tert*-butoxide.[36] The solvent free reaction was reported to avoid the use of chromatography and organic solvents for work up and the products could be obtained through simply washing with water. Finally, the Watson group developed an amidation method using aminoalcohols under sustainable reaction conditions (Scheme 3.09b).[37] This focus required the use of environmentally benign solvent where *iso*-propanol was found the most effective with the use of potassium phosphate tribasic as the catalyst. Although there developed conditions did require elevated temperature dipeptides could be formed without epimerization and with good chemoselectivity using *tert*-butyl esters as the protecting group for the amino acid C-terminus.

a) Base mediated amidation of esters applicable to a broad scope of esters and amines

i) Alcazar and coworkers	ii) Szostak and coworkers	iii)Ohshima and coworkers
2.2 equiv. LHMDS DMF, 0.25 M RT, 2 min	3.0 equiv. LHMDS PhMe, 0.25 M, RT	5.0 mol% NaOMe PhMe, 4.0 M 20 - 48 h, 50 °C

iv)Yoon and coworkers	v) Qin and coworkers
2.0 equiv. KO*t*Bu THF, 0.1 M, RT, 1 h	1.5 equiv. NaO*t*Bu neat, 1 h, RT
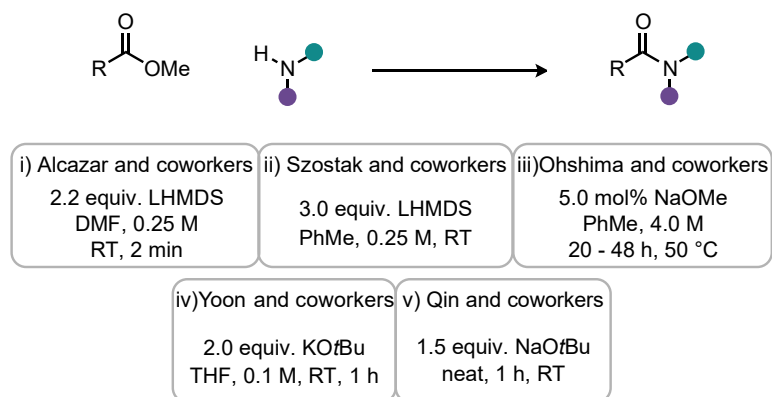
b) Watson and coworkers sustainable catalytic amidation of esters with aminoalcohols
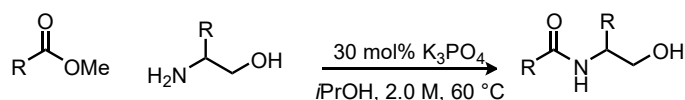
Scheme 3.09 Base mediated direct amidation of esters.

The direct amidation of esters offers an alternate method for the preparation of amides and in situations where the deprotection of an acid can be avoided may provide an attractive approach. This benefit is beginning to be utilized in industrial research and development, such as the TBD catalysed synthesis of the HPGDS inhibitor **200**. Although the metal catalysed procedures are yet to be adopted which is possibly due to the

sensitivity of the catalysts systems requiring the use of strictly controlled environments with dry and degassed solvents. This level of complexity in the methodology may lead to more traditional coupling procedures still being preferential.

3.1.3 Non-Canonical Methods for the Synthesis of Amides

The amidation methods reviewed thus far have focused on improvements made in the areas regarding the use of carboxylic acids and esters. Although these are some of the most utilized methods for the synthesis of amides being developed other avenues to produce amides have also seen breakthroughs.[38] This includes oxidative methods where amides can be formed from lower oxidation state carbons, or utilizing carbonylation techniques which can produce carbonyl containing compounds.

Palladium catalysed methods for the oxidation of aldehydes to amides has seen some development (Scheme 3.10). Yoshida and coworkers developed an amidation of aldehydes where bromobenzene could be used as the terminal oxidant in the reaction (Scheme 3.10a).[39] A hemiaminal formed between the amine and aldehyde component which could then be oxidized by a palladium(II) intermediate via a β-hydride elimination. The scope of the reaction with regard to the aldehyde was modest with alkyl and aryl examples demonstrated in good yield. Although the amine component was limited to strongly nucleophilic cyclic amines such as morpholine **120**. In 2008, Torisawa and coworkers published another palladium catalysed oxidative amidation of aldehydes employing urea hydrogen peroxide as the oxidant (Scheme 3.10b).[40] Under these new conditions the scope of the reaction could be improved to include heteroaromatic aldehydes as well as less nucleophilic primary amines.

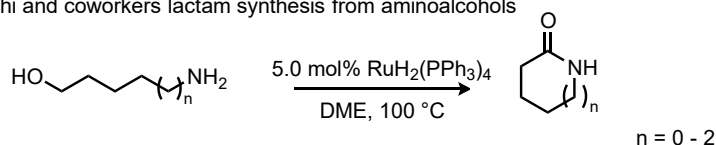a) Tamaru and coworkers oxidative amidation of aldehydes by palladium catalysis
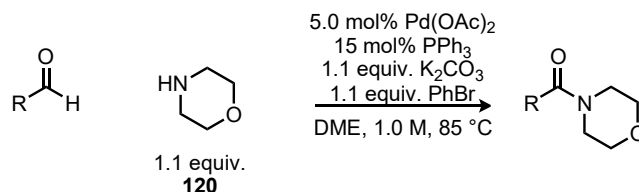
b) Torisawa and coworkers palladium catalysed oxidative amidation of aldehydes
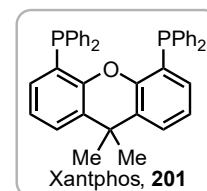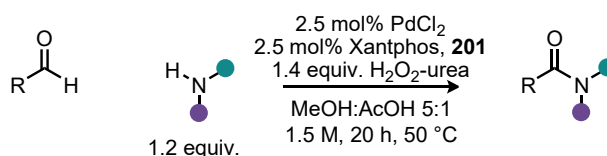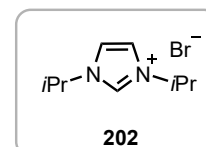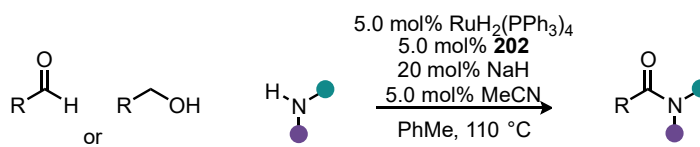

Scheme 3.10. Palladium catalysed oxidative amidation of aldehydes.

Ruthenium catalysed oxidations of aminoalcohols were initially discovered by Murahashi and coworkers for the synthesis of lactams (Scheme 3.11a).[41] A decade later Hyeok-Hong and coworkers applied the same ruthenium catalyst for the synthesis of linear amides from aldehydes or primary alcohols (Scheme 3.11b).[42] Addition of an imidazolium NHC **202** ligand increased the reactivity of the system such that intermolecular amidation could take place. Further ligand system development was made by Milstein and coworkers with the use of dearomatized PNN ligand which allowed for very low loading of the catalyst **203** (0.1 mol%) (Scheme 3.11c).[43] Even at catalyst loading this low the reaction was still complete in 24 h. These transformations are highly efficient with the only waste product being hydrogen gas.

a) Murahashi and coworkers lactam synthesis from aminoalcohols

b) Hyeok Hong and coworkers ruthenium catalysed oxidative amidation of aldehydes and alcohols

c) Milstein and coworkers ruthenium catalysed oxidative amidation of alcohols
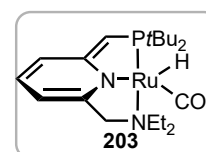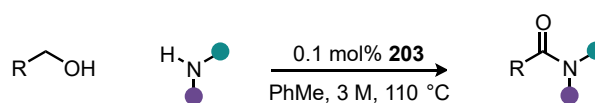
Scheme 3.11 Oxidative amidation of aldehydes and alcohols using ruthenium catalysis.

NHC organocatalysis has also been applied to the oxidative amidation of aldehydes. The groups of Rovis and Bode both presented an amidation of aldehydes containing reducible bonds in 2007 (Scheme 3.12).[44] These transformations were applicable to a range of functionalized aldehydes including those with strained rings, α,β-unsaturated, and α-halo aldehydes. These reactions could be carried out at room temperature without the need for additional oxidizing agent due to the built-in nature of the reducible bonds. A range of oxidative methods for the amidation of aldehydes have also been developed allowing the derivatization of unfunctionalized aldehydes increasing the range of accessible amides.[45]
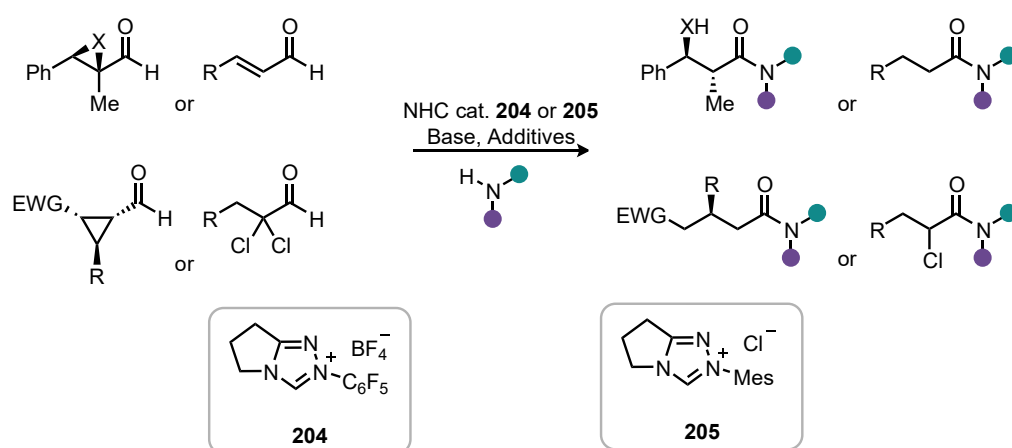
Scheme 3.12 Amidation of aldehydes containing reducible bonds using NHC catalysis.

Carbonylative amidation of aryl halides has been demonstrated as a powerful method for the synthesis of aryl amides utilizing palladium catalysis.[46] Milstien and coworkers initial discovery required harsh reaction conditions with high temperatures (150 °C) and high CO pressure (5 atm).[47] These conditions were also limited in scope of the amide product with only three examples of amides being produced. Significant development has taken place since this seminal discovery improving reaction conditions. Buchwald and coworkers have established milder conditions for the aminocarbonylation of aryl chlorides (Scheme 3.13a).[48] Under their conditions only 1 atm of CO pressure is required which can be supplied simply from a balloon, negating the need for specialized pressure vessels. These conditions could also be applied to a broad range of aryl chloride substrates including electron rich and poor examples, sterically encumbered, and heterocyclic. The amine scope being similarly broad with primary, aryl, and cyclic amines coupling with ease, although secondary amines required increased reaction temperature. Even though the palladium catalysed methodology can access a broad range of amide products it is limited to aryl halides due to competing β-hydride

elimination of alkyl halides at the high reaction temperatures necessary due to CO catalyst poisoning.[49] To overcome some of these disadvantages Polyzos and coworkers applied iridium photoredox catalysis to the aminocarbonylation of alkyl iodides and aryl iodides or bromides (Scheme 3.13b). Utilizing flow chemistry for the transformation allowed for the use of high pressures to maintain CO solvation while also providing a high surface area and short path length for optimum photo absorbance.[50] The photoredox conditions could then be applied to a broad scope of 90 examples including natural product derivatives, heterocycles, unprotected amino acids, and varying electronics and sterics of aryl halides. Although these conditions have been applied to a broad range of substrates, there greatest limitation currently is the use alkyl iodides which have limited commercial availability.

a) Buchwald and coworkers palladium catalysed amincarbonylation of arylchlorides
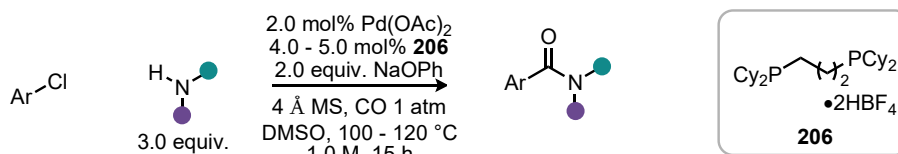
b) Polyzos and coworkers Ir catalysed photoredox carbonylative amidation
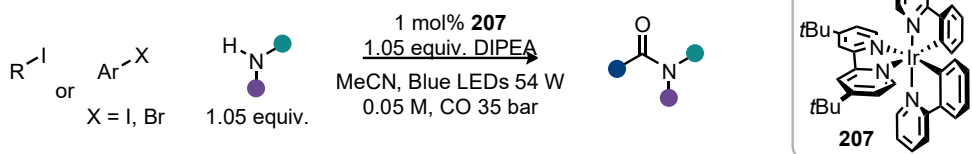
Scheme 3.13 Catalytic carbonylative amidation methods.

These amidation methods from alternate starting materials than that of the more traditional synthesis have provided new methods to access this valuable functional group. Although many of these methods require the use of functional groups which require prior synthesis which is likely the cause for the minimal adoption in synthetic laboratories. Also, carboxylic acids, esters, and amines are amongst the most readily available starting materials with 1000's being commercially available.

3.1.4 Prior Exploration of Amidation Using Ball Milling

These alternate methods only go so far in addressing the need for a viable alternative to the synthesis of amides in a more environmentally benign fashion. Within the challenge of finding an alternative amidation strategy the use of chlorinated (DCM, DCE) or polar aprotic solvents (DMF, DMP, etc.) needs to be addressed as the reduction of the use of

these solvents was another key point for the ACS Green Chemistry Roundtables.[5] These solvents are often used in conjunction with the high molecular weight activating reagents used in amidation showing the clear need for an alternative approach.[4, 51]

One possibility is to forgo the use of solvent in the reaction entirely and to use a method such as ball milling to carry out these transformations. A great deal of the previous work on the synthesis of amides through ball milling has focused on the activation of carboxylic acids (Scheme 3.14). Activating reagents such as carbonyldiimidazole (CDI) **208** and 1-ethyl-3-(3-dimethylaminopropyl)carbodiimide (EDC) **209** have been shown to be highly efficient in the synthesis of amides under ball milling conditions.[52] Lamaty and coworkers have been at the forefront of amide synthesis under ball milling conditions with the use of activating reagents, improving upon the previous synthetic methods producing fast reactions with minimal epimerization on challenging peptide couplings, **214**, and towards the synthesis of pharmaceuticals **212** and **213** in a solvent free manner.[53] Uronium based activating reagents (1-Cyano-2-ethoxy-2-oxoethylidenaminooxy)dimethylamino-morpholino-carbenium hexafluorophosphate (COMU) **210** and chloro-N,N,N′,N′-tetramethylformamidinium hexafluorophosphate (TCFH) **211** have also been implemented by Aav and coworkers in the synthesis of amides including the hexa-amidation of biotin[6]uril **215** which is especially challenging under solution conditions due to its poor solubility.[54]
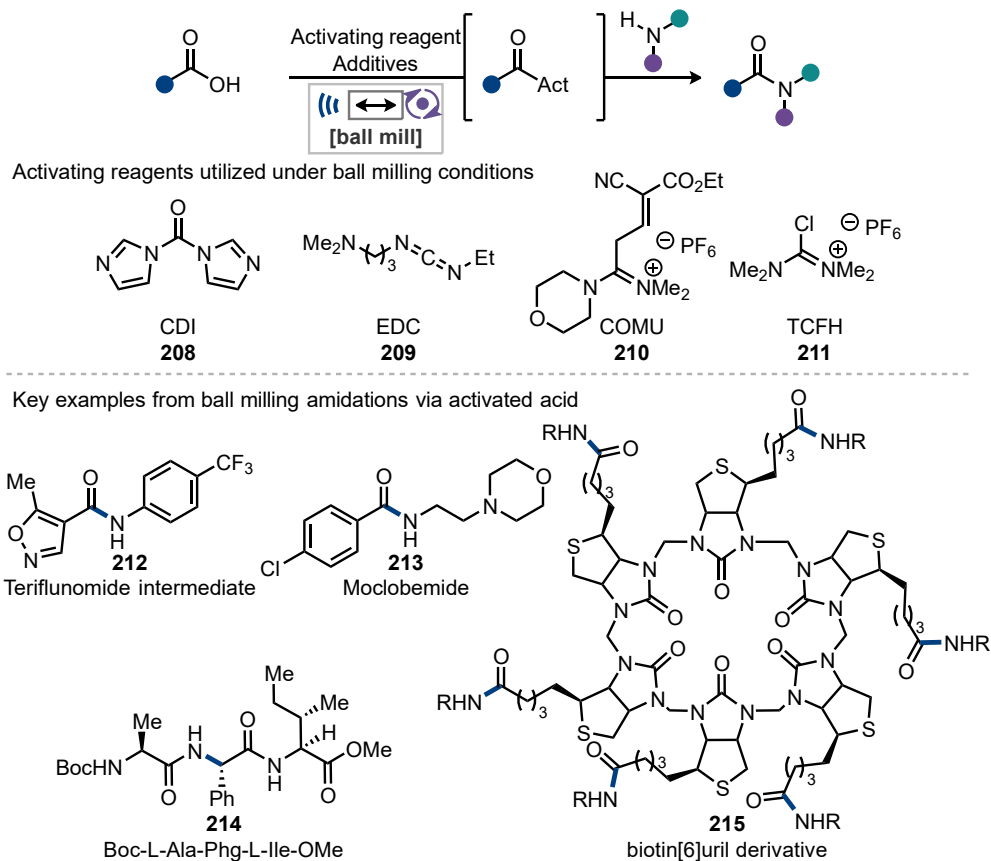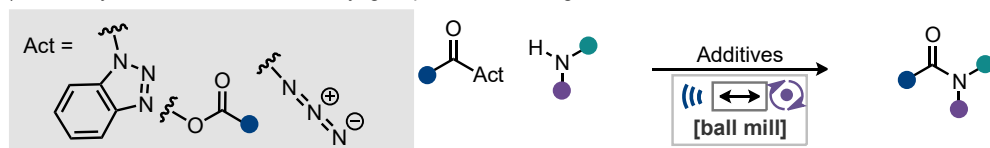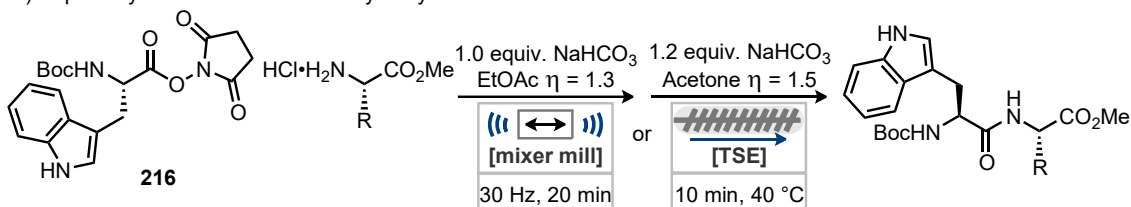
Scheme 3.14 Amidation via *in situ* activation of carboxylic acids by ball milling.

The synthesis of amides using activated carboxylic acid surrogates has also been thoroughly explored under ball milling conditions (Scheme 3.15). Activated acyl compounds such as acyl azides, anhydrides, and *N*-acyl benzotriazoles have been shown to give rapid access to amides under mechanochemical conditions (Scheme 3.15a).[55] Amino acid derivatives including hydroxysuccinimide esters such as Boc-Trp-OSu **216** have been shown to be applicable for the synthesis of di- and tri-peptides under ball milling as well as continuous extrusion methods (Scheme 3.15b).[56] This continuous technology has the potential of allowing access to these peptides on large scales with very little waste when compared to the current solution batch procedures. Traceless activation through the use of urethane protected amino acids allowed Lamaty and coworkers to synthesize di- and tri- peptides without any organic solvent or purification (Scheme 3.15c). The reaction mixture could simply be filtered and washed with water to provide the products in high yields and purity.[57] Juaristi and coworkers achieved similar results using *N*-Boc-*N*-carboxyanhydride derivatives for the synthesis α,β- and β,β-dipeptides, although requiring the use of organic solvent for work up and purification (Scheme 3.15d).[58]
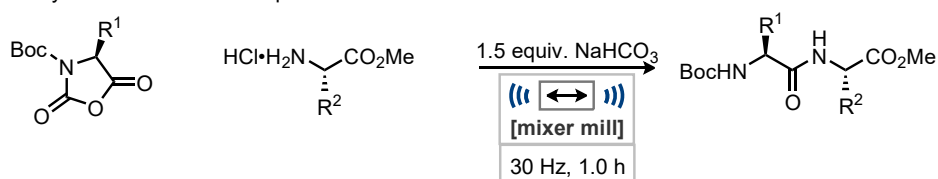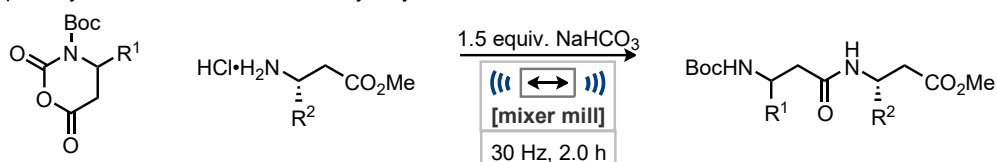
**Scheme 3.15.** Amidation of activated acid surrogates.

Alternative amide synthesis methods studied under mechanochemical conditions include the Beckman rearrangement of O-tosyl oximes (Scheme 3.16a). This method unfortunately suffers from selectivity issues due to competing migratory aptitudes leading to mixtures of amide products in many cases. Despite this challenge the synthesis of paracetamol was successfully caried out in good yield using the Beckman rearrangement under ball milling conditions.[59] Mechanoenzymatic peptide and amide synthesis has also been achieved with the use of ball milling and transferred to twin screw extrusion through collaboration of Hernández and James and coworkers (Scheme 3.16b).[60] Despite the high energy collisions experienced within the ball mill the enzyme, papain, was still able to efficiently catalyse the reaction without suffering from degradation.

a) Mechanochemical one pot oxime formation and Beckmann rearrangement
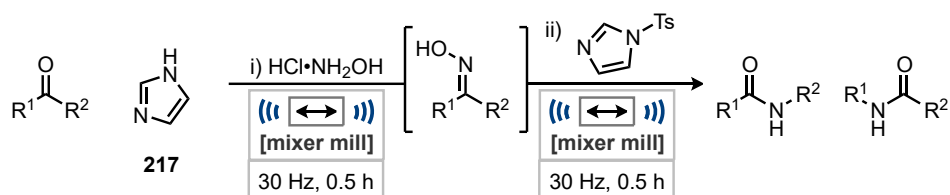
b) Mechanoenzyatic amide and peptide synthesis
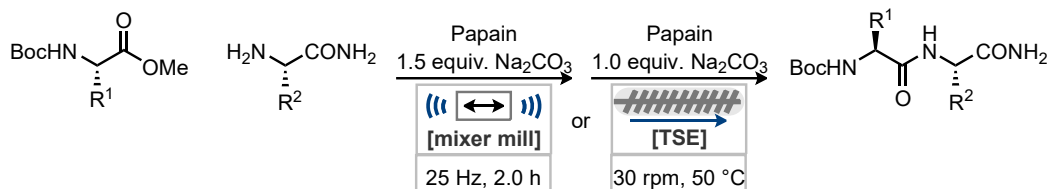
Scheme 3.16 Alternate amidation strategies by mechanochemical methods.

Progress towards new amidation strategies using mechanochemistry has been well established and has shown many benefits compared to that of solution methods. Reduction in solvent waste for the reaction and purification can be significant, providing high purity products in a shortened reaction time. However, many of the developed methods still heavily rely on the use of stoichiometric reagents for the activation of carboxylic acids or the prior synthesis of activated reagents many of which still require the activation of carboxylic acids using the same wasteful reagents to be synthesized. The application of simple inactivated esters has been shown to be a plausible substrate for the synthesis of amides in solution but has only been demonstrated once under mechanochemical conditions through the use of an enzymatic reaction.

## 3.2 Direct Amidation of Esters - Results and discussion

Presented in the previous chapter was the observation of the direct amidation of **156** while undertaking the substrate scope of the ball milling Buchwald-Hartwig reaction (Scheme 3.17).[61] Initial inquiry into the reactivity found that the Pd-PEPPSI-IPent **118** catalyst was not required for the transformation. Described herein is the continued investigation and optimization of the direct amidation of esters by ball milling.
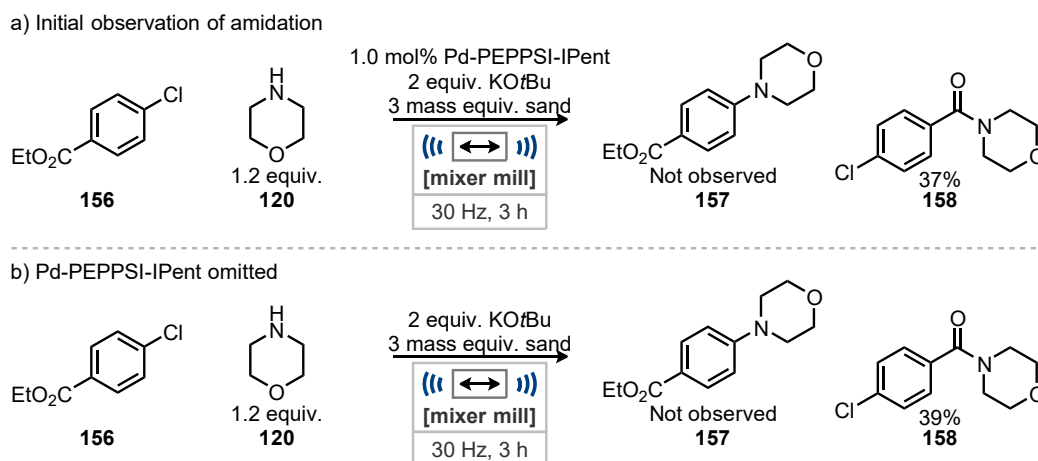
Scheme 3.17. Initial observation of direct amidation of esters.

3.2.1 Optimization

The initial conditions for the optimization of the direct amidation of esters were modified from those which were used for discovery of the transformation (Scheme 3.17). Ethyl benzoate **218** and morpholine **150** were chosen as model substrates for the transformation. At first these compounds were milled along with a range of bases as the amidation of esters has previously been established in solution with the use Bronsted bases and it was postulated that the potassium *tert*-butoxide within the Buchwald-Hartwig conditions could have been responsible for the observed reactivity.
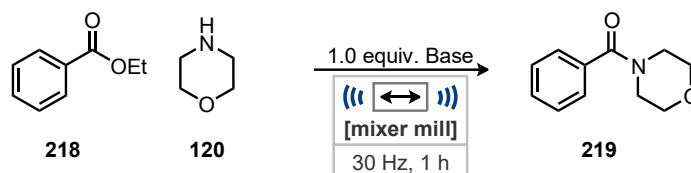
Entry	Base	Solution pKa[b]62	Yield of **219**[a] / %
1	-	-	0
2	NaHCO$_3$	6.4	0
3	NEt$_3$	10.6	0
4	K$_2$CO$_3$	10.3	0
5	KOH	15.7	0
6	NaO*t*Bu	17	62
7	KO*t*Bu	17	75

[a] Yield of isolated product. [b] pKa reported of conjugate acid.

Table 3.01 Direct amidation base screening.

Without any base present or in the presence of weak bases no conversion to the amide was observed (Table 3.01, entries 1 – 4), also the use of a stronger hydroxide base failed to facilitate the transformation (Table 3.01, entry 5). Alkoxide bases did permit the generation of the desired amide product in moderate to good yields (Table 3.01, entries 6 and 7). Potassium *tert*-butoxide performed superiorly and was carried forward through the optimization and confirmed that this was the likely aspect of the Buchwald-Hartwig reaction conditions that produced this reactivity.

If the reaction proceeds through a simple substitution mechanism, then it is plausible that the reaction could be carried out using a sub-stoichiometric or potentially catalytic quantity of base due to regenerating an equivalent of base during each substitution. The optimization was continued by decreasing the quantity of base being used.

218 **120** X equiv. KO*t*Bu
[mixer mill]
30 Hz, 1 h
219

| Entry	Equiv. of KO*t*Bu	Yield of **219**[a] / %
1	0.25	55
2	0.50	66
3	0.75	66
4	0.80	66
5	0.85	85
6	0.90	64

[a] Yield of isolated product.

Table 3.02 Direct amidation base stoichiometry optimization.

Decreasing the quantity of base still allowed the reaction to proceed in moderate to good yields with 0.85 equiv. of potassium *tert*-butoxide being the optimal amount of base (Table 3.02, entry 5). This unusual quantity required for the transformation could be due to a fine balance between filling ratio and the energy of the impact while also containing sufficient base to facilitate the reaction. It could also be plausible that the solid base could also be acting as grinding auxiliary improving the mixing and mass transfer which may explain the reduced yields at lower loadings of base (Table 3.02, entries 1-3).

To further investigate if the base is also acting as a grinding auxiliary 0.25 equiv. of base was used while several grinding auxiliaries were screened. If this is the case the use of grinding auxiliaries with the lower loading of base could lead to increased yields. The quantity of potassium tert-butoxide being used was decreased to 0.25 equiv. along with 67 mg of the solid additives as this is the reduction in mass of the base compared to the current optimal loading of 0.85 equivalents.
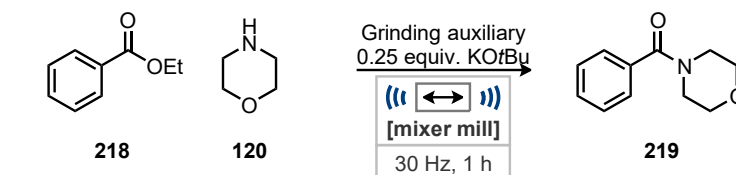
Entry	Grinding auxiliary[b]	Yield of **219**[a] / %
1	NaCl	41
2	Na₂SO₄	48
3	SiO₂	27
4	Sand	35
5	KCl	58

[a] Yield of isolated product. [b] 67 mg of grinding auxiliary used.

Table 3.03 Direct amidation grinding auxiliary screening.

Generally, lower yields were observed with these grinding auxiliaries (Table 3.03, entries 1-4) in place than the in reaction without the use of the grinding auxiliaries (Table 3.02, entry 1). This suggests that the reduction in yields observed at lower base loadings previously are in fact due to the reduced quantity of base rather than poor mixing or energy transfer. Potassium chloride was the only additive to lead to any improvement increasing the yield by 3% (Table 3.03, entry 5). Due to only marginal improvements on the yields being made using solid additives further optimization continued with the use of 0.85 equiv. of base which was clearly superior for this amidation reaction.

Final alterations to the conditions focused on reaction time and the stoichiometry of the starting materials.
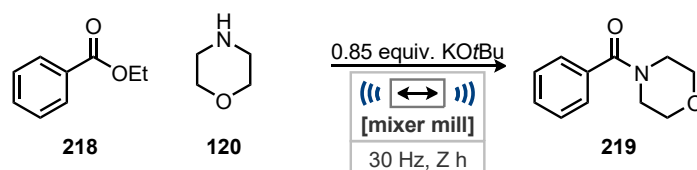
Entry	Time / h	Equiv. of **218**	Equiv. of **120**	Yield of **219**[a] / %
1	1.25	1.0	1.0	72
2	0.75	1.0	1.0	70
3	1	1.2	1.0	98
4	1	1.0	1.2	83

[a] Yield of isolated product.

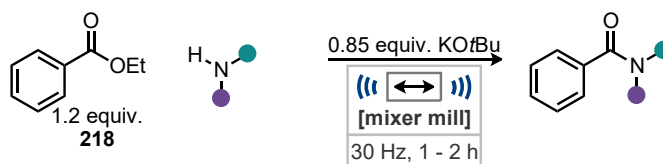**Table 3.04** Direct amidation time and stoichiometry optimization.

Increasing or decreasing the reaction time failed to improve on the yield with 1 hour remaining optimum (Table 3.04, entries 1 and 2). Increasing the quantity of ester to 1.2 equiv. the yield of the reaction significantly increased to 98% (Table 3.04, entry 3).

However, altering the stoichiometry of the amine made little effect on the reaction, decreasing the yield by 2% when 1.2 equiv. was used (Table 3.04, entry 4).
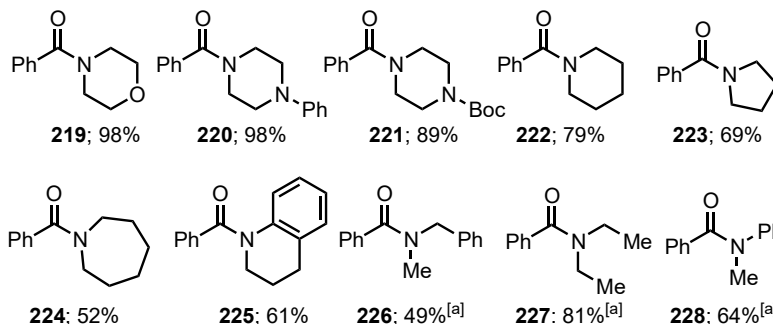
3.2.2 Substrate Scope

With conditions that lead to near quantitative formation of the desired product in hand (Table 3.04, entry 3) the project proceeded to a significant substrate scope exploring a variety esters and amines utilizing 1.2 equiv. of the ester and 0.85 equiv. of potassium *tert*-butoxide with the amine being the limiting reagent. The model substrate of ethyl benzoate **218** will continue to be used to investigate a range of amines (Scheme 3.18).
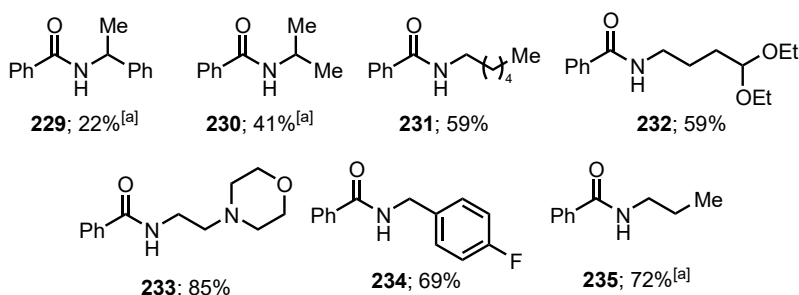
Scheme reaction conditions: 0.85 equiv. KO*t*Bu, [mixer mill], 30 Hz, 1 - 2 h. Benzoate ester **218** (1.2 equiv.) with amine.

Cyclic and Secondary amines

219; 98% **220**; 98% **221**; 89% **222**; 79% **223**; 69%

224; 52% **225**; 61% **226**; 49%[a] **227**: 81%[a] **228**; 64%[a]

Primary amines

229; 22%[a] **230**; 41%[a] **231**; 59% **232**; 59%

233; 85% **234**; 69% **235**; 72%[a]

Anilines and Amino Pyridines

236; 27%[a] **237**; 36% **238**; 79% **239**; 45%

240; 55%[a] **241**; 28%[a] **242**; 11% **243**; 49%[a]
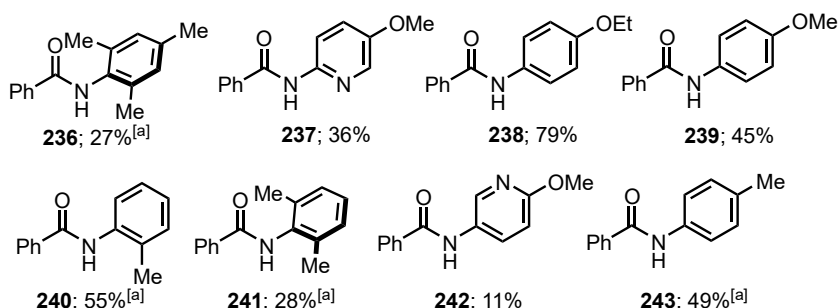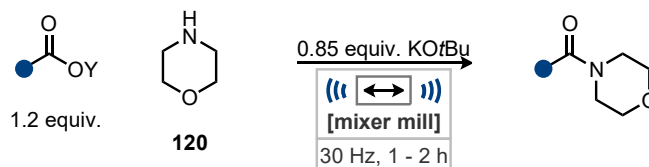
[a] 2 h reaction time.

Scheme 3.18 Amine substrate scope.

Initial exploration of the amine substrate scope focused on examples most similar to that of the model substrate, morpholine **120**, with cyclic and secondary amines. Cyclic amines provided good to excellent yields for all examples **219** – **225**. Secondary amines also achieved good yields in the amidation process but required increased reaction times of 2 hours to allow for more effective conversion to the desired amides **226** – **228**. The increase in reaction time may be due to the greater degree of rotational freedom of the substituents leading to a greater impact from the steric encumbrance whereas cyclic amines the substituents are pinned back reducing these interactions. Primary alkyl amine examples also produced moderate to good yields with some substrates also requiring

extended reaction times of 2 hours to provide more synthetically useful yields **229** – **235**. The most sterically encumbered examples such as α-methylbenzylamine **229** and *iso*-propyl amine **230** led to the lowest yields and show the sensitivity of this reaction to the size of the nucleophile. Other primary amines without α functionalization provided good yields **231** – **235** especially 4-(2-aminoethyl)-morpholine **287** providing an excellent 85% yield of the product **233** in only 1 hour. Aniline and amino pyridine derivatives **236** – **243** also requiring extended reaction times and the yields being slightly reduced compared to other primary amine examples. This reduction in yield is likely due to their reduced nucleophilicity. The most sterically demanding substrates in this class 2,6-dimethylaniline and 2,4,6-trimethylaniline provided almost identical yields of **236** and **241** in 2 hours with only 1% separating them likely due to the similar size of both amines. Reducing the steric strain to only one flanking methyl group with *o*-toluidine **240** improved the yield significantly to 55% which in fact outperformed *p*-toluidine **243** surprisingly. Another surprising observation is the significant difference in yield for 4-ethoxyanilne **238** and *p*-anisidine **239** of almost 25%. The nucleophilicity and size of these amines is similar and correlating from other examples explored these have been the key factors in determining the yields of the transformation. It is still unclear what leads to this disparity in the reaction outcomes for the production of **238** and **239**.

With a number of amides successfully explored through variation of the amine fragment the substrate scope was expanded through variation of the ester. Returning to the model amine morpholine **120** to investigate a variety of methyl and ethyl esters, initially altering the substitution of benzoate esters (Scheme 3.19).
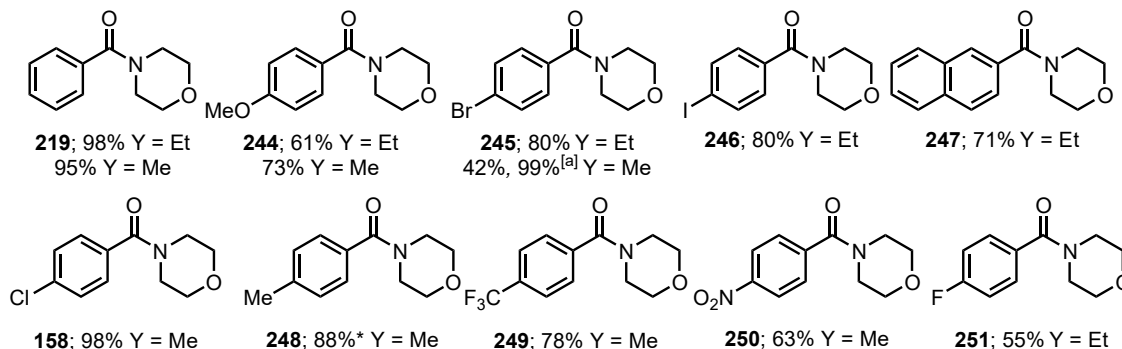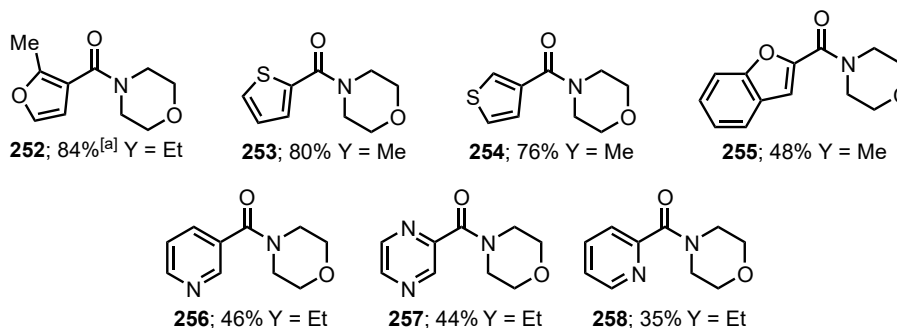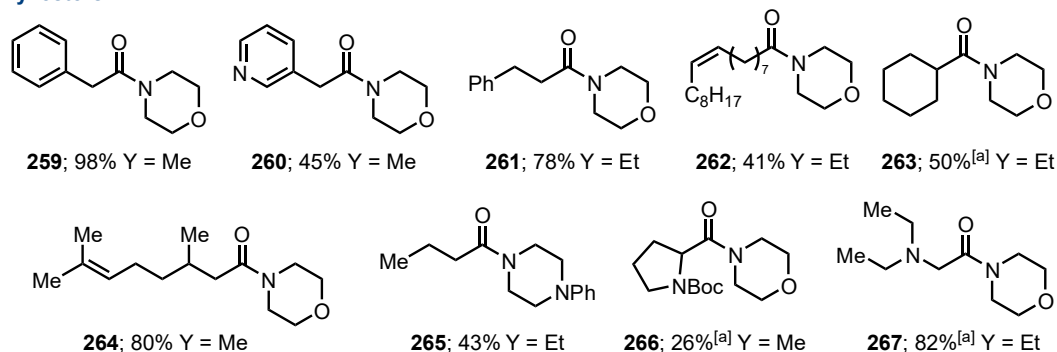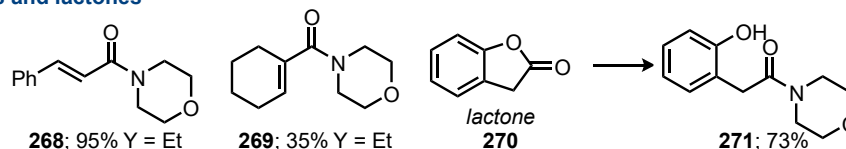
Scheme 3.19 Ester substrate scope.

Benzoate esters provided good to excellent yields with a range of substitutions including electron rich and poor examples **219** – **251**. Comparison of methyl and ethyl esters led to similar yields for substrates where both starting materials had the same initial form. Whereas, for 4-bromobenzoate the methyl ester is a solid at room temperature while the

ethyl ester a liquid. This mismatch in form leads to a significant difference in the reactivity of the esters under the neat ball milling conditions. In 1 hour, the ethyl ester achieves an 80% yield of **245** with the methyl only reaching 42% in the same time frame. Increasing the reaction time to 2 hours for the solid methyl ester resulted in a 99% yield of the amide showing this decreased reactivity could easily be overcome. Heteroaromatic esters were also found to be highly successful in the reaction providing good to excellent yields for a variety of heteroaromatics **252** – **258**. Alkyl esters were also found to be effective partners in this transformation with most examples providing good yields in only 1 hour **259** – **267**. For the amidation of ethyl butyrate, 1-phenylpiperazine was used as an alternate to morpholine **120** due to difficulties in isolating the morpholino amide, using 1-phenylpiperazine a good yield to the alkyl amide **265** could be achieved. Alkyl esters derived from naturally occurring compounds such as oleic acid **262** or amino acids **266** and **267** provided moderate to good yields. Unfortunately for Boc-proline methyl ester complete epimerization of the chiral centre occurred during the reaction. Vinylic esters were also investigated with ethyl cinnamate leading to an excellent yield of **268** whereas ethyl cyclohex-1-ene-1-caxboxylate only could achieve 35% of **269** in 1 hour. Unfortunately, extended reaction times could not improve on the yield of **269**. Finally, the lactone benzofuran-2(3H)-one **270** could be ring opened to produce the linear amide **271** in a very good yield of 73%.

Amines can be stored as ammonium salts as these are often safer and easier to handle solids rather than malodorous and often highly toxic free amines. Ammonium salts can easily then be unveiled as amines during a reaction with the addition of base. As this transformation is base mediated it was proposed by the use of an additional equiv. of base that it may be possible to employ ammonium salts as substrates.
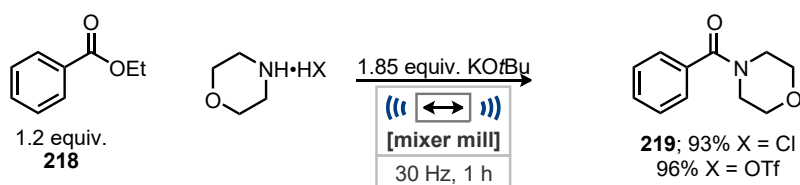

Scheme 3.20 Ammonium chloride and triflate salts as substrates.

With an additional equivalent of potassium *tert*-butoxide in the reaction, chloride and triflate ammonium salts could easily be transferred to these conditions (Scheme 3.20). Both provided excellent yields of the model substrate **219** comparable to that of the optimized reaction conditions using the free amine without lengthening the reaction time.

Due to the large number of amides present in industrially relevant compounds such as pharmaceuticals or other functional materials the substrate scope was continued by attempting to synthesize examples of these compounds using this newly established method (Scheme 3.21).
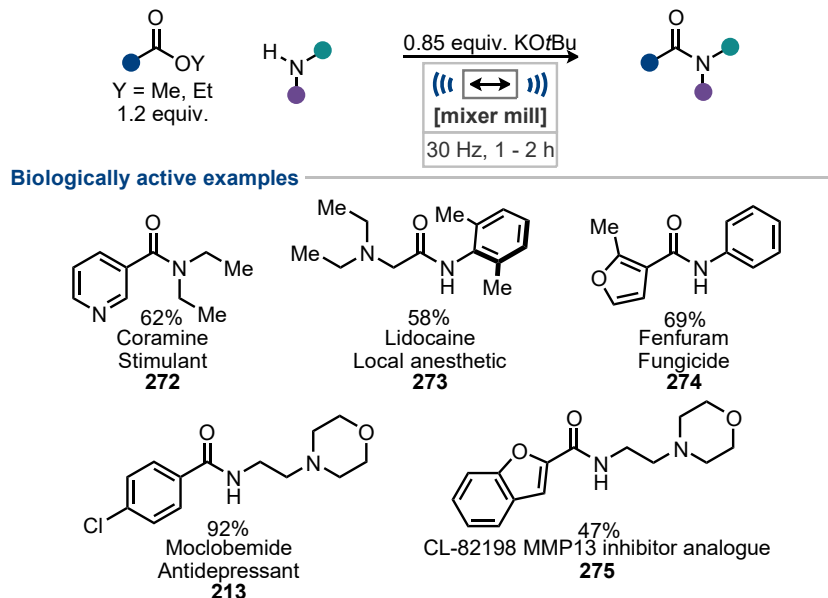
Scheme 3.21 Application to industrially relevant examples.

While exploring biologically active materials good to excellent yields could be achieved for a broad range of functionalities in the synthesis five examples including, moclobemide **213**, coramine **272**, lidocaine **273**, fenfuram **274**, and an analogue of a CL-82198 MMP13 inhibitor **275**. These examples showcase the broad range of amides possible to synthesize using this method with a variety of functionalities present in the ester and amine components of these reactions.

During the substrate scope several examples failed to participate in the reaction, these compounds are presented in Scheme 3.22.
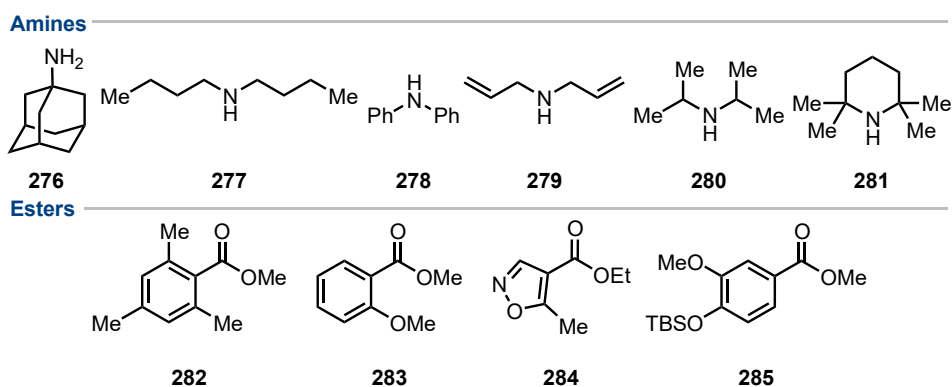
Scheme 3.22 Unproductive amides and esters attempted during the substrate scope.

The only primary amine that was attempted and failed to partake in the reaction was 1-adamantylamine **276**, possibly due to its large size. Secondary amines with flanking substituents larger than ethyl, such as **277** – **279** were unproductive in the reaction providing less than 10% of the amide in 2 hour or more. The low yields could possibly be improved on with longer reaction time, the use of a stronger base, or through elevated reaction temperature. Finally, the highly sterically encumbered 2,2,6,6-tetramethylpiperidine **281** resulted in no detectable amide product and returned the starting materials. Throughout the amines that struggled in the reaction the large size of the nucleophile appears to be the key factor preventing the reaction.

The first ester which did partake in the reaction was methyl 2,4,6-trimethylbenzoate **282** likely due to the pendant methyl groups preventing attack at the carbonyl. The synthesis of amides from this and similar substrates often struggle due to the blocking effect of the methyl groups. Methyl 2-methoxybenzoate **283** which is less sterically encumbered than **282** also failed to produce any product. This could be due to the combined effect on steric encumbrance and a more electron rich aromatic system reducing its electrophilicity. Furthermore, the highly electron rich **285** was unproductive in the reaction producing less than a 10% yield of the product in 2 hours. This slow reaction is likely due to the poor electrophilicity of this ester due its highly electron rich nature. Finally, ethyl 5-methylisoxazole-4-carboxylate **284**, precursor to teriflunomide **212** an immunosuppressant, completely decomposed on addition of potassium *tert*-butoxide demonstrating that to further expand the heterocycle substrate scope alternate bases may be required to prevent decomposition of base sensitive substrates.

3.2.3 Scale Up

The scalability of this process was next to be investigated as this can provide a significant challenge in ball milling synthetic procedures due to the energy provided by the mixer mill does not directly scale when altering the size of the reactor vessel.[63] Initial trials at increasing the scale of the method increased the jar volume to 25 mL (from 14 mL) and the ball mass to 12 g (from 4 g) as these were the largest sizes available at the time. The reaction time (1 h) and frequency (30 Hz) remained the same as to make comparisons to the original scale.
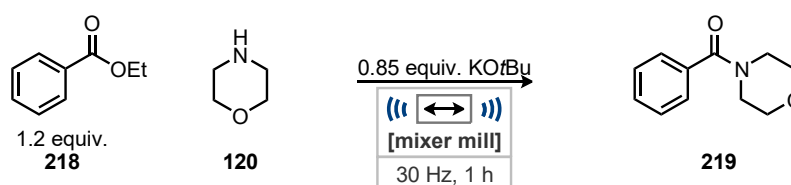
Entry	Scale / mmol	Yield of **219**[a] / %
1	5	93
2	7.5	74

[a] Yield of isolated product.

Table 3.05 Scale up investigation.

Running the reaction at a 5 mmol scale decreased the yield by only 5% compared to the optimized reaction showing that the conditions could easily be transferred to this scale (Table 3.05, entry 1). Although further attempts to increase the scale of the reaction preceded to dwindling returns (Table 3.05, entry 2) possibly indicating the 5 mmol scale was close to the maximum capable for the volume of the milling vessel. Access to larger vessels or heavier milling balls may allow for further increase in scale.

With the success of the increase in the scale of the transformation to 5 mmol using the model substrates these new conditions were applied to the synthesis of moclobemide **213**. Also, due to the mixer mill being able to run two reactions in parallel these new increased scale conditions were carried out in both vessels simultaneously and the reaction mixtures combined.
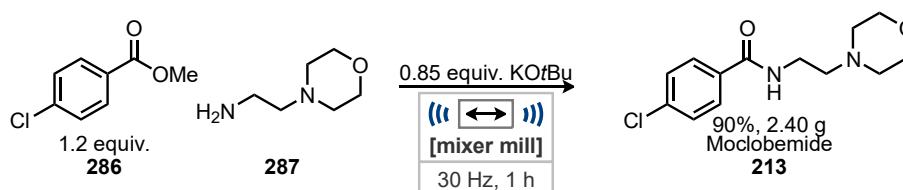

Scheme 3.23 Scale up of moclobemide.

These parallel reactions led to a 90% yield of moclobemide **213** for a total of 2.40 g of the antidepressant, representing a 10-fold increase in the reaction scale, which was still achievable in only 1 h (Scheme 3.23). These initial results in the scale up of this process indicates to the possibility of a directly scalable reaction that is only limited by the milling vessel volumes available.

3.2.4 Leaving Group Variations

Through the substrate scope (Scheme 3.18 - 3.20) it has been demonstrated that methyl and ethyl esters can be effectively amidated with little difference in yields between to two esters so long as the form of the reagents remains the same. Further variation of the leaving group allows its size and leaving group ability to be varied along with the form of the reagent. These variations can be used to compare the effectiveness of these substrates under the solvent free conditions developed. To study these variations a range of benzoate esters bearing different leaving groups of varying size and functionalization's were used under the optimized reaction conditions.
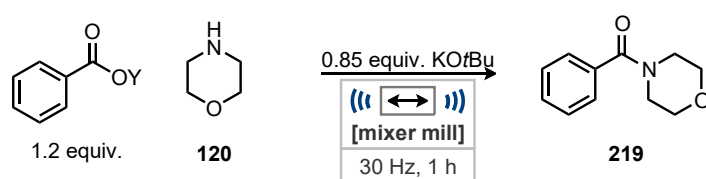
| Entry	Y group	Form	A Value[64]	pKa of alcohol biproduct[62]	Yield of 219[a] / %
1	Methyl	Liquid	1.70	15.5	95
2	Ethyl	Liquid	1.75	16.0	98
3	*iso*-Propyl	Liquid	2.15	16.5	42
4	*tert*-Butyl	Liquid	>4.50	17.0	6
5	Benzyl	Solid	1.81	15.4	70
6	Phenyl	Solid	3.00	9.9	83
7	Menthyl	Solid	-	16.4	5

[a] Yield of isolated product.

Table 3.06 Leaving group variation.

As the size of the leaving group is increased from methyl to *tert*-butyl (Table 3.06, entries 1 – 4) the yield decreases significantly with almost no production of **219** for the largest leaving group. Across these variations the substrates remained liquid at room temperature making their direct comparison straightforward while the remaining leaving groups all provided solid starting materials. The benzyl leaving group (Table 3.06, entry 5) has an A value suggesting only a moderate increase in the size compared to methyl and ethyl though the yield has decreased by almost 30% which could be due to the solid form of the ester starting material. Although the phenyl group (Table 3.06, entry 6) is much larger than that of the benzyl or *iso*-propyl groups the ester containing the phenol leaving group outperformed esters containing these smaller leaving groups. This is due to the phenol group benefiting from a lower pKa than other leaving groups

which is indicative of a more stable anion and greater leaving group ability. Although this substrate is a solid this can be overcome with a more activated leaving group improving the yield. Finally, a menthol derived benzoate ester (Table 3.06, entry 7) was used in the reaction and the large size of this leaving group and solid form of the starting material all but completely prevented the amidation from occurring only reaching only a 5% yield in the reaction.

3.2.5 Stirred Neat and Solution Control Reactions

As the amidation of esters is well known in solution the conditions developed under ball milling were transferred to solution alongside stirring neat. Furthermore, previously reported methods for the amidation of esters utilizing alkoxide bases were also carried out for comparison.[35-36]
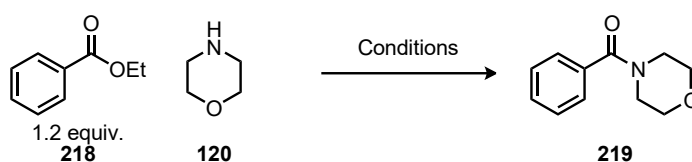
Entry	Conditions	Yield of **219**[a] / %
1	0.85 equiv. KO*t*Bu Stirred neat, 1h	34
2	0.85 equiv. KO*t*Bu 1.0 M EtOH, RT, 1 h	0
3	0.85 equiv. KO*t*Bu 1.0 M EtOH, 78 ˚C, 1 h	8
4	2.0 equiv. KO*t*Bu, 0.1 M THF, RT, 1 h	0 (80[b])[35b]
5	5.0 mol% NaOMe, 4.0 M PhMe, 50 ˚C, 24 h	53 (94[b])[35a]
6	1.5 equiv. NaO*t*Bu Stirred neat, 1h	48 (94)[78]

[a] Yield of isolated product. [b] Piperidine used in place of morpholine. Yields in parentheses are those reported in the original publication of the respective reaction conditions.

Table 3.07 Stirred neat and solution control reactions.

With the ball milling conditions directly transferred to neat stirring (Table 3.07, entry 1) a moderate yield of **219** could be achieved, demonstrating the improved mass transfer within the ball mill for solvent free reactions. With the addition of ethanol as solvent (Table 3.07, entries 2 and 3) no product was observed at room temperature and in refluxing ethanol only 8% of **219** was produced in 1 h. This clearly shows the advantage of carrying this reaction out without solvent as the neat stirring or ball milling conditions outperformed both solution conditions. As the conditions developed in this work had

shown not to transfer to solution or solvent free stirring, procedures that had previously been reported in the literature using alkoxide bases were repeated.

Yoon and coworkers previously reported the rapid amidation of esters in THF using potassium *tert*-butoxide (Table 3.07, entry 4) though when repeated using these conditions no product was observed at room temperature for 1 h. Their report suggested that piperidine could reach 80% yield in the same timeframe, although they did not report the yield for morpholine **120**. Ohshima and coworkers established a sodium methoxide catalysed amidation of esters (Table 3.07, entry 5) and while repeating this method a good yield of 53% could be achieved. But again, this is significantly below the reported yield of 94% achieved with piperidine. Finally, the solvent free method reported by Qin and coworkers was attempted resulting in a good yield of 48% of the amide **219**. This result is also significantly lower than the reported yield of 94% for this reaction. These procedures are clearly challenging to reproduce, or details of the reaction conditions have not been reported fully leading to significant discrepancy. This difficulty may result in the lack of uptake of these methods for synthesis of amides within the chemistry community.

3.3 Conclusion and future work

In conclusion the first base mediated mechanochemical direct amidation of esters has been demonstrated expanding the possible methods for the synthesis of amides under ball milling conditions. The developed method offers an alternative to the use of activating reagents or activated substrates that may require prior synthesis. Furthermore, the substrate scope has shown that the reaction is highly effective towards a broad range of functionality for both esters and amines. This broad scope allowed for the successful synthesis of five biologically active compounds in good yields. The scale up of this procedure though limited by the milling vessel volume has been initially shown to be easily transferable such that 2.40 g of moclobemide **212** could be synthesized in only one hour. Finally, through variation of the leaving group the effects of sterics and form of the starting materials on the reaction could be further investigated and shown to be able to effectively prevent reactions from taking place and slowing down the rate of the reaction when solid starting materials were used or esters containing large enough leaving groups.

The substrate scope is broad for both the ester and amine components, but some more sterically demanding substrates did fail to participate in the reaction. Possibly through further optimization on these more demanding substrates could result in these challenging substrates being included. Further expansion of the scope of the reaction could also be made by application of ammonium chloride as the ammonium salt which may be able to lead to the synthesis of primary amides by this method. Also, through further optimization of the base the reaction could be expanded to sensitive heterocycles which decomposed on addition of potassium *tert*-butoxide. Furthermore, an alternate base may prevent the epimerization observed with the current conditions for chiral esters.

Although the initial results of the scale up of this reaction were promising it is still limited to only relatively small quantities of material. This reaction could potentially benefit through application of twin-screw extrusion as a continuous mechanochemical reactor for scale up to kilogram quantities. This reaction is well suited due to its limited number of components and short reaction time under ball milling conditions. Reactions under similar ball milling conditions have been successfully transferred to this continuous method.[65]

3.4 Bibliography

1. a) E. Massolo, M. Pirola and M. Benaglia, *Eur. J. Org. Chem.*, 2020, **2020**, 4641-4651; b) V. R. Pattabiraman and J. W. Bode, *Nature*, 2011, **480**, 471-479.
2. D. G. Brown and J. Boström, *J. Med. Chem.*, 2016, **59**, 4443-4458.
3. a) S. D. Roughley and A. M. Jordan, *J. Med. Chem.*, 2011, **54**, 3451-3479; b) A. El-Faham and F. Albericio, *Chem. Rev.*, 2011, **111**, 6557-6602; c) E. Valeur and M. Bradley, *Chem. Soc. Rev.*, 2009, **38**, 606-631.
4. J. R. Dunetz, J. Magano and G. A. Weisenburger, *Org. Process Res. Dev.*, 2016, **20**, 140-177.
5. a) M. C. Bryan, P. J. Dunn, D. Entwistle, F. Gallou, S. G. Koenig, J. D. Hayler, M. R. Hickey, S. Hughes, M. E. Kopach, G. Moine, P. Richardson, F. Roschangar, A. Steven and F. J. Weiberth, *Green Chem.*, 2018, **20**, 5082-5103; b) D. J. C. Constable, P. J. Dunn, J. D. Hayler, G. R. Humphrey, J. J. L. Leazer, R. J. Linderman, K. Lorenz, J. Manley, B. A. Pearlman, A. Wells, A. Zaks and T. Y. Zhang, *Green Chem.*, 2007, **9**, 411-420.
6. J. B. Sperry, C. J. Minteer, J. Tao, R. Johnson, R. Duzguner, M. Hawksworth, S. Oke, P. F. Richardson, R. Barnhart, D. R. Bill, R. A. Giusto and J. D. Weaver, *Org. Process Res. Dev.*, 2018, **22**, 1262-1275.
7. G. A. Weisenburger and P. F. Vogt, *Org. Process Res. Dev.*, 2006, **10**, 1246-1250.
8. T. Narendar Reddy, A. Beatriz, V. Jayathirtha Rao and D. P. De Lima, *Chem.: Asian J*, 2019, **14**, 344-388.
9. R. M. Lanigan and T. D. Sheppard, *Eur. J. Org. Chem.*, 2013, **2013**, 7453-7465.
10. X. Wang, *Nat. Catal.*, 2019, **2**, 98-102.
11. C. L. Allen and J. M. J. Williams, *Chem. Soc. Rev.*, 2011, **40**, 3405.
12. C. L. Allen, A. R. Chhatwal and J. M. J. Williams, *Chem. Commun.*, 2012, **48**, 666-668.
13. H. Lundberg, F. Tinnis and H. Adolfsson, *Chem. Eur. J.*, 2012, **18**, 3822-3826.
14. H. Adolfsson, H. Lundberg and F. Tinnis, *Synlett*, 2012, **23**, 2201-2204.
15. D. G. Hall, *Chem. Soc. Rev.*, 2019, **48**, 3475-3496.
16. K. Ishihara, S. Ohara and H. Yamamoto, *J. Org. Chem.*, 1996, **61**, 4196-4197.
17. S. Arkhipenko, M. T. Sabatini, A. S. Batsanov, V. Karaluka, T. D. Sheppard, H. S. Rzepa and A. Whiting, *Chem. Sci.*, 2018, **9**, 1058-1072.
18. K. Arnold, A. S. Batsanov, B. Davies and A. Whiting, *Green Chem.*, 2008, **10**, 124-134.
19. a) N. Gernigon, R. M. Al-Zoubi and D. G. Hall, *J. Org. Chem.*, 2012, **77**, 8386-8400; b) R. M. Al-Zoubi, O. Marion and D. G. Hall, *Angew. Chem. Int. Ed.*, 2008, **47**, 2876-2879.
20. S. Fatemi, N. Gernigon and D. G. Hall, *Green Chem.*, 2015, **17**, 4016-4028.
21. D. J. C. Constable, P. J. Dunn, J. D. Hayler, G. R. Humphrey, J. J. L. Leazer, R. J. Linderman, K. Lorenz, J. Manley, B. A. Pearlman, A. Wells, A. Zaks and T. Y. Zhang, *Green Chem.*, 2007, **9**, 411-420.
22. C. W. Cheung, M. L. Ploeger and X. Hu, *Nat. Commun.*, 2017, **8**, 14878.
23. T. Ben Halima, J. K. Vandavasi, M. Shkoor and S. G. Newman, *ACS Catal.*, 2017, **7**, 2176-2180.
24. S. Shi and M. Szostak, *Chem. Commun.*, 2017, **53**, 10584-10587.
25. a) L. Ielo, V. Pace, W. Holzer, M. M. Rahman, G. Meng, R. Szostak and M. Szostak, *Chem. Eur. J.*, 2020, **26**, 16246-16250; b) M. Szostak and G. Li, *Synthesis,* 2020, **52**, 2579-2599; c) C. Liu and M. Szostak, *Chem. Eur. J.*, 2017, **23**, 7157-7173.
26. L. Hie, N. F. Fine Nathel, X. Hong, Y.-F. Yang, K. N. Houk and N. K. Garg, *Angew. Chem. Int. Ed.*, 2016, **55**, 2810-2814.

27. a) Y.-L. Zheng and S. G. Newman, *ACS Catal.*, 2019, **9**, 4426-4433; b) T. Ben Halima, J. Masson-Makdissi and S. G. Newman, *Angew. Chem. Int. Ed.*, 2018, **57**, 12925-12929.
28. M. Movassaghi and M. A. Schmidt, *Org. Lett.*, 2005, **7**, 2453-2456.
29. X. Yang and V. B. Birman, *Org. Lett.*, 2009, **11**, 1499-1502.
30. K. E. Price, C. LarrivéE-Aboussafy, B. M. Lillie, R. W. McLaughlin, J. Mustakis, K. W. Hettenbach, J. M. Hawkins and R. Vaidyanathan, *Org. Lett.*, 2009, **11**, 2003-2006.
31. C. Sabot, K. A. Kumar, S. Meunier and C. Mioskowski, *Tetrahedron Lett.*, 2007, **48**, 3863-3866.
32. J. L. Vrijdag, F. Delgado, N. Alonso, W. M. De Borggraeve, N. Pérez-Macias and J. Alcázar, *Chem. Commun.*, 2014, **50**, 15094-15097.
33. G. Li and M. Szostak, *Nat. Commun.*, 2018, **9**.
34. G. Li, C.-L. Ji, X. Hong and M. Szostak, *J. Am. Chem. Soc.*, 2019, **141**, 11161-11172.
35. a) T. Ohshima, Y. Hayashi, K. Agura, Y. Fujii, A. Yoshiyama and K. Mashima, *Chem. Commun.*, 2012, **48**, 5434; b) J. Park, Y.-J. Yoon, B. Kim, H.-G. Lee, S.-B. Kang, G. Sung, J.-J. Kim and S.-G. Lee, *Synthesis*, 2012, **44**, 42-50.
36. R. Zhang, W.-Z. Yao, L. Qian, W. Sang, Y. Yuan, M.-C. Du, H. Cheng, C. Chen and X. Qin, *Green Chem.*, 2021, DOI: 10.1039/d1gc00720c.
37. N. Caldwell, C. Jamieson, I. Simpson and A. J. B. Watson, *ACS Sustain. Chem. Eng.*, 2013, **1**, 1339-1344.
38. R. M. De Figueiredo, J.-S. Suppo and J.-M. Campagne, *Chem. Rev.*, 2016, **116**, 12029-12122.
39. Y. Tamaru, Y. Yamada and Z.-I. Yoshida, *Synthesis*, 1983, **1983**, 474-476.
40. Y. Suto, N. Yamagiwa and Y. Torisawa, *Tetrahedron Lett.*, 2008, **49**, 5732-5735.
41. T. Naota and S.-I. Murahashi, *Synlett*, 1991, **1991**, 693-694.
42. S. Muthaiah, S. C. Ghosh, J.-E. Jee, C. Chen, J. Zhang and S. H. Hong, *J. Org. Chem.*, 2010, **75**, 3002-3006.
43. C. Gunanathan, Y. Ben-David and D. Milstein, *Science*, 2007, **317**, 790.
44. a) J. W. Bode and S. S. Sohn, *J. Am. Chem. Soc.*, 2007, **129**, 13798-13799; b) H. U. Vora and T. Rovis, *J. Am. Chem. Soc.*, 2007, **129**, 13796-13797.
45. a) S. De Sarkar and A. Studer, *Org. Lett.*, 2010, **12**, 1992-1995; b) S. Kuwano, S. Harada, R. Oriez and K.-I. Yamada, *Chem. Commun.*, 2012, **48**, 145-147.
46. A. Brennführer, H. Neumann and M. Beller, *Angew. Chem. Int. Ed.*, 2009, **48**, 4114-4133.
47. Y. Ben-David, M. Portnoy and D. Milstein, *J. Am. Chem. Soc.*, 1989, **111**, 8742-8744.
48. J. R. Martinelli, T. P. Clark, D. A. Watson, R. H. Munday and S. L. Buchwald, *Angew. Chem. Int. Ed.*, 2007, **46**, 8460-8463.
49. a) L. Wu, X. Fang, Q. Liu, R. Jackstell, M. Beller and X.-F. Wu, *ACS Catal.*, 2014, **4**, 2977-2989; b) R. Grigg and S. P. Mutton, *Tetrahedron*, 2010, **66**, 5515-5548.
50. C. Sambiagio and T. Noël, *Trends Chem.*, 2020, **2**, 92-106.
51. a) N. Schneider, D. M. Lowe, R. A. Sayle, M. A. Tarselli and G. A. Landrum, *J. Med. Chem.*, 2016, **59**, 4385-4402; b) M. T. Sabatini, L. T. Boulton, H. F. Sneddon and T. D. Sheppard, *Nat. Catal.*, 2019, **2**, 10-17.
52. a) C. Duangkamol, S. Jaita, S. Wangngae, W. Phakhodee and M. Pattarawarapan, *RSC Adv.*, 2015, **5**, 52624-52628; b) V. Strukil, B. Bartolec, T. Portada, I. Dilovic, I. Halasz and D. Margetic, *Chem. Commun.*, 2012, **48**, 12100-12102.
53. a) T. X. Metro, J. Bonnamour, T. Reidon, J. Sarpoulet, J. Martinez and F. Lamaty, *Chem. Commun.*, 2012, **48**, 11781-11783; b) V. Porte, M. Thioloy, T. Pigoux, T.-X. Métro, J. Martinez and F. Lamaty, *Eur. J. Org. Chem.*, 2016, **2016**, 3505-3508; c) Y. Yeboue, M. Jean, G. Subra, J. Martinez, F. Lamaty and T. X. Metro, *Org. Lett.*, 2021, **23**, 631-635.

54.   T. Dalidovich, K. A. Mishra, T. Shalima, M. Kudrjašova, D. G. Kananovich and R. Aav, *ACS Sustain. Chem. Eng.*, 2020, **8**, 15703-15715.
55.   a) N. Cindro, M. Tireli, B. Karadeniz, T. Mrla and K. Užarević, *ACS Sustain. Chem. Eng.*, 2019, **7**, 16301-16309; b) L. Gonnet, T. Tintillier, N. Venturini, L. Konnert, J.-F. Hernandez, F. Lamaty, G. Laconde, J. Martinez and E. Colacino, *ACS Sustain. Chem. Eng.*, 2017, **5**, 2936-2941; c) G. Kaupp, J. Schmeyers and J. Boy, *Tetrahedron*, 2000, **56**, 6899-6911.
56.   a) J. Bonnamour, T.-X. Métro, J. Martinez and F. Lamaty, *Green Chem.*, 2013, **15**, 1116-1120; b) Y. Yeboue, B. Gallard, N. Le Moigne, M. Jean, F. Lamaty, J. Martinez and T.-X. Métro, *ACS Sustain. Chem. Eng.*, 2018, **6**, 16001-16004.
57.   V. R. Declerck, P. Nun, J. Martinez and F. D. R. Lamaty, *Angew. Chem. Int. Ed.*, 2009, **48**, 9318-9321.
58.   J. G. Hernandez and E. Juaristi, *J. Org. Chem.*, 2010, **75**, 7107-7111.
59.   R. Mocci, E. Colacino, L. D. Luca, C. Fattuoni, A. Porcheddu and F. Delogu, *ACS Sustain. Chem. Eng.*, 2021, **9**, 2100-2114.
60.   a) K. J. Ardila-Fierro, D. E. Crawford, A. Körner, S. L. James, C. Bolm and J. G. Hernández, *Green Chem.*, 2018, **20**, 1262-1269; b) J. G. Hernández, K. J. Ardila-Fierro, D. Crawford, S. L. James and C. Bolm, *Green Chem.*, 2017, **19**, 2620-2625.
61.   Q. Cao, W. I. Nicholson, A. C. Jones and D. L. Browne, *Org. Biomol. Chem.*, 2019, **17**, 1722-1726.
62.   D. H. Ripin and D. A. Evans, https://tinyurl.com/78uxjta5, (accessed 16/06/2021, 2021).
63.   A. Stolle, R. Schmidt and K. Jacob, *Faraday Discuss.*, 2014, **170**, 267-286.
64.   J. A. Hirsch, in *Topics in Stereochemistry*, eds. N. L. Allinger and E. L. Eliel, Wiley, New York, 1967, pp. 199-222.
65.   Q. Cao, J. L. Howard, D. E. Crawford, S. L. James and D. L. Browne, *Green Chem.*, 2018, **20**, 4443-4447.

4   Reductive Coupling of Electron Poor Alkenes

4.1   Introduction to Alternate Reactivity

Opportunities for chemical activation by mechanical force have been well established across a broad range of chemistry and material sciences.[1] These have allowed multiple disciplines to utilize mechanochemical approaches for the induction of chemical change within; organic, inorganic, medicinal, and organometallic chemistry. Many of these approaches have been complementary towards more traditional chemical activation methods such as thermal- or photo- chemistry. Although examples of contrasting reactivity have been demonstrated sporadically.

The earliest examples of alternate reactivity observed through the application of mechanical energy came from inorganic chemistry. Lea and coworkers reported the decomposition of silver halide salts upon grinding whereas heating simply led to the melting of these compounds.[2] Another example from inorganic chemistry came from Boldyrew and coworkers through an investigation detailing the decomposition of alkali metal bromates.[3] Mechanical treatment of the alkali metal bromates led to an entirely different decomposition pathway than the thermally induced reaction. The new pathway was found to resemble more closely that of the irradiative decomposition.

Currently examples of novel reactivity through mechanochemical methods are limited and as such it is extremely challenging to predict when new reactivity or alternate product formations will occur.[4] Most discoveries of differing reaction pathways being accessed mechanochemically have been serendipitous, rather than predicted.

Further investigations into new reactivity will allow a greater understanding and may permit predictability of the outcomes to be achieved. This could then give access to materials not accessible to solution chemistry as the reactivity relies on mechanical activation.

4.1.1   Alternate and New Reactivity Discovered *via* Ball Milling

Discussion of various examples of new reactivity and alternate products undertaken mechanochemically follows. The examples chosen demonstrate the broad range of areas in which these discoveries have been made.

The synthesis of cyclopalladated compounds has been studied extensively due to the wide applications of these compounds in organic synthesis, catalysis, and for functional

materials with bioactive or photoluminescent properties.[5] Through work exploring the first solid state transition-metal mediated C-H bond activation Ćurić and co-workers discovered the synthesis of the doubly palladated complex **290** via the monopalladated intermediate **289**, which is the major product of this C-H activation in solution (Scheme 4.01).[6] Attempts were made to synthesize the new complex **290** in solution, but all attempts only furnished the previously reported monopalladated complex **289**. Through this work *in situ* raman spectroscopy was used to optimize the reaction conditions such that quantitative yields of **289** and **290** could be achieved in 4.5 or 7.5 h respectively. This is in contrast to the solution conditions which require 3 days for the synthesis of **289**.[5a] They suggest that this methodology could be used for the generation of catalytic systems for the functionalization of C-H bonds that are not hampered by the need of suitable solubility but can be used in the absence of solvent.
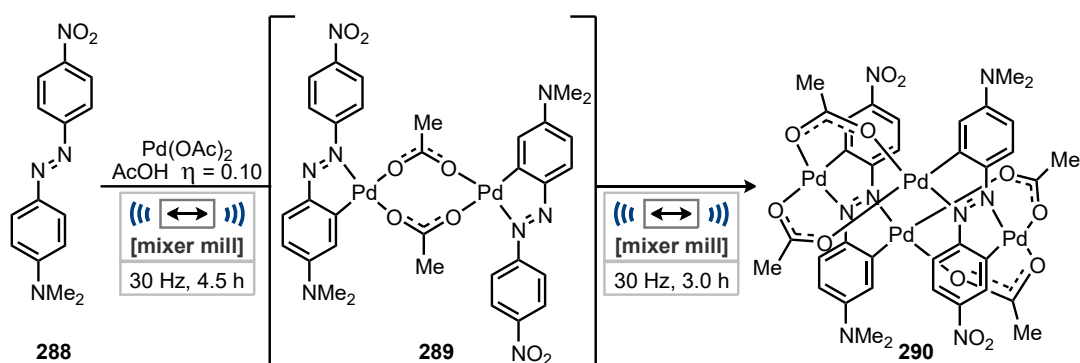
Scheme 4.01 New products accessed through C-H bond activation through ball milling.

The importance of cyclophosphazanes arises from their structural versatility with applications as multi-dentate ligands[7], catalysts for organic synthesis[8], and antitumor drugs[9]. The synthesis of adamantoid phosphazanes as well as other non-carbon covalent structures remains an underdeveloped area of synthesis due to their high moisture and air sensitivity.[10] García and co-workers explored the synthesis of these challenging molecules with the use of ball milling from their double decker macrocyclic isomers **291** and **293** (Scheme 4.02).[11] Under solution conditions the *iso*-propyl functionalised isomer **292** has only been prepared through very harsh conditions requiring heating neat at 160 °C for 12 days.[12] The ball milling synthesis of this compound could be achieved in only 90 mins with lithium chloride being used as an additive. Furthermore, the same structure bearing *tert*-butyl groups **294**, previously considered a textbook example of a sterically inaccessible molecule in main-group chemistry, was also synthesized for the first time under the same ball milling conditions.[13] These results demonstrate a break-through for main group chemistry by the application of mechanochemical synthesis to access new materials thought to be inaccessible.

Although, it is still not yet understood how the mechanical activation of these compounds occurs.
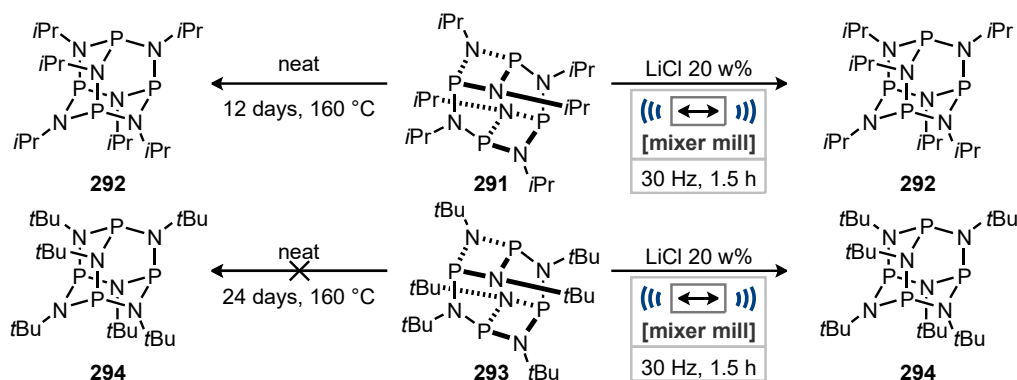
Scheme 4.02 Mechanical activation of cyclophosphazanes.

The synthesis of sulfonyl guanidines, an important functional group for pharmaceuticals[14] and herbicides[15], is traditionally carried out from activated sulfonyl or carbodiimide derivatives.[14, 16] Friščić and co-workers following on from their established copper catalysed coupling of sulfonamides and isocyanates[17], have developed a synthesis of sulfonyl guanidines.[18] Inactivated arylsulfonamides and carbodiimides were coupled using a copper(I) catalyst with nitromethane or acetone as a liquid additive (Scheme 4.03). The method established by ball milling could not be reproduced under any solution conditions, which at best only achieved minimal conversion. This increased reactivity demonstrates the necessity of ball milling to effectively carry out this reaction. Initial mechanistic analysis of the reaction suggested activation of the carbodiimide π-system through coordination with the copper catalyst with further investigations ongoing to elucidate the requirement of ball milling for this transformation.
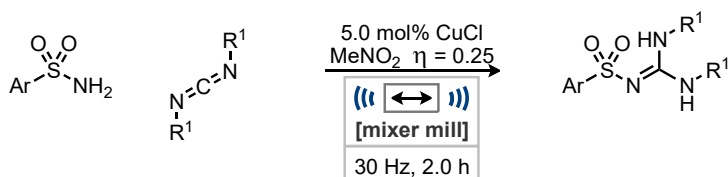

Scheme 4.03 Synthesis of sulfonyl guanidines by ball milling.

Currently there are limited examples of alternate or new reactivity that has been accessed by ball milling. This is likely due to the serendipitous nature of many of these discoveries and as of yet predicting when this new or alternate reactivity will exist is not possible. Investigating these transformations may allow for a greater level of understanding of why this new reactivity is observed and then allow for its prediction.

4.1.2 Previous Work

Prior work in the group discovered the dimerization of benzylidene malonates **295** while investigating the generation of organomanganese halides from alkyl halides and manganese metal (Scheme 4.04).[19] In this work ethyl 4-bromobutyrate **294** was proposed to generate the organomanganese halide while using lithium chloride and THF as additives. The generated nucleophile could then attack diethyl benzylidene malonate **295** via a conjugate addition to form a new C-C bond, although this desired product has not yet been observed.
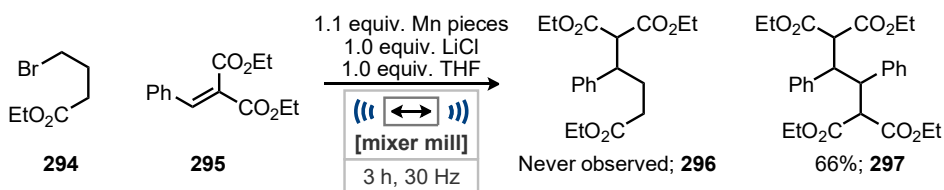
Scheme 4.04 Initial observation of reductive dimerization. Results obtained by Dr Joseph L. Howard.

4.1.3 Reductive Dimerisations

This unexpected reactivity is similar to previous work from Cahiez and co-workers who had shown the β-reductive dimerization of 2-cyclohexen-1-one **299** by dibutyl manganese **298** (Table 4.01).[20] The authors reported a significant temperature dependence on the product selectivity, with reactions at higher temperature leading to largely the dimerized product **301** over the desired conjugate addition **300**. Although this dimerization process was exclusively observed for 2-cyclohexen-1-one derived substrates and was not displayed by benzylidene malonates which exclusively led to the 1,4-addition product regardless of temperature.
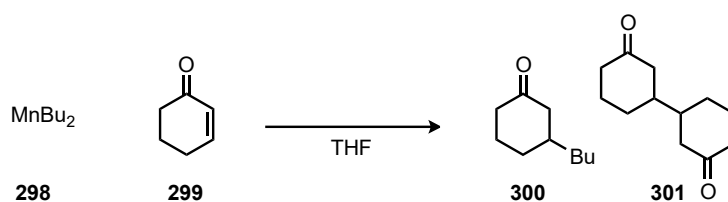
Entry	Temperature / ˚C	Yield of **300** / %	Yield of **301** / %
1	20	29	68
2	-30	70	25

**Table 4.01** Previous observation of reductive dimerization by Cahiez and co-workers.

Further investigation into the β-reductive dimerization of 2-cyclohexen-1-one derivatives by Cahiez and co-workers established a poor synthetic scope for the transformation. Such that 2-cyclohexen-1-one **299** and isophorone **302** were the only compounds leading to satisfactory yields of the dimerization. Other 2-cyclohexen-1-one derivatives led to poor yields due to considerable amounts of the addition products with the organomanganese. Through their further investigations they found that the reaction could be catalysed by dialkyl manganese through experiments using a catalytic quantity of a manganese(II) chloride and 2.5 equivalents of butyl magnesium chloride (Scheme 4.05).[20-21]
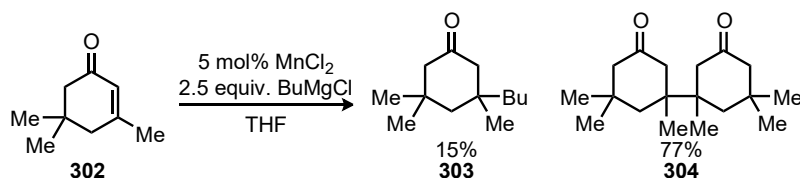
**Scheme 4.05** Catalytic dimerization of isophorone via dialkyl organomanganese.

The dimerization of diethyl benzylidene malonate **295** has also been previously observed by Nishiguchi and co-workers in 2011 while developing a method for the carboxylation of ethyl cinnamate with magnesium and carbon dioxide (Scheme 4.06).[22] This reaction provided the dimer as part of a mixture of products resulting from both the desired carboxylation **304** and the reduction of the double bond **305**. They suggest that a single electron reduction of the substrate provides a radical anion intermediate which can either undergo dimerization or further reduction to generate the nucleophile that may then attack carbon dioxide or become protonated. Although there is no report of dimerization of the less activated cinnamate esters which only underwent carboxylation and reduction of the double bond.
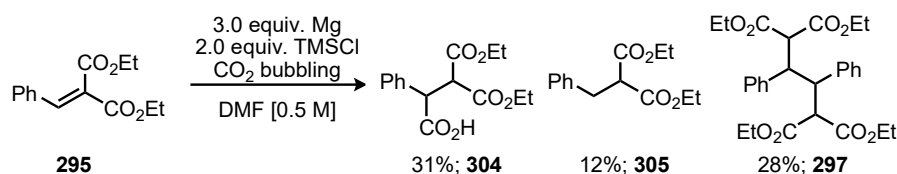
Scheme 4.06 Dimerization observed through reduction of benzylidene malonates by magnesium.

Yamashita and co-workers have also established dimerization reaction using samarium(II) diiodide as the single electron reductant (Scheme 4.07).[23] The radical conjugate addition dimerization reaction was applicable to a small number of activated double bonds including alkylidene and benzylidene malonates. Zhang and co-workers also established a similar dimerization process employing samarium(II) diiodide.[24] They also found the samarium(II) diiodide mediated reaction to be applicable to a small range of benzylidene and alkylidene malonates.
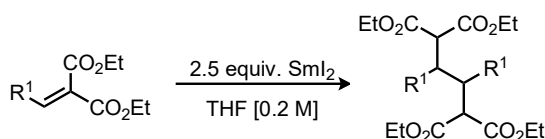
Scheme 4.07 Samarium diiodide mediated dimerization of benzylidene malonates.

More recently Scheidt and co-workers have undertaken a rigorous development of the functionalization of benzylidene malonates through the use of photoredox and Lewis acid cooperative catalysis (Scheme 4.08).[25] Their initial report regarded the intermolecular radical-radical cross-coupling, for the alkylation of the benzylidene malonates (Scheme 4.08a). This method avoided the previously reported radical conjugate addition for the synthesis of the dimers. They expanded on the range of possible transformations to include arylation of the generated radical (Scheme 4.08b) and an annulation reaction (Scheme 4.08c) from difunctionalized arylidene malonates. They also demonstrated the formation of dimers through a radical-radical coupling when tributylamine was used as the reductive quench for the photocatalyst. Finally, the reduction of the double bond in benzylidene malonates could be carried out selectively when the organic photocatalyst DPAIPN **306** was exchanged for the iridium-based system **307**. In these examples from Scheidt and co-workers the application of Lewis or Bronsted acids to activate the benzylidene malonate system was key to successful reactions; this activation was shown to lower the reduction potentials of the substrates through cyclic voltammetry measurements.
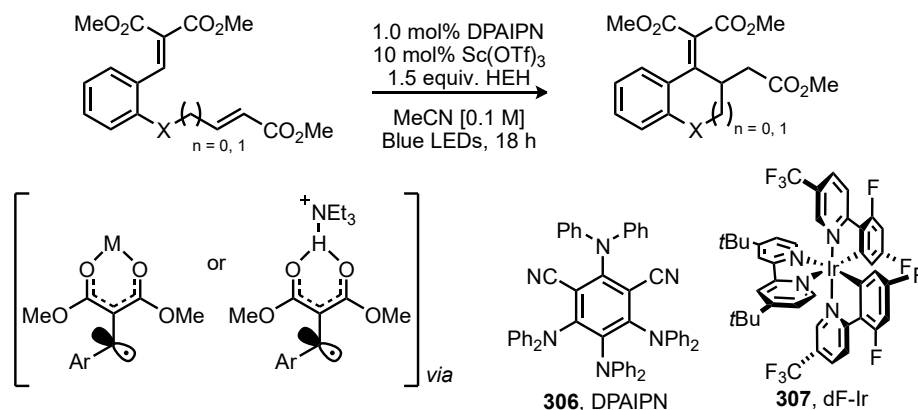
a) Radical-radical coupling of arylidene malonates via cooperative lewis acid photoredox catalysis.
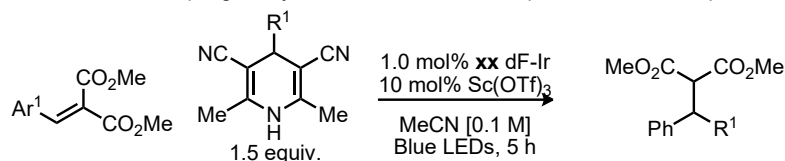
b) Radical arylation of arylidene malonates via photoredox catalysis
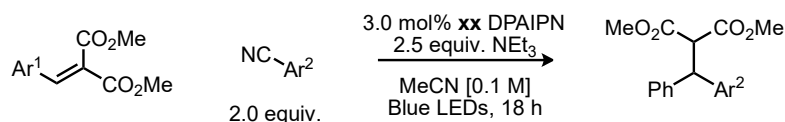
c) Reductive annulation of arylidene malonates via cooperative lewis acid photoredox catalysis.

Scheme 4.08 Photoredox reduction of benzylidene malonate derivatives.

Previously Cahiez and coworkers established a reductive dimerization of 2-cyclohexen-1-one derivatives but found the reaction unamenable to the dimerization of benzylidene malonates. [20] More recently stronger reducing agents such as magnesium or samarium(II) diiodide have been able to enable this dimerization via proposed radical-radical coupling. [22-24] Schiedt and coworkers have since gone on to utilize photoredox catalysis for the functionalization of arylidene malonates via the benzyl radical intermediate.[25] Currently ball milling has established conditions under which manganese can facilitate the dimerization of benzylidene malonates potentially revealing increased reactivity of the metal under ball milling conditions. In this work the established reaction will be optimized, and its mechanism studied.

4.2 Results and discussion

4.2.1 Investigation of Manganese Induced Reductive Dimerization

To aid in the optimization of the newly discovered reaction diethyl benzylidene malonate **295**, was exchanged for a fluorine labelled variant **308**, so that ^{19}F NMR spectroscopy could be used for analysis of the crude reaction mixture and determine yields utilizing an internal standard. Initial control reactions were focused on determining the necessity of each of the reagents (Table 4.02).

Entry	Variation of conditions	Conversion of 308[a] / %	Yield of 309[a] / %	Yield of 310[a] / %
1	No variation	100	0	85
2	Mn pieces omitted	0	0	0
3	LiCl omitted	5	0	0
4	THF omitted	12	0	0
5	**294** omitted	28	-	10

[a] Determined by ^{19}F NMR spectroscopy using α,α,α-trifluorotoluene as an internal standard.

Table 4.02 Variation of discovered reaction conditions.

The fluorinated substrate achieved a greater yield of 85% (Table 4.02, entry 1) than the unfunctionalized phenyl derivative (66%) that was used to when this reactivity was discovered. This increased reactivity could be due to the inductive electron withdrawing ability of the fluorine atom which may aid reduction.[26] With any variation in these conditions the reaction yield was dramatically decreased (Table 4.02, entries 2 – 5). With the reductant manganese removed (Table 4.02, entry 2) no conversion was observed showing no background reaction from the stainless-steel jar and ball, and no side reactions caused by any other reagents present. With lithium chloride omitted (Table 4.02, entry 3) conversion was significantly reduced and no product formation was observed. This could be due to the lithium cation acting as a Lewis acid, possibly activating the substrate by decreasing the reduction potential, as observed by Scheidt and co-workers using scandium(III) triflate or ammonium salts.[25] The liquid additive THF was also found to be vital for the transformation and without it (Table 4.02, entry 4) there

was a significant decrease in the conversion of the starting material producing a complex mixture of products. Finally, a reduced yield of only 10% was observed with ethyl 4-bromobutyrate **294** omitted (Table 4.02, entry 5) suggesting it may not be directly involved in the mechanism to generate the dimer **310**.

With the uncovered conditions shown to require all the reagents, attention was switched to attempting to change the reaction selectivity to the initially desired conjugate addition. Multiple examples from the literature display alternating liquid additives can alter the product selectivity or improve on reaction yields.[27] Liquid additives were screened to see what effects could be observed by changing the polarity and coordinating abilities of the solvents (Table 4.03).

Entry	Liquid additive	ε_r	Conversion of **308**[a] / %	Yield of **309**[a] / %	Yield of **310**[a] / %
1	Et$_2$O	4.27	15	0	trace
2	THF	7.58	100	0	85
3	DCM	8.93	8	0	0
4	iPrOH	17.9	100	0	67
5	NMP	32.2	32	0	15
6	DMF	36.7	8	0	0
7	MeCN	37.5	25	0	0

[a] Determined by ^{19}F NMR spectroscopy using α,α,α-trifluorotoluene as an internal standard.
Table 4.03 Screen of different liquid additives (LAG).

Utilizing different liquid additives failed to alter the selectivity of the reaction to the conjugate addition product **309**, though (Table 4.03, entries 1 – 7) some of the screened examples still allowed access to the dimer product (Table 4.03, entries 2, 4, and 5). This reaction manifold is sensitive, with highly polar and strongly coordinating solvents such as DMF and acetonitrile (Table 4.03, entries 6 – 7) preventing any products from forming. Furthermore, the moderately polar solvent DCM (Table 4.03, entry 3), with a similar dielectric constant to that of THF, prevented the reaction occurring. This may be due to it not being a coordinating solvent. However, THF which is moderately polar, and coordinating does provide sufficient reaction conditions for complete conversion and a high yield of the product (Table 4.03, entry 2) but diethyl ether which is also an ethereal

solvent does not lead to significant conversion (Table 4.03, entry 1). The only other additive which led to quantitative conversion of **308** was *i*PrOH (Table 4.03, entry 4) which is slightly more polar than THF and able to coordinate through oxygen. Also, if any organometallic intermediates were present its likely that *i*PrOH would be able to protonate them. The need for a coordinating liquid additive suggests the possibility of organometallic intermediates that require the stabilization of solvation from a coordinating solvent.[28] All examples of liquid additives that allowed the dimerization to take part are moderately to strongly coordinating and that reactivity seems to be limited by the addition of the most and least polar additives as well as the most strongly coordinating.[28]

The role of ethyl 4-bromobutyrate **294** in the reaction was then investigated as it had not been observed to take part in its proposed chemistry. It had already been demonstrated not to be crucial to the reaction proceeding (Table 4.02, entry 5).
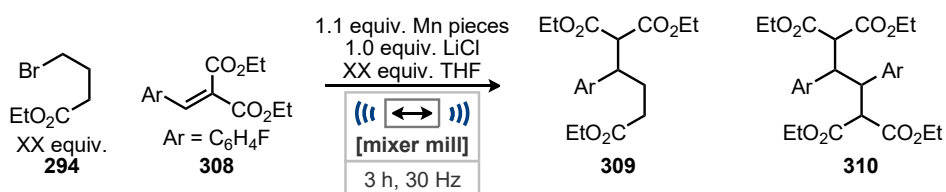
Entry	Equiv. of **294**	Equiv. of THF	Conversion of **308**[a] / %	Yield of **309**[a] / %	Yield of **310**[a] / %
1	1.0	1.0	100	0	85
2	0.5	1.0	100	0	86
3	0	1.0	28	-	10
4	0	2.0	100	-	80 (80[b])
5	0	3.0	62	-	43

[a] Determined by ^{19}F NMR spectroscopy using α,α,α-trifluorotoluene as an internal standard.
[b] Yield of isolated product.

Table 4.04 Determination of role of ethyl 4-bromobutyrate **294**.

Initial reduction in the stoichiometry of **x** to from 1 to 0.5 equivalents (Table 4.04, entries 1 and 2) the reaction yield marginally increased from 85% to 86% but with **294** completely removed from the reaction formation of the product almost entirely ceased (Table 4.04, entry 3). It is well known in ball milling reactions altering the amount or form of material present in the reaction can have drastic implications for the mixing and energy transfer, and therefore reaction outcomes.[27d, 29] To correct for the smaller quantity of liquid with **294** omitted, an additional equivalent of THF was used (Table 4.04, entry 4), improving the yield of **310** to 80% but further increasing the equivalence of THF did not lead to any further improvements (Table 4.04, entry 5). These results suggest that **294** was simply

acting as a liquid additive and possibly taking no other part in the dimerization reaction. Although with the presence of ethyl 4-bromobutyrate **294** the reaction produced a marginally improved yield it was decided that moving forward that (Table 4.04, entry 4) using 2 mmol of THF would be taken forward for simplicity. Also, this would prevent the possibility of organomanganese halides being generated from the alkyl halide. Further investigations into the ball milling generation of organomanganese halides from manganese metal and alkyl halides is presented in chapter 5.

As the likely role of ethyl 4-bromobutyrate **294** had been deciphered, the reductant would be the next attribute of the conditions to be optimized (Table 4.05).
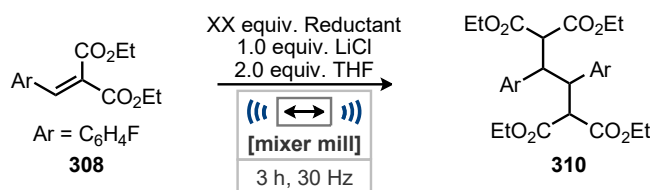
Entry	Reductant	Equiv. of reductant	Conversion of **308**[a] / %	Yield of **310**[a] / %
1	Mn pieces	0.55	69	47
2	Mn pieces	1.1	100	80 (80[b])
3	Mn pieces	2.0	100	63
4	Zn granular	1.1	83	43
5	Mn powder	1.1	100	79 (78)

[a] Determined by ^{19}F NMR spectroscopy using α,α,α-trifluorotoluene as an internal standard.
[b] Yield of isolated product.

Table 4.05 Optimization of reductant.

Altering the stoichiometry of the manganese in the reaction led to decreased yields of the product (Table 4.05, entries 1 and 3). With the stoichiometry reduced full conversion of the starting material **308** was not achieved and an increase in manganese in the reaction led to significant degradation of the product. Upon changing the reductant to zinc metal, the reaction still took place albeit in reduced yield, this is most likely due to the greater reduction potential of manganese metal over zinc. As previous examples using ball milling to activate metals have shown improved tolerance to the starting form of the metal over solution conditions this was also explored.[30] Unfortunately compared to other metals fewer forms of manganese metal are commercially available that would be applicable to use in a ball mill. Manganese powder, 40 mesh, is similarly reactive than the irregular pieces form (Table 4.05, entry 5) with 79% yield of **310** still being produced.

This has again confirmed that through the use of ball milling different forms of metals can be used without significant change in reactivity.[30]

With seemingly optimal conditions for the stoichiometry and form of the reductant in place (Table 4.05, entry 2) optimization continued with the Lewis acid activator.
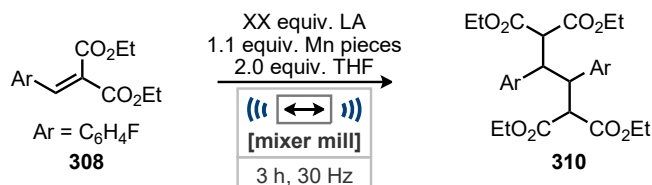
Entry	Lewis acid	Equiv. of Lewis acid	Conversion of 308[a] / %	Yield of 310[a] / %
1	Mg(OTf)$_2$	1.0	<1	0
2	MnCl$_2$•4H$_2$O	1.0	<1	0
3	Mn(OTf)$_2$	1.0	4	0
4	ZnCl$_2$	1.0	78	63
5	Sc(OTf)$_3$	1.0	9	0
6	LiBr	1.0	68	66
7	LiI	1.0	25	0
8	LiOTf	1.0	<1	0
9	LiCl	1.0	95	83 (80[b])
10	LiCl	0.5	83	72
11	LiCl	1.5	71	68

[a] Determined by ^{19}F NMR spectroscopy using α,α,α-trifluorotoluene as an internal standard.
[b] Yield of isolated product.

Table 4.06 Optimization of Lewis acid.

Lewis acids were selected that had been reported to activate 1,3-bicarbonyl systems including those demonstrated by Schiedt and co-workers.[25] Magnesium and manganese salts (Table 4.06, entries 1 – 3) led to no product formation potentially due to not adequately activating the system. Zinc(II) chloride (Table 4.06, entry 4) led to the greatest conversion of all the newly screened Lewis acids but led to significant amount of an unidentified side product. Further investigation into this unidentified side product is reported in table 4.08. Surprisingly, scandium(III) triflate (Table 4.06, entry 5) which has been reported as the most effective Lewis acid for similar systems prevented the reaction from occurring in the ball mill. This is potentially due to poor mass transfer in this reaction due to the large molecular weight of scandium(III) triflate, 492 gmol[-1], compared to only 42 gmol[-1] for the optimal lithium chloride. The large quantity of scandium(III) triflate required led to the jar being over filled preventing efficient mass and energy transfer.

Lithium salts (Table 4.06, entries 6 – 9) showed a similar trend that with higher molecular weight halides, or pseudo-halides, leading to poorer yields (LiCl 42.39 gmol^{-1}, LiBr 86.85 gmol^{-1}, LiI 133.85 gmol^{-1}, LiOTf 156.01 gmol^{-1}). However this contrast with what may be expected as with increasing halide mass the lithium salt should become a stronger Lewis acids due to a more available lithium cation as the difference in hard soft cation anion pairing decreasing the bond strength (Li-Cl 469 kJmol^{-1}, Li-Br 423 kJmol^{-1}, Li-I 352 kJmol^{-1}, Li-O 341 kJmol^{-1}).[31] Finally, altering the equivalents of lithium chloride (Table 4.06, entries 10 – 11) led to decreased conversion whether the stoichiometry was increased or decreased. With a reduced quantity the reaction may be slowed leading to decreased conversion, although with more lithium chloride available an accelerated rate could be expected. Perhaps with the larger quantity present the texture of the reaction mixture is altered enough to prevent efficient reactivity which is observed when higher molecular weight lithium salts are employed. Summarizing these results, it seems that not only the species of the of the Lewis acid but the counterion plays a key role in the reactivity with lower molecular weight species leading to greater conversion. This is potentially due to more efficient mass transfer and careful consideration of the balance of the reactivity and mechanical effects of using differing reagents.

Solid additives were screened in the reaction as grinding auxiliaries in mechanochemical reactions can be used to improve mixing within the jar by altering the texture of the reaction mixture (Table 4.06). The solvent free nature of the reaction mixtures can become sticky especially in the presence of liquids such as the starting material **308** and THF. The potential benefits of using solid additives have been demonstrated amongst previous reports. [32]
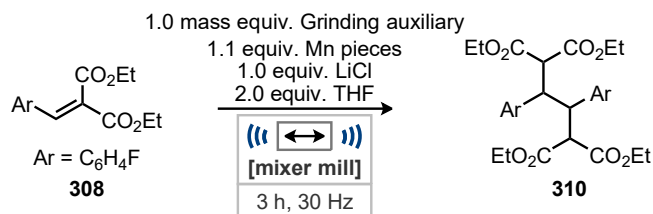
Entry	Grinding auxiliary	Conversion of **308**[a] / %	Yield of **310**[a] / %
1	-	95	80 (80[b])
2[c]	LiCl	<1	0
3	NaCl	<1	0
4	MgSO$_4$	<1	0
5	Sand	98	81
6	Celite	100	72
7	Alumina (neutral)	50	10

[a] Determined by ^{19}F NMR spectroscopy using α,α,α-trifluorotoluene as an internal standard.
[b] Yield of isolated product. [c] 1.0 equiv. of LiCl Omitted.

Table 4.07. Grinding auxiliary screen.

Unsurprisingly when using lithium chloride as the grinding auxiliary (Table 4.07, entry 2) rather than just 1.0 equivalent conversion of **308** was prevented as similar observations were made in (table 4.06, entry 11) when the stoichiometry of lithium chloride was increased to 1.5 equivalents. The use of sodium chloride (Table 4.07, entry 3), one of the most commonly utilized grinding auxiliaries, also completely shut down the reaction.[32] Often grinding auxiliaries serve multiple purposes within the reaction, not only to improve mixing, but can be used to dry reaction mixtures or stabilize metal catalysts.[33] Magnesium sulfate was used as a grinding auxiliary as the reaction potentially occurred *via* an organometallic intermediate and that the use of a desiccant such as this could remove any moisture present and improve reaction yields. Unfortunately, magnesium sulfate prevented the reaction entirely leading to no conversion (Table 4.06, entry 4). Using sand as the grinding agent (Table 4.07, entry 5) the reaction proceeded, leading to a marginally improvement in yield than without the grinding auxiliary present (Table 4.07, entry 1). Unfortunately, its presence caused the work up to be much more arduous as it caused emulsions to form during liquid-liquid extraction. Celite also allowed for some reactivity (Table 4.07, entry 6) with a slightly reduced yield of the product but led to a range of unknown side products that consumed the starting material. Lastly, alumina (Table 4.07, entry 7) also produced several unknown side products consuming the starting material, but the reaction still proceeded albeit in greatly reduced yield and conversion. The production of these unknown side products seems to be related to the

acidity of the grinding auxiliaries being used in the reaction although no further investigation into their formation took place.

Finally, the reaction time was varied as a last avenue of investigation to increase the reaction yield with shorter and longer reaction times.
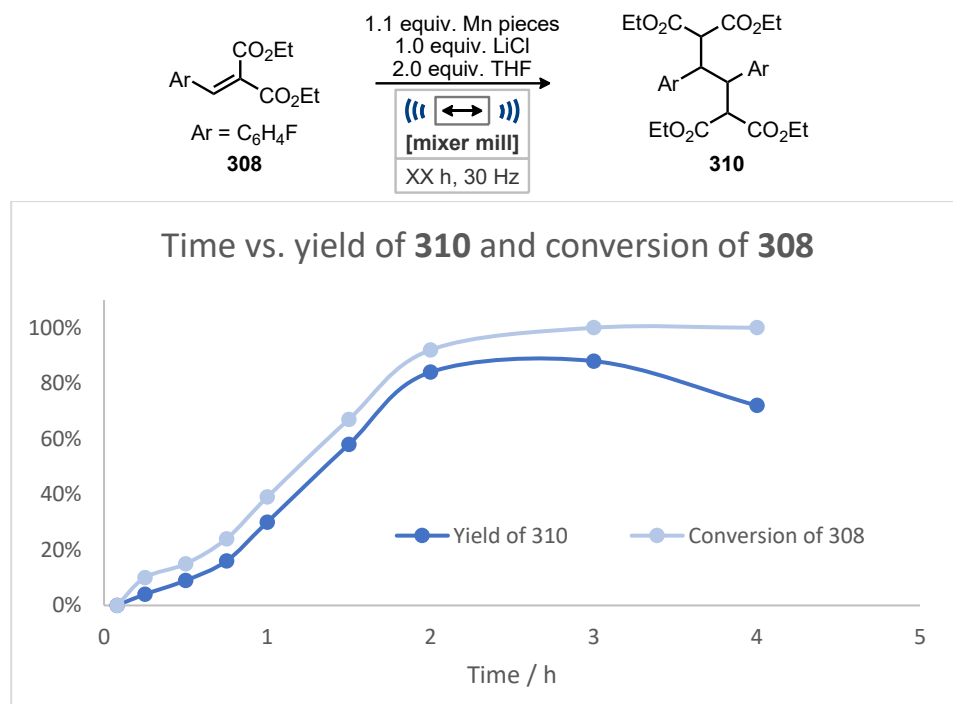

Yield and conversion determined by ^{19}F NMR spectroscopy using α,α,α-trifluorotoluene as an internal standard.

Figure 4.01 Optimization of reaction time.

From the shortest reaction times (Figure 4.01) at 5 minutes there is no conversion of product formation suggesting a brief induction period before the reaction begins. This induction period could facilitate the particle size reduction of the manganese metal revealing fresh metal surfaces free from passivation. Once the induction period is over the reaction yield increases steadily until reaction time reaches 2 hours. At 2 hours conversion is not yet complete at 92% with a good yield of 80%. The following hour the reaction is considerably slower reaching a peak of 83% with complete conversion. Further increasing the reaction time to 4 hours only leads to marginal degradation of the product **310**. The reaction time of 3 h was carried through to further exploration of the reaction as other substrates may require longer reaction times if their reduction is slower and this reaction time should allow for sufficient conversion of any other starting materials.

4.2.2 Optimization Summary

The reaction showed little tolerance to changing conditions from those used for the initial discovery (Scheme 4.09a). Through optimization it has been shown that the ethyl 4-bromo butyrate **294** present initially was unnecessary, and this was likely assisting the THF acting as a liquid additive. It would be plausible for the ester functionality to stabilize any organomanganese intermediates as ester containing solvents such as ethyl acetate have been shown to stabilize these species.[21b] Furthermore, the removal of this reagent suggests a potentially alternate reaction mechanism than that of the dimerization of 2-cyclohexen-1-one demonstrated by Cahiez and co-workers which requires a dialkyl organomanganese as a stoichiometric reagent or catalyst (Table 4.01).[20-21] Through screening alternate liquid additives moderately polar solvents containing coordinating groups provided the highest yields. The effectiveness of Lewis acids in the reactions seems to inversely correlate to the molecular weight of the compounds with the lightest Lewis acids providing the best yields. Upon screening grinding auxiliaries, sand was the only additive which did not decrease reaction yield or led to a variety of unknown side products. Although as the gain in yield was only minimal and the increased difficulty of the work up it was not pursued any further. Through the thorough investigation of reaction conditions, it was decided that the optimal conditions for the reaction are as follows (Scheme 4.09b).
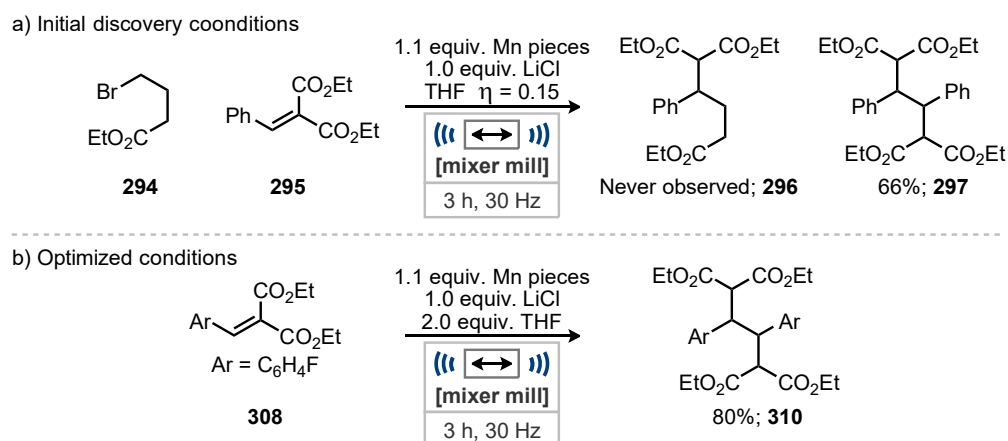
Scheme 4.09 Comparison of initial discovery to Optimized reaction conditions.

4.2.3 Substrate scope

To probe the pertinence of the optimized conditions a range of benzylidene and alkylidene malonates they were first synthesized by the Knoevenagel condensation of the respective activated methylenes and aldehydes. These reactions were carried out either under Dean Stark conditions, for large scale preparations, or with the use of molecular sieves as desiccant, for smaller scale reactions (see Chapter 6, Supporting Information).
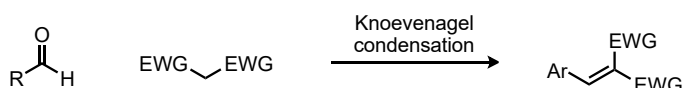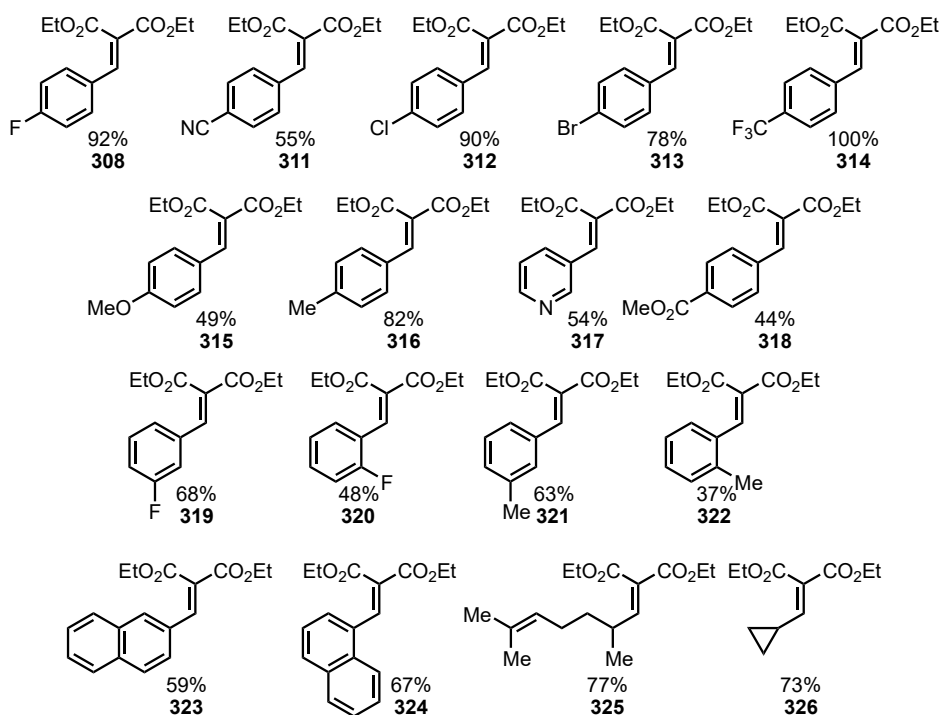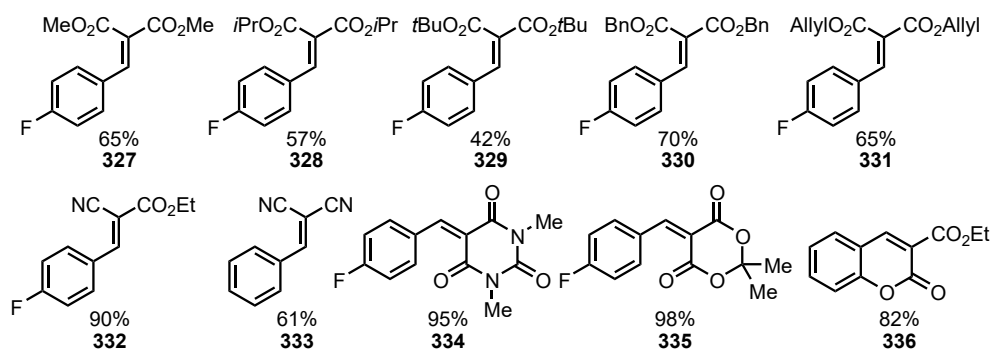
Scheme 4.10. Benzylidene and alkylidene malonate synthesis. Compound **333** was synthesized by Dr Joseph L. Howard.

Initially derivatives of benzylidene malonate were synthesized varying the nature of the substituents on the aromatic ring including electron withdrawing and donating groups. These products were often obtained in good to excellent yields **311**-**324**. Alkylidene malonates based on melonal, **325**, and cyclopropanecarboxaldehyde, **326**, were synthesised as it was hypothesised that if the mechanism operated *via* a radical intermediate that these compounds may be able to assist in elucidating the mechanism. For **325** may undergo 5-exo-trig cyclization if a radical were formed and **326** may undergo strain release ring opening.

The activated methylene in the Knoevenagel condensation was also varied for the synthesis of a range activated double bonds with a variety of electron withdrawing groups. When these variations were made the aldehyde remained 4-fluorobenzaldehyde except for **333**. This included varying the ester substituents and the use of ethyl cyanoacetate **332**, malononitrile **333**, barbituric acid **334**, and meldrums acid **335**. Finally, ethyl 2-oxo-2H-chromene-3-carboxylate **336** was synthesised through Knoevenagel condensation with salicylaldehyde.

With these compounds in hand the substrate scope was undertaken. Initial change focussed on the activation of the π-system using different malonate esters and unexplored electron withdrawing groups. This comprised of compounds **327** – **336**.
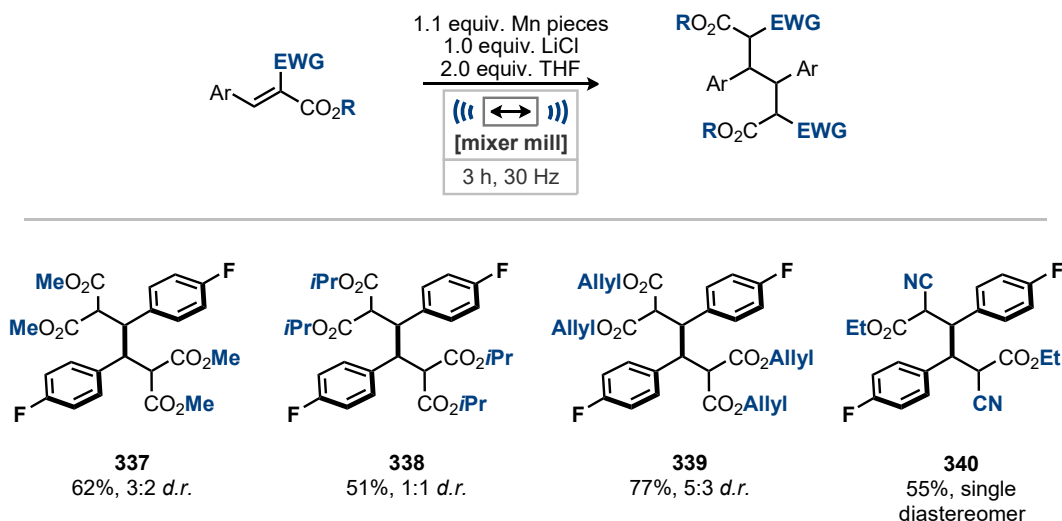
Yields of isolated product. Ratio of anti:syn diastereomers calculated using ^{19}F NMR spectroscopy. Diastereomer of **340** unknown.

Scheme 4.11 Substrate scope of varied malonate esters and double bond activation.

Altering the substituent on the malonate esters was largely successful, methyl, allyl, and *iso*-propyl were all successful in the coupling reaction, albeit in slightly reduced yield for the bulkier *iso*-propyl compound. Allyl substituents were unaffected by the reaction

showing the tolerance to inactivated double bonds to the reaction conditions. Finally, ethyl 2-cyano-3-(4-fluorophenyl)acrylate **340** was successful, leading to a single diastereomer of the product unlike every other substrate which gave a mixture of both syn and anti-products. However, this reaction did lead to only a moderate yield of this dimer. Also, ethyl 2-cyano-3-(4-fluorophenyl)acrylate **332** was the only example containing an alternate electron withdrawing group that successfully underwent the dimerization all other successful examples were based on malonate esters.
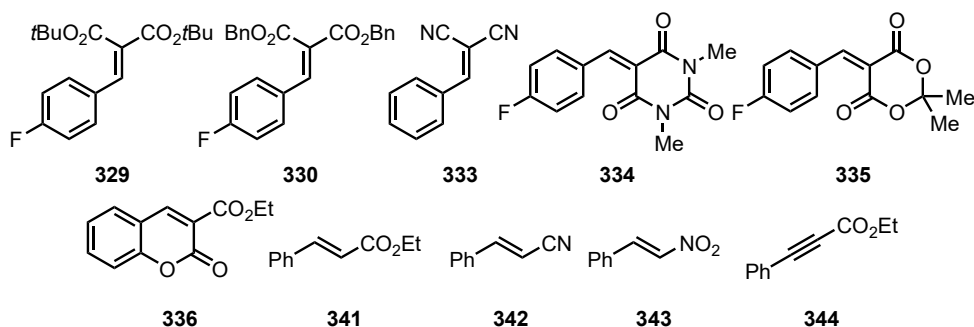
Scheme 4.12 Unsuccessful substrates with varied activation and malonate esters.

Several compounds were screened which were unsuccessful during the scope with varying electron withdrawing groups. The only failed malonate esters derivatives were the *tert*-butyl **329** and benzyl **330** substituted examples. This was possibly due to the steric encumbrance of the *tert*-butyl and benzyl groups as the smaller *iso*-propyl substituents led to a reduced yield in the reaction. Unfortunately, **334** derived from dimethyl barbituric acid did not partake possibly due to weaker coordination with lithium cation. If this substrate had undertaken the reaction the possibility of a two-step one pot process was postulated where the substrate was produced via a mechanochemical Knoevenagel condensation followed by dimerization, as Knoevenagel condensations are well known to proceed in ball mills.[29a, 34] The Meldrum's acid derived substrate **335** completely decomposed during the reaction with no starting material remaining but also no product being observed. This decomposition also took place on milling just the substrate **335** with no other reagents. All the substrates that contain only one electron withdrawing group, **341** – **344**, were unable to be coupled by this reaction likely due to higher reduction potentials. Ethyl 2-chromenone-3-carboxylate **336** was unreactive under the developed conditions possibly due to the increased aromatic nature of the double bond leading to a higher reduction potential. Finally, the benzylidene malononitrile substrate **333**, also failed to participate probably due to poorer coordination with the Lewis acid. This weaker coordination then fails to further activate the substrate similarly to the dimethyl barbituric acid functionalised compound.

With sufficient investigation into the possible variation of the electron withdrawing groups having taken place the substrate scope moved towards varying the substitution of the aromatic ring and investigating alkylidene malonates.
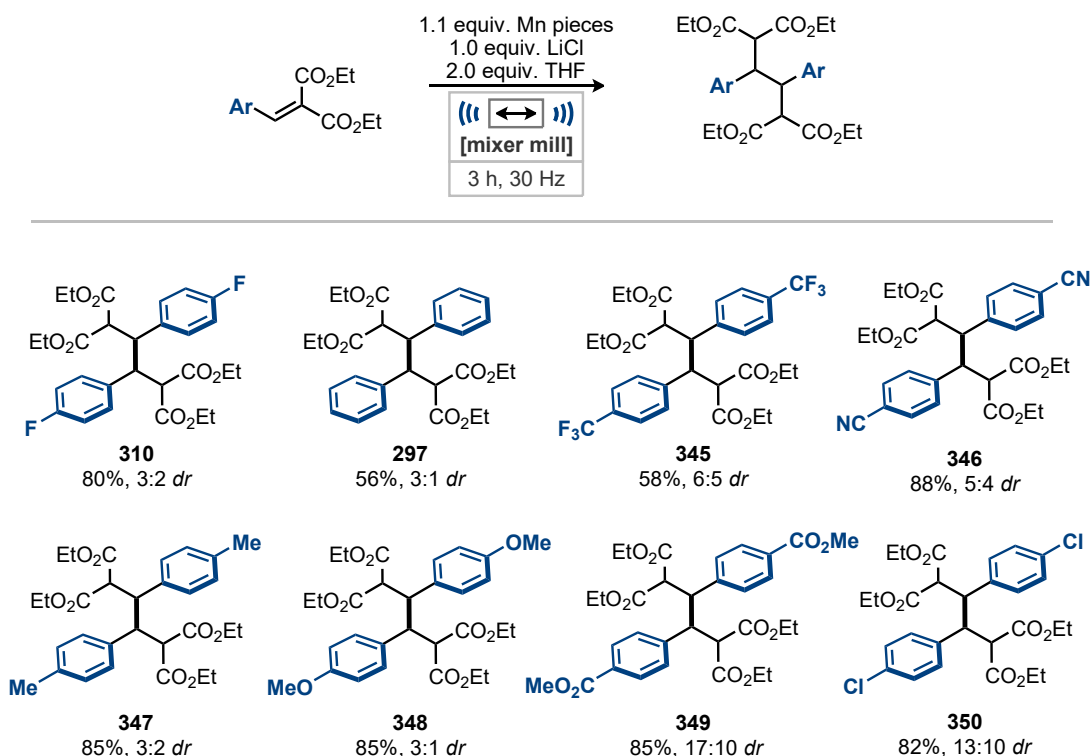

Yield of isolated products. Ratio of anti:syn diastereomers calculated using ^{1}H NMR or ^{19}F NMR spectroscopy.

Scheme 4.13 Aryl substituent substrate scope.

Substrates containing electron withdrawing groups were successfully coupled, including **345**, **346**, and **349** producing good to excellent yields. Also tolerated were electron donating substituents such as methyl and methoxy, **347** and **348** producing excellent yields. The only halides tolerated in the reaction were chloride and fluoride **350** and **310**, with heavier halides such as bromide substituents leading to complex mixtures of products, which likely arise from oxidative insertion of manganese into the C-Br bond followed by protonation. Finally, the unfunctionalized **295** used for the reaction discovery was amenable to these new conditions although producing the dimer product **297** in slightly reduced yield when compared to the initial discovery (66%).

The ratio of the product diastereomers follows a general trend of those with electron withdrawing substituents leading to a mixture of anti:syn diastereomers closer to 1:1 and electron donating substituents giving a greater proportion of the major anti diastereomer. The variation in diastereomers provides a possible insight into the thermodynamic nature of the reaction as it is likely that any reduced intermediates stability will vary with the

electronics of the system, whether the intermediate is a radical or anionic species. Electron withdrawing substituents will stabilize the intermediate, this stabilization may allow a reversable formation of the dimer producing a greater proportion of the thermodynamic syn-diastereomer. In the examples where electron donating groups are present a greater proportion of the anti-diastereomer is observed. This is possibly due to this stereoisomer being the kinetic product and that the reversibility of the addition is not possible for these substrates leading to this diastereomer forming in excess. However, this hypothesis has not been confirmed.
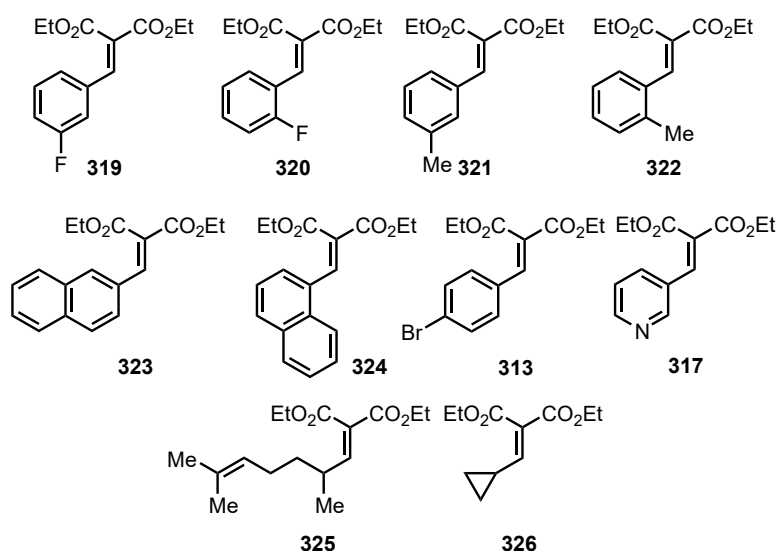
Scheme 4.14. Unreactive substrates for aryl substituent scope.

Similarly, to the previous scope multiple starting materials failed to undergo the transformation. The use of either isomer of naphthaldehyde **323** and **324** led to minimal conversion of starting material and no products were observed. Similarly reduced reactivity was observed in the use of larger malonate ester derivatives. Unfortunately, starting materials containing either fluoro or methyl groups at the *ortho* or *meta* positions **319** - **322** did not participate in the reaction. This is again possibly due to the sensitivity of this reaction to traditional steric factors. As mentioned previously the aryl bromide bearing substrate **313** did undergo the reaction although leading to a complex mixture of inseparable dimer products. Through mass spectrometry analysis of this mixture it seems to include de-halogenated dimers suggesting manganese addition to the C-Br bond followed by proto-demetallation of these species. The pyridyl derived starting material **317** also failed to participate in the reaction with minimal product conversion observed. Although other electron deficient species succeeded in the dimerization it is still unclear as to why this compound did not participate. Finally, alkylidene malonates **325** and **326** did not undergo the reaction with no consumption of starting material being

observed in either reaction. It is likely that these compounds have a higher reduction potential such that they are not amenable to reduction by manganese in this reaction.

## 4.3 Mechanistic Study

4.3.1 Proposed mechanisms

From the results obtained from this reaction thus far two potential mechanisms were postulated for the dimerization. These mechanisms were based either around a single two electron reduction by manganese or multiple single electron reductions (SET) taking place.
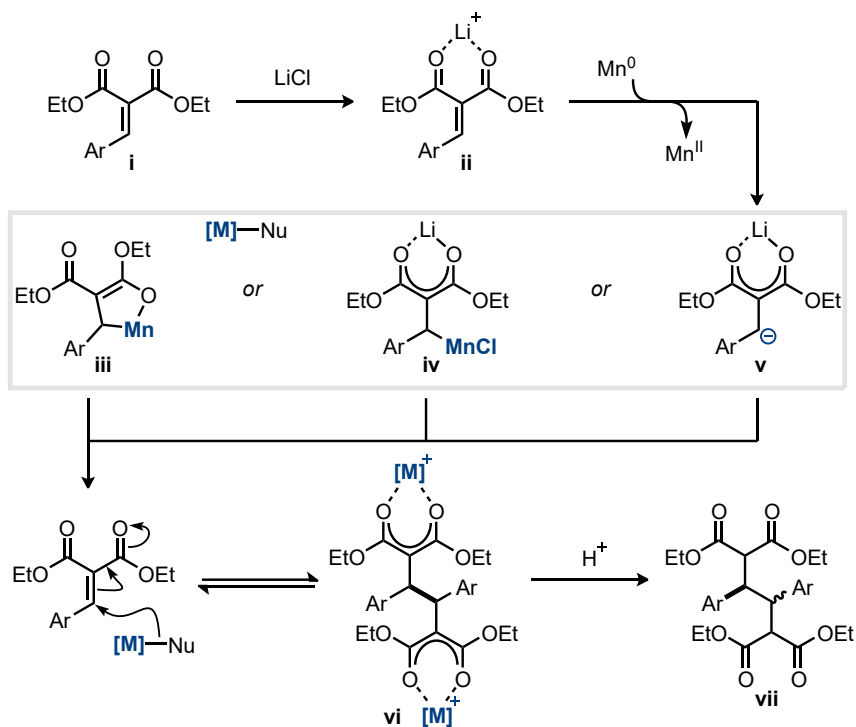
Scheme 4.15 Proposed two electron reduction mechanism.

The first proposed mechanism is based on a single two electron reduction. The reaction is initiated by coordination of a lithium cation to the 1,3-dicarbonyl to activate the substrate **i** forming the adduct **ii**, as the reaction does not take place without lithium chloride present. This activated species is then reduced by the manganese metal via a two-electron reduction to generate a nucleophile. The nucleophile could occupy multiple forms including, a cyclic organomanganese enolate **iii**, a linear organomanganese halide with a lithium enolate **iv**, or a free benzylic anion **v**. Any of these intermediate species then act as the nucleophile that partakes in a conjugate addition with another molecule

of the starting material to form the dimer as a dienolate **vi** which is then protonated upon workup to reveal the final product **vii**. The second equivalent of the starting material acting as the electrophile could also be activated by lithium in a similar manner but could be sufficiently electrophilic enough without it.
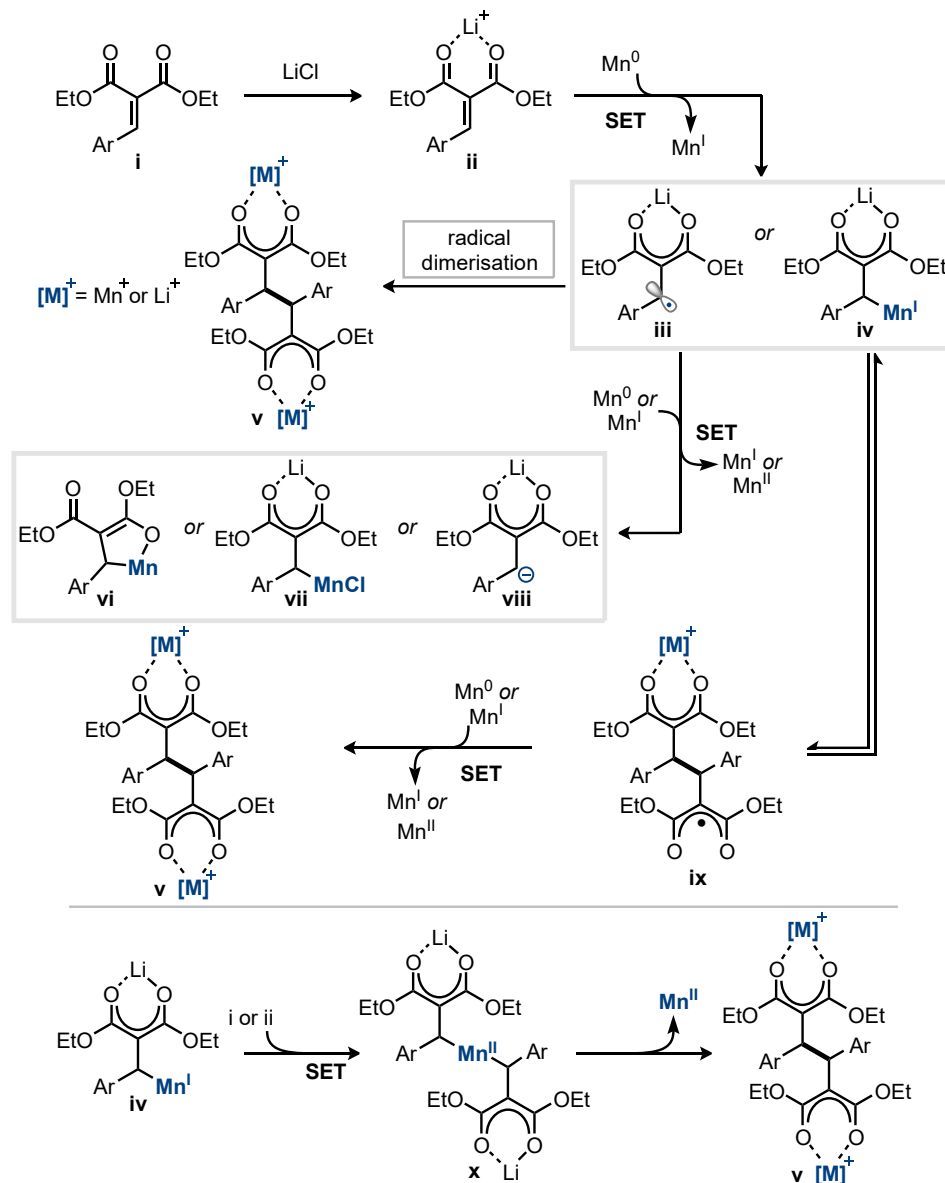
Scheme 4.16 Possible reaction pathways via initial single electron reduction.

The second mechanistic proposal is initiated by the same coordination of lithium acting as a Lewis acid to further activate the double bond forming **ii**. This adduct then being reduced by manganese *via* a single electron transfer. This reduction could then furnish a free radical intermediate **iii** or manganese(I) bound organometallic **iv**. These reduced intermediates could undergo direct dimerization with another equivalent of themselves. The manganese(I) species **iv** or the free radical **iii** could undergo further reduction

forming the intermediates **vi**, **vii**, or **viii**. These would then undergo the reaction postulated in scheme 4.15. Another distinct possibility is these intermediates **iii** or **iv** may act as a radical nucleophile attacking a further equivalent of the starting material, acting as the somophile, forming a radical enolate intermediate **ix**. This is then reduced by a manganese(0) or manganese(I) to furnish the final dienolate **v** which can again be protonated during the workup. Finally, the manganese(I) bound intermediate **iv** could undergo a Pinacol type coupling reaction where the manganese(I) reduces another molecule of the lithium adduct **ii** or the starting material **i** to form the dialkyl manganese(II) intermediate **x**.

These proposed mechanisms allowed the design of a series of control reactions and investigations to uncover the reaction mechanism.

4.3.2 Cyclic Voltammetry

From the optimization of this reaction, it was abundantly clear that the lithium chloride or other Lewis acids are essential for this reaction (Table 4.06). To gain insight into the role of lithium chloride the reduction potential of compounds **314** and **315** were measured with and without the presence of lithium chloride. It has previously been shown by Schiedt and co-workers that the addition of a Lewis acid to similar substrates can alter the reduction potential so that they are more easily reduced.[25] The reduction potentials were measured against ferrocene ($E_{1/2}$ = 0.382 V vs. SCE in MeCN).[31b]

a) Known reduction potentials of manganese and zinc

$$Mn^{II} + 2e^- \longrightarrow Mn^0 \qquad E_{1/2} = \text{-1.185 V } vs.\text{ SCE}$$

$$Zn^{II} + 2e^- \longrightarrow Zn^0 \qquad E_{1/2} = \text{-0.762 V } vs.\text{ SCE}$$
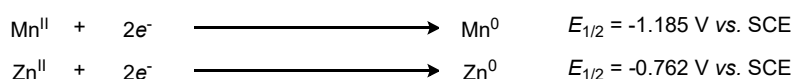
b) Substrates which the reduction potentials were measured
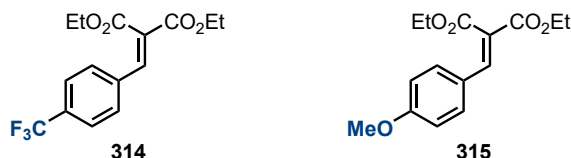
Scheme 4.17 Known reduction potentials for manganese(II) and zinc(II) and compounds **314** and **315** which the reductions potentials were measured.

Entry	Substrate	Without LiCl	With LiCl	Δ
1	**314** CF$_3$	-1.65	-1.59	0.06
2	**315** OMe	-2.00	-1.63	0.37

Table 4.08 Reductive potentials referenced to SCE. Thanks to Alex C. Seastram for assisting with the cyclic voltammetry measurements.

Compounds **314** and **315** were chosen to illustrate the range of reduction potentials which could be accessed across electron rich and poor examples. Each substrate was measured with and without the presence of lithium chloride so that the change in reduction potentials could also be compared. In solution addition of lithium chloride decreased the reduction potentials of these substrates by between 0.06 V (4-CF$_3$, **314**) and 0.37 V (4-OMe, **315**) showing the benefit of the addition of a Lewis acid to the system. The reduction potentials that have been measured are greater than the known reducing ability of manganese metal (E$_{1/2}$ = -1.185 V vs. SCE) suggesting that it should not be possible for manganese to reduce these substrates.[31b] Although, the precise conditions that each of these reduction potentials were measured under and the reaction are significantly different which may account for the discrepancy.

The measured reduction potential of compound **314** bearing the trifluoro methyl group without the presence of lithium chloride is similar to that of compound **315** with LiCl present (-1.65 V vs. -1.63 V respectively). If the lithium chlorides only role in the reaction is to act as a Lewis acid to activate the substrates, then in may be possible for compound **314** to undergo the dimerization reaction without LiCl present.
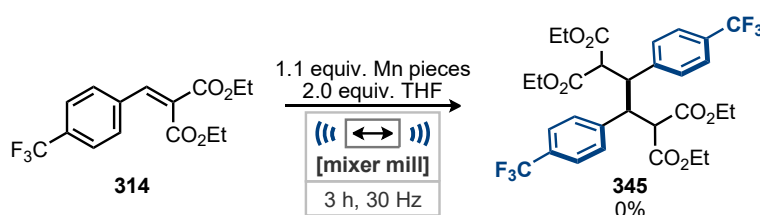
Scheme 4.18 Dimerization of **314** with LiCl omitted.

When these conditions were applied no conversion of the starting material **314** was observed. This suggests that LiCl may have more than one role in the reaction or under the conditions within the ball mill the activation of the substrate is more significant than under the conditions which the reduction potentials were measured.

4.3.3 Control Reactions

Initial control reactions focused on attempts to protonate any organometallic intermediates. It is likely that the three intermediates suggested for the two-electron reduction (Scheme 4.15) would be highly sensitive to the presence of water in the reaction as they could succumb to proto-demetallation resulting in the reduced starting material **351** being observed. To investigate the presence of these organometallic intermediates water and metal hydrate salts were included using both manganese and zinc as reductants.

Entry	Reductant	Additives	Yield of 310[a] / %	Yield of 351[a] / %
1	Mn	-	80	0
2	Zn	-	43	0
3	Mn	H_2O (4.0 equiv.)	20	0
4	Zn	H_2O (4.0 equiv.)	4	41
5	Zn	$MnCl_2 \cdot 4H_2O$ (2.0 equiv.)	18	51
6[b]	Zn	$MnCl_2 \cdot 4H_2O$ (2.0 equiv.)	11	64
7	Mn	$MnCl_2 \cdot 4H_2O$ (2.0 equiv.)	19	0
8[b]	Mn	$MnCl_2 \cdot 4H_2O$ (2.0 equiv.)	0	0

[a] Determined by ^{19}F NMR spectroscopy using α,α,α-trifluorotoluene as an internal standard.
[b] LiCl omitted from reaction.

Table 4.09 Attempts to protonate organometallic intermediates with water.

The proposed product of the proto-demetallation, compound **351**, was believed to not have been previously observed during the optimization studies, so for accurate comparison it was synthesized from a literature procedure. On addition of 4.0 equiv. of water to the optimized reaction conditions (Table 4.09, entry 3) none of the protonated intermediate **351** was observed with the product, **310**, being observed albeit in diminished yield. To check the validity of this study it was repeated using zinc as the reductant as that had previously showed some activity in the reaction (Table 4.09, entry 2). When 4.0 equiv. of water was added to this reaction (Table 4.09, entry 4) compound **351** was the major product of this reaction in 41% yield with only 4% of the

dimer **310** being observed. This abrupt difference in selectivity for the reduced starting material on the use of different reductants is likely caused by the operation of differing mechanisms with zinc and manganese. Alternately, the organomanganese intermediate could be more challenging to proto-demetallate. The intermediate present with the use of zinc is clearly easily protonated by water.

Further reactions attempted to use a manganese salt to trans-metalate any organozinc intermediate to form the equivalent manganese intermediate which may have increased stability to water (Table 4.09, entries 5 and 6). Manganese(II) chloride tetrahydrate was chosen to run these reactions so that a known amount of water would be used in each reaction as anhydrous manganese(II) salts are often highly hygroscopic so may contain unknown quantities of water. With the manganese salt present in the reaction using zinc as the reductant the dimer was observed in increased yields, but the reduced starting material was still the major product. This suggests that if the trans-metalation to a manganese species may be occurring but that this is sluggish compared to the protonation by water. Although the organomanganese species that forms could be more resilient to protonation and therefore form the desired dimer product in increased yield. Furthermore, when lithium chloride was omitted from the reaction using zinc as a reductant and manganese(II) chloride tetrahydrate as an additive conversion to both products was still observed (Table 4.09, entry 6). Omitting lithium chloride also increased the production of the reduced starting material **351** showing that addition of lithium chloride can improve the selectivity for the dimer product. As lithium chloride is able to alter this selectivity it is possible that in some instances the electrophile is in fact the adduct of **308** with lithium chloride. This result also suggests that the manganese(II) chloride tetrahydrate may also be sufficiently Lewis acidic to promote the reduction by zinc. Although when manganese was used as the reductant in the presence of manganese(II) chloride tetrahydrate (Table 4.08, entries 7 and 8) this additive impaired reactivity but none of the reduced starting material **351** was observed. Finally, when lithium chloride was omitted from this reaction no reactivity was observed which is in accordance with previous observations made in the optimization (Table 4.02, entry 3).

These observations do not confirm the mechanism as exclusively a two-electron or single electron process for zinc and manganese but do show the increased stability of any manganese intermediate to proto-demetalation by water. They suggest that the reaction mediated by zinc is likely to have some form of organozinc intermediate which is able to react with water.

Within this investigation as the spectroscopic data of **351** was now known previous results were re-examined to determine if this side product was present. This found that during the Lewis acid optimization zinc(II) chloride (Table 4.06, entry 4) led to a 10% yield of the reduced starting material **351**. This is possibly due to the generation of the organozinc which, as shown, is more prone to protonation.

As THF is vital for the reaction to take place it was investigated to determine if it was a hydrogen atom source in the formation of the product. The liquid additive was simply replaced with d^8-THF and if any transfer occurs the detection of deuterium incorporation could easily be carried out by variation in the ^{1}H NMR spectrum of the product (Scheme 4.19).
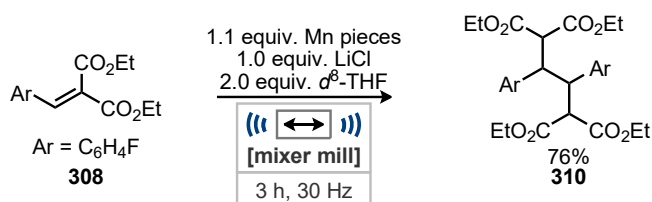
Scheme 4.19 Control reaction employing d^8-THF as liquid additive.

This reaction provided 76% of the product **310** without any deuterium atom incorporation demonstrating that the THF is not acting as a hydrogen atom source.

A competition experiment between two substrates with differing reduction potentials was also carried out. The hypothesized outcome is that if the reaction occurs via a radical-radical dimerization process that the more readily reduced starting material will react initially to generate the intermediate radicals and then these species will combine to form the AA dimer (where A is the more reducible substrate). Once the A starting material has been sufficiently consumed the reduction of the less reactive substrate B will begin initially consuming the remaining A radicals forming the mixed AB dimer as a minor product and with the consumption of A complete the reaction will then continue to exclusively produce BB. For this experiment the chosen substrates were **308** and **315** as their reduction potentials should be significantly different and using ^{1}H and ^{19}F NMR spectroscopy it will be possible to determine the crude yields of all products.
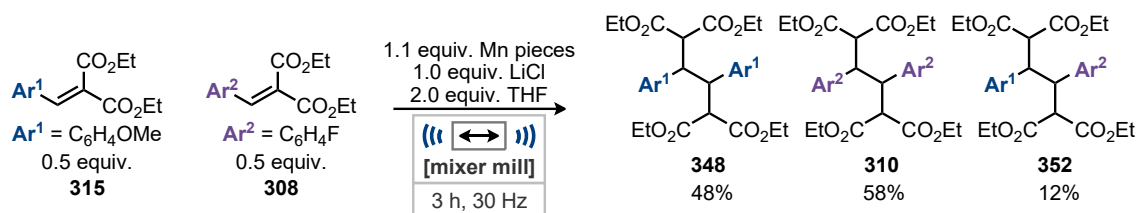
Scheme 4.20 Competition experiment to probe diradical combination mechanism. Yields and assignment carried out by ^{1}H NMR spectroscopy and ^{19}F NMR spectroscopy of the crude reaction mixture containing 4-fluorotoluene an internal standard.

The competition reaction using two substrates of differing reduction potentials was moderately selective for the symmetric products **310** and **348**. If there was no difference in the rate of reduction of either of the substrates a statistical mixture outcome would be expected of 1:2:1 (AA:AB:BB). This competition reaction shows differing rates of reduction and that there is a possibility for the radical dimerization mechanism for this transformation (Scheme 4.20). Although to gain a more detailed insight into this process it should be repeated, and the yield of each product measured at a variety of reaction times.

Experiments were carried out using the radical traps TEMPO and 1,1-diphenylethylene to attempt to trap any of the possible radical intermediates. To sufficiently probe the reaction the inhibitor was present from the beginning of the milling process and in a separate experiment added after half of the reaction time (1.5 h). This was envisioned to potentially trap the initial radical of the reduced starting material or trapping the radical enolate that could exist if the reaction were to pursue that mechanism.
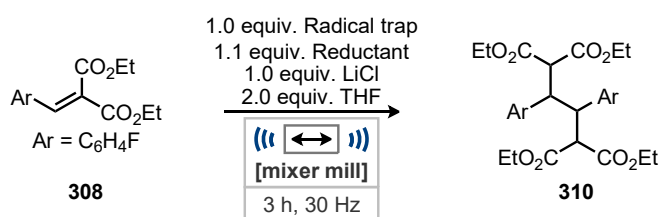
Entry	Radical Trap	Conversion of **308**[a] / %	Yield of **310**[a] / %
1[b]	TEMPO	5	trace
2[c]	TEMPO	61	58
3[b]	1,1-diphenyl ethylene	3	Trace (90)[d]
4[c]	1,1-diphenyl ethylene	65	61 (87)[d]

[a] Determined by ^{19}F NMR spectroscopy using α,α,α-trifluorotoluene as an internal standard. [b] Radical trap present from the beginning of the reaction. [c] Radical trap added after 1.5 h. [d] 1,1-diphenyl ethylene recovered.

Table 4.10 Radical trapping experiments.

136

In the reactions where the traps were in place from the beginning of the reaction (Table 4.10, entries 1 and 3) they both prevented the reaction from taking place with only a trace of the product being detected by ^{19}F NMR spectroscopy. But no adduct of either trap with any hypothesized intermediate was detected by ^{19}F NMR spectroscopy or mass spectrometry. Also, in the reaction where 1,1-diphenyl ethylene was used as the trapping agent 90% of 1,1-diphenyl ethylene was recovered.

The trapping experiments were then attempted again with TEMPO and 1,1-diphenylethylene added after 90 mins. When TEMPO was used as the trap under these conditions (Table 4.10, entry 2) 58% of **310** was still obtained. Showing that once the trap was added that the reaction was significantly inhibited. Similar results were obtained while using 1,1-diphenylethylene as the radical trap with considerable inhibition of the reaction occurring (Table 4.10, entry 4). Again, no adducts of the radical traps could be observed in either of these reactions. Furthermore, it was possible to recover 87% of the 1,1-diphenyl ethylene (Table 4.10, entry 4) showing it had not likely undergone any other reactions. It is still unclear by what mechanisms the reaction is being inhibited using these radical traps but throughout the optimization it was clear that the reaction was highly sensitive to changing conditions.

As these radical trap experiments proved to be inconclusive the observation of an intermediate radical was attempted using Electron Paramagnetic Resonance (EPR) spectroscopy. EPR spectroscopy was chosen as this could potentially provide direct observations of an organic radical and any compound containing an unpaired spin such as manganese(II) species if they were present in the reaction mixture.

4.3.4 EPR Study

Initial investigations using EPR spectroscopy was used to determine the species of manganese at the end of the reaction. For this the crude mixture from the milling vessel was dissolved in ethyl acetate, the usual workup solvent, the aqueous layer following the reaction work up, and manganese(II) acetate as a known comparison, were analysed using EPR spectroscopy. The EPR spectrum of the crude reaction mixture (Figure 4.02a) contained a sextet multiplet feature, with six equal-intensity hyperfine lines separated by 260 MHz (92.77 G), which is characteristic of a d^5 Mn^{II} species with $I(^{55}$Mn$)$ = 5/2. This however does not confirm whether the mechanism occurs via a two-electron reduction or two single electron reductions but that some manganese is oxidized to its second oxidation state. A similar signal was then observed from the aqueous phase (Figure

4.02b) following the work-up of the reaction and the organic phase post work-up had very little remaining manganese(II) signal (Figure 4.02c). Attempts were made to quantify the amount of manganese(II) present though these were unsuccessful due to the quantity of iron present in the samples from the stainless steel jar making accurate measurements difficult to obtain.[35]
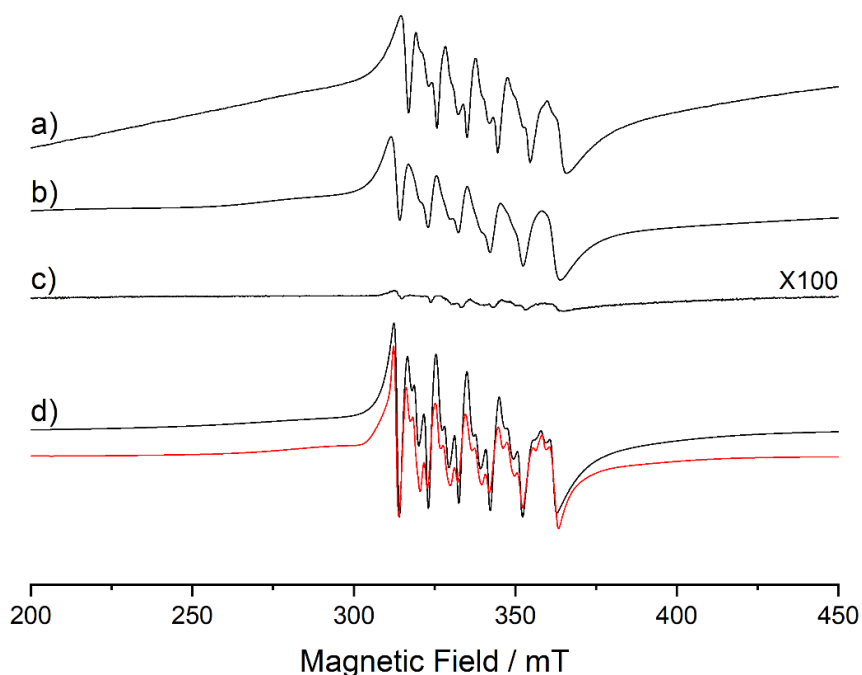
Figure 4.02 CW X-band EPR spectra (T = 120 K) of **a)** Crude reaction mixture dissolved in ethyl acetate, **b)** aqueous layer after work-up with HCl, **c)** organic layer after work-up; **d)** Mn(OAc)$_2$ (10 mM) in a water:glycerol (50:50) solvent, and red trace showing a simulation of Mn(OAc)$_2$. A simulation of Mn(OAc)$_2$ has been included above for comparative purposes, showing the extremely similarities in spectral appearance between the crude product and its Mn(OAc)$_2$ counterpart. Thanks to Giuseppina Magri for measuring the EPR spectrum.

Due to the high sensitivity of EPR if an organic radical were present, it would likely be detectable unless it is obscured by another signal. So, in a final attempt to detect a carbon based radical a spin trap, N-tertbutyl nitrone (PBN), was employed for its detection.[36] For this reaction the spin trap was again added after 90 mins and then the whole reaction mixture was subjected to a further 90 mins of milling. If the spin trap were successful it would react with the carbon centred radical to generate a more stable, long-lived radical that could then be detected. The reaction was then worked up as normal to

138

remove any manganese(II) salts and the EPR spectrum was measured on the organic phase. Unfortunately, no conclusive assignment could be made to any of the observed findings from these experiments.

Although no evidence of a carbon-based radical could be established by EPR spectroscopy the final oxidation state of manganese could be eluded. Continued investigation into this reaction moved focus from a mechanochemical environment into establishing the reactivity in solution.

4.3.5 Solution Reactions

To investigate the effect on changing particle size of the manganese metal during the ball milling reaction attempts were made to establish reactivity under solution conditions using metal in its original form and post ball milling. Through ball milling not only will the particle size be reduced but new metal surfaces will be revealed free from contamination which can result in increased reactivity along with a greater number of reactive defects in the surface of the metal.[37] Furthermore, increased surface area will increase rate of the reaction.
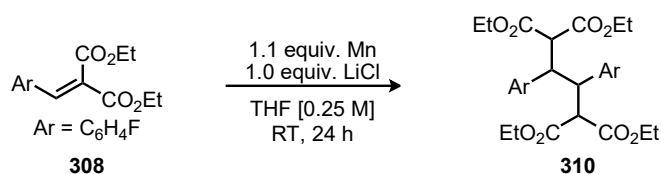
Entry	Mn Form	Milling Time[b] / min	Conversion of 308[a] / %	Yield of 310[a] / %
1	Pieces	-	2	0
2	Powder	-	12	trace
3[c]	Pieces	-	5	trace
4[c]	Powder	-	18	11
5	Pieces	2	71	69
6	Powder	2	69	65
7	Pieces	5	89	86
8	Powder	5	83	78
9	Pieces	15	99	95
10	Pieces	20	70	65
11	Pieces	25	71	38
12	Pieces	30	27	21
13	Pieces	45	13	trace
14	Pieces	60	5	trace

[a] Determined by ^{19}F NMR spectroscopy using α,α,α-trifluorotoluene as an internal standard. [b] 275 mg of Mn pieces milled at 30 Hz with a 4 g ball for the specified length of time. [c] Reactions carried out at 66 ˚C.

Table 4.11 Solution reactions using various forms of Manganese.

Using commercially available forms of manganese (Table 4.11, entries 1 and 2) minimal conversion was observed with powder being the most reactive providing 12% conversion but only a trace of the product in 24 h. With this limited reactivity observed in solution using the unaltered commercially available sources of manganese, the reactions were then repeated at elevated temperature (Table 4.11, entries 4 and 5). At 66 ˚C increased conversion was observed for both manganese powder and pieces (Table 4.11, entries 3 and 4) and for manganese powder a small yield of 11% was achieved although pieces only provided a trace of the product. This is likely due to the higher surface area of the metal powder than the pieces.

Once manganese of either form had been milled for a short period of time 2 – 5 minutes (Table 4.11, entries 5 – 8) its reactivity significantly increased such that with 5 minutes of milling 89% conversion and an 86% yield was observed for milled manganese pieces.

The reactivity of the milled metal then further increased until 15 minutes of milling (Table 4.11, entry 9). However, continued milling of 25 minutes or more led to a decrease in reactivity and further prolonged milling led to significant deactivation (Table 4.11, entries 11 – 14). As the metal is being milled under an air atmosphere it may be possible for prolonged milling to lead to oxidation of the metal reducing the quantity of active manganese metal present.

During these experiments, it seems that the manganese is significantly less reactive after 60 minutes of milling although the ball milling dimerization conditions requires 3 hours. This extended reactivity during the dimerization reaction under ball milling conditions could be due to the addition of the reagents reducing the rate of the particle size reduction as these components will also absorb some of the energy. These additional components may also be able to coat any manganese surfaces potentially preventing the metal being oxidised during the reaction.

4.4   Conclusion and Future Work

In conclusion, a novel dimerization of electron poor alkenes has been serendipitously discovered and optimized. The discovered reactivity has not been previously observed for manganese metal. A substrate scope varying electronics and sterics was then carried out which supported the understanding of the tolerance of the reaction. To delve deeper into the mechanism of the reaction the redox potentials of a two of substrates were measured which showed the addition of a Lewis acid could make the reduction potential more amenable to manganese metal. Several control experiments were performed in an attempt to ascertain if radical intermediate(s) are present during this reaction, including radical traps and spin traps. EPR spectroscopy was then employed to try and detect these organic radicals without success but did confirm the presence of manganese(II) in the reaction. With the evidence collected it seems most likely that the manganese metal is reducing the activated substrate. This reduced species seems to be stable to proto-demetallation so perhaps exists as a Mn^{II} metallacycle (scheme 4.15 **iii**) or as a radical intermediate that was not possible to detect (scheme 4.16 **iii**). This intermediate is then able to act as a soft nucleophile to perform the conjugate addition with another equivalent of the starting material.

Future work on this transformation could investigate the reaction mechanism under solution conditions that have now been established. Attention could also be made to

expand the scope of the transformation as currently the products are not of any use. Addition of stronger Lewis acid activators may allow substrates which are more challenging to reduce to be accessed. Alternatively, the use of alternate electrophiles could allow for extension of the reaction to a range of new products. Electrophiles could include the radical coupling reagents accessed by Scheidt and coworkers under their photoredox approach to the functionalization of benzylidene malonates. Alternatively, manganese or other metals could be explored further to determine the effects on their reactivity initiated by ball milling. Finally, the use of manganese metal under ball milling conditions could be explored for the original aim of the generation of organomanganese halides.

4.5 Bibliography

1.   a) S. L. James, C. J. Adams, C. Bolm, D. Braga, P. Collier, T. Friscic, F. Grepioni, K. D. Harris, G. Hyett, W. Jones, A. Krebs, J. Mack, L. Maini, A. G. Orpen, I. P. Parkin, W. C. Shearouse, J. W. Steed and D. C. Waddell, *Chem. Soc. Rev.*, 2012, **41**, 413-447; b) R. T. O'Neill and R. Boulatov, *Nat. Rev. Chem.*, 2021, **5**, 148-167; c) C. Kung, *Nature*, 2005, **436**, 647-654; d) Y. Zhang, J. Yu, H. N. Bomba, Y. Zhu and Z. Gu, *Chem. Rev.*, 2016, **116**, 12536-12563.
2.   a) L. Takacs, *Bull. Hist. Chem.*, 2003, **28**, 26-34; b) L. Takacs, *J. Mater. Sci.*, 2004, **39**, 4987-4993.
3.   W. W. Boldyrew, E. G. Awwakumow, H. Harenz, G. Heinicke and L. I. Z. Strugowa, *Anorg. Allg. Chem.*, 1672, **393**, 152-158.
4.   J. G. Hernández and C. Bolm, *J. Org. Chem.*, 2017, **82**, 4007-4019.
5.   a) I. Omae, *Coord. Chem. Rev.*, 2004, **248**, 995-1023; b) K. Godula, *Science*, 2006, **312**, 67-72; c) D. Morales-Morales, in *Palladacycles*, eds. J. Dupont and M. Pfeffer, Wiley-VCH, Weinheim, Germany, 2008, pp. 1-12; d) M. Albrecht, *Chem. Rev.*, 2010, **110**, 576-623; e) T. W. Lyons and M. S. Sanford, *Chem. Rev.*, 2010, **110**, 1147-1169; f) J. Yamaguchi, A. D. Yamaguchi and K. Itami, *Angew. Chem. Int. Ed.*, 2012, **51**, 8960-9009; g) M. Albrecht, in *Palladacycles*, eds. J. Dupont and M. Pfeffer, Wiley-VCH, Weinheim, Germany, 2008, pp. 13-33.
6.   M. Juribasic, K. Uzarevic, D. Gracin and M. Curic, *Chem. Commun.*, 2014, **50**, 10287-10290.
7.   a) T. Roth, H. Wadepohl, D. S. Wright and L. H. Gade, *Chem. Eur. J.*, 2013, **19**, 13823-13837; b) M. S. Balakrishna, D. Suresh and J. T. Mague, *Inorg. Chim. Acta*, 2011, **372**, 259-265.
8.   H. Klare, J. M. Neudorfl and B. Goldfuss, *Beilstein J. Org. Chem.*, 2014, **10**, 224-236.
9.   D. Suresh, M. S. Balakrishna, K. Rathinasamy, D. Panda and S. M. Mobin, *Dalton Trans.*, 2008, DOI: 10.1039/b804026p, 2812-2814.
10.   D. S. Wright, in *Comprehensive Inorganic Chemistry II*, Elsevier, Oxford, United Kingdom, 2 edn., 2013, vol. 1, pp. 953-967.
11.   Y. X. Shi, K. Xu, J. K. Clegg, R. Ganguly, H. Hirao, T. Friscic and F. Garcia, *Angew. Chem. Int. Ed.*, 2016, **55**, 12736-12740.
12.   O. J. Scherer, K. Andres, C. Krüger, Y.-H. Tsay and G. Wolmerhäser, *Angew. Chem. Int. Ed.*, 1980, **19**, 571-572.
13.   a) J. K. Brask, T. Chivers, M. L. Krahn and M. Parvez, *Inorg. Chem.*, 1999, **38**, 290-295; b) Y. X. Shi, R. Z. Liang, K. A. Martin, D. G. Star, J. Diaz, X. Y. Li, R. Ganguly and F. Garcia, *Chem. Commun.*, 2015, **51**, 16468-16471; c) A. Bashall, E. L. Doyle, F. García, G. T. Lawson, D. J. Linton, D. Moncrieff, M. McPartlin, A. D. Woods and D. S. Wright, *Chem. Eur. J.*, 2002, **8**, 5723-5731.
14.   J. H. M. Lange, H. K. A. C. Coolen, H. H. Van Stuivenberg, J. A. R. Dijksman, A. H. J. Herremans, E. Ronken, H. G. Keizer, K. Tipker, A. C. McCreary, W. Veerman, H. C. Wals, B. Stork, P. C. Verveer, A. P. Den Hartog, N. M. J. De Jong, T. J. P. Adolfs, J. Hoogendoorn and C. G. Kruse, *J. Med. Chem.*, 2004, **47**, 627-643.
15.   a) H. Küçükbay, R. Durmaz, N. Okyucu and S. Günal, *Folia Microbiol.*, 2003, **48**, 679-681; b) M. A. Gonzalez, D. B. Gorman, C. T. Hamilton and G. A. Roth, *Org. Process Res. Dev.*, 2008, **12**, 301-303.
16.   a) J. Zhang and Y. Shi, *Tetrahedron Lett.*, 2000, **41**, 8075-8078; b) J. H. M. Lange, S. Verhoog, H. J. Sanders, A. Van Loevezijn and C. G. Kruse, *Tetrahedron Lett.*, 2011, **52**, 3198-3200; c) C. Bolm and C. Worch, *Synthesis*, 2007, **2007**, 1355-1358.

17. D. Tan, V. Strukil, C. Mottillo and T. Friscic, *Chem. Commun.*, 2014, **50**, 5248-5250.
18. D. Tan, C. Mottillo, A. D. Katsenis, V. Strukil and T. Friscic, *Angew. Chem. Int. Ed.*, 2014, **53**, 9321-9324.
19. J. L. Howard, PhD, Cardiff University, 2018.
20. G. Cahiez and M. Alami, *Tetrahedron Lett.*, 1986, **27**, 569-572.
21. a) Y. Hideki, H. Yasuhiro, T. Jun, S. Hiroshi and O. Koichiro, *Bulletin Chem. Soc. Japan*, 1997, **70**, 2297-2300; b) G. Cahiez, C. Duplais and J. Buendia, *Chem. Rev.*, 2009, **109**, 1434-1476.
22. M. Hirofumi, M. Taro, M. Takeshi and N. Ikuzo, *Chem. Lett.*, 2011, **40**, 368-369.
23. M. Yamashita, K. Okuyama, I. Kawasaki, S. Nakamura, R. Nagamine, T. Tsujita and S. Ohta, *Chem. Pharm. Bull.*, 2000, **48**, 1799-1802.
24. J. HUAJIANG and Z. YONGMIN, *Chinese J. Org. Chem.*, 1997, **17**, 242-246.
25. a) R. C. Betori, B. R. McDonald and K. A. Scheidt, *Chem. Sci.*, 2019, **10**, 3353-3359; b) R. C. Betori and K. A. Scheidt, *ACS Catal.*, 2019, **9**, 10350-10357; c) B. R. McDonald and K. A. Scheidt, *Org. Lett.*, 2018, **20**, 6877-6881.
26. C. Hansch, S. D. Rockwell, P. Y. C. Jow, A. Leo and E. E. Steller, *J. Med. Chem.*, 1977, **20**, 304-306.
27. a) L. Chen, M. Regan and J. Mack, *ACS Catal.*, 2016, **6**, 868-872; b) J. L. Howard, Y. Sagatov, L. Repusseau, C. Schotten and D. L. Browne, *Green Chem.*, 2017, **19**, 2798-2802; c) Z.-J. Jiang, Z.-H. Li, J.-B. Yu and W.-K. Su, *J. Org. Chem.*, 2016, **81**, 10049-10055; d) K. L. Denlinger, L. Ortiz-Trankina, P. Carr, K. Benson, D. C. Waddell and J. Mack, *Beilstein J. Org. Chem.*, 2018, **14**, 688-696; e) P. Ying, J. Yu and W. Su, *Adv. Synth. Catal.*, 2021, **363**, 1246-1271; f) J. L. Howard, Y. Sagatov and D. L. Browne, *Tetrahedron*, 2018, **74**, 3118-3123.
28. C. Elschenbroich and A. Salzer, *Organometallics: A Concise Introduction*, VCH, 1992.
29. a) B. P. Hutchings, D. E. Crawford, L. Gao, P. Hu and S. L. James, *Angew. Chem. Int. Ed.*, 2017, **56**, 15252-15256; b) K. Kubota, T. Seo, K. Koide, Y. Hasegawa and H. Ito, *Nat. Commun.*, 2019, **10**, 111.
30. a) Q. Cao, R. T. Stark, I. A. Fallis and D. L. Browne, *ChemSusChem*, 2019, **12**, 2554-2557; b) Q. Cao, J. L. Howard, E. Wheatley and D. L. Browne, *Angew. Chem. Int. Ed.*, 2018, **57**, 11339-11343; c) J. Yin, R. T. Stark, I. A. Fallis and D. L. Browne, *J. Org. Chem.*, 2020, **85**, 2347-2354.
31. a) J. A. Kerr, *Chem. Rev.*, 1966, **66**, 465-500; b) W. M. Haynes, *CRC Handbook of Chemistry and Physics*, CRC Press, Taylor & Francis Group, Boca Raton, Florida, United States of America, 92 edn., 2014; c) S. W. Benson, *J. Chem. Educ.*, 1965, **42**, 502.
32. a) M. T. J. Williams, L. C. Morrill and D. L. Browne, *ACS Sustainable Chem. Eng.*, 2020, **8**, 17876-17881; b) J.-L. Do, C. Mottillo, D. Tan, V. Štrukil and T. Friščić, *J. Am. Chem. Soc.*, 2015, **137**, 2476-2479; c) M. Leonardi, M. Villacampa and J. C. Menéndez, *Chem. Sci.*, 2018, **9**, 2042-2064; d) J. L. Howard, W. Nicholson, Y. Sagatov and D. L. Browne, *Beilstein J. Org. Chem.*, 2017, **13**, 1950-1956.
33. G. W. Wang, *Chem. Soc. Rev.*, 2013, **42**, 7668-7700.
34. a) R. Schmidt, C. F. Burmeister, M. Baláž, A. Kwade and A. Stolle, *Org. Process Res. Dev.*, 2015, **19**, 427-436; b) C. F. Burmeister, R. Schmidt, K. Jacob, S. Breitung-Faes, A. Stolle and A. Kwade, *Chem. Eng. J.*, 2020, **396**, 124578; c) C. F. Burmeister, A. Stolle, R. Schmidt, K. Jacob, S. Breitung-Faes and A. Kwade, *Chem. Eng. Technol.*, 2014, **37**, 857-864; d) H. Kulla, S. Haferkamp, I. Akhmetova, M. Röllig, C. Maierhofer, K. Rademann and F. Emmerling, *Angew. Chem. Int. Ed.*, 2018, **57**, 5930-5933; e) N. Cindro, M. Tireli, B. Karadeniz, T. Mrla and K. Užarević, *ACS Sustain. Chem. Eng.*, 2019, **7**, 16301-16309; f) S. Lukin, M. Tireli, I. Lončarić, D. Barišić, P. Šket, D. Vrsaljko, M. Di Michiel, J. Plavec, K. Užarević and I. Halasz, *Chem. Commun.*, 2018, **54**, 13216-13219.

35. A. P. Golombek and M. P. Hendrich, *J. Magn. Reson.*, 2003, **165**, 33-48.
36. H.-M. Huang, M. Koy, E. Serrano, P. M. Pflüger, J. L. Schwarz and F. Glorius, *Nat. Cat.*, 2020, **3**, 393-400.
37. C. E. Teerlinck and W. J. Bowyer, *J. Org. Chem.*, 1996, **61**, 1059-1064.

5 Generation of Organomanganese Halides *via* Ball Milling

5.1 Introduction to Organomanganese Halides

The discovery of organometallics such as Grignard, organolithium, and organozinc reagents has profoundly influenced synthetic chemistry. These are highly versatile reagents that are among the most common nucleophilic at carbon synthons. Their applications to synthetic transformations are numerous and their generation is well understood. However, the use of these reagents is not without difficulty due to the reactivity of these species, often stringently dry reaction conditions can be required, alongside low reaction temperatures. Furthermore, as Grignard or organolithium reagents are such powerful nucleophiles they have limited functional group tolerance prohibiting the use of these compounds with complex molecules. Organozinc compounds do have superior functional group tolerance, than that of the forementioned organometallics, but often their synthesis is more capricious than that of more reactive organometallics.[1]

A possible alternative to these well-established reagents are organomanganese compounds, which exhibit superior stability and functional group tolerance, only bested by organoindium compounds.[2] With manganese metal itself being toxicologically benign and the second most common transition metal in the earth's crust after iron, it is a safer and more sustainable feedstock over other transition metal elements.[3] The first preparation of an organomanganese compound was performed by Gilman and Bailie, in 1937, from phenyl magnesium iodide **353** and manganese(II) iodide (Scheme 5.01).[4] The report concerned the preparation of both phenyl manganese iodide **354** and diphenyl manganese **355** and briefly studied there interaction with electrophiles. In the following 40 years there were sporadic reports of the synthesis and reactivity of other organomanganese reagents but detailed study into these compounds only started appearing in the 1970s.[5]
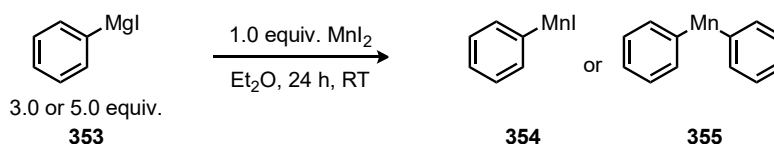
Scheme 5.01 Gilman and Bailie preparation of organomanganese compounds.

5.1.1 The Synthesis of Organomanganese Halides

The first report of the generation of organomanganese from the bulk metal came from Cahiez and coworkers in 1989, where organomanganese formation was limited to only allyl bromides and α-halo-esters (Scheme 5.02a).[6] Through optimization of this reaction the choice of solvent was key to access the reactive species, only EtOAc produced good yields for the addition of the organomanganese to a ketone initially. Further issues were encountered with expanding the substitution of the allyl halide to the γ position, and with the use of aldehydes as an electrophile also proving unproductive. Through the addition of a catalytic quantity of zinc(II) chloride (10 mol%), the scope of the reaction could be extended to crotyl and prenyl bromides (Scheme 5.02b).[6] Furthermore, through the use of the zinc-manganese couple produced by the addition of zinc(II) chloride, the solvent could be exchanged for THF, further extending the reactivity to allyl chlorides.[6] Takai and coworkers subsequently went on to reveal that catalytic lead(II) chloride (1 mol%) along with TMSCl (40 mol%) could also be used for the activation of the manganese metal surface to generate allyl manganese from allyl chloride (Scheme 5.02c).[7] This alternate method could also achieve this synthesis at room temperature in only 30 minutes, whereas previous reports from Cahiez and coworkers required elevated temperatures. Knochel and coworkers have disclosed a method for the generation of functionalized aryl organomanganese species from aryl bromides and iodides using catalytic indium(III) chloride (2.5 mol%) and lead(II) chloride (2.5 mol%) in the presence of lithium chloride (Scheme 5.02d). This method could also be applied for the generation of benzyl organomanganese from benzyl chlorides in good yields.[8] This work did expand on the range of organomanganese halides which could be generated directly from the metal but was limited to electron poor aryl halides. Although significant efforts have been made, the generation of organomanganese halides directly from the reaction of the bulk metal and a carbon halide bond it is currently limited to only activated species.[9] To access a broader range of organomanganese halides alternate methods have been developed.

a) Cahiez and coworkers demonstrating the first direct synthesis of organomanganese

R^1 and R^1, Br; R^2, R^3, O; 1.5 equiv. Mn granular; EtOAc [1.0 M]; N$_2$, 60 °C → R^1, OH, R^3, R^2
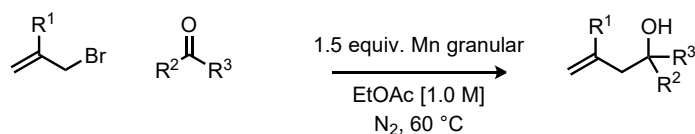
b) Cahiez and coworkers discovery of the zinc-managanese couple

R^1, R^2, R^3, Cl; R^4, R^5, O; 1.5 equiv. Mn granular; 10 mol% ZnCl$_2$; THF [1.0 M]; N$_2$, 60 °C → R^1, R^2, R^3, OH, R^5, R^4

c) Takai and coworkers activating the surface of manganese with TMSCl

R^1O_2C, Cl or R^1, Cl; R^2, R^3, O; 2.0 equiv. Mn; 40 mol% TMSCl; 1.0 mol% PbCl$_2$; THF [1.0 M], N$_2$ → R^1O_2C, OH, R^3, R^2 or R^1, OH, R^3, R^2
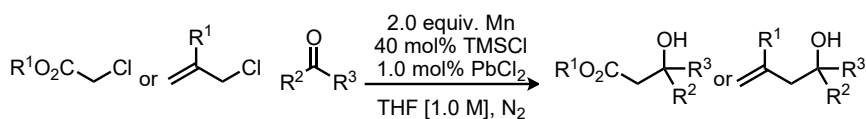
d) Knochel and coworkers indium and lead catalysed generation of organomanganese

EWG, X or Ar, Cl; X = Br or I; 3.0 equiv. Mn; 2.5 mol% InCl$_3$; 2.5 mol% PbCl$_2$; THF [1.0 M], N$_2$; 50 °C or 25 °C → EWG, MnX or Ar, MnCl
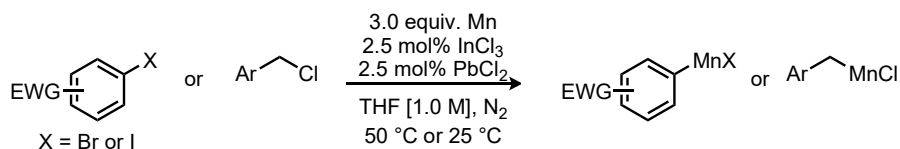
Scheme 5.02 Synthesis of organomanganese from commercially available bulk manganese metal.

The production of organomanganese directly from less reactive alkyl and aryl halides is possible using highly active manganese metal. Rieke and coworkers have pioneered the application of highly reactive metals for the generation of organometallics.[10] The methodology developed requires the reduction of metal salts by lithium or sodium to produce metal particles (Ø <1 µm) free from any passivation. Rieke and coworkers have applied this methodology to a range of metals including manganese.[10-11] The Rieke manganese was accessed through reduction of manganese(II) chloride by lithium in the presence of naphthalene as an electron carrier (Scheme 5.03a). The highly reactive manganese could then be used to access organomanganese reagents from alkyl and aryl bromides.[12] Work then continued to further expand the range of accessible organomanganese reagents to include heteroaryl bromides and iodides.[13] Furthermore, Rieke and coworkers also accessed benzyl and alkyl organomanganese reagents from the tosylates and mesylates, providing access through the oxidative addition to a C-O bond for the first time.[14] Inspired by the work of Rieke, alternate reducing reagents have been utilized for the production of highly reactive manganese metal particles including lithium aluminium hydride, magnesium, or potassium graphite (Scheme 5.03b).[15] Cahiez and coworkers also improved on the generation of Rieke manganese by successfully

replacing the naphthalene used as an electron carrier with 2-phenyl pyridine **356** (Scheme 5.03c).[15b] This alternate method is more attractive for the large-scale preparation of Rieke manganese which is often disadvantaged due to the difficulty in removing the remaining naphthalene.

a) Generation and application of Rieke manganese

$$R = \text{Alkyl, Aryl, Heteroaryl}$$
$$X = \text{Br, I, OTs, OMs}$$

$$MnBr_2 \xrightarrow[\text{THF [0.5 M], Ar}]{\substack{\text{2.0 equiv. Li} \\ \text{30 mol\% Naphthalene}}} \left[Mn^* \right] \xrightarrow{R-X} R-MnX$$
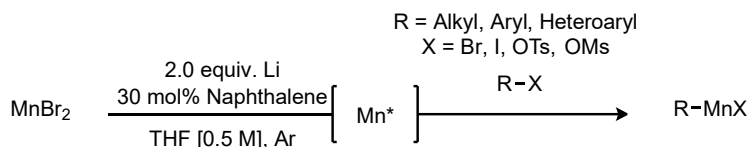
b) Various methods for the generation activated manganese metal

$$MnCl_2 \xrightarrow[\substack{\text{THF [0.4 M]} \\ \text{0 °C, Ar}}]{\text{1.0 equiv. LiAlH}_4} \left[Mn^* \right] \xleftarrow[\text{THF [0.35 M], Ar}]{\text{2.7 equiv. Mg turnings}} Li_2MnCl_4$$

$$MnBr_2 \bullet LiBr \xrightarrow[\substack{\text{THF [0.12 M]} \\ \text{-15 °C, Ar}}]{\text{2.0 equiv. C}_8\text{K}} \left[C_8Mn \right]$$
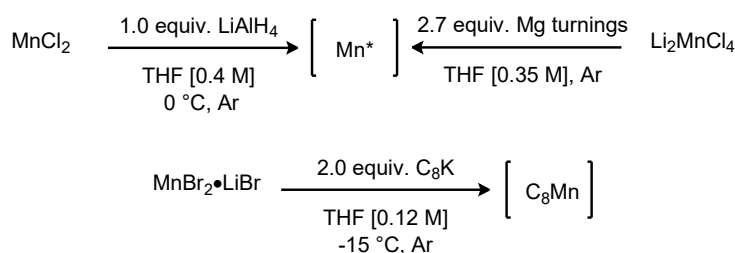
c) Cahiez and coworkers generation of activated manganese

$$R = \text{Alkyl, Aryl, Heteroaryl}$$

$$MnCl_2 \bullet 2LiCl \xrightarrow[\text{THF [0.5 M], Ar}]{\substack{\text{2.0 equiv. Li} \\ \text{30 mol\%} \\ \text{2-Phenylpyridine \textbf{356}}}} \left[Mn^* \right] \xrightarrow{R-Br} R-MnBr$$
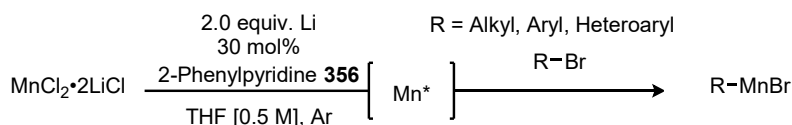
Scheme 5.03 Generation of activated manganese and application to production of organomanganese.

Transmetallation of organolithium or organomagnesium halides with manganese(II) halides allows access to a range of organomanganese halides including alkyl, allyl, benzyl, alkenyl, alkynyl, aryl, and heteroaryl (Scheme 5.04).[6b, 16] The limits of the possible organomanganese compounds that can be prepared through transmetallation is dependent on the stability of the organolithium or organomagnesium starting materials. The functional group tolerance of organomanganese halides can be demonstrated by the addition of cosolvents (EtOAc, MeCN, CH$_2$Cl$_2$, etc.) that would readily react with the organometallic precursor.[9, 17] This method of preparation has provided a reliable access to the organomanganese halides and permitted the study of their stability and reactivity in detail.[18] This has shown that the formation of ate complexes from the corresponding lithium or tetraalkyl ammonium salts can stabilize the organomanganese.[19] Also, the use of coordinating solvent such as THF or DMF can reduce the rate of β-hydride elimination.[20] Organomanganese halides prepared from manganese(II) iodide undergo much faster β-hydride elimination than those prepared from other manganese(II) salts.[9, 21] This instability means that they must be handled at low temperatures. Contrastingly,

organomanganese halides generated from the corresponding chlorides and bromides are much more stable and can often be handled at room temperature or even in refluxing solvent without significant degradation. Methyl organomanganese chloride, for example, can even be stored for months in THF at room temperature under an argon atmosphere.[9] Due to the moderate solubility of manganese(II) chloride and manganese(II) bromide in THF, often the ate complexes must be pre-formed using the corresponding lithium or tetra-alkylammonium halides salts to increase their solubility. The resulting ate complexes can then undergo transmetallation with organomagnesium halides at higher concentrations, reducing the reaction time.[6b, 16] One benefit of using organolithium reagents for the generation of organomanganese halides is that the ate complexes can be formed *in situ* by the lithium halide salts formed as the biproduct of transmetallation.

Preparation of organomanganese halides via transmetallation

$$MnX_2 \quad \xrightarrow[\text{THF or Et}_2O]{\textbf{R}-\text{Li} \quad \text{or} \quad \textbf{R}-\text{MgX}} \quad \textbf{R}-MnX$$

X = Cl, Br, I

Possible additives
LiX, NR$_4$X, DMF

R = Alkyl, allyl, benzyl, alkenyl, alkynyl, aryl, or heteroaryl
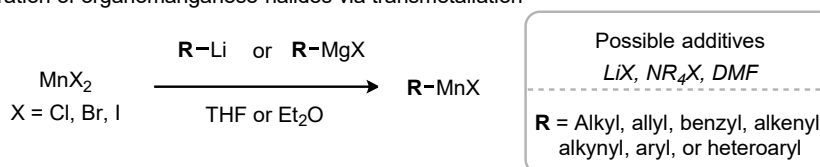
Scheme 5.04 Preparation of organomanganese through transmetallation.

Currently the synthesis of organomanganese halides has mostly been accomplished through the transmetallation of more reactive organometallics and employing this method significant examination of their reactivity and stability has been carried out. However, this method reduces the scope of the organomanganese being generated due to poor functional group tolerance of the more reactive organometallics. The use of activated manganese generated through the reduction of manganese(II) salts has provided access to a broader scope of organomanganese halides. Although, this method does require the manipulation of highly reactive finely divided metal powders and strong reducing agents. Ideally it would be possible to access the same range of organomanganese halides directly from the bulk metal without the need for strenuous prior activation, unfortunately such a general method does not yet exist.

5.1.2 The Chemistry of Organomanganese Halides

Organomanganese halides display good functional group tolerance as they are unreactive with esters, amides, and nitriles at elevated temperatures, and at room temperature they do not react with alkyl chlorides and bromides, or trifluoromethyl and trichloromethyl groups.[22] This tolerance often leads to high selectivity in reactions where

other organometallics would lead to a mixture of products. This benefit can be demonstrated through reactions with CO_2 in which organomanganese exclusively produces the acid product due to not reacting with the carboxylate whereas organolithium or Grignard reagents may undergo multiple additions (Scheme 5.05a).[9] Furthermore, the acylation of organomanganese with anhydrides or acyl chlorides can produce exclusively the ketone without 1,2-addition also observed with other nucleophiles (Scheme 5.05b).[16b, 17c, 20b] This leads to much higher yields being obtained than for the organolithium or Grignard mediated acylation's.[23] This high selectivity and good functional group tolerance have allowed Cahiez and coworkers to synthesize over 1000 functionalized ketones from various organomanganese halides and acylating reagents.[9, 24] These high selectivity's can still be achieved as organomanganese reagents require the use of elevated temperature or Lewis acids to undergo 1,2-addition to ketones and aldehydes in a similar fashion to other organometallics. Through competition experiments using electrophiles containing multiple reactive ketones or aldehydes, organomanganese halides show surprising selectivity for the less sterically demanding substrates indicating the sensitivity to steric effects even over electronic factors (Scheme 5.05c).[25] This sensitivity to steric effects has allowed organomanganese species to be successfully applied to highly diastereoselective additions to aldehydes during natural product synthesis.[26] The diastereoselectivity achieved also outperforms both Grignard or organolithium reagents in the same transformations such as addition to boc protected amino aldehydes **360** and **363** (Scheme 5.05d).[26-27]

a) Addition of organomanganese halides to CO_2
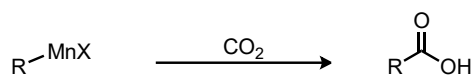
b) Acylation of organomanganese halides with acyl chlorides or anhydides
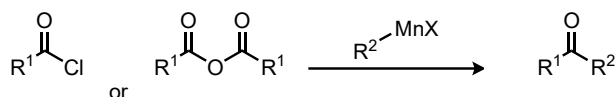
c) Selectivity driven by sensitivity to steric effects on organomanganese halide
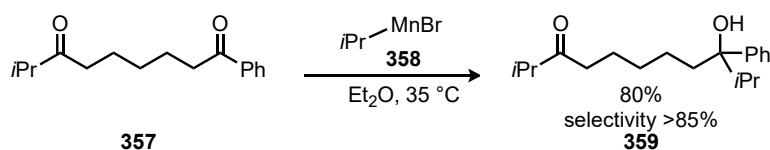
d) Diastereoselectivity of organomanganese halide compared to other organometallics

[M]	361:362
MnBr	89:11
MgI	54:46

[M]	364:365
MnBr	96:4
Li	39:61
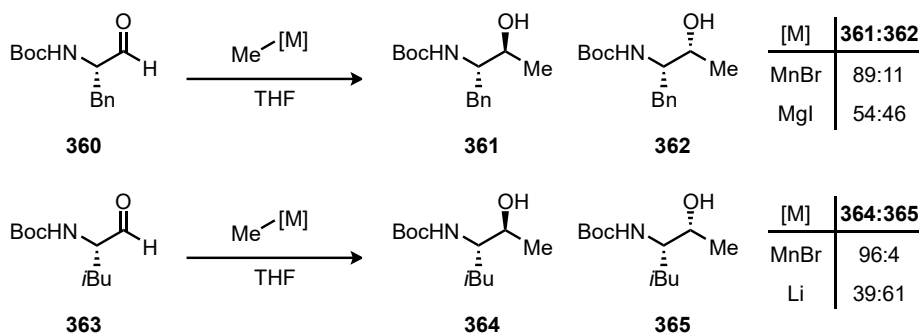
Scheme 5.05 1,2-Additions and acylation reactions of organomanganese halides.

Organomanganese halides have been shown to be moderately selective for 1,4-additions in the presence of various Michael acceptors.[16a, 28] The application of various Lewis acids such as boron trifluoride or lithium halide salts improve this selectivity but yields could not exceed 70% for the desired conjugate addition product due to competing 1,2-addition reactions.[29] With the use of a copper catalyst highly selective conjugate addition procedures could be performed with loadings of copper as low as 0.1 mol%.[30] Organomanganese halides have also been shown to be competent partners in cross-coupling reactions with various metal catalysts including, Pd, Ni, Fe, and Cu.[31] Both palladium and nickel catalysis have been applied for the synthesis of biaryls in good yields. Cahiez and coworkers used palladium catalysis to synthesize challenging *o,o'*-biarlys in excellent yields from organomanganese halides (Scheme 5.06a). During this work, they discovered that the sterically hindered aryl bromide coupling partners were more reactive than their iodide counterparts. This sterically challenging coupling often provides low yields using other cross-coupling reaction partners.[32] The nickel catalysed process developed by Schneider and coworkers (Scheme 5.06b) could also

produce a broad range of biaryl products under mild conditions. They found this procedure to be amenable to the challenging *o,o'*-biarlys but in reduced yields compared to that of the palladium catalysed reaction.

a) Palladium catalysed cross-coupling of organomanganese halides with aryl halides

90%
366

95%
367

X = Br 93%, X = I 0%
368
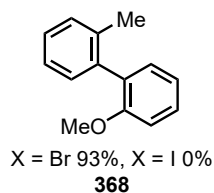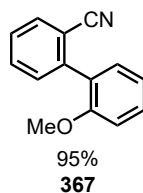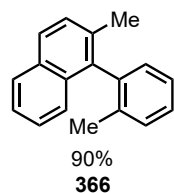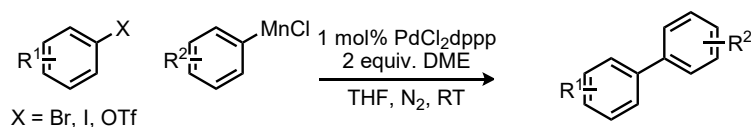
b) Nickel catalysed cross-coupling of aryl organomanganese halides and aryl halides

R = *i*Pr   **191**
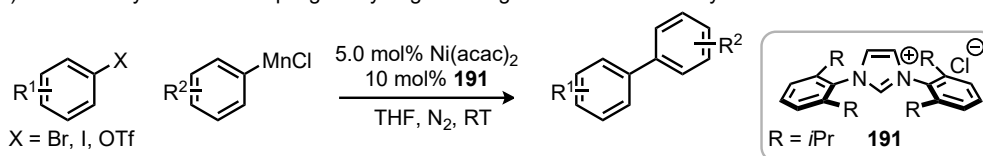
Scheme 5.06 Organomanganese halides utilized in cross-coupling reactions.

The reactivity of organomanganese halides with various electrophiles and its involvement in metal catalysed processes has been well established. This has highlighted a number of benefits, including increased diastereoselectivity with chiral electrophiles compared to other organometallics, which is likely caused by the sensitivity of organomanganese reagents to steric interactions. However, in the majority of these studies the generation of the organomanganese has been carried out through the transmetallation of a more reactive organometallic. This has therefore limited the scope of many of these investigations.

5.1.3 Use of Elemental Metals in Ball Milling

The first example of an organometallic species for the synthesis of C-C bonds under ball milling conditions came from Harrowfield and coworkers for the generation of Grignard reagents (Scheme 5.07a).[33] Through grinding napthyl chlorides and bromides with magnesium metal, the intermediate Grignard reagents could be generated and then trapped by the addition of benzophenone **369**, producing the tertiary alcohol product **370**. Due to the large excess of magnesium present in the reaction mixture, side products from both Pinacol coupling **371** and McMurry coupling **372** were observed. Further

investigation of these coupling reactions with benzophenone **369** and acetophenone would always produce a mixture of products including the diol, alkene, and the direct reduction of the ketone to either alcohol or alkane. This work established the use of ball milling to be able to remove the passivized metal surface allowing access to the reactive metal surface, without the addition of activating reagents often required in solution, such as iodine, TMSCl, or 1,2-dibromoethane.

Hanusa and coworkers expanded on this work in 2020 establishing the generation of Grignard reagents from naphthyl fluorides through the use of ball milling (Scheme 5.07b).[34] Activation of C-F bonds for the generation of Grignard reagents is particularly challenging due to the increased bond strength compared to other C-halide bonds (146 kJmol^{-1} stronger than C-Cl).[35] Indirect access to fluoro Grignards is possible through the use of fluorinating reagents in the presence of MgR$_2$ (R = Me, Et, Bu, or Ph), and Grignard reagents can be catalytically converted to the fluoro Grignards with a transition metal catalyst and perfluoroaryl compounds.[36] Direct insertion of magnesium into a C-F bond often requires the use of highly activated forms of magnesium metal such as Rieke magnesium or magnesium anthracene, and often these methods only achieve low yields.[37] Through the application of ball milling, access to fluoro Grignards was possible for 1-fluoronapthalene and 2-fluoronapthalene followed by successful homocoupling to the bi-naphthyls **373** in the presence of iron(III) chloride, in comparable yields to the bromonaphthalene equivalents. However, this work also required a significant excess of magnesium (6 equiv.) and both examples of ball milling enabled generation of Grignard reagents required the use of glove boxes to carry out these reactions under protective atmospheres.

a) Harrowfield and coworkers generation of Grignard reagents

b) Hanusa and coworkers ball milling enabled generation of fluoro Grignards
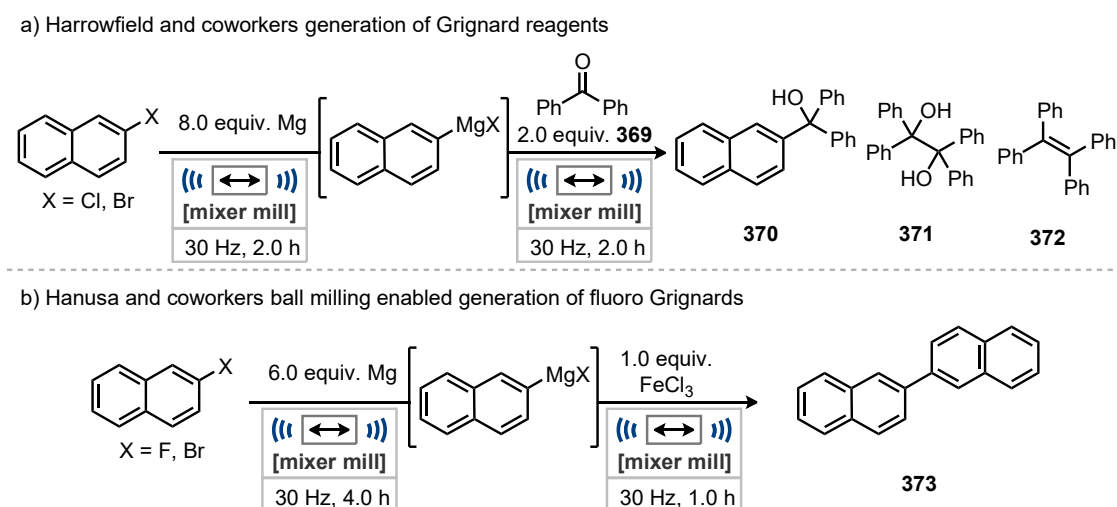
Scheme 5.07 Generation of Grignard and fluoro Grignard reagents *via* ball milling.

Recently Dai and coworkers established a ball milling mediated synthesis of conjugated porous networks **374** (CPNs) (Scheme 5.08).[38] These materials contain nano-porous skeletons with high surface areas and superb stability leading to their applications in a range of uses including energy storage, gas separation, and catalysis.[39] The mechanochemical synthesis of these materials utilised magnesium metal for the dehalogenative coupling of tetra-halo benzene to generate the 2D molecular architectures **374**. The materials produced were then investigated for energy storage applications and were found to be promising candidates as electrode materials in lithium-ion batteries due to efficient intercalation of lithium ions. The mechanochemical method established may provide a more sustainable method for the synthesis of these materials due to the significantly reduced solvent requirement.
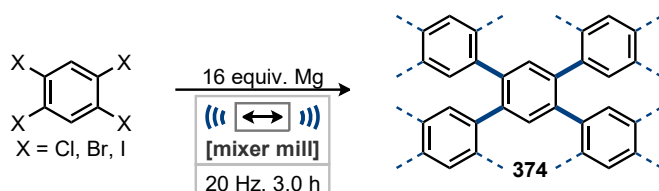
Scheme 5.08 Ball milling dehalogenative Ullman coupling for the synthesis of CPNs.

Lumb and coworkers developed a redox promoted self-assembly of metal organic materials through the reduction of *ortho*-quinones **375** with zinc in the presence of a range of ligands (Scheme 5.09).[40] This one pot multicomponent strategy allowed for the synthesis of discrete and extended metal-organic materials including the complex **378**. The envisaged reaction would occur through single electron reduction of two *ortho*-quinones **375** by zinc for the generation of the paramagnetic intermediate **377**, which could then coordinate to the ligands within the reaction mixture to generate the final complexes. Ligand design and stoichiometry could then be tailored for the generation of mono or multinuclear complexes including metal-organic polymers. Through optimization, the use of toluene and water as liquid additives provided a high yielding process without the production of any biproducts. This procedure demonstrated excellent efficiency in the synthesis of metal organic compounds by combining both the metal oxidation and ligand coordination steps into a one pot multicomponent procedure.
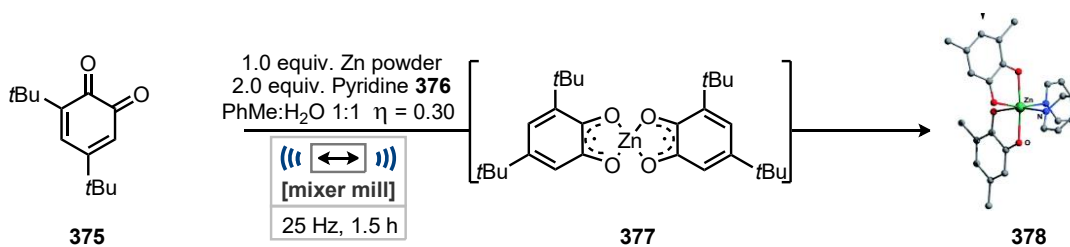
Scheme 5.09 Redox promoted complexation of *ortho*-quinone with Zn.[v]

Previously the group has developed the generation of organozinc reagents *via* ball milling through the reaction of zinc metal with alkyl and aryl halides (Scheme 5.10).[41] The initial report of this process generated the organozinc and then successfully applied this intermediate in a Negishi cross-coupling reaction with an aryl halide as a two-step one pot procedure (Scheme 5.10a). This reaction could be carried out without the protection of moisture or air and all the reagents could simply be added to the milling vessel on the bench. Using ball milling, a one pot process for the Negishi cross-coupling was also established for the first time where both coupling partners, zinc metal, and the palladium catalyst, along with any additives were present from the start of the reaction, simplifying the method for this vital cross-coupling reaction (Scheme 5.10b). Organozinc reagents generated by ball milling have then been applied to a Barbier reaction and allylation reaction in one-pot methods, again without the necessity for a protective atmosphere or dry solvent which are commonly required in solution (Scheme 5.10c – d). Ball milling has also been shown to be able to generate the organozinc intermediate from a range of forms of zinc metal whereas in solution differing forms can lead to significant discrepancies in the generation of the organometallic, leading to challenging reproducibility.

---

[v] Crystal structures reproduced from ref. 40 with permission from the RSC. Further permissions for reproduction of this scheme should be directed to the RSC.

a) Two-step one-pot procedure for the mechonchemical Negishi cross-coupling

b) One pot procedure for the mechonchemical Negishi cross coupling

c) Zinc mediated Barbier reaction

d) Zinc mediated allyation reaction
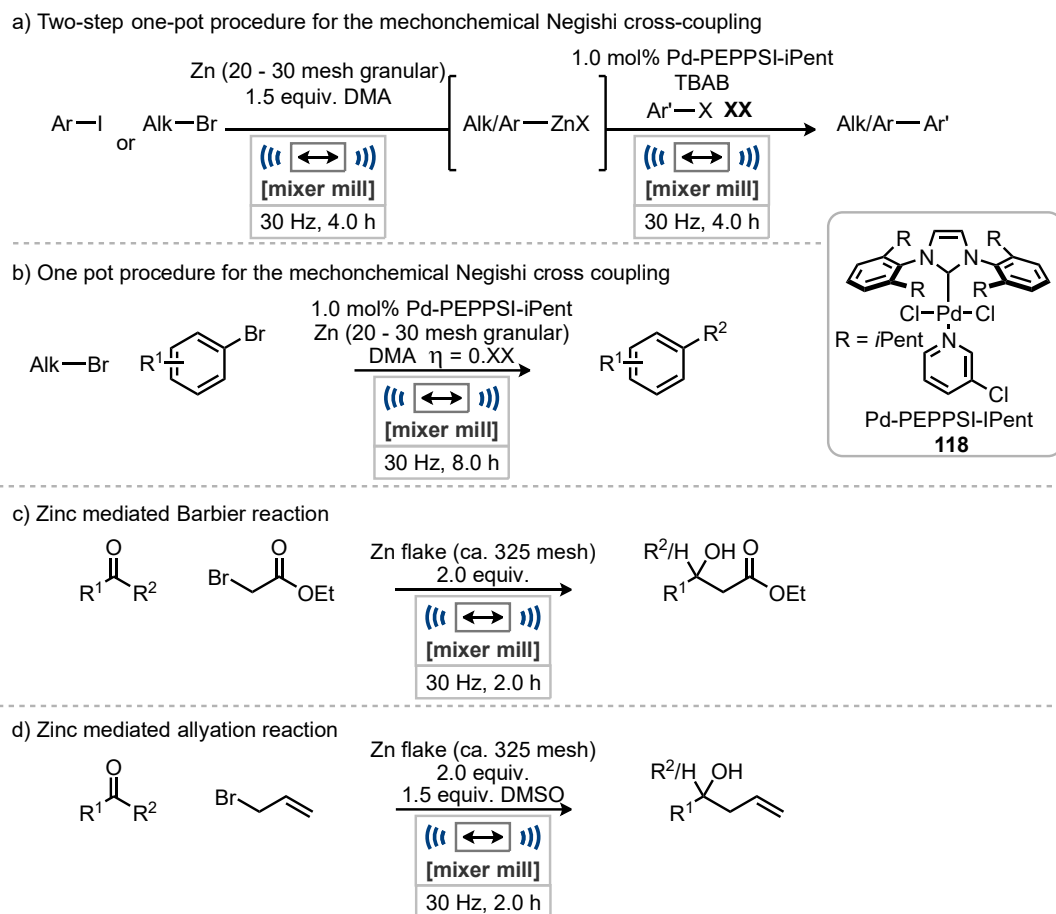
Scheme 5.10 Generation and application of organozinc enabled by ball milling.

The application of the elemental form of metals in ball milling reactions as catalysts is a growing area of research.[42] Recently termed direct mechanocatalysis by Borchardt, where the milling vessel or grinding balls are either made directly from, or coated with, the metal catalyst. The pre-functionalization of these milling vessels can be achieved simply by milling the metal in the absence of any other reagents to distribute the catalytic surface within the vessel and onto the grinding balls. Mack and coworkers have pioneered this method of mechanocatalysis producing several examples using Cu, Ag, and Ni catalytic systems, simply by milling the metal prior to the reaction.[43] Their first example of this method utilized pre-milled copper coating the jar and ball, followed by the addition of a phenyl acetylene **36** and benzyl azide **379** for a click reaction (Scheme 5.11a). Su and coworkers, inspired by the use of copper metal as a catalyst found that application of copper balls could facilitate dehydrogenative couplings of tetrahydroisoquinolines **35** with terminal alkynes **36** or indoles **381** (Scheme 5.11b).[44]

a) Mack and coworkers using a copper vial for a click reaction

Ph ≡   Ph–N₃

36   **379**

Cu vial
Cu Ball
[mixer mill]
15 min

Ph–N⟨N=N⟩–Ph

380
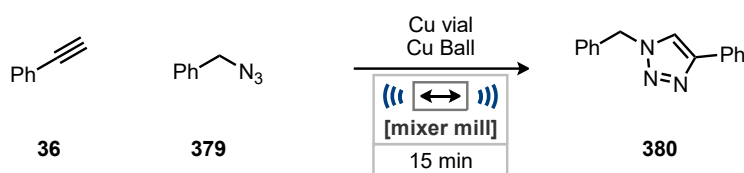
b) Su and coworkers dehydrogenative coupling of tetrahydroisoquinolines

Ph ≡   (indole, N–H)   or

36   **381**   **35** N–Ph

1.1 equiv. DDQ
Cu Balls
[mixer mill]
30 Hz, 0.5 h

N–Ph, R
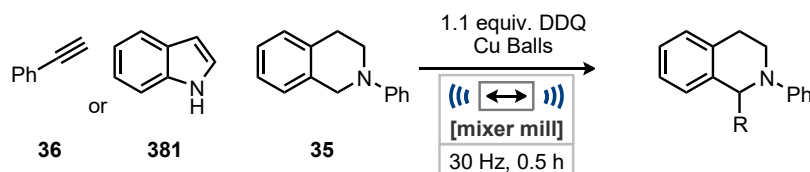
Scheme 5.11 Copper utilized in mechanocatalysis for click chemistry and dehydrogenative coupling.

Borchardt and coworkers have developed a range of methods for the synthesis of linear and branched polyphenylene polymers.[45] Their most recent example has successfully utilized palladium balls or palladium black metal powder for the Suzuki cross-coupling of 4-bromophenylboronic acid **382** to produce poly(*para*-phenylene) **383** (Scheme 5.12). During their investigation into the mechanism of the polymerization, *in situ* PXRD and Raman measurements confirmed the heterogeneous catalysis mechanism. Furthermore, addition of ligands typically able to assist the homogeneous catalysis provided no benefit in this procedure. Finally, the degree of polymerization of poly(*para*-phenylene) produced using the mechanochemical method surpassed those obtained through solution and electrochemical processes.[46]

Br––B(OH)₂

382

4.7 mol% Pd black or
2 Pd Balls
[mixer mill]
20 Hz, 8.0 h

(–⟨ ⟩–)ₙ

383
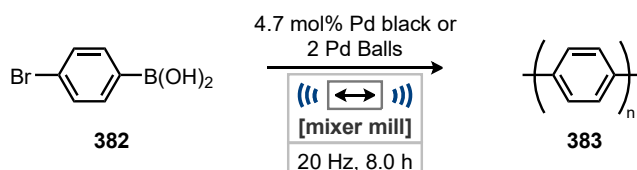
Scheme 5.12 Mechanocatalytic synthesis of poly(*para*-phenylene) **383**.

Through these examples the application of base metals in synthetic reactions under ball milling conditions can produce a range of benefits for stoichiometric or catalytic reactions. In the case of organometallic generation, the rapid production of these species compared to solution along with the simplification of the procedure provides a great benefit. Furthermore, in the case of organozinc compounds the ability to carry out their synthesis without the need for a protective atmosphere is very impressive. This area, however, is still very much in its infancy with limited examples of the use and generation of

organometallics under ball milling conditions. Numerous possible areas of exploration, including the synthesis of organometallics from other metals, are still to be investigated.

5.2 Results and discussion

5.2.1 Previous Work

Prior work in the group on the generation of organomanganese halides by ball milling had been carried out using ethyl 4-bromobutyrate, **294**, and manganese pieces under ball milling conditions with a variety of additives.[47] Due to the brittle nature of manganese metal, it will form a fine powder under ball milling conditions. The newly exposed metal surfaces should be highly reactive for the formation of organomanganese halides, due it being free of any contaminants or passivation. Furthermore, the presence of microcrystalline regions of the metal and defects in the metal surface containing low valent metal atoms should be highly reactive for the formation of organometallics.[48] These reactive surfaces have previously been shown to exist in higher concentrations on metal surfaces after ball milling of brittle metals.[48]
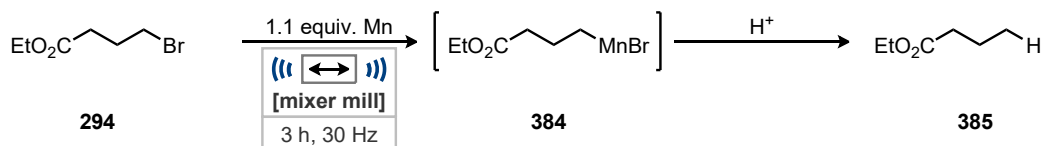
Entry	Time / h	Additive (equiv.)	Conversion of **294**[a]	Yield of **385**[a]
1	3	DMA (0.5)	77%	23%
2	3	DMA (1.0)	80%	37%
3	3	DMA (1.5)	84%	16%
4	3	LiCl (1.0)	52%	21%
5	3	LiCl (2.0)	33%	12%
6	3	THF (1.0)	69%	20%
7	3	LiCl (1.0) THF (1.0)	75%	36%
8	3	DMF (1.0)	75%	28%
9	3	EtOAc (1.0)	0%	0%
10	3	NMP (1.0)	81%	23%

[a] Measured by GC.

Table 5.01 Previous screening of conditions. Results obtained by Dr Joseph L. Howard.

Through this initial screening for the generation of organomanganese halides, addition of 1.0 equivalent of DMA (Table 5.01, entry 2) or 1.0 equivalent of lithium chloride and THF (Table 5.01, entry 7) had shown promising conversion and yields. These promising conditions were then applied to a two-step one-pot approach where the organomanganese halide intermediate would be produced in the first step and then an electrophile would be added in the second. All the electrophiles screened had been previously reported to undergo addition reactions with organomanganese halides.[9]
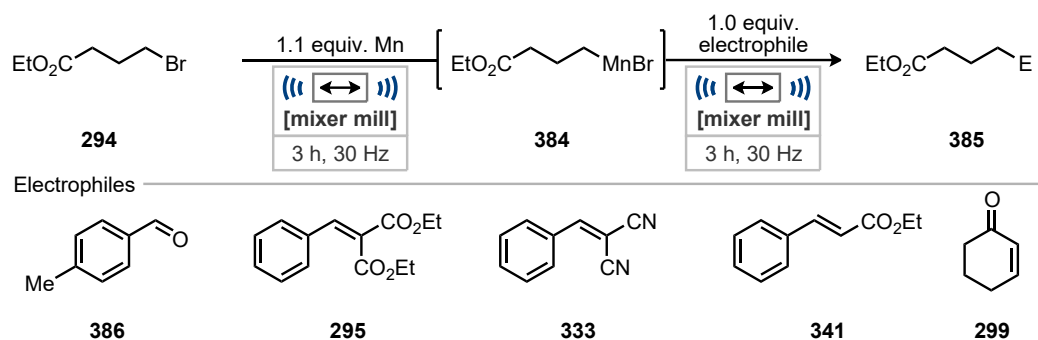
Scheme 5.13 One-pot two-step electrophile screen. Results obtained by Dr Joseph L. Howard.

All attempts to intercept the organomanganese halide using this one-pot two-step system were unsuccessful. The reaction method was then altered to include the electrophile from the initial onset of milling. Unfortunately, the desired addition products were also not observed under these reaction conditions either. Although this did lead to the discovery of the dimerization reaction of benzylidene malonates discussed in the previous chapter.

This work guided by the previous study and the results regarding the dimerization of benzylidene malonates aims to generate organomanganese halides from manganese metal and organic halides under ball milling conditions and successfully intercept them with a nucleophile.

5.2.2 Initial Conditions Screening

As using the conditions that had been developed thus far had failed to produce the desired organometallic nucleophile from ethyl 4-bromobutyrate **294**, a range of pro-nucleophiles **387** – **391** were screened under similar reaction conditions to the previous work. 2-Cyclohexen-1-one **299** and ethyl cinnamate **341** were chosen as conjugate electrophiles as they are both known to readily react with organomanganese halides.[9]

Finally, THF and lithium chloride were chosen as additives as they had both been vital for the dimerization reactivity previously explored and have both been reported to be able to stabilize organomanganese species.[49]
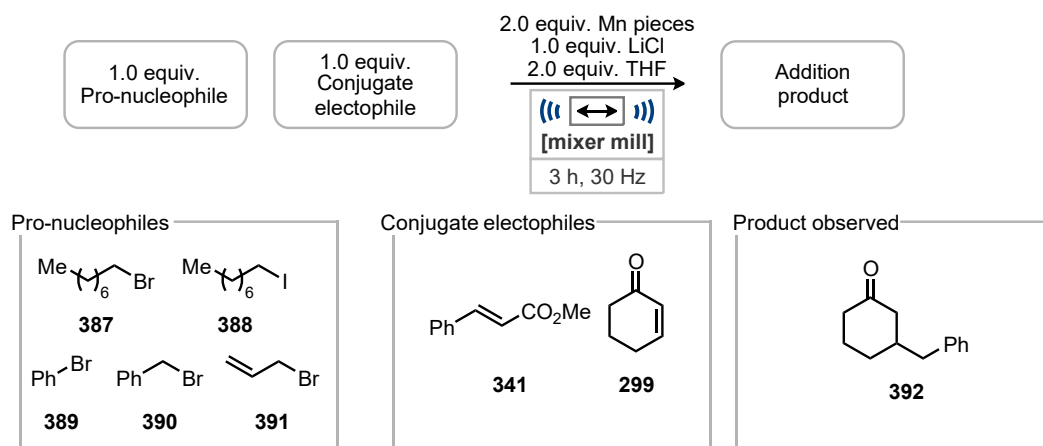
Scheme 5.14 Screening pro-nucleophiles and conjugate electrophiles.

Under these modified conditions only benzyl bromide showed any product formation with the desired conjugate addition product **392** being isolated in 8% yield (Scheme 5.14). This was the first confirmed production of the desired organomanganese halide successfully acting as a nucleophile. With this initial reactivity identified this reaction was then repeated using a 4-fluorobenzyl bromide **393** so that for the optimization ^{19}F NMR spectroscopy could be utilized for measuring reaction yields and conversion.
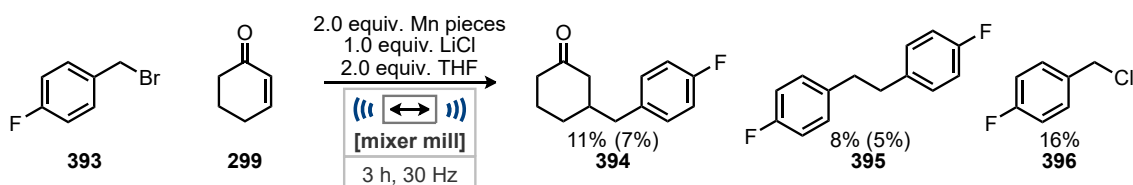
Yields determined by ^{19}F NMR spectroscopy using α,α,α-trifluorotoluene as an internal standard. Yield of isolated product in parentheses.

Scheme 5.15 Repeat of initial result with the fluorinated benzyl bromide **393**.

The initial reaction conditions were successfully repeated on the fluorinated variant in a similar yield of isolated product of **394**, 7% (Scheme 5.15). Also, through repeating this reaction side products including bibenzyl **395** and benzyl chloride **396** could be identified. The bibenzyl is likely generated through attack of the organomanganese on the remaining benzyl halide which is often observed in the generation of benzyl organometallics.[50] The benzyl chloride may be produced by Finkelstein reactivity with

the bromide being displaced by lithium chloride. These initial conditions show some promise confirming the ability to generate the desired organomanganese halide under ball milling conditions. Although further optimization and refinement of the reaction to improve selectivity and the yield of the transformation was clearly required.

5.2.3 Optimization

Initial optimization focused on the stoichiometry of the manganese metal and 4-fluorobenzyl bromide **393**. This was an attempt to maximise the quantity of the organomanganese being generated, which should lead to an increase in the yield of **394** by producing more of the nucleophile.
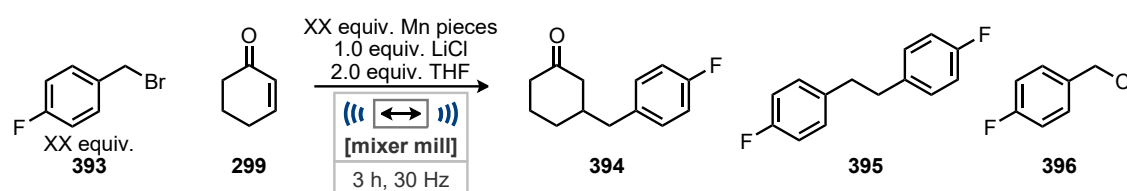
Entry	Equiv. of Mn	Equiv. of **393**	Conversion of **393**[a] / %	Yield of **394**[a] / %	Yield of **395**[a] / %	Yield of **396**[a] / %
1	1.0	1.0	80	4	8	16
2	1.5	1.0	93	3	15	7
3	2.0	1.0	98	11 (7)[b]	19 (5)[b]	6
4	2.5	1.0	99	3	24	5
5	2.0	1.25	98	21	47	12
6	2.0	1.5	87	10	13	8
7	2.0	1.75	81	12	35	16
8	2.0	2.0	75	13	23	18

[a] Determined by ^{19}F NMR spectroscopy using α,α,α-trifluorotoluene as an internal standard.
[b] Yield of isolated product.

Table 5.02 Optimization of manganese pieces and 4-fluorobenzyl bromide stoichiometry.

Through altering the equivalents of manganese metal (Table 5.02, entries 1 – 4) it was clear that with greater than 1.0 equivalents complete conversion of **393** was achieved. With a greater or reduced quantity of manganese than 2.0 equivalents the selectivity of reaction altered towards producing more of bibenzyl **395** decreasing the yield of the desired addition product **394**. This made it clear that with only 1.0 equivalent of

4-fluorobenzyl bromide **393** that 2.0 equivalents of manganese were optimal. Optimization continued by increasing the quantity of **393** attempting to generate more of the organomanganese halide. Increasing the equivalents of **393** to 1.25 increased the yield of all products (Table 5.02, entry 5) likely due to a greater quantity of the organometallic intermediate being generated. Although further increases in the equivalents of **393** (Table 5.02, entries 6 – 8) led to diminished yields possibly due to dilution of the reaction mixture or large quantities of liquid in the reaction causing poorer energy transfer.

As 4-fluorobenzyl chloride, **396**, had been observed as a side product of the reaction the current optimal conditions (Table 5.02, entry 5) were carried out with this **396**, in place of the benzyl bromide **393** that was being used for the reaction optimization. This was to assess if this was a valid starting material to produce the organomanganese halide or if the optimization should focus on preventing this side product from occurring.
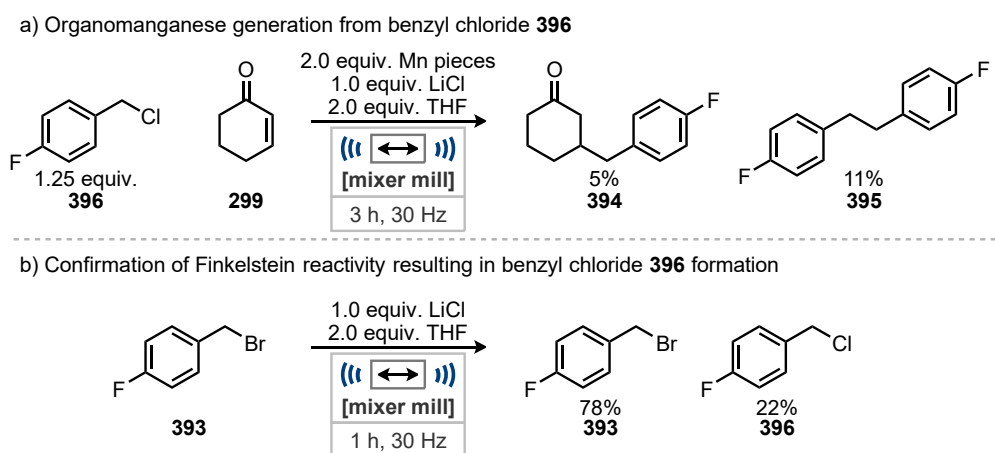
Scheme 5.16 4-fluorobenzyl chloride **396** reactivity and confirmation of Finkelstein reactivity. Yields determined by ^{19}F NMR Spectroscopy using α,α,α-trifluorotoluene as an internal standard.

Using the benzyl chloride **396** as the starting material still provided some reactivity with a moderate yield of **394** compared to the current best yield achieved (Scheme 5.16a). Although this activity has been shown it seems that avoiding the formation of **396** would likely assist in improving reaction yields, by ensuring the more reactive starting benzyl bromide stays intact. To probe how the benzyl chloride **396** was forming in the reaction a simple test was made by milling lithium chloride with 4-fluorobenzyl bromide **393** together for 1 hours (Scheme 5.16b). Moderate conversion to the benzyl chloride **396** was observed under these reaction conditions. This confirmed that the lithium chloride alone is responsible for this reaction and in an attempt to prevent this unwanted reactivity

from taking place a range of alternate Lewis acids were screened in the reaction conditions.
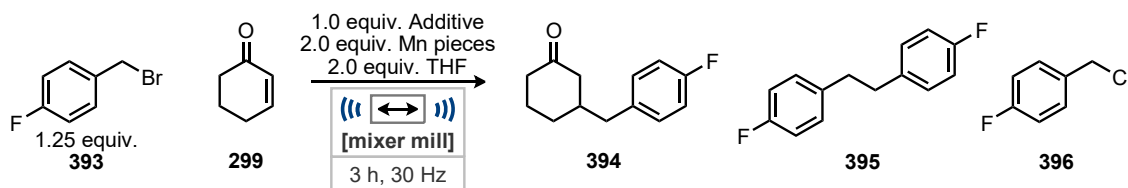
Entry	Additive	Conversion of 393[a] / %	Yield of 394[a] / %	Yield of 395[a] / %	Yield of 396[a] / %
1	-	80	2	37	NA
2	LiCl	98	11	19	6
3	LiBr	78	18	17	NA
4	LiI	100	20	34	NA
5	LiOTf	51	0	Trace	NA
6	ZnCl$_2$	98	16	13	0
7	Sc(OTf)$_3$	23	3	0	NA
8[b]	LiBr	76	24	18	NA
9[c]	LiBr	100	16	38	NA

[a] Determined by ^{19}F NMR spectroscopy using α,α,α-trifluorotoluene as an internal standard. [b] 2.25 equiv. of Mn pieces used. [c] 2.5 equiv. of Mn pieces used.

Table 5.03 Optimization of additive.

Without the presence of a metal salt additive the generation of the organomanganese still occurred but the selectivity shifted towards the production of the bibenzyl **395** and away from the desired product (Table 5.03, entry 1). Addition of lithium halide salts (Table 5.03, entries 2 – 4) improved the selectivity to the desired addition product likely acting as Lewis acids increasing the electronegativity of **299**. The yields of these reactions increased with the increasing size of the halide. The larger halides will have weaker bonding with the lithium cation, potentially increasing its Lewis acidity. Although the use of lithium triflate (Table 5.03, entry 5) seemingly prevented the generation of the organomanganese and neither **394** nor **395** were observed after this reaction. Zinc(II) chloride (Table 5.03, entry 6), which had previously been shown to assist the addition of organomanganese halides to conjugated electrophiles, performed moderately with slightly increased yields than lithium chloride but without the generation of **396**.[29] The strongly Lewis acidic scandium(III) triflate (Table 5.03, entry 7) significantly inhibited the conversion of **393** this may be due to the high molecular weight of this compound meaning the milling vessel is overfilled preventing mixing and mass transfer. Similar

observations were observed during the dimerization of benzylidene malonates in the previous chapter, during the optimization scandium(III) triflate also prevented that reaction. Although lithium iodide (Table 5.03, entry 4) produced the highest yield of the desired product and the greatest quantity of organomanganese, its difficulty in handling due to being extremely hygroscopic made repeating these yields challenging. As lithium bromide performed similarly well (Table 5.03, entry 5), it was taken forward as the optimal additive which also prevented the unwanted side product 4-fluorobenzyl chloride **396** from being produced.

With the additive changed to lithium bromide complete conversion of the benzyl bromide **393** was no longer being achieved (Table 5.03, entry 5). Attempting to increase this conversion was carried out by increasing the equivalents of manganese metal in the reaction (Table 5.03, entries 8 – 9). Increasing from 2.0 to 2.25 equiv. (Table 5.03, entry 9) produced a similar conversion of **393** (76%) but increased the yield of the desired addition product **394** by 6% and marginally increased the bibenzyl **395** yield by 1% demonstrating an increased generation of the organomanganese halide. Further increasing the equivalents of manganese metal to 2.5 equivalents (Table 5.03, entry 9) did achieve complete conversion of the benzyl bromide **393** but led to a significant selectivity switch towards the formation of bibenzyl **395** over the desired product **394**. Due to this switch in selectivity using lithium bromide and 2.25 equivalents of manganese pieces was taken forward through the optimization (Table 5.03, entry 8).

With lithium bromide being found to be the optimal Lewis acid additive its stoichiometry in the reaction was optimized.
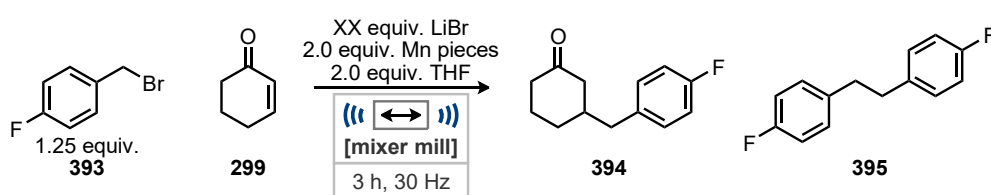
| Entry	Equiv. of LiBr	Conversion of 393[a] / %	Yield of 394[a] / %	Yield of 395[a] / %
1	0.5	100	0	59
2	0.75	100	0	59
3	1.0	76	24	18
4	1.5	91	17	33
5	2.0	73	12	18

[a] Determined by ^{19}F NMR spectroscopy using α,α,α-trifluorotoluene as an internal standard.

Table 5.04 Optimization of additive stoichiometry.

Sub-stoichiometric quantities of lithium bromide (Table 5.04, entries 1 and 2) prevented the formation of the desired addition product **394** and bibenzyl **395** was the only observed product in 59% yield in both cases. When greater than 1.0 equivalent was used (Table 5.04, entries 4 and 5) the desired product was formed, although in reduced yields. Furthermore, the selectivity again switched to prefer the formation of bibenzyl **395** over the desired product **394** with increasing equivalents of lithium bromide. The quantity of organomanganese halide being generated in the reactions also seems to reduce with increased quantity of lithium bromide. From the variations made to the conditions it remains that 1.0 equivalent of lithium bromide is optimal in the reaction (Table 5.04, entry 3).

The reactions so far have attempted the addition reaction with 2-cyclohexen-1-one **299** as the electrophile. However, accurately measuring the conversion of this compound has been challenging and, although not yet observed, it may be possible for **299** to undergo either conjugate or direct addition, producing multiple products. For these reasons a brief electrophile screen was carried out with electrophiles reported to effortlessly undergo addition with organomanganese halides.[9]
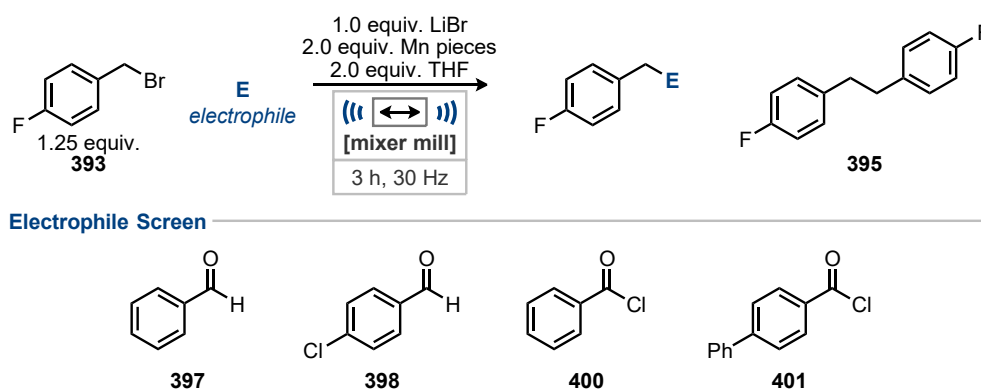
Entry	Electro-phile	Conversion of 393[a] / %	Conversion of electrophile[b] / %	Yield of addition product[a] / %	Yield of 395[a] / %
1	**397**	77	11	0	30
2	**398**	46	8	0	46
3	**400**	38	NA	0	12
4	**401**	24	NA	0	9

[a] Determined by ^{19}F NMR spectroscopy using α,α,α-trifluorotoluene as an internal standard.
[b] Determined by ^{1}H NMR spectroscopy using mesitylene as an internal standard.

Table 5.05 Optimization of additive stoichiometry.

Unfortunately, the electrophiles screened all failed to react with the organomanganese halides being generated during the reactions, leading to the bibenzyl **395** being the only product being observed in all cases. As none of these electrophiles successfully intercepted the organomanganese the optimization continued with 2-cyclohexen-1-one **299** as the electrophile.

Through the optimization thus far THF has been used as a liquid additive in the reaction, as it was the optimal choice in the previously established dimerization and is well known for its ability to stabilise organometallic species. To ensure that THF is the optimal choice a range of solvents were screened as liquid additives with varying dielectric constants.
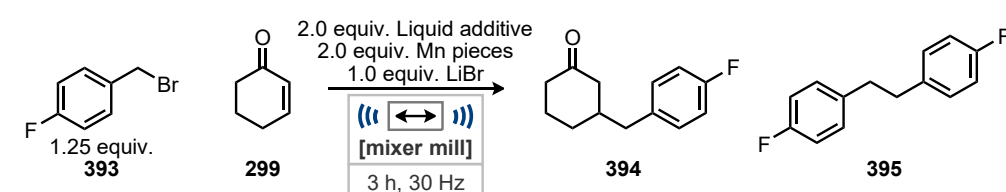
Entry	Liquid Additive	Conversion of 393[a] / %	Yield of 394[a] / %	Yield of 395[a] / %
1	-	30	2	4
2	Hexane (1.88)	71	1	Trace
3	PhMe (2.38)	55	2	Trace
4	Et$_2$O (4.33)	78	0	Trace
5	THF (7.58)	76	24	18
6	DCM (8.93)	62	9	12
7	HFIP (15.7)	96	14	45
8	iPrOH (19.92)	89	31	18
9	EtOH (24.55)	94	15	41
10	NMP (32.2)	74	17	14
11	MeCN (37.5)	84	15	23
12	DMA (37.78)	90	11	12
13	DMSO (46.68)	47	0	Trace

[a] Determined by ^{19}F NMR spectroscopy using α,α,α-trifluorotoluene as an internal standard.

Table 5.06 Liquid additive screen (values in brackets are the dielectric constant of the respective liquid additive).[51]

Without a liquid additive or using solvents with lower dielectric constants than THF (Table 5.06, entries 1 – 4) low conversions of **393** were observed as well as low yields of the desired product **394** or bibenzyl **395**. Without a liquid additive present or using a

less polar solvent the formation of the organomanganese halide seems to be inhibited. Although DCM and THF have similar dielectric constants (8.93 and 7.58 respectively), THF significantly outperformed DCM (Table 5.06, entries 5 and 6) in the reaction likely due to its coordinative nature aiding in stabilising organometallics. Alcoholic solvents HFIP, *i*PrOH, and EtOH (Table 5.06, entries 7 – 9) performed surprisingly well in the reaction considering the possibility that the alcohol could protonate any organomanganese halide intermediate. As the polarities of the liquid additives increased in the final examples (Table 5.06, entries 10 – 13) reaction yields began to decrease with DMSO (Table 5.06, entry 13) completely preventing the formation of the desired product **394** and only a trace of the bibenzyl **395**. This screen of liquid additives revealed that *i*PrOH (Table 5.06, entry 8) to be the most effective choice producing the highest yield of **394**, 31%, although the selectivity of the reaction is still only moderate with 18% of the bibenzyl **395** still being produced. With it clear that *i*PrOH is the optimal choice for liquid additive the optimization of its stoichiometry was carried out.
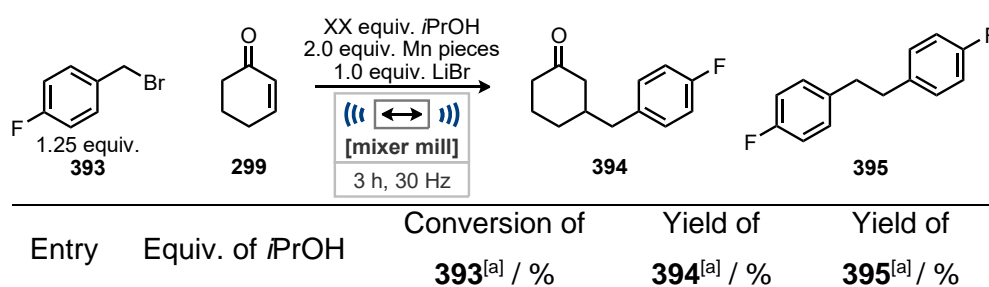
Entry	Equiv. of *i*PrOH	Conversion of 393[a] / %	Yield of 394[a] / %	Yield of 395[a] / %
1	1.0	80	25	17
2	1.5	88	36	24
3	2.0	86	31	18
4	2.5	100	11	34

[a] Determined by ^{19}F NMR spectroscopy using α,α,α-trifluorotoluene as an internal standard.

Table 5.07 Optimization of iPrOH stoichiometry.

Increasing the quantity of *i*PrOH to 2.5 equiv. (Table 5.07, entry 4) led to a shift in selectivity with the bibenzyl product being significantly preferred. A slight reduction from 2.0 to 1.5 equiv. (Table 5.07, entry 2) marginally increased the yield of the desired product **394**, but also led to a significant increase in the quantity of bibenzyl **395**. This increase suggests a greater quantity of the organomanganese nucleophile being produced. Further decreasing the quantity of *i*PrOH (Table 5.07, entry 1) led to diminishing yields.

So far through this investigation the pro-nucleophile has been limited to benzyl halides **390** and **393**. Although these compounds have allowed for the investigation into the formation of the organomanganese halides they are an activated starting material that will more readily form the organometallic. Thus, for the development of a broader method for the formation of organomanganese halides, a range of less activated alkyl and aryl bromide and iodide compounds were applied to the reaction. Although many of these compounds failed to produce the desired organometallic during the initial screening of compounds (Scheme 5.14) it was hoped that with the improved conditions now developed these substrates may be more susceptible to the formation of a range of organomanganese halides.
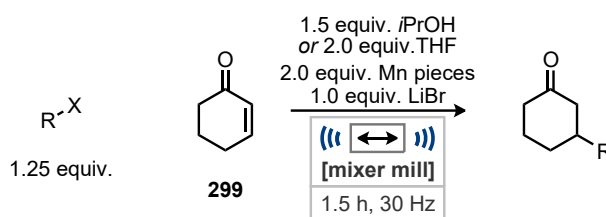
Pro-nucleophile Screen
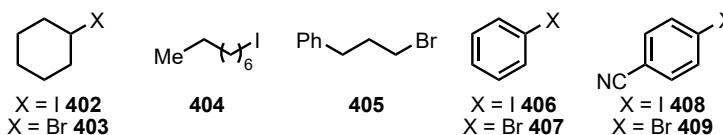
Entry	Liquid Additive / equiv.	Pro-nucleophile	Conversion of pro-nucleophile[a] / %	Yield of addition product[a] / %
1	*i*PrOH (1.5)	A	12	0
2	THF (2.0)	A	16	0
3	*i*PrOH (1.5)	B	11	0
4	THF (2.0)	B	9	0
5	*i*PrOH (1.5)	C	2	0
6	THF (2.0)	C	1	0
7	*i*PrOH (1.5)	D	3	0
8	THF (2.0)	D	2	0
9	*i*PrOH (1.5)	E	14	0
10	THF (2.0)	E	12	0
11	*i*PrOH (1.5)	F	18	0
12	THF (2.0)	F	16	0
13	*i*PrOH (1.5)	G	7	0
14	THF (2.0)	G	8	0
15	*i*PrOH (1.5)	H	7	0
16	THF (2.0)	H	5	0

[a] Determined by ^{1}H NMR spectroscopy using mesitylene as an internal standard.

Table 5.08. Pro-nucleophile screen.

Unfortunately, none of the alkyl and aryl halides screened showed any significant conversion and detection of any addition products could not be made. This confirmed that the conditions that had currently been developed were not suitable for application to general organomanganese halide generation.

In a final attempt to improve the yield of the transformation due to the increasing quantity of bibenzyl being produced using *i*PrOH as the liquid additive (Table 5.07, entry 2), the addition of a copper(I) catalyst was investigated. This was to improve the selectivity of

the reaction as copper catalysed conjugate addition of organomanganese halides and other organometallics are well known.[31b, 52]

Table 5.09 Addition of copper catalyst.
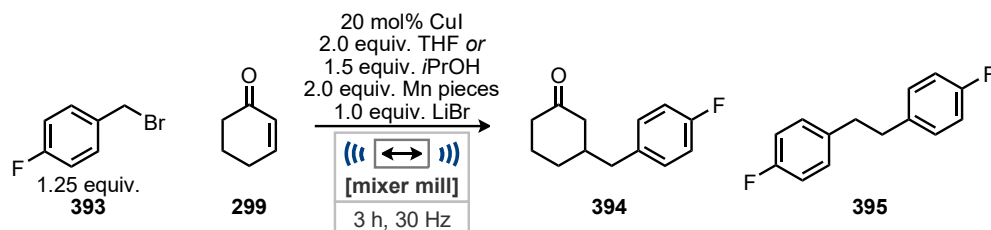
Entry	Liquid additive	Conversion of 393[a] / %	Yield of 394[a] / %	Yield of 395[a] / %
1	*i*PrOH	93	55 (48)	16 (12)
2	THF	90	42	30

[a] Determined by ^{19}F NMR spectroscopy using α,α,α-trifluorotoluene as an internal standard.

The addition of the copper catalyst provided a significant increase in the selectivity and yield of the transformation. With *i*PrOH as the liquid additive (Table 5.09, entry 1) a good yield of 55% of **394** was found and the quantity of bibenzyl **395** formed reduced to only 16%. To confirm the *i*PrOH was in fact the optimal liquid additive the effect of the copper(I) catalyst was also investigated using THF. There was also an increase in yield of the conjugate addition product while using THF as the liquid additive (Table 5.09, entry 2) than the previous results without the copper catalyst. Although the selectivity of this reaction was still quite poor with the yield of bibenzyl **395** also increasing upon addition of the copper(I) catalyst. The addition of the copper catalyst was able to not only improve the yield of the desired product and the selectivity, but it also resulted in a greater quantity of the organomanganese being generated. This could be due to the reduced quantity of the benzyl bromide **393** being consumed by the formation of the side product and allowing more to generate the organometallic.

5.3   Conclusion and Future Work

In summary, access to organomanganese halides from benzyl bromides has been established under ball milling conditions for the first time. Through optimization of the process the addition of metal salt additives and liquid additives have been key in controlling the yield of the process. Initially lithium chloride was chosen but due to

unwanted Finkelstein reactivity being displayed further optimization found lithium bromide to be more suitable. While screening liquid additives it was clear that the polarity and intermolecular bonding attributes of the liquid additives were key in enabling the reactivity, and this found that *i*PrOH was the best choice in this reaction. Unfortunately, the reaction is currently limited in scope of both electrophile and pro-nucleophile. Finally, initial results suggest significant benefit on addition of a copper catalyst improving the selectivity and the yield of the desired product.

Future work on the direct generation of organomanganese halides *via* ball milling could benefit by investigating a number of factors. Firstly, the use of copper catalysts in this transformation has shown significant benefit and investigation into all attributes while using this catalyst could further improve on the yield of the addition product. Also, if high yields are achievable with the use of a copper catalyst chiral ligands may be able to render the transformation asymmetric. The use of co-catalysts, which assist in the generation of the organomanganese from Takai ($PbCl_2$), Knochel ($InCl_3$ and $PbCl_2$) and Cahiez ($ZnCl_2$) could be further investigated alongside the use of lithium bromide and a copper catalyst.[6-8] Furthermore, the use of additives known to form stabilizing ate complexes such as tetraalkyl ammonium salts could be of some benefit.[19] Finally, to allow the current method to expand to a broader scope of organomanganese compounds, longer reaction times and possibly elevated reaction temperatures may be required. In solution it is not uncommon for organomanganese halide formation of less reactive alkyl bromides to require 10 – 16 h with activated manganese metal such as Rieke manganese.[12a, 15b]

A concept which is yet to receive much attention for the formation of organometallics is to generate an activated metal powder *via* ball milling and then add this to a solution reaction for the formation of the organometallic. It may then be possible to conduct the reactions under more stringently inert conditions removing air and moisture. In the previous chapter the use of ball milled manganese was able to induce the dimerization reaction in solution whereas the commercially available metals struggled. Although this method does have the inherent risk of handling finally divided metal powders which may spontaneously ignite. To prevent this from occurring it may be possible to produce a suspension of the metal powder that could then be bench stable, similar to sodium hydride which is suspended in mineral oil. This would provide a powder which could be easily manipulated under air that could then be used in solution. This could possibly improve the reproducibility of the formation of many challenging organometallic species.

5.4 Bibliography

1. P. Knochel and C. Diène, *Comptes Rendus Chimie*, 2011, **14**, 842-850.
2. Z.-L. Shen, S.-Y. Wang, Y.-K. Chok, Y.-H. Xu and T.-P. Loh, *Chem. Rev.*, 2013, **113**, 271-401.
3. a) C. L. Keen, J. L. Ensunsa, B. Lönnerdal and S. Zidenberg-Cherr, in *Encyclopedia of Human Nutrition (Second Edition)*, ed. B. Caballero, Elsevier, Oxford, 2005, DOI: https://doi.org/10.1016/B0-12-226694-3/00202-7, pp. 217-225; b) ed. WileyVCH, WileyVCH, Weinheim, Germany, 6 edn., 2003, vol. 20, p. 497.
4. a) H. Gilman and J. C. Bailie, *J. Org. Chem.*, 1937, **02**, 84-94; b) H. Gilman and R. H. Kirby, *J. Am. Chem. Soc.*, 1941, **63**, 2046-2048.
5. G. Cahiez and O. Gager, in *PATAI'S Chemistry of Functional Groups*, DOI: https://doi.org/10.1002/9780470682531.pat0539.
6. a) G. Cahiez and P.-Y. Chavant, *Tetrahedron Lett.*, 1989, **30**, 7373-7376; b) G. Cahiez and B. Laboue, *Tetrahedron Lett.*, 1989, **30**, 3545-3546.
7. K. Takai, T. Ueda, T. Hayashi and T. Moriwake, *Tetrahedron Lett.*, 1996, **37**, 7049-7052.
8. Z. Peng and P. Knochel, *Org. Lett.*, 2011, **13**, 3198-3201.
9. G. Cahiez, C. Duplais and J. Buendia, *Chem. Rev.*, 2009, **109**, 1434-1476.
10. a) R. D. Rieke, *Science*, 1989, **246**, 1260-1264; b) R. D. Rieke, *Acc. Chem. Res.*, 1977, **10**, 301-306.
11. R. D. Rieke, Berlin, Heidelberg, 1975.
12. a) S.-H. Kim, M. V. Hanson and R. D. Rieke, *Tetrahedron Lett.*, 1996, **37**, 2197-2200; b) S.-H. Kim and R. D. Rieke, *Synth. Commun.*, 2006, **28**, 1065-1072.
13. R. D. Rieke, S.-H. Kim and X. Wu, *J. Org. Chem.*, 1997, **62**, 6921-6927.
14. R. D. Rieke, Y. Suh and S.-H. Kim, *Tetrahedron Lett.*, 2005, **46**, 5961-5964.
15. a) T. Hiyama, M. Obayashi and A. Nakamura, *Organometallics*, 1982, **1**, 1249-1251; b) G. Cahiez, A. Martin and T. Delacroix, *Tetrahedron Lett.*, 1999, **40**, 6407-6410; c) J. Tang, H. Shinokubo and K. Oshima, *Synlett*, 1998, **1998**, 1075-1076; d) J. Tang, H. Shinokubo and K. Oshima, *Tetrahedron*, 1999, **55**, 1893-1904; e) A. Fürstner and H. Brunner, *Tetrahedron Lett.*, 1996, **37**, 7009-7012.
16. a) G. Cahiez and M. Alami, *Tetrahedron*, 1989, **45**, 4163-4176; b) G. Cahiez, D. Bernard and J. F. Normant, *Synthesis*, 1977, **1977**, 130-133; c) G. Friour, G. Cahiez and J. F. Normant, *Synthesis*, 1984, **1984**, 37-40.
17. a) W. E. Parham and C. K. Bradsher, *Acc. Chem. Res.*, 1982, **15**, 300-305; b) I. Klement, H. Stadtmüller, P. Knochel and G. Cahiez, *Tetrahedron Lett.*, 1997, **38**, 1927-1930; c) G. Cahiez, D. Bernard and J. F. Normant, *Synthesis*, 1976, **1976**, 245-248.
18. M. Tamura and J. Kochi, *J. Organomet. Chem.*, 1971, **29**, 111-129.
19. G. Cahiez, L. Razafintsalama, B. Laboue and F. Chau, *Tetrahedron Lett.*, 1998, **39**, 849-852.
20. a) G. Cahiez and B. Laboue, *Tetrahedron Lett.*, 1989, **30**, 7369-7372; b) G. Friour, A. Alexakis, G. Cahiez and J. Normant, *Tetrahedron*, 1984, **40**, 683-693.
21. G. Cahiez, D. Bernard and J. F. Normant, *J. Organomet. Chem.*, 1976, **113**, 99-106.
22. a) G. Cahiez and E. Metais, *Tetrahedron Lett.*, 1995, **36**, 6449-6452; b) Q. T. Do, D. Elothmani, G. Le Guillanton and J. Simonet, *Tetrahedron Lett.*, 1997, **38**, 3383-3384; c) G. Cahiez, J. Rivas-Enterrios and P. Clery, *Tetrahedron Lett.*, 1988, **29**, 3659-3662.
23. a) K. Ritter and M. Hanack, *Tetrahedron Lett.*, 1985, **26**, 1285-1288; b) G. Boche and R. Eiben, *Tetrahedron Lett.*, 1985, **26**, 1289-1292.
24. G. Cahiez, P.-Y. Chavant and E. Metais, *Tetrahedron Lett.*, 1992, **33**, 5245-5248.

25. G. Cahiez and F. Mahuteau-Betzer, in *Handbook of Functionalized Organometallics*, ed. P. Knochel, Wiley-VCH, Weinheim, 2005, vol. 2, pp. 541-567.
26. C. Boucley, G. Cahiez, S. Carini, V. Cerè, M. Comes-Franchini, P. Knochel, S. Pollicino and A. Ricci, *J. Organomet. Chem.*, 2001, **624**, 223-228.
27. a) M. T. Reetz, H. Haning and S. Stanchev, *Tetrahedron Lett.*, 1992, **33**, 6963-6966; b) M. T. Reetz, K. Rölfing and N. Griebenow, *Tetrahedron Lett.*, 1994, **35**, 1969-1972.
28. I. N. N. Namboothiri and A. Hassner, *J. Organomet. Chem.*, 1996, **518**, 69-77.
29. G. Cahiez and M. Alami, *J. Organomet. Chem.*, 1990, **397**, 291-298.
30. a) M. A. S. Marquais, and G. Cahiez, *Organic Synth*, 1995, **72**, 135; b) G. Cahiez and M. Alami, *Tetrahedron Lett.*, 1989, **30**, 3541-3544; c) G. Cahiez and M. Alami, *Tetrahedron Lett.*, 1989, **30**, 7365-7368; d) G. Cahiez and M. Alami, *Tetrahedron Lett.*, 1990, **31**, 7423-7424.
31. a) F. Keigo, O. Koichiro and U. Kiitiro, *Chem. Lett.*, 1987, **16**, 2203-2206; b) G. Cahiez and S. Marquais, *Synlett*, 1993, **1993**, 45-47; c) G. Cahiez and S. Marquais, *Tetrahedron Lett.*, 1996, **37**, 1773-1776; d) A. Fürstner, A. Leitner, M. Méndez and H. Krause, *J. Am. Chem. Soc.*, 2002, **124**, 13856-13863; e) A. Leleu, Y. Fort and R. Schneider, *Adv. Synth. Catal.*, 2006, **348**, 1086-1092; f) J. G. Donkervoort, J. L. Vicario, J. T. B. H. Jastrzebski, R. A. Gossage, G. Cahiez and G. Van Koten, *J. Organomet. Chem.,* 1998, **558**, 61-69; g) E. Riguet, M. Alami and G. Cahiez, *Tetrahedron Lett.*, 1997, **38**, 4397-4400; h) E. Riguet, M. Alami and G. Cahiez, *J. Organomet. Chem.*, 2001, **624**, 376-379.
32. a) S. P. Stanforth, *Tetrahedron*, 1998, **54**, 263-303; b) A. F. Littke, C. Dai and G. C. Fu, *J. Am. Chem. Soc.*, 2000, **122**, 4020-4028.
33. J. M. Harrowfield, R. J. Hart and C. R. Whitaker, *Aust. J. Chem.*, 2001, **54**, 423-425.
34. I. R. Speight and T. P. Hanusa, *Molecules*, 2020, **25**, DOI: 10.3390/molecules25030570.
35. J. E. Huheey, *Inorganic Chemistry: Principles of Structure and Reactivity*, Harper & Row, United States of America, Michigan, 3 edn., 1983.
36. a) J. Paterová, M. Skalický, M. Rybáčková, M. Kvíčalová, J. Cvačka and J. Kvíčala, *J. Fluorine Chem.*, 2010, **131**, 1338-1343; b) E. C. Ashby and J. Nackashi, *J. Organomet. Chem.*, 1974, **72**, 11-20.
37. a) R. D. Rieke and P. M. Hudnall, *J. Am. Chem. Soc.*, 1972, **94**, 7178-7179; b) C. M. Beck, Y.-J. Park and R. H. Crabtree, *Chem. Commun.*, 1998, **1998**, 693-694.
38. H. Chen, J. Fan, Y. Fu, C.-L. Do-Thanh, X. Suo, T. Wang, I. Popovs, D.-e. Jiang, Y. Yuan, Z. Yang and S. Dai, *Adv. Mater.*, 2021, **33**, 2008685.
39. a) J.-S. M. Lee and A. I. Cooper, *Chem. Rev.*, 2020, **120**, 2171-2214; b) A. G. Slater and A. I. Cooper, *Science*, 2015, **348**, aaa8075; c) P. Xu, X. Han, B. Zhang, Y. Du and H.-L. Wang, *Chem. Soc. Rev.*, 2014, **43**, 1349-1360.
40. M. Glavinovic, F. Qi, A. D. Katsenis, T. Friscic and J. P. Lumb, *Chem. Sci.*, 2016, **7**, 707-712.
41. a) Q. Cao, J. L. Howard, E. Wheatley and D. L. Browne, *Angew. Chem. Int. Ed.*, 2018, **57**, 11339-11343; b) Q. Cao, R. T. Stark, I. A. Fallis and D. L. Browne, *ChemSusChem*, 2019, **12**, 2554-2557; c) J. Yin, R. T. Stark, I. A. Fallis and D. L. Browne, *J. Org. Chem.*, 2020, **85**, 2347-2354.
42. W. Pickhardt, S. Gratz and L. Borchardt, *Chem. Eur.J.*, 2020, **26**, 12903-12911.
43. a) R. A. Haley, A. R. Zellner, J. A. Krause, H. Guan and J. Mack, *ACS Sustainable Chem. Eng.*, 2016, **4**, 2464-2469; b) L. Chen, D. Leslie, M. G. Coleman and J. Mack, *Chem. Sci.*, 2018, **9**, 4650-4661; c) T. L. Cook, J. A. Walker and J. Mack, *Green Chem.*, 2013, **15**, 617-619; d) D. A. Fulmer, W. C. Shearouse, S. T. Medonza and J. Mack, *Green Chem.*, 2009, **11**, 1821-1825.

44. W. Su, J. Yu, Z. Li and Z. Jiang, *J. Org. Chem.*, 2011, **76**, 9144-9150.
45. a) C. G. Vogt, S. Grätz, S. Lukin, I. Halasz, M. Etter, J. D. Evans and L. Borchardt, *Angew. Chem. Int. Ed.*, 2019, **58**, 18942-18947; b) S. Grätz, B. Wolfrum and L. Borchardt, *Green Chem.*, 2017, **19**, 2973-2979.
46. a) P. Kovacic and A. Kyriakis, *J. Am. Chem. Soc.*, 1963, **85**, 454-458; b) S. Geetha and D. C. Trivedi, *Synth. Met.*, 2005, **148**, 187-194.
47. J. L. Howard, PhD, Cardiff University, 2018.
48. G. Kaupp, *CrystEngComm*, 2011, **13**.
49. C. Elschenbroich and A. Salzer, *Organometallics: A Concise Introduction*, Wiley-VCH, Germany, 3 edn., 1992.
50. A. Kadam, M. Nguyen, M. Kopach, P. Richardson, F. Gallou, Z.-K. Wan and W. Zhang, *Green Chem.*, 2013, **15**, 1880-1888.
51. I. Colomer, A. E. R. Chamberlain, M. B. Haughey and T. J. Donohoe, *Nat. Rev. Chem.*, 2017, **1**, 0088.
52. A. Alexakis, J. E. Bäckvall, N. Krause, O. PàMies and M. DiéGuez, *Chem. Rev.*, 2008, **108**, 2796-2823.

6 Experimental Section

6.1   General Information

All chemicals recently obtained from commercial sources were used without further purification unless stated otherwise. Amines which were discoloured or not recently purchased were purified by either passing through a plug of basic alumina or an acid/base wash. Morpholine was stored over 4 Å molecular sieves to ensure low water content. Potassium *tert*-butoxide was used as supplied and the bottle was flushed with nitrogen after use and sealed with parafilm. Older bottles of potassium tert-butoxide which had not been stored in sufficiently rigorous manner could be purified by sublimation.

^{1}H, ^{19}F, and ^{13}C NMR spectra were obtained on Bruker 400 MHz and Bruker 500 MHz spectrometers with chloroform-d as deuterated solvent. The obtained chemical shifts δ are reported in ppm and are referenced to the residual solvent signal (CDCl$_3$ 7.26 and 77.16 ppm, Methanol-d$_4$ 3.31 and 49.00 ppm, DMSO-d$_6$ 2.50 and 39.52, D$_2$O 4.79 ppm for ^{1}H and ^{13}C respectively). Spin-spin coupling constants J are given in Hz and refer to apparent multiplicities rather than true coupling constants. Data are reported as: chemical shift, multiplicity and integration. ^{1}H NMR yields were obtained using 0.33 mmol of mesitylene as an internal standard, ^{19}F NMR yields were obtained using 0.33 mmol of α,α,α-trifluorotoluene as an internal standard.

High resolution mass spectral (HRMS) data were obtained on a Thermo Scientific LTQ Orbitrap XL by the EPSRC UK National Mass Spectrometry Facility at Swansea University or on a Waters MALDI-TOF mx in Cardiff University. Spectra were obtained using electron impact ionization (EI), chemical ionization (CI), positive electrospray (ES), pneumaticallyassisted electrospray (pNSI) or atmospheric solids analysis probe (ASAP+).

Infrared spectra were recorded on a Shimadzu IR-Affinity-1S FTIR spectrometer or a Agilent Cary 630 FTIR spectrometer.

Melting points were measured using a Stuart SMP10 apparatus or a Gallenkamp apparatus and are reported uncorrected.

Optical rotation measurements were taken on a Bellingham and Stanley ADP410 polarimeter at ambient temperature, using a LED light source filtered to 589.3 nm.

Gas chromatography analysis was carried out using a Bruker Scion 456 gas chromatograph. An Agilent 19091J-413HP-5 column (30.0 m × 320 µm × 0.25 µm

nominal) was employed for all of the separations using the following conditions: initial column temperature, 40 °C; initial hold time, 2 min; next temperature, 100 °C; hold time, 5 min; rate of temperature ramp 1, 4 °C/min, final temperature 300 °C; hold time, 5 min; rate of temperature ramp 2, 15 °C/min; injection temperature, 250 °C; injection volume 1 μL; detection temperature, 300 °C, split mode. The effluent was combusted in an H2/air flame and detected using FID (flame ionization detector).

The GC yield of products and conversion of substrates were determined by using the internal standard method. The response factor (RF) of analytes was determined by analysing known S3 quantities of internal standard (mesitylene) against known quantities of substrate and product:

$$RF = \frac{Area_{Internal\ Standard}\ X\ Moles_{Analyte}}{Area_{Analyte}\ X\ Moles_{Internal\ Standard}}$$

The quantity of an analyte was then calculated according to the following equation:

$$Moles_{Analyte} = \frac{RF\ X\ Moles_{Internal\ Standard}\ X\ Area_{Analyte}}{Area_{Internal\ Standard}}$$

The preparatory HPLC was carried out with a Japan Analytical Industry LC-9110 II Next equipped with a normal phase column (JAIGEL-SIL, 043-10), a UV-Vis detector and set to recycling with a 10 mLmin^{-1} flow rate.

Cyclic voltammetry (CV) experiments were conducted using an Autolab PGSTAT204, controlled using Nova 2.1 software. The working electrode was a GC disc (3 mm dia., BASi part number MF-2012), the counter electrode was a Pt-wire (BASi part number MW-4130) and a Ag/AgCl reference electrode was used (BASi part number – MF-2052) in a 10 mL glass vial. The solution of interest was purged with N_2 for 10 minutes before data collection. After data collection, ferrocene (5 mM) was added and an additional scan was run. The parent data was referenced relative to the Fc$^{+/0}$ couple that was recorded ($E_{1/2}$ = 0.382 V).

All EPR spectra were recorded on a Bruker EMX utilising an ER4102_shqe resonator, at 120 K using a Bruker Variable Temperature Unit, operating at 10 mW MW power, 100 kHz field modulation and 5 G modulation depth. Spin-trap samples were recorded at room temperature, utilising the ER4102_shqe resonator, operating at 0.64 mW MW power, 100 kHz field modulation and 0.5 G modulation depth.

6.2 Milling Equipment
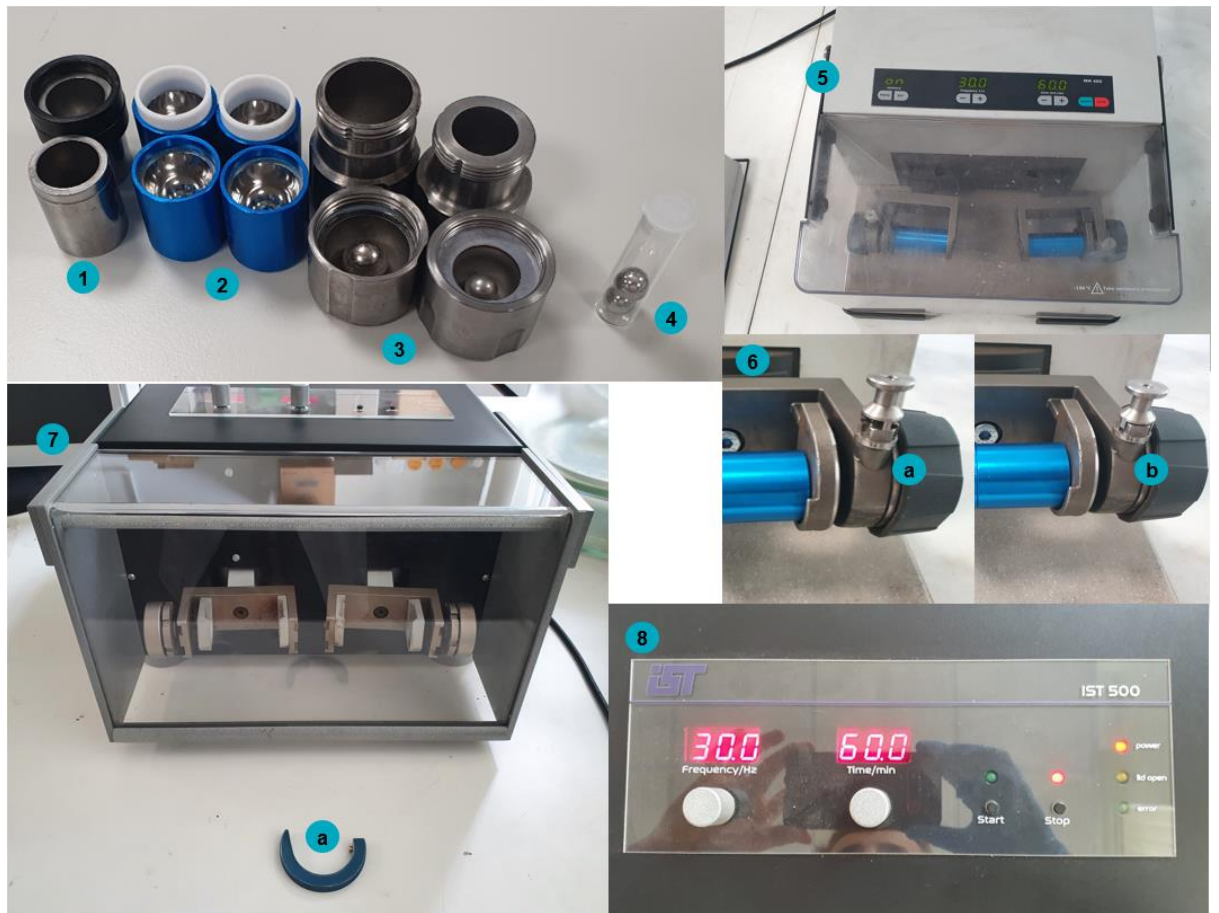
1)   IST milling jar 14 mL stainless steel with retaining collar
      (http://www.insolidotech.org/accessories.html)

2)   FTS Smartsnap™ grinding jars, 15 mL stainless steel with PTFE retaining washer
      (https://formtechscientific.com/fts-1000-shaker-
      mill/products.html?section=accessories&accessory=smartsnap-grinding-jars)

3)   Retsch stainless steel milling jars 25 mL and 15 mL
      (https://www.retsch.com/products/milling/ball-mills/mixer-mill-mm-400/order-
      data-quote-request/)

4)   4 g stainless steel milling balls from Retsch
      (https://www.retsch.com/products/milling/ball-mills/mixer-mill-mm-400/order-
      data-quote-request/)

5)   Retsch MM 400 control panel and FTS Smartsnap™ grinding jars mounted
      (https://www.retsch.com/products/milling/ball-mills/mixer-mill-mm-400/function-
features/)

6)   Retsch jar mounting with FTS Smartsnap™ grinding jars, (a) unlocked and (b)
      locked

7)   IST 500 ball mill jar mountings with the jar (a) removal tool
      (http://www.insolidotech.org/ist500.html)

8)   IST 500 ball mill controls set to 30 Hz and 60 minutes

6.3 Robust Buchwald-Hartwig Amination via Ball Milling

6.3.1 General Procedure 1: Ball Milling Buchwald-Hartwig Amination

To a 15 mL stainless steel milling vessel (Form-Tech Scientific) was added a stainless-steel ball (12 g), sand (0.338 g), potassium *tert*-butoxide (2 mmol, 0.224 g), aryl halide (1 mmol), amine (1.2 mmol) and Pd-PEPPSI-IPent (0.01 mmol, 8.0 mg) under an air atmosphere. The milling jar was then closed, and the mixture was milled at 30 Hz for 3 hours. After the desired reaction time, the black solid mixture was scratched out using spatula and the jar was raised with EtOAc (10 mL) twice. Then the mixture was filtered and the solvent was removed *in vacuo*. The crude reaction mixture was then purified by silica gel flash chromatography.

6.3.2 General Procedure 2: Solution Buchwald-Hartwig Amination Under Air

To a 50 mL round bottom flask a stir bar, potassium tert-butoxide (2 mmol, 0.224 g) and Pd-PEPPSI-IPent (0.01 mmol, 8.0 mg) were added. Then a premixed solution of the desired solvent (10 mL), chlorobenzene (1 mmol, 0.113 g), morpholine (1.2 mmol, 0.105 g) and the internal standard mesitylene (0.5 mmol, 0.060 g). The reaction was then stirred at room temperature under air. The reaction was analyzed by GC by talking an aliquot (~50 μL), every hour, and passed through a pipette containing a small plug of silica gel using diethyl ether as eluent. The GC yield was calculated relative to mesitylene as the internal standard.

4-phenyl morpholine (121)
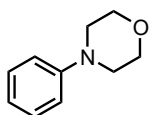
The title compound was prepared according to General Procedure 1 as a beige solid (0.149 g, 91%). **MP** 61 - 63 °C. **^{1}H NMR** (500 MHz, CDCl$_3$) δ 7.31 - 7.26 (m, 2H), 6.95 - 6.85 (m, 3H), 3.87 (t, J = 4.5 Hz, 4H), 3.16 (t, J = 4.5 Hz, 4H). **^{13}C NMR** (126 MHz, CDCl$_3$) δ 151.4, 129.3, 120.2, 115.9, 67.1, 49.2. **HRMS** (EI) [C$_{10}$H$_{13}$NO] calc. 163.0997, found 163.1002. Characterization data is in accordance with previous report.[1]

2-morpholinobenzo[*d*]oxazole (126)
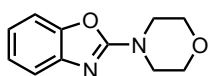
The title compound was prepared according to General Procedure 1 as white solid (0.082 g, 40%). **MP** 79 - 81 °C. **^{1}H NMR** (500 MHz, CDCl$_3$) δ 7.30 (dd, J = 7.8, 0.5 Hz, 1H),

7.21 - 7.17 (m, 1H), 7.10 (td, J = 7.7, 1.0 Hz, 1H), 6.97 (td, J = 7.8, 1.2 Hz, 1H), 3.77 - 3.72 (m, 4H), 3.64 - 3.57 (m, 4H). **^{13}C NMR** (126 MHz, CDCl$_3$) δ 162.1, 148.8, 142.9, 124.1, 121.0, 116.5, 108.9, 66.2, 45.8. **HRMS** (EI) [C$_{11}$H$_{12}$N$_2$O$_2$] calc. 204.0899, found 204.0899. Characterization data is in accordance with previous report.[2]

4-mesitylmorpholine (127)
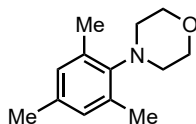
The title compound was prepared according to General Procedure 1 as white crystal (0.144 g, 70%). **MP** 64 - 66 °C. **^{1}H NMR** (500 MHz, CDCl$_3$) δ 6.84 (s, 2H), 3.86 - 3.75 (m, 4H), 3.13 - 3.05 (m, 4H), 2.33 (s, 6H), 2.26 (s, 3H). **^{13}C NMR** (126 MHz, CDCl$_3$) δ 145.5, 137.0, 135.0, 129.8, 68.4, 50.2, 20.8, 19.6. **HRMS** (ESI) [C$_{13}$H$_{19}$NO+H] calc. 206.1545, found 206.1541. Characterization data is in accordance with previous report.[3]

4-(3,5-dimethoxyphenyl)morpholine (128)
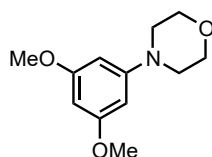
The title compound was prepared according to General Procedure 1 as white solid (0.185 g, 83%). **MP** 85 - 86 °C. **^{1}H NMR** (500 MHz, CDCl$_3$) δ 6.08 (d, J = 1.9 Hz, 2H), 6.04 (t, J = 2.0 Hz, 1H), 3.87 - 3.81 (t, J = 4.8 Hz, 4H), 3.78 (s, 6H), 3.14 (t, J = 7.22 Hz, 4H). **^{13}C NMR** (126 MHz, CDCl$_3$) δ 160.7, 152.4, 93.9, 91.0, 66.0, 54.4, 48.5. **HRMS** (ESI) [C$_{12}$H$_{17}$NO$_3$+H] calc. 224.1287, found: 224.1286. Characterization data is in accordance with previous report.[4]

4-(benzo[*d*][1,3]dioxol-5-yl)morpholine (129)
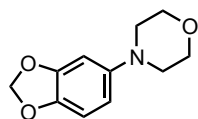
The title compound was prepared according to General Procedure 1 as yellow solid (0.122 g, 59%). **MP** 64 - 65 °C. **^{1}H NMR** (500 MHz, CDCl$_=$) δ 6.73 (d, J = 8.4 Hz, 1H), 6.54 (d, J = 2.4 Hz, 1H), 6.35 (dd, J = 8.4 Hz, 1H), 5.90 (s, 2H), 3.84 (t, J = 4.8 Hz, 4H), 3.03 (t, J = 4.8 Hz, 4H). **^{13}C NMR** (126 MHz, CDCl$_3$) δ 148.5, 147.5, 141.9, 108.8, 108.4, 101.1, 99.7, 67.1, 51.2. **HRMS** (ESI) [C$_{11}$H$_{13}$NO$_3$+H] calc. 208.0974, found 208.0969. Characterization data is in accordance with previous report.[5]

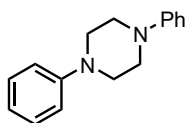## 4-(4-(methylthio)phenyl)morpholine (130)
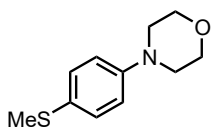
The title compound was prepared according to General Procedure 1 as an off-white solid (0.136 g, 65%). **MP** 93 - 95 °C. **^{1}H NMR** (500 MHz, CDCl$_3$) δ 7.21 - 7.16 (m, 2H), 6.80 - 6.76 (m, 2H), 3.77 (t, J = 5.0 Hz, 4H), 3.05 (t, J = 5.0 Hz, 4H), 2.36 (s, 3H). **^{13}C NMR** (126 MHz, CDCl$_3$) δ 149.8, 130.0, 128.0, 116.4, 67.0, 49.4, 18.1. **HRMS** (EI) [C$_{11}$H$_{15}$NOS] calc. 209.0874, found: 209.0873. Characterization data is in accordance with previous report.[6]

4-(pyridin-3-yl)morpholine (131)
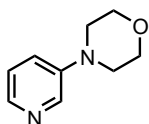
The title compound was prepared according to General Procedure 1 as a yellow solid (0.099 g, 60%). **MP** 37 - 39 °C. **^{1}H NMR** (500 MHz, CDCl$_3$) δ 8.31 (s, 1H), 8.13 (s, 1H), 7.17 (t, J = 2.0 Hz, 2H), 3.91 - 3.82 (m, 4H), 3.20 - 3.17 (m, 4H). **^{13}C NMR** (126 MHz, CDCl$_3$) δ 147.1, 141.2, 138.4, 123.7, 122.2, 66.8, 48.7. **HRMS** (EI) [C$_9$H$_{12}$N$_2$O] calc. 164.0950, found 164.0953. Characterization data is in accordance with previous report.[7]

4-(4-(pyridin-2-ylmethyl)phenyl)morpholine (132)
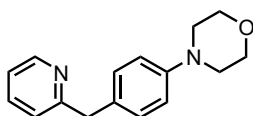
The title compound was prepared according to General Procedure 1 as yellow oil (0.082 g, 32%). **^{1}H NMR** (500 MHz, CDCl$_3$) δ 8.53 (d, J = 3.7 Hz, 1H), 7.55 (t, J = 7.6 Hz, 1H), 7.17 (d, J = 8.4 Hz, 2H), 7.09 (d, J = 7.7 Hz, 2H), 6.86 (d, J = 8.5 Hz, 1H), 4.08 (s, 1H), 3.88 - 3.78 (m, 4H), 3.15 - 2.92 (m, 4H). **^{13}C NMR** (126 MHz, CDCl$_3$) δ 161.6, 150.0, 149.4, 136.6, 131.2, 130.0, 123.1, 121.3, 116.1, 67.1, 49.7, 44.0. **HRMS** (EI) [C$_{16}$H$_{18}$N$_2$O] calc. 254.1419, found 254.1416.

4-(2-(phenoxymethyl)phenyl)morpholine (133)
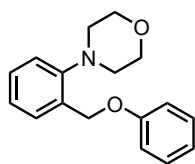
The title compound was prepared according to General Procedure 1 as white crystal (0.194 g, 72%). **MP** 85 - 88 °C. **^{1}H NMR** (500 MHz, CDCl$_3$) δ 7.57 - 7.51 (m, 1H), 7.37 - 7.27 (m, 3H), 7.19 - 7.12 (m, 2H), 7.01 - 6.93 (m, 3H), 5.16 (s, 2H), 3.82 (t, J = 4.6 Hz, 4H), 2.98 (t, J = 4.6 Hz, 4H). **^{13}C NMR** (126 MHz, CDCl$_3$) δ 159.1, 151.5, 132.0, 130.1, 129.6, 129.2, 124.4, 121.0, 120.0, 114.9, 67.6, 66.0, 53.6. **HRMS** (ESI) [C$_{17}$H$_{19}$NO$_2$+H] calc. 270.1489, found 270.1492.:
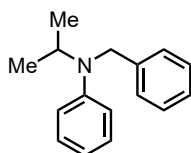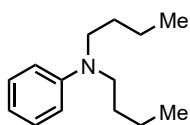
4-(p-tolyl)morpholine (134)
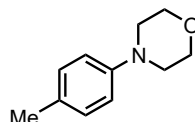
The title compound was prepared according to General Procedure 1 as white solid (0.092 g, 52%). **MP** 43 - 46 °C. **^{1}H NMR** (500 MHz, CDCl$_3$) δ 7.09 (d, J = 8.2, 2H), 6.84 (d, J = 8.4 Hz, 2H), 3.86 (t, J = 4.8 Hz, 4H), 3.11 (t, J = 4.8 Hz, 4H), 2.28 (s, 3H). **^{13}C NMR** (126 MHz, CDCl$_3$) δ 149.3, 129.9, 129.8, 116.2, 67.1, 50.1, 20.6. **HRMS** (EI) [C$_{15}$H$_{15}$NO] calc. 177.1154, found 177.1149. Characterization data is in accordance with previous report.[4]

4-(4-fluorophenyl)morpholine(135)
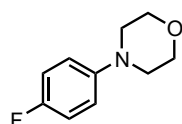
The title compound was prepared according to General Procedure 1 as yellow oil (0.076 g, 42%). **^{1}H NMR** (500 MHz, CDCl$_3$) δ 7.03 - 6.92 (m, 2H), 6.90 - 6.82 (m, 2H), 3.90 - 3.80 (m, 4H), 3.13 - 3.03 (m, 4H). **^{13}C NMR** (126 MHz, CDCl$_3$) δ 157.5 (d, J = 239 Hz), 148.1 (d, J = 2 Hz), 117.6 (d, J = 8 Hz), 115.76 (d, J = 22 Hz), 67.1, 50.5. **^{19}F NMR** (471 MHz, CDCl$_3$) δ -124.2. **HRMS** (ASAP+) [C$_{10}$H$_{12}$NOF+H] calc. 182.0981, found: 182.0983. Characterization data is in accordance with previous report.[8]

4-morpholinobenzonitrile (136)
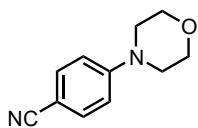
The title compound was prepared according to General Procedure 1 as a white solid (0.096 g, 51%). **MP** 81- 83 °C. **¹H NMR** (500 MHz, CDCl₃) δ 7.55 - 7.48 (m, 2H), 6.90 - 6.83 (m, 2H), 3.85 (t, J = 5.0 Hz, 4H), 3.27 (t, J = 5.0 Hz, 4H). **¹³C NMR** (126 MHz, CDCl₃) δ 153.6, 133.6, 120.0, 114.2, 101.1, 66.6, 47.4. **HRMS** (EI) [C₁₁H₁₂N₂O] calc. 188.0950, found 188.0952. Characterization data is in accordance with previous report.[7]

1,4-diphenylpiperidine (138)
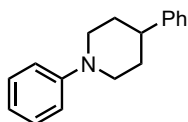
The title compound was prepared according to General Procedure 1 as a white solid (0.192 g, 81%). **MP** 85 - 87 °C. **¹H NMR** (500 MHz, CDCl₃) δ 7.35 - 7.20 (m, 6H), 7.00 (d, J = 7.8 Hz, 2H), 6.86 (t, J = 6.9 Hz, 1H), 3.82 (d, J = 12.3 Hz, 2H), 2.83 (t, J = 11.2 Hz, 2H), 2.76 - 2.58 (m, 1H), 2.01 - 1.89 (m, 4H). **¹³C NMR** (126 MHz, CDCl₃) δ 152.0, 146.2, 129.3, 128.6, 127.0, 126.4, 119.7, 116.8, 50.7, 42.7, 33.5. **HRMS** (ESI) [C₁₇H₁₉N] calc. 237.1517, found 237.1519. Characterization data is in accordance with previous report.[9] Result obtained by Andrew C. Jones.
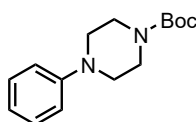
4-phenylthiomorpholine (139)
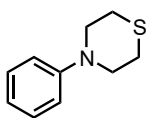
The title compound was prepared according to General Procedure 1 as a dark yellow oil (0.158 g, 88%). **¹H NMR** (500 MHz, CDCl₃) δ 7.22 - 7.12 (m, 2H), 6.86 - 6.72 (m, 3H), 3.44 (t, J = 5.1 Hz, 4H), 2.65 (t, J = 5.1 Hz, 4H). **¹³C NMR** (126 MHz, CDCl₃) δ 151.4, 129.3, 119.9, 117.2, 52.2, 26.9. **HRMS** (ESI) [C₁₀H₁₃NS] calc. 179.0769, found 179.0760. Characterization data is in accordance with previous report.[10] Result obtained by Andrew C. Jones.

1-phenylpiperidine (140)
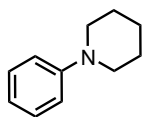
The title compound was prepared according to General Procedure 1 as a brown oil (0.124 g, 77%). **^{1}H NMR** (500 MHz, CDCl$_3$) δ 7.27 - 7.21 (m, 2H), 6.95 (d, *J* = 7.9 Hz, 2H), 6.82 (t, *J* = 7.3 Hz, 1H), 3.16 (t, *J* = 5.5 Hz, 4H), 1.77 - 1.67 (m, 4H), 1.62 - 1.53 (m, 2H). **^{13}C NMR** (126 MHz, CDCl$_3$) δ 152.4, 129.1, 119.3, 116.7, 50.8, 26.0, 24.5. **HRMS** (ESI) [C$_{11}$H$_{15}$N] calc. 161.1204, found 161.1204. Characterization data is in accordance with previous report.[11] Result obtained by Andrew C. Jones.

8-phenyl-1,4-dioxa-8-azaspiro[4.5]decane (141)
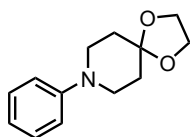
The title compound was prepared according to General Procedure 1 as a dark yellow oil (0.171 g, 78%). **^{1}H NMR** (500 MHz, CDCl$_3$) δ 7.55 (t, *J* = 7.8 Hz, 2H), 7.25 (d, *J* = 8.1 Hz, 2H), 7.13 (t, *J* = 7.2 Hz, 1H), 4.29 (s, 4H), 3.64 - 3.62 (t, *J* = 5.5 Hz, 4H), 2.27 - 2.03 (t, *J* = 5.5 Hz, 4H). **^{13}C NMR** (126 MHz, CDCl$_3$) δ 151.1, 129.2, 119.6, 116.8, 107.3, 64.5, 47.9, 34.7. **HRMS** (ESI) [C$_{13}$H$_{17}$NO$_2$+H] calc. 220.1336, found 220.1338. Characterization data is in accordance with previous report.[12] Result obtained by Andrew C. Jones.

1-phenylazepane (142)
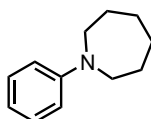
The title compound was prepared according to General Procedure 1 as a brown oil (0.126 g, 72%). **^{1}H NMR** (500 MHz, CDCl$_3$) δ 7.23 - 7.17 (m, 2H), 6.69 (d, *J* = 8.2 Hz, 2H), 6.62 (t, *J* = 7.2 Hz, 1H), 3.47 - 3.44 (t, *J* = 6.0 Hz, 4H), 1.82 -1.74 (m, 4H), 1.58 - 1.52 (m, 4H). **^{13}C NMR** (126 MHz, CDCl$_3$) δ 149.1, 129.4, 115.3, 111.3, 49.2, 27.9, 27.3. **HRMS** (ESI) [C$_{12}$H$_{17}$N+H] calc. 175.1361, found 175.1362. Characterization data is in accordance with previous report.[13] Result obtained by Andrew C. Jones.

2-phenyl-1,2,3,4-tetrahydroisoquinoline (135)
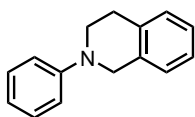
The title compound was prepared according to General Procedure 1 as an off-white solid (0.151 g, 72%). **MP** 57 - 60°C. **^{1}H NMR** (500 MHz, CDCl$_3$) δ 7.39 - 7.28 (m, 2H), 7.22 - 7.18 (m, 4H), 7.06 - 6.97 (m, 2H), 6.86 (t, J = 7.3 Hz, 1H), 4.44 (s, 2H), 3.59 (t, J = 5.8 Hz, 2H), 3.02 (t, J = 5.7 Hz, 2H). **^{13}C NMR** (126 MHz, CDCl$_3$) δ 150.7, 135.0, 134.6, 129.3, 128.7, 126.7, 126.5, 126.2, 118.8, 115.3, 50.9, 46.7, 29.3. **HRMS** (EI) [C$_{15}$H$_{15}$N] calc. 209.1204, found 209.1204. Characterization data is in accordance with previous report.[14] Result obtained by Andrew C. Jones.

4-benzyl-1-phenylpiperidine (143)
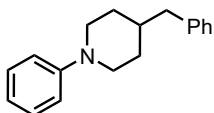
The title compound was prepared according to General Procedure 1 as a red solid (0.200 g, 80%). **MP** 67 - 70 °C. **^{1}H NMR** (500 MHz, CDCl$_3$) δ 7.24 - 7.04 (m, 7H), 6.83 (d, J = 8.0 Hz, 2H), 6.72 (t, J = 7.3 Hz, 1H), 3.52 (t, J = 28.9 Hz, 2H), 2.54 (td, J = 12.2, 2.1 Hz, 2H), 2.48 (d, J = 7.1 Hz, 2H), 1.82 - 1.44 (m, 3H), 1.38 - 1.21 (m, 2H). **^{13}C NMR** (126 MHz, CDCl$_3$) δ 151.96, 140.59, 129.25, 129.13, 128.33, 125.99, 119.34, 116.62, 50.08, 43.29, 38.00, 32.15. **HRMS** (EI) [C$_{18}$H$_{21}$N] calc. 251.1674, found 251.1674. Result obtained by Andrew C. Jones.

1,4-diphenylpiperazine (144)

The title compound was prepared according to General Procedure 1 as a white solid (0.190 g, 80%). **MP** 173 - 175 °C. **^{1}H NMR** (500 MHz, CDCl$_3$) δ 7.37 - 7.27 (m, 4H), 7.01 (d, J = 7.9 Hz, 4H), 6.91 (t, J = 7.3 Hz, 2H), 3.36 (s, 8H). **^{13}C NMR** (126 MHz, CDCl$_3$) δ 151.4, 129.3, 120.2, 116.5, 49.6. **HRMS** (ESI) [C$_{16}$H$_{18}$N] calc. 238.1517, found 238.1519. Characterization data is in accordance with previous report.[11] Result obtained by Andrew C. Jones.

N-benzyl-*N*-methylaniline (145)
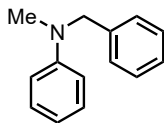
The title compound was prepared according to General Procedure 1 as a light-yellow liquid (0.134 g, 68%). **¹H NMR** (500 MHz, CDCl₃) δ 7.24 - 7.17 (m, 2H), 7.17 - 7.07 (m, 5H), 6.69 - 6.58 (m, 3H), 4.43 (s, 2H), 2.92 (s, 3H). **¹³C NMR** (126 MHz, CDCl₃) δ 149.8, 139.1, 129.3, 128.7, 127.0, 126.8, 116.6, 112.4, 56.7, 38.6. **HRMS** (ASAP+) [C₁₄H₁₅N+H] calc. 198.1283, found 198.1277. Characterization data is in accordance with previous report.[11] Result obtained by Andrew C. Jones.

N-benzyl-*N*-*iso*propylaniline (146)

The title compound was prepared according to General Procedure 1 as yellow liquid (0.160 g, 71%). **¹H NMR** (500 MHz, CDCl₃) δ 7.34 - 7.28 (m, 4H), 7.25 - 7.14 (m, 3H), 6.75 - 6.66 (m, 3H), 4.43 (s, 2H), 4.34 - 4.25 (m, 1H), 1.22 (d, *J* = 6.6 Hz, 6H). **¹³C NMR** (126 MHz, CDCl₃) δ 149.4, 140.9, 129.2, 128.5, 126.5, 126.3, 116.4, 113.1, 48.5, 48.2, 20.0. **HRMS** (ASAP+) [C₁₆H₁₉N+H] calc. 226.1596, found 226.1294. Characterization data is in accordance with previous report.[15] Result obtained by Andrew C. Jones.

N,N-dibutylaniline (147)

The title compound was prepared according to General Procedure 1 as yellow liquid (0.095 g, 61%). **¹H NMR** (500 MHz, CDCl₃) δ 7.24 - 7.19 (m, 2H), 6.69 - 6.61 (m, 3H), 3.28 (t, *J* = 7.5 Hz, 4H), 1.63 - 1.55 (m, 4H), 1.42 - 1.33 (m, 4H), 0.97 (t, *J* = 7.4 Hz, 6H). **¹³C NMR** (126 MHz, CDCl₃) δ 148.3, 129.3, 115.2, 111.8, 50.9, 29.6, 20.5, 14.2. **HRMS** (ASAP+) [C₁₄H₂₃N+H] calc. 206.1909, found 206.1910. Characterization data is in accordance with previous report.[11] Result obtained by Andrew C. Jones.

N-methyl-*N*-phenethylaniline (148)
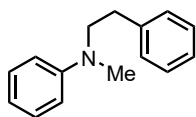
The title compound was prepared according to General Procedure 1 as yellow liquid (0.152 g, 72%). **^{1}H NMR** (500 MHz, CDCl$_3$) δ 7.33 - 7.04 (m, 7H), 6.72 - 6.59 (m, J = 16.4, 3H), 3.47 (t, J = 7.5 Hz, 2H), 2.79 (s, J = 7.1 Hz, 3H), 2.78 - 2.72 (m, 2H). **^{13}C NMR** (126 MHz, CDCl$_3$) δ 148.8, 139.9, 129.4, 128.9, 128.6, 126.3, 116.2, 112.2, 54.8, 38.6, 32.9. **HRMS** (EI) [C$_{15}$H$_{17}$N] calc. 211.1361, found 211.1363. Characterization data is in accordance with previous report.[16] Result obtained by Andrew C. Jones.

tert-butyl 4-phenylpiperazine-1-carboxylate (149)

The title compound was prepared according to General Procedure 1 as a white solid (0.157 g, 60%). **^{1}H NMR** (500 MHz, CDCl$_3$) δ 7.30 - 7.27 (m, 2H), 6.95 - 6.90 (m, 3H), 3.59 (t, J = 5.2 Hz, 4H), 3.14 (t, J = 5.1 Hz, 4H), 1.50 (s, 9H). **^{13}C NMR** (126 MHz, CDCl$_3$) δ 154.9, 151.4, 129.3, 120.4, 116.8, 80.0, 49.6, 43.5, 28.6. **HRMS** (EI) [C$_{15}$H$_{22}$N$_2$O$_2$] calc. 262.1681, found: 262.1682. Characterization data is in accordance with previous report.[11] Result obtained by Andrew C. Jones.

tert-butyl 4-(2-((2,4-dimethylphenyl)thio)phenyl)piperazine-1-carboxylate/ N-Boc vortioxetine (154)
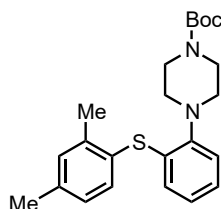
The title compound was prepared according to General Procedure 1 as an light yellow solid (0.275 g, 69%). **MP** 78 - 80 °C. **^{1}H NMR** (500 MHz, CDCl$_3$) δ 7.36 (d, J = 7.8 Hz, 1H), 7.15 (s, 1H), 7.09 - 7.00 (m, 3H), 6.90 - 6.84 (m, 1H), 6.53 (dd, J = 7.9, 1.4 Hz, 1H), 3.62 (t, J = 5.0 Hz, 4H), 3.02 (t, J = 4.9 Hz, 4H), 2.36 (s, 3H), 2.32 (s, 3H), 1.49 (s, 9H). **^{13}C NMR** (126 MHz, CDCl$_3$) δ 155.1, 149.1, 142.5, 139.4, 136.3, 134.8, 131.8, 127.99, 127.96, 126.5, 125.7, 124.8, 120.1, 79.8, 51.8, 43.8, 28.6, 21.3, 20.7. **HRMS** (ESI+)

[C$_{23}$H$_{30}$N$_2$O$_2$S+H] calc. 399.2106, found 399.2102. Characterization data is in accordance with previous report.[17]

tert-butyl 4-(2-((2,4-dimethylphenyl)thio)phenyl)piperazine-1-carboxylate hydrobromide/ Vortioxetine (155)
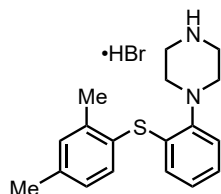
N-Boc vortioxetine (0.275 g, 0.7 mmol,) was dissolved in 2 mL methanol and slowly added 0.2 mL 48 wt% HBr (aq.) followed by heating to reflux for 2 hours. Then the mixture was cooled to room temperature then the solvent was removed by evaporation. After the addition of diethyl ether (2 mL), the mixture was stirred at room temperature for 2 h before leaving the mixture in the freezer overnight. Filtration and washing with 5 mL diethyl ether to produce brownish solid. Then the brownish solid was dried under high vaccum (0.215 g, 81%). **MP** 218 °C. **^{1}H NMR** (500 MHz, CDCl$_3$) δ 9.36 (s, 2H), 7.31 (d, *J* = 7.8 Hz, 1H), 7.17 - 7.06 (m, 3H), 7.02 (d, *J* = 7.8 Hz, 1H), 6.96 - 6.90 (m, 1H), 6.55 (d, *J* = 7.7 Hz, 1H), 3.68 - 3.35 (m, 8H), 2.35 (s, 3H), 2.30 (s, 3H). **^{13}C NMR** (126 MHz, CDCl$_3$) δ 147.0, 142.3, 139.6, 136.0, 134.7, 132.0, 128.1, 127.2, 126.9, 126.0, 126.0, 120.6, 48.6, 44.2, 21.3, 20.7. **HRMS** (ESI+) [C$_{18}$H$_{22}$N$_2$S+H] calc. 299.1582, found 299.1588. Characterization data is in accordance with previous report.[18]

tert-butyl piperazine-1-carboxylate (153)
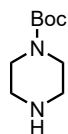
The titled compound was prepared using a method modified from literature.[19] To a 50 mL flask was added piperazine (0.86 g, 10 mmol, 2.5 equiv), sodium hydroxide (0.16 g, 4.0 mmol, 1.0 equiv), isopropanol (12 mL) and water (1.3 mL). di-tert-butyl dicarbonate (0.92 mL, 4.0 mmol, 1.0 equiv) was added and the reaction was stirred at room temperature for 18 h. The solution was concentrated to remove isopropanol. The mixture was diluted with water, filtered through a fritted funnel to remove di-tert-butyl piperazine-1,4-dicarboxylate, and the filtrate was extracted with DCM (×3). The combined organic fractions were dried over magnesium sulphate and concentrated to yield the titled

compound as a white crystalline solid (1.06 g, 5.7 mmol, 57%). **^{1}H NMR** (500 MHz, CDCl$_3$) δ 1.47 (s, 9H), 2.94 - 2.71 (m, 4H), 3.72 - 3.36 (m, 4H). **^{13}C NMR** (126 MHz, CDCl$_3$) δ 155.0, 79.7, 46.0, 44.9, 28.6. **HRMS** (EI) [C$_9$H$_{18}$N$_2$O$_2$] calc. 186.1386, found 186.1386. Characterization data is in accordance with previous report.[19]

S-(2,4-dimethylphenyl) ethanethioate (151)
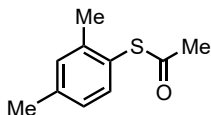
The titled compound was prepared using a method modified from the literature.[20] A 100 mL, three-necked, round-bottomed flask equipped with an argon inlet adapter, glass stopper, and a rubber septum was charged with 2,4-dimethylbenzenethiol (1.381 g, 10 mmol), 35 mL of dichloromethane, and pyridine (1.15 mL, 1.12 g, 14.2 mmol) and cooled to 0 °C. Acetyl chloride (1.0 mL, 1.10 g, 14.1 mmol) was added slowly via syringe over ca. 8 min. The resulting mixture was stirred at 0 °C for 10 min and then at 25 °C for 2 h. The resulting cloudy white mixture was poured into 20 mL of water, and the aqueous phase was separated and extracted with two 10 mL portions of dichloromethane. The combined organic phases were washed with 20 mL of brine, dried over magnesium sulpohate, filtered, and concentrated under reduced pressure. Then the crude material was then purified by silica gel flash chromatography (Ethyl Acetate/Petroleum ether = 1:20) to give the title compound as light yellow liquid (1.028 g, 57%). **^{1}H NMR** (500 MHz, CDCl$_3$) δ 7.24 (s, 1H), 7.14 - 7.11 (m, 1H), 7.04 - 7.00 (m, 1H), 2.39 (s, 3H), 2.32 (s, 3H), 2.30 (s, 3H). **^{13}C NMR** (126 MHz, CDCl$_3$) δ 194.4, 141.9, 140.5, 135.9, 131.8, 127.6, 124.2, 30.3, 21.4, 20.8. **HRMS** (EI) [C$_{10}$H$_{12}$OS] calc. 180.0609, found: 180.0616. Characterization data is in accordance with previous report.[21] Result obtained by Qun Cao.

(2-bromophenyl)(2,4-dimethylphenyl)sulfane (152)
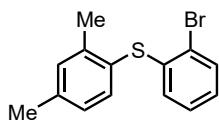
The titled compound was prepared using a method modified from literature.[22] To a 50 mL round bottomed flask, Pd(dba)$_2$ (0.144 g, 0.25 mmol), Xantphos (0.203 g, 0.35 mmol), 1,2- dibromobenzene (0.702 g, 1.5 mmol), S-(2,4-dimethylphenyl)ethanethioate (0.901 g, 5 mmol) sodium tert-butoxide (0.577 g, 6 mmol), toluene (10 mL) were added. The reaction mixture was stirred at 6 h at 110 °C under nitrogen atmosphere and then cooled

to room temperature. Then the reaction mixture was poured into a 10 mL saturated aqueous ammonium chloride and extracted with Et2O (20 mL) three times. The combined organic phase was dried over magnesium sulphate, filtered and concentrated under reduced pressure. Then the crude material was then purified by silica gel flash chromatography (Ethyl acetate/Petroleum ether = 1:20) to give the titled compound as light yellow liquid (1.232 g, 84%). **¹H NMR** (500 MHz, CDCl₃) δ 7.53 (dd, J = 7.9, 1.4 Hz, 1H), 7.40 (d, J = 7.8 Hz, 1H), 7.19 - 7.15 (m, 1H), 7.10 - 7.04 (m, 2H), 6.96 (td, J = 7.9, 7.3 Hz, 1H), 6.57 (dd, J = 8.0, 1.6 Hz, 1H), 2.37 (s, 3H), 2.34 (s, 3H). **¹³C NMR** (126 MHz, CDCl₃) δ 142.5, 140.1, 139.6, 136.4, 132.9, 132.1, 128.2, 127.8, 127.5, 127.2, 126.2, 121.3, 21.4, 20.7. **HRMS** (EI) [$C_{14}H_{13}SBr$] calc. 291.9921, found: 291.9925. Characterization data is in accordance with previous report.[23] Result obtained by Qun Cao.

Diphenylsulfane (160)
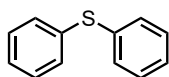
To a 15 mL stainless steel milling vessel (Form-Tech Scientific) was added a stainless-steel ball (12 g), sand (0.338 g), potassium *tert*-butoxide (2 mmol, 0.224 g), chlorobenzene (1 mmol, 0.113 g), thiophenol (1.2 mmol, 0.132 g) and Pd-PEPPSI-IPent (0.01 mmol, 8.0 mg) under an air atmosphere. The milling jar was then closed, and the mixture was milled at 30 Hz for 3 hours. After the desired reaction time, the black solid mixture was scratched out using spatula and the jar was raised with EtOAc (10 mL) twice. Then the mixture was filtered and the solvent was removed *in vacuo*. The crude reaction mixture was then purified by silica gel flash chromatography to provide the title compound as a colourless oil (0.089 g, 0.48 mmol, 48%). **¹H NMR** (500 MHz, CDCl₃) δ 7.37 (d, J = 7.4 Hz, 4H), 7.32 (t, J = 7.6 Hz, 4H), 7.27 (d, J = 7.1 Hz, 2H).**¹³C NMR** (126 MHz, CDCl₃) δ 135.9, 131.2, 129.3, 127.2. **HRMS** (EI) [$C_{12}H_{10}S$] calc. 186.0503, found 186.0499. Characterization data is in accordance with previous report.[24]

6.4 Direct Amidation of Esters Enabled by Ball Milling

6.4.1 General Procedure 3: Ball Milling Direct Amidation of Esters with amines

To a 14 mL stainless steel milling jar (Insolido Technologies) was added a stainless-steel ball (4 g), the ester (1.2 mmol), the amine (1 mmol), and potassium *tert*-butoxide (0.85 mmol, 96 mg). The jar was then closed and milled for 1 hour at 30 Hz. Once the reaction was complete the jar was opened, and EtOAc (~2 mL) and brine (~1 mL) was added to the jar which was then closed shaken and the mixture transferred to a separating funnel, this was then repeated with an additional aliquot of EtOAc (~2 mL) and water (~1 mL). For examples that caused large amounts of emulsion NaOH aq. (2 M, 1 mL) was added to aid in separation. The organic phase was then separated and dried over magnesium sulphate. The solvent was removed *in vacuo* and the crude mixture purified by silica gel chromatography if required.

6.4.2 General Procedure 4: Ball Milling Direct Amidation of Esters with ammonium salts

To a 14 mL stainless steel milling jar (Insolido Technologies) was added a stainless-steel ball (4 g), the ester (1.2 mmol), the ammonium salt (1 mmol), and potassium *tert*-butoxide (1.85 mmol, 209 mg, 1.85 equiv.). The jar was then closed and securely fitted to the mill which was set for 1 hour at the frequency of 30 Hz. Once the reaction was complete the jar was opened, and EtOAc (~2 mL) and brine (~1 mL) was added to the jar which was then closed shaken and the mixture transferred to a separating funnel, this was then repeated with an additional aliquot of EtOAc (~2 mL) and water (~1 mL). For examples that caused large amounts of emulsion NaOH aq. (2 M, 1 mL) was added to aid in separation. The organic phase was then separated and dried over magnesium sulphate. The solvent was removed *in vacuo* and the crude mixture purified by silica gel chromatography.

6.4.3 General Procedure 5: Large scale Direct Amidation of Esters with Amines

To a 25 mL stainless steel milling (Retsch) jar was added a stainless-steel ball (12 g), the ester (1.2 equivalents), the amine (1 equivalent), and potassium *tert*-butoxide (0.85 equivalents). The jar was then closed and milled for 1 hour at 30 Hz. Once the reaction was complete the reaction mixture washed from the jar with EtOAc (~5 mL) and water (~5 mL) into a separating funnel. Additional EtOAc (~50 mL) and water (~50 mL) was then added and the aqueous extracted. The layers were separated and the aqueous phase was re-extracted with EtOAc (2 x 25 mL). The organic phases were combined and

dried over magnesium sulphate and solvent removed *in vacuo*. The crude product was purified by flash column chromatography.
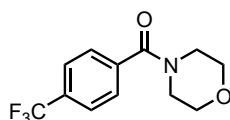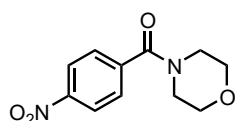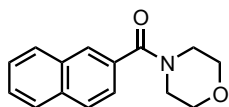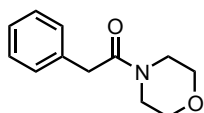
phenyl(morpholino)methanone (219)
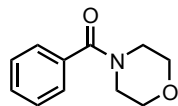
The title compound was prepared according to General Procedure 3, as a white solid (187 mg, 98%). **MP** 62 – 68 °C. **^{1}H NMR** (500 MHz, CDCl$_3$) δ 7.49 – 7.36 (m, 5H), 3.92 – 3.33 (m, 8H). **^{13}C NMR** (126 MHz, CDCl$_3$) δ 170.6, 135.5, 130.0, 128.7, 127.2, 67.1. **IR:** ν_{max}: 2859, 1624, 1423, 1269, 1109, 1018, 710 cm^{-1}. **HRMS** (pNSI+) [C$_{11}$H$_{13}$NO$_2$ + H]: calc. 192.1019, found 192.1018. Characterization data is in accordance with prior reports.[25]
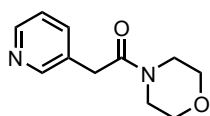
(4-methoxyphenyl)(morpholino)methanone (244)
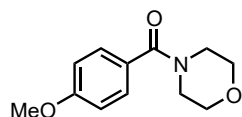
The title compound was prepared according to General Procedure 3, as a white solid (161 mg, 73%). **MP** 37 – 40 °C (EtOAc), **^{1}H NMR** (500 MHz, CDCl$_3$) δ 7.41 – 7.35 (m, 2H), 6.93 – 6.89 (m, 2H), 3.83 (s, 3H), 3.69 (d, *J* = 3.6 Hz, 8H). **^{13}C NMR** (126 MHz, CDCl$_3$) δ 170.4, 160.9, 129.2, 127.4, 113.8, 66.9, 55.4. **IR**: ν_{max}: 1607, 1435, 1252, 1109, 1007, 849, 762, 550 cm^{-1}. **HRMS** (pNSI+) [C$_{12}$H$_{15}$NO$_3$ + H]: calc. 222.1125, found 222.1125. Characterization data is in accordance with prior reports.[26]

(4-bromophenyl)(morpholino)methanone (245)
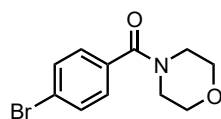
The title compound was prepared according to General Procedure 3, as a white solid (267 mg, 99%). **MP** 50 – 53 °C (EtOAc). **^{1}H NMR** (500 MHz, CDCl$_3$) δ 7.58 (d, *J* = 8.3 Hz, 2H), 7.31 (d, *J* = 8.3 Hz, 2H), 3.61 (d, *J* = 140.3 Hz, 8H). **^{13}C NMR** (126 MHz, CDCl$_3$) δ 169.6, 134.3, 132.0, 129.0, 124.4, 67.0. **IR**: ν_{max}: 2980, 1618, 1435, 1271, 1111, 1010, 843, 752, 540 cm^{-1} **HRMS** (ES+) [C$_{11}$H$_{12}$BrNO$_2$ + H]: calc. 270.0130, found 270.0125. Characterization data is in accordance with prior reports.[27]

(4-iodophenyl)(morpholino)methanone (246)
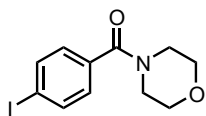
The title compound was prepared according to General Procedure 3, as a white solid prepared according to **GP1** (253 mg, 80%). **MP** 102 – 105 ˚C (EtOAc) **^{1}H NMR** (500 MHz, CDCl$_3$) δ 7.80 – 7.73 (m, 2H), 7.18 – 7.11 (m, 2H), 3.59 (d, J = 151.3 Hz, 8H). **^{13}C NMR** (126 MHz, CDCl$_3$) δ 169.5, 137.8, 134.7, 128.9, 96.1, 66.9. **IR**: v_{max}: 2853, 1622, 1429, 1269, 1109, 1005, 831, 752, 538 cm^{-1}. **HRMS** (pNSI+) [C11H12INO$_2$ + H]: calc. 317.9985, found 317.9987. Characterization data is in accordance with prior reports.[26]

(4-fluorophenyl)(morpholino)methanone (251)
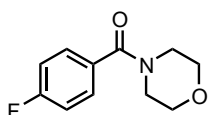
The title compound was prepared according to General Procedure 3, as a yellow liquid (115 mg, 55%). **^{1}H NMR** (400 MHz, CDCl$_3$) δ 7.48 – 7.39 (m, 2H), 7.16 – 7.05 (m, 2H), 3.70 (bs, 8H). **^{13}C NMR** (126 MHz, CDCl$_3$) δ 169.59 (s), 163.57 (d, J = 250.2 Hz), 131.39 (d, J = 3.5 Hz), 129.54 (d, J = 8.5 Hz), 115.76 (d, J = 21.8 Hz), 66.93 (s), 48.33 (s), 42.82 (s). **^{19}F NMR** (471 MHz, CDCl$_3$) δ -105.84 – -112.49 (m). **IR**: v_{max}: 2980, 1626, 1427, 1111,843, 733, 573 cm^{-1} **HRMS** (pNSI+) [C$_{11}$H$_{12}$O$_2$NF + H]: calc. 210.0925, found 210.0925. Characterization data is in accordance with prior reports.[27]

(4-chlorophenyl)(morpholino)methanone (158)
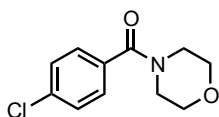
The title compound was prepared according to General Procedure 3, as a white solid (221 mg, 98%). **MP** 64 – 66 ˚C (EtOAc). **^{1}H NMR** (500 MHz, CDCl$_3$) δ 7.45 – 7.34 (m, 2H), 7.13 – 7.01 (m, 2H), 3.59 (*br* s, 8H). **^{13}C NMR** (126 MHz, CDCl$_3$) δ 169.4, 136.1, 133.7, 129.0, 128.8, 66.9, 48.3, 42.7. **IR**: v_{max}: 2860, 1622, 1435, 1111, 1011, 837, 554 cm^{-1} **HRMS** (EI+) [C$_{11}$H$_{12}$ClNO$_2$]: calc. 225.0557, found 225.0556. Characterization data is in accordance with prior reports.[27]

4-tolyl(morpholino)methanone (248)
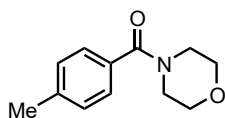
The title compound was prepared according to General Procedure 3, as a white solid (127 mg, 62%). **MP** 61 – 63 ˚C (EtOAc) **¹H NMR** (400 MHz, CDCl₃) δ 7.31 (d, *J* = 8.1 Hz, 2H), 7.21 (d, *J* = 7.8 Hz, 2H), 3.70 (*br* s, 8H), 2.38 (s, 3H). **¹³C NMR** (126 MHz, CDCl₃) δ 170.8, 140.2, 132.5, 129.3, 127.4, 67.1, 21.5. **IR**: ν$_{max}$: 2949, 1616, 1273, 1111, 833, 750, 542 cm⁻¹ **HRMS** (pNSI+) [C₁₂H₁₅O₂N + H]: calc. 206.1176, found 206.1175. Characterization data is in accordance with prior reports.[28]

morpholino(4-(trifluoromethyl)phenyl)methanone (249)

The title compound was prepared according to General Procedure 3, as a white solid (201 mg, 78%). **MP** 48 -51 ˚C (EtOAc) **¹H NMR** (500 MHz, CDCl₃) δ 7.67 (d, *J* = 8.1 Hz, 1H), 7.51 (d, *J* = 8.0 Hz, 1H), 4.01 – 3.16 (m, 4H). **¹⁹F NMR** (471 MHz, CDCl₃) δ -62.95 (s). **¹³C NMR** (126 MHz, CDCl₃) δ 169.0 (s), 139.0 (s), 139.0 (s), 131.9 (q, *J* = 32.8 Hz), 127.6 (s), 127.0 (s), 125.8 (q, *J* = 3.7 Hz), 124.8 (s), 122.7 (s), 120.5 (s), 66.9 (s), 48.2 (s), 42.6 (s). **IR**: ν$_{max}$: 1636, 1429, 1319, 1107, 1063, 1012, 841 cm⁻¹ **HRMS** (ES+) [C₁₂H₁₂NO₂F₃ + H]: calc. 260.0898, found 260.0891. Characterization data is in accordance with prior reports.[28]

4-nitrophenyl(morpholino)methanone (250)

The title compound was prepared according to General Procedure 3, as a white solid (149 mg, 63%). **MP** 91 – 93 ˚C (EtOAc) **¹H NMR** (400 MHz, CDCl₃) δ 8.33 – 8.26 (m, 2H), 7.62 – 7.56 (m, 2H), 3.93 – 3.27 (m, 8H). **¹³C NMR** (126 MHz, CDCl₃) δ 168.2, 148.7, 141.6, 128.3, 124.1, 66.9. **IR**: ν$_{max}$: 2868, 1620, 1512, 1441, 1348, 1260, 1107, 835, 723, 546 cm⁻¹ **HRMS** (pNSI+) [C₁₁H₁₂O₄N₂ + H]: calc. 237.0870, found 237.0872. Characterization data is in accordance with prior reports.[28]

morpholino(naphthalen-2-yl)methanone (247)

The title compound was prepared according to General Procedure 3, as a white solid (176 mg, 71%). **MP** 85 – 88 ˚C (EtOAc) **^{1}H NMR** (500 MHz, CDCl$_3$) δ 7.94 – 7.80 (m, 4H), 7.58 – 7.43 (m, 3H), 4.01 – 3.32 (m, 8H). **^{13}C NMR** (126 MHz, CDCl$_3$) δ 170.5, 133.8, 132.7, 132.6, 128.5, 128.4, 127.9, 127.2, 127.1, 126.8, 124.3, 67.0, 48.4, 42.7. **IR**: ν$_{max}$: 1618, 1425, 1298, 1232, 1111, 1028, 872, 810, 750 cm^{-1} **HRMS** (ES+) [C$_{15}$H$_{15}$NO$_2$ + H]: calc. 242.1181, found 242.1187. Characterization data is in accordance with prior reports.[26]

1-morpholino-2-phenylethan-1-one (259)

The title compound was prepared according to General Procedure 3, as a white solid (153 mg, 74%). **MP** 45 – 49 ˚C (EtOAc) **^{1}H NMR** (500 MHz, CDCl$_3$) δ 7.25 (t, J = 7.4 Hz, 2H), 7.20 – 7.13 (m, 3H), 3.66 (s, 2H), 3.57 (s, 4H), 3.38 (dt, J = 9.1, 3.9 Hz, 4H). **^{13}C NMR** (126 MHz, CDCl$_3$) δ 169.6, 134.8, 128.8, 128.5, 126.9, 66.8, 66.5, 46.5, 42.2, 40.9. **IR**: ν$_{max}$: 2851, 1639, 1433, 1277, 1229, 1111, 1036, 845, 733, 698, 575 cm^{-1} **HRMS** (EI+) [C$_{12}$H$_{15}$NO$_2$]: calc. 205.1103, found 205.1103. Characterization data is in accordance with prior reports.[26]

1-morpholino-2-(pyridin-3-yl)ethan-1-one (260)

The title compound was prepared according to General Procedure 3, as a white solid (93 mg, 45%). **MP** 45 – 47 ˚C (EtOAc). **^{1}H NMR** (500 MHz, CDCl$_3$) δ 8.60 – 8.40 (m, 2H), 7.74 – 7.67 (m, 1H), 7.34 (dd, J = 7.8, 4.9 Hz, 1H), 3.73 (s, 2H), 3.66 (dd, J = 10.2, 4.1 Hz, 4H), 3.63 – 3.56 (m, 2H), 3.54 – 3.44 (m, 2H). **^{13}C NMR** (126 MHz, CDCl$_3$) δ 168.4, 149.2, 147.5, 138.0, 131.3, 124.0, 66.9, 66.6, 46.5, 42.4, 37.5. **IR**: ν$_{max}$: 1635, 1436, 1420, 1234, 1224, 1110, 1031, 847, 713, 577 cm^{-1} **HRMS** (EI+) [C$_{11}$H$_{14}$N$_2$O$_2$ + H]: calc. 207.1134, found 207.1136. Characterization data is in accordance with prior reports.[28]

1-morpholino-3-phenylpropan-1-one (261)
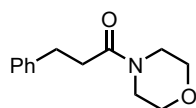
The title compound was prepared according to General Procedure 3, as a colourless oil (172 mg, 79%). **^{1}H NMR** (500 MHz, CDCl$_3$) δ 7.33 – 7.27 (m, 2H), 7.24 – 7.17 (m, 3H), 3.62 (s, 4H), 3.55 – 3.46 (m, 2H), 3.41 – 3.28 (m, 2H), 3.02 – 2.93 (m, 2H), 2.66 – 2.57 (m, 2H). **^{13}C NMR** (126 MHz, CDCl$_3$) δ 171.0, 141.2, 128.7, 128.6, 126.4, 67.0, 66.6, 46.1, 42.1, 34.9, 31.6. **IR**: ν$_{max}$: 1637, 1430, 1270, 1226, 1112, 1024, 751, 699 cm^{-1} **HRMS** (ES+) [C$_{13}$H$_{17}$NO$_2$ + H]: calc. 220.1318, found 220.1340. Characterization data is in accordance with prior reports.[26]

(Z)-1-morpholinooctadec-9-en-1-one (262)
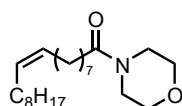
The title compound was prepared according to General Procedure 3, as a colourless oil (142 mg, 41%). **^{1}H NMR** (500 MHz, CDCl$_3$) δ 5.45 – 5.25 (m, 2H), 3.72 – 3.63 (m, 4H), 3.63 - 3.58 (m, 2H), 3.54 – 3.37 (m, 2H), 2.75 (d, J = 6.6 Hz, 1H), 2.35 – 2.23 (m, 2H), 2.10 – 1.92 (m, 3H), 1.66 – 1.55 (m, 2H), 1.40 – 1.15 (m, 20H), 0.87 (td, J = 6.9, 5.0 Hz, 3H). **^{13}C NMR** (126 MHz, CDCl$_3$) δ 171.9, 171.9, 171.9, 130.2, 130.0, 130.0, 129.8, 128.1, 127.9, 67.0, 66.7, 46.1, 41.9, 33.2, 33.1, 31.9, 31.9, 31.5, 29.8, 29.7, 29.7, 29.7, 29.7, 29.7, 29.6, 29.5, 29.5, 29.5, 29.5, 29.4, 29.4, 29.4, 29.3, 29.2, 27.2, 27.2, 27.2, 25.6, 25.3, 25.3, 22.7, 22.6, 14.1, 14.1. **IR**: ν$_{max}$: 2922, 2851, 1647, 1456, 1427, 1227, 1115 cm^{-1} **HRMS** (ES+) [C$_{22}$H$_{41}$NO$_2$]: calc. 352.3216, found 352.3218. Characterization data is in accordance with prior reports.[29]

3,7-dimethyl-1-morpholinooct-6-en-1-one (264)
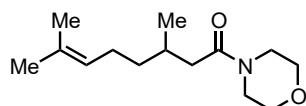
The title compound was prepared according to General Procedure 3, as a colourless oil (191 mg, 80%). **^{1}H NMR** (500 MHz, CDCl$_3$) δ 5.13 – 5.03 (m, 1H), 3.65 (dt, J = 12.9, 6.7 Hz, 6H), 3.46 (s, 2H), 2.31 (dd, J = 14.5, 5.8 Hz, 1H), 2.12 (dd, J = 14.5, 8.3 Hz, 1H), 1.98 (ddt, J = 12.3, 8.2, 6.2 Hz, 3H), 1.67 (d, J = 1.1 Hz, 3H), 1.60 (s, 3H), 1.43 – 1.33

(m, 1H), 1.22 (dddd, *J* = 13.6, 9.2, 8.0, 6.0 Hz, 1H), 0.95 (d, *J* = 6.6 Hz, 3H). **¹³C NMR** (126 MHz, CDCl₃) δ 171.4, 131.7, 124.5, 67.2, 66.9, 46.4, 42.1, 40.5, 37.2, 30.2, 25.9, 25.6, 20.0, 17.8. **IR**: ν_{max}: 1636, 1457, 1420, 1229, 1114, 1036 cm⁻¹ **HRMS** (ES+) [C₁₄H₂₅NO₂ + H]: calc. 240.1964, found 240.1965.
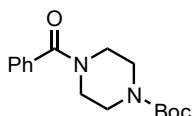
1-(4-phenylpiperazin-1-yl)butan-1-one (265)
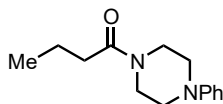
The title compound was prepared according to General Procedure 3, as a colourless oil (62 mg, 43%). **¹H NMR** (500 MHz, CDCl₃) δ 7.28 (dd, *J* = 8.4, 7.4 Hz, 2H), 6.92 (dd, *J* = 16.7, 7.8 Hz, 3H), 3.84 – 3.57 (m, 4H), 3.23 – 3.11 (m, 4H), 2.41 – 2.30 (m, 2H), 1.74 – 1.65 (m, 2H), 0.99 (t, *J* = 7.4 Hz, 3H). **¹³C NMR** (126 MHz, CDCl₃) δ 171.6, 151.0, 129.3, 120.5, 116.7, 49.8, 49.5, 45.6, 41.4, 35.3, 18.8, 14.0. **IR**: ν_{max}: 1638, 1597, 1495, 1431, 1207, 1024, 756, 692 cm⁻¹ **HRMS** (EI+) [C₁₄H₂₀N₂O]: calc. 232.1576, found 232.1572
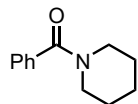
tert-butyl 2-(morpholine-4-carbonyl)pyrrolidine-1-carboxylate (266)
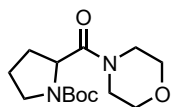
The title compound was prepared according to General Procedure 3, as a white solid (74 mg, 26%). **MP** 67 – 71 ˚C (EtOAc) **¹H NMR** (500 MHz, CDCl₃) δ 4.55 (ddd, *J* = 12.0, 8.3, 3.0 Hz, 1H), 3.82 – 3.28 (m, 10H), 2.23 – 1.76 (m, 4H), 1.40 (d, *J* = 22.3 Hz, 9H). **¹³C NMR** (126 MHz, CDCl₃) δ 171.2, 171.0, 154.5, 153.9, 79.6, 67.0, 66.6, 56.7, 56.2, 46.8, 46.6, 46.0, 45.7, 42.4, 30.6, 29.8, 28.5, 24.3, 23.6. **IR**: ν_{max}: 1683, 1652, 1398, 1364, 1231, 1154, 1112 cm⁻¹ **HRMS** (ES+) [C₁₄H₂₄N₂O₄ + Na]: calc. 307.1634, found 307.1636. $[\alpha]_D^{25}$ = -0.01 (*c* =1.1 CH₂Cl₂). Characterization data is in accordance with prior reports.[30]

2-(diethylamino)-1-morpholinoethan-1-one (267)
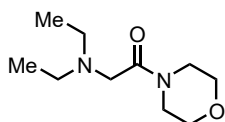
The title compound was prepared according to General Procedure 3, as a pale-yellow oil (164 mg, 82%). **¹H NMR** (500 MHz, CDCl₃) δ 3.66 (dd, *J* = 8.9, 5.1 Hz, 3H), 3.63 – 3.52 (m, 1H), 3.24 (s, 1H), 2.56 (q, *J* = 7.1 Hz, 2H), 1.02 (t, *J* = 7.1 Hz, 3H). **¹³C NMR** (126 MHz, CDCl₃) δ 169.8, 67.1, 57.4, 47.4, 46.2, 42.3, 11.8. **IR**: ν_{max}: 1641, 1436, 1272,

1233, 1113, 1068, 964, 583 cm^{-1} **HRMS** (EI+) [C$_{10}$H$_{18}$N$_2$O$_2$ + H]: calc. 199.14410, found 199.1436.

cyclohexyl(morpholino)methanone (263)
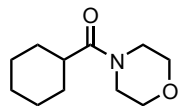
The title compound was prepared according to General Procedure 3, as a white solid (99 mg, 50%). **MP** 46 – 48 ˚C (EtOAc) **¹H NMR** (500 MHz, CDCl$_3$) δ 3.87 – 3.26 (m, 8H), 2.40 (tt, J = 11.6, 3.3 Hz, 1H), 1.77 (dd, J = 5.7, 3.8 Hz, 2H), 1.68 (d, J = 13.2 Hz, 3H), 1.58 – 1.42 (m, 2H), 1.22 (dd, J = 12.2, 5.5 Hz, 3H).**¹³C NMR** (126 MHz, CDCl$_3$) δ 174.8, 67.0, 46.0, 42.0, 40.3, 29.4, 25.9, 25.9. **IR**: ν$_{max}$: 1629, 1424, 1213, 1116, 1014, 865 cm^{-1} **HRMS** (ES+) [C$_{11}$H$_{19}$NO$_2$]: calc. 197.14103, found 197.1409. Characterization data is in accordance with prior reports.[31]

1-morpholino-2-(2-hydroxyphenyl)ethan-1-one (271)
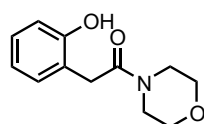
The title compound was prepared according to General Procedure 3, as a white solid (162 mg, 73%). **MP** 100 – 103 ˚C (EtOAc) **¹H NMR** (500 MHz, CDCl$_3$) δ 9.51 (s, 1H), 7.19 (td, J = 8.0, 1.6 Hz, 1H), 7.03 – 6.94 (m, 2H), 6.83 (td, J = 7.4, 1.1 Hz, 1H), 3.74 (s, 2H), 3.72 – 3.62 (m, 8H). **¹³C NMR** (126 MHz, CDCl$_3$) δ 171.8, 157.0, 130.2, 129.3, 120.7, 120.4, 118.4, 66.7, 66.6, 47.3, 42.6, 36.4. **IR**: ν$_{max}$: 2980, 1483, 1387, 1250, 1109, 968, 847, 756, 692, 592 cm^{-1} **HRMS** (EI+) [C$_{12}$H$_{15}$NO$_3$]: calc. 221.1052, found 221.1056. Characterization data is in accordance with prior reports.[32]

(E)-1-morpholino-3-phenylprop-2-en-1-one (268)
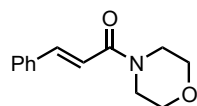
The title compound was prepared according to General Procedure 3, as a white solid (206 mg, 95%). **mp** 74 – 76 ˚C (EtOAc). **¹H NMR** (500 MHz, CDCl$_3$) δ 7.70 (d, J = 15.4 Hz, 1H), 7.56 – 7.48 (m, 2H), 7.41 – 7.32 (m, 3H), 6.84 (d, J = 15.4 Hz, 1H), 3.71 (dd, J = 16.9, 14.8 Hz, 8H). **¹³C NMR** (126 MHz, CDCl$_3$) δ 165.7, 143.3, 135.3, 129.9, 129.0, 127.9, 116.7, 67.0, 46.4, 42.6. **IR**: ν$_{max}$: 1653, 1596, 1456, 1227, 1116, 1044, 972, 763,

703 cm^{-1} **HRMS** (ES+) [$C_{13}H_{15}N_2$ + H]: calc. 218.1181, found 218.1181. Characterization data is in accordance with prior reports.[28]

cyclohex-1-en-1-yl(morpholino)methanone (269)
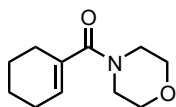
The title compound was prepared according to General Procedure 3, as a colourless oil (68 mg, 35%). **¹H NMR** (500 MHz, CDCl₃) δ 5.81 (tt, J = 3.7, 1.8 Hz, 1H), 3.75 – 3.46 (m, 8H), 2.22 – 2.15 (m, 2H), 2.13 – 2.06 (m, 2H), 1.73 – 1.66 (m, 2H), 1.66 – 1.59 (m, 2H). **¹³C NMR** (126 MHz, CDCl₃) δ 172.1, 134.0, 128.4, 67.2, 26.1, 24.8, 22.2, 21.7. **IR**: ν$_{max}$: 1616, 1424, 1276, 1244, 1112, 1008 cm^{-1} **HRMS** (ES+) [$C_{11}H_{17}NO_2$]: calc. 196.1338, found 196.1339. Characterization data is in accordance with prior reports.[25]

phenyl(4-phenylpiperazin-1-yl)methanone (220)
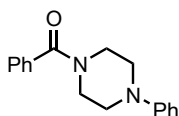
The title compound was prepared according to General Procedure 3, as a white solid (261 mg, 98%). **MP** 75 – 78 ˚C (EtOAc) **¹H NMR** (500 MHz, CDCl₃) δ 7.36 (s, 5H), 7.21 (dd, J = 14.6, 6.8 Hz, 2H), 6.85 (dd, J = 15.0, 7.6 Hz, 3H), 3.70 (d, J = 171.2 Hz, 4H), 3.12 (d, J = 60.5 Hz, 4H). **¹³C NMR** (126 MHz, CDCl₃) δ 170.6, 151.1, 135.8, 130.0, 129.4, 128.7, 127.3, 120.8, 116.9. **IR**: ν$_{max}$: 1599, 1495, 1431, 1231, 1153, 1013, 694 cm^{-1} **HRMS** (EI+) [$C_{17}H_{18}N_2O$]: calc. 266.1419, found 266.1425. Characterization data is in accordance with prior reports.[2]

***tert*-butyl 4-benzoylpiperazine-1-carboxylate (221)**

The title compound was prepared according to General Procedure 3, as a white solid (284 mg, 98%). **MP** 91 – 94 ˚C (EtOAc) **¹H NMR** (500 MHz, CDCl₃) δ 7.38 – 7.30 (m, 1H), 3.51 (d, J = 165.0 Hz, 2H), 1.41 (s, 2H). **¹³C NMR** (126 MHz, CDCl₃) δ 170.6, 154.6, 135.5, 129.9, 128.6, 127.1, 80.4, 47.5, 43.8, 42.1, 28.4. **IR**: ν$_{max}$: 1690, 1620, 1427, 1287,

1242, 1119, 710, 540 cm^{-1} **HRMS** (ES+) [C$_{16}$H$_{22}$N$_2$O$_3$ + H]: calc. 291.1709, found 291.1702. Characterization data is in accordance with prior reports.[28]

phenyl(piperidin-1-yl)methanone (222)

The title compound was prepared according to General Procedure 3, as a white solid (159 mg, 79%). **MP** 29 – 32 ˚C (EtOAc) **^{1}H NMR** (500 MHz, CDCl$_3$) δ 7.38 (s, 5H), 3.70 (s, 2H), 3.33 (s, 2H), 1.82 – 1.43 (m, 6H). **^{13}C NMR** (126 MHz, CDCl$_3$) δ 170.3, 136.6, 129.3, 128.4, 126.8, 48.8, 43.1, 26.6, 25.7, 24.6. **IR**: ν_{max}: 2933, 1614, 1429, 1275, 1256, 1111, 1001, 793, 708 cm^{-1} **HRMS** (pNSI+) [C$_{12}$H$_{15}$NO + H]: calc. 190.1226, found 190.1225. Characterization data is in accordance with prior reports.[33]

phenyl(pyrrolidin-1-yl)methanone (223)
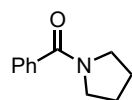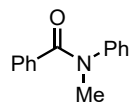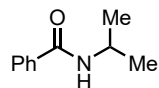

The title compound was prepared according to General Procedure 3, as a colourless oil (122 mg, 69%). **^{1}H NMR** (500 MHz, CDCl$_3$) δ 7.54 – 7.47 (m, 2H), 7.43 – 7.34 (m, 3H), 3.65 (t, J = 7.0 Hz, 2H), 3.42 (t, J = 6.6 Hz, 2H), 1.99 – 1.92 (m, 2H), 1.86 (p, J = 6.6 Hz, 2H). **^{13}C NMR** (126 MHz, CDCl$_3$) δ 169.9, 137.4, 129.9, 128.4, 127.2, 49.7, 46.3, 26.5, 24.6. **IR**: ν_{max}: 2874, 1614, 1574, 1447, 1339, 793, 719, 660 cm^{-1} **HRMS** (EI+) [C$_{11}$H$_{13}$NO]: calc. 175.0997, found 175.0996. Characterization data is in accordance with prior reports.[26]

azepan-1-yl(phenyl)methanone (224)
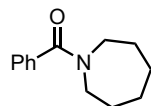
The title compound was prepared according to General Procedure 3, as a colourless oil (106 mg, 52%). **^{1}H NMR** (500 MHz, CDCl$_3$) δ 7.37 (q, J = 2.8 Hz, 5H), 3.78 – 3.60 (m, 2H), 3.36 (t, J = 5.7 Hz, 2H), 1.84 (dt, J = 11.9, 5.9 Hz, 2H), 1.61 (ddd, J = 13.9, 10.3, 5.6 Hz, 6H). **^{13}C NMR** (126 MHz, CDCl$_3$) δ 171.7, 137.5, 129.1, 128.5, 126.6, 49.9, 46.4, 29.7, 28.0, 27.4, 26.6. **IR**: ν_{max}: 1622, 1420, 1304, 1281, 702, 631 cm^{-1} **HRMS** (ES+)

$[C_{13}H_{17}NO + H]$: calc. 204.1388, found 204.1382. Characterization data is in accordance with prior reports.[28]

(3,4-dihydroquinolin-1(2*H*)-yl)(phenyl)methanone (225)
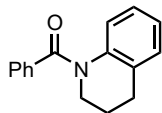
The title compound was prepared according to General Procedure 3, as a white solid (144 mg, 61%). **MP** 116 – 119 ˚C (EtOAc) **¹H NMR** (500 MHz, CDCl₃) δ 7.39 – 7.31 (m, 3H), 7.27 (t, J = 7.4 Hz, 2H), 7.15 (dd, J = 7.5, 0.7 Hz, 1H), 6.99 (td, J = 7.5, 1.1 Hz, 1H), 6.90 – 6.82 (m, 1H), 3.91 (t, J = 6.5 Hz, 2H), 2.85 (t, J = 6.6 Hz, 2H), 2.05 (p, J = 6.6 Hz, 2H). **¹³C NMR** (126 MHz, CDCl₃) δ 170.3, 139.4, 136.3, 131.6, 130.1, 128.6, 128.4, 128.1, 125.7, 125.5, 124.6, 44.5, 27.0, 24.2. **IR**: v_{max}: 2361, 1636, 1489, 1375, 1146, 1067, 758, 702 cm⁻¹ **HRMS** (EI+) $[C_{16}H_{15}NO]$: calc. 237.1154, found 237.1158. Characterization data is in accordance with prior reports.[28]

N-benzyl-*N*-methylbenzamide (226)
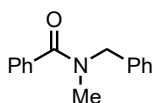
The title compound was prepared according to General Procedure 3, as a yellow oil (110 mg, 49%). **¹H NMR** (500 MHz, CDCl₃) δ 7.55 – 7.27 (m, 9H), 7.17 (d, J = 6.0 Hz, 1H), 4.64 (d, J = 125.3 Hz, 2H), 2.95 (d, J = 84.6 Hz, 3H). **¹³C NMR** (126 MHz, CDCl₃) δ 172.5, 171.7, 137.2, 136.7, 136.4, 136.3, 129.8, 129.0, 128.9, 128.6, 128.5, 128.3, 127.7, 127.7, 127.1, 126.9, 55.3, 50.9, 37.2, 33.3. **IR**: v_{max}: 1626, 1445, 1396, 1261, 1067, 1026, 716, 694 cm⁻¹ **HRMS** (ES+) $[C_{15}H_{15}NO + H]$: calc. 226.1232, found 226.1223. Characterization data is in accordance with prior reports.[28]

N,N-diethylbenzamide (227)
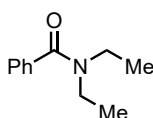
The title compound was prepared according to General Procedure 3, as a colourless oil (144 mg, 81%). **¹H NMR** (500 MHz, CDCl₃) δ 7.45 – 7.30 (m, 5H), 3.40 (d, J = 148.1 Hz, 4H), 1.17 (d, J = 73.1 Hz, 6H). **¹³C NMR** (126 MHz, CDCl₃) δ 171.4, 137.5, 129.2, 128.5, 126.4, 43.4, 39.3, 14.3, 13.1. **IR**: v_{max}: 1624, 1425, 1286, 1096, 785, 703 cm⁻¹ **HRMS** (Es+)

[$C_{10}H_{13}NO$ + H]: calc. 164.1075, found 164.1075. Characterization data is in accordance with prior reports.[28]

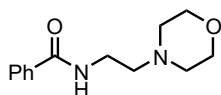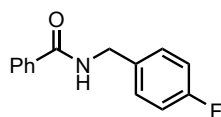### *N*-methyl-*N*-phenylbenzamide (228)

The title compound was prepared according to General Procedure 3, as a white solid (135 mg, 64%). **MP** 56 – 58 ˚C (EtOAc) **¹H NMR** (500 MHz, CDCl₃) δ 7.29 (d, *J* = 7.6 Hz, 2H), 7.25 – 7.18 (m, 3H), 7.18 – 7.08 (m, 3H), 7.03 (d, *J* = 7.8 Hz, 2H), 3.50 (s, 3H). **¹³C NMR** (126 MHz, CDCl₃) δ 170.8, 145.0, 136.0, 129.7, 129.3, 128.8, 127.8, 127.0, 126.6, 38.5. **IR**: ν_max: 1639, 1593, 1493, 1360, 1302, 1281, 1103, 768, 725, 694, 654, 577 cm⁻¹ **HRMS** (ES+) [$C_{14}H_{13}NO$ + H]: calc. 212.1075, found 212.1075. Characterization data is in accordance with prior reports.[28]
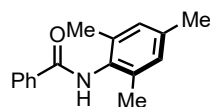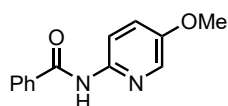
N-(1-phenylethyl)benzamide (229)
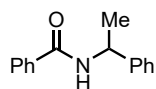
The title compound was prepared according to General Procedure 3, as a white solid (50 mg, 22%). **MP** 104 – 106 ˚C (EtOAc) **¹H NMR** (500 MHz, CDCl₃) δ 7.69 (d, *J* = 7.1 Hz, 2H), 7.43 – 7.37 (m, 1H), 7.35 – 7.24 (m, 6H), 7.22 – 7.17 (m, 1H), 6.45 – 6.25 (m, 1H), 5.26 (p, *J* = 7.0 Hz, 1H), 1.52 (d, *J* = 6.9 Hz, 3H). **¹³C NMR** (126 MHz, CDCl₃) δ 166.7, 143.3, 134.7, 131.6, 128.9, 128.7, 127.6, 127.1, 126.4, 49.3, 21.8. **IR**: ν_max: 3287, 1632, 1516, 1489, 1321, 1211, 1147, 1092, 758, 698, 631, 552 cm⁻¹ **HRMS** (EI+) [$C_{15}H_{15}NO$]: calc. 225.1154, found 225.1146. Characterization data is in accordance with prior reports.[26]

N-*iso*propylbenzamide (230)

The title compound was prepared according to General Procedure 3, as a white solid (66 mg, 41%). **MP** 84 – 87 ˚C (EtOAc) **¹H NMR** (500 MHz, CDCl₃) δ 7.74 (d, *J* = 7.0 Hz, 2H), 7.47 – 7.41 (m, 1H), 7.37 (t, *J* = 7.5 Hz, 2H), 6.18 (s, 1H), 4.30 – 4.21 (m, 1H), 1.23 (d, *J* = 6.6 Hz, 6H). **¹³C NMR** (126 MHz, CDCl₃) δ 166.7, 135.0, 131.3, 128.5, 126.8, 41.9, 22.9. **IR**: ν_max: 3294, 1628, 1531, 1346, 1288, 1169, 692 cm⁻¹ **HRMS** (EI+) [$C_{10}H_{13}NO$]:

calc. 163.0997, found 163.0998. Characterization data is in accordance with prior reports.[25]

N-hexylbenzamide (231)
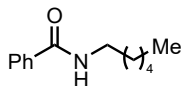
The title compound was prepared according to General Procedure 3, as a colourless oil (122 mg, 59%). **^{1}H NMR** (500 MHz, CDCl$_3$) δ 7.78 – 7.74 (m, 2H), 7.51 – 7.46 (m, 1H), 7.44 – 7.40 (m, 2H), 6.27 – 6.03 (bs, 1H), 3.45 (td, *J* = 7.2, 5.8 Hz, 2H), 1.68 – 1.55 (m, 2H), 1.44 – 1.27 (m, 6H), 0.97 – 0.84 (m, 3H). **^{13}C NMR** (126 MHz, CDCl3) δ 167.64, 135.04, 131.44, 128.7, 127.0, 40.3, 31.7, 29.8, 26.8, 22.7, 14.2. **IR**: v_{max}: 3312, 2926, 1634, 1539, 1489, 694 cm^{-1} **HRMS** (EI+) [C$_{13}$H$_{19}$NO]: calc. 205.1467, found 205.1471. Characterization data is in accordance with prior reports.[26]

N-(4,4-diethoxybutyl)benzamide (232)
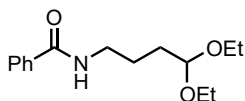
The title compound was prepared according to General Procedure 3, as a colourless oil (127 mg, 48%,). **^{1}H NMR** (500 MHz, CDCl$_3$) δ 7.78 – 7.74 (m, 2H), 7.51 – 7.46 (m, 1H), 7.44 – 7.39 (m, 2H), 6.42 (bs, 1H), 4.59 – 4.47 (m, 1H), 3.72 – 3.60 (m, 2H), 3.56 – 3.43 (m, 4H), 1.79 – 1.67 (m, 4H), 1.20 (dd, *J* = 8.8, 5.4 Hz, 6H). **^{13}C NMR** (126 MHz, CDCl$_3$) δ 167.6, 135.0, 131.4, 128.7, 127, 102.9, 61.7, 39.9, 31.2, 24.7, 15.5. **IR**: v_{max}: 2972, 1636, 1541, 1125, 1057, 694, 403 cm^{-1} **HRMS** (EI+) [C$_{15}$H$_{23}$NO$_3$ + Na]: calc. 288.1576, found 288.1585. Characterization data is in accordance with prior reports.[34]

N-(2-morpholinoethyl)benzamide (233)

The title compound was prepared according to General Procedure 3, as a white solid (201 mg, 85%). **MP** 116 – 119 ˚C (CH$_2$Cl$_2$) **^{1}H NMR** (500 MHz, CDCl$_3$) δ 7.82 – 7.72 (m, 2H), 7.54 – 7.39 (m, 3H), 6.77 (s, 1H), 3.76 – 3.68 (m, 4H), 3.56 (dd, J = 11.2, 5.7 Hz, 2H), 2.60 (t, J = 6.0 Hz, 2H), 2.51 (s, 4H). **^{13}C NMR** (126 MHz, CDCl$_3$) δ 167.5, 134.8, 131.5, 128.7, 127.0, 67.2, 57.0, 53.5, 36.2. **IR**: v_{max}: 3296, 2361, 1638, 1458, 1115, 1009, 862, 694 cm^{-1} **HRMS** (EI+) [C$_{13}$H$_{18}$N$_2$O$_2$ + H]: calc. 235.1477, found 235.1451. Characterization data is in accordance with prior reports.[35]
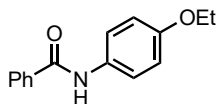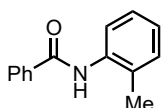
N-(4-fluorobenzyl)benzamide (234)

The title compound was prepared according to General Procedure 3, as a white solid (130 mg, 57%). **MP** 102 – 104 ˚C (EtOAc) **^{1}H NMR** (500 MHz, CDCl$_3$) δ 7.81 – 7.77 (m, 2H), 7.54 – 7.49 (m, 1H), 7.46 – 7.41 (m, 2H), 7.36 – 7.31 (m, 2H), 7.07 – 7.01 (m, 2H), 6.39 (bs, 1H), 4.62 (d, J = 5.7 Hz, 2H). **^{13}C NMR** (126 MHz, CDCl$_3$) δ 167.5, 162.4 (d, J = 246.0 Hz), 134.4, 134.2 (d, J = 3.3 Hz), 131.8, 129.8 (d, J = 8.1 Hz), 128.8, 127.1, 115.8 (d, J = 21.5 Hz), 43.6. **^{19}F NMR** (471 MHz, CDCl$_3$) δ -114.76 – -114.85 (m). **IR**: ν$_{max}$: 3291, 3069, 2930, 1636, 1545, 1508, 1219, 843, 802, 691, 492 cm^{-1} **HRMS** (EI+) [C$_{14}$H$_{12}$NOF]: calc 229.0903, found 229.0903. Characterization data is in accordance with prior reports.[36]

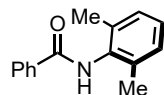### *N*-mesitylbenzamide (236)

The title compound was prepared according to General Procedure 3, as a white solid (65 mg, 27%). **MP** 187 – 189 ˚C (EtOAc) **^{1}H NMR** (500 MHz, CDCl$_3$) δ 7.94 – 7.90 (m, 2H), 7.59 – 7.54 (m, 1H), 7.53 – 7.48 (m, 2H), 6.95 (s, 2H), 2.30 (s, 3H), 2.25 (s, 6H). **^{13}C NMR** (126 MHz, CDCl$_3$) δ 166.2, 137.3, 135.4, 134.8, 131.9, 131.3, 129.2, 128.9, 127.3, 21.1, 18.6. **IR**: ν$_{max}$: 3267, 2916, 1638, 1514, 1487, 1294, 851, 710, 667 cm^{-1} **HRMS** (EI+) [C$_{16}$H$_{17}$NO]: calc. 239.1310, found 239.1313. Characterization data is in accordance with prior reports.[37]

N-(5-methoxypyridin-2-yl)benzamide (237)

The title compound was prepared according to General Procedure 3, as a white solid (82 mg, 36%). **MP** 86 – 88 ˚C (EtOAc) **^{1}H NMR** (500 MHz, CDCl$_3$) δ 8.68 (s, 1H), 8.35 – 8.24 (m, 1H), 7.93 – 7.78 (m, 3H), 7.54 – 7.37 (m, 3H), 7.26 (dd, J = 5.7, 3.1 Hz, 1H), 3.79 (d, J = 5.0 Hz, 3H). **^{13}C NMR** (126 MHz, CDCl$_3$) δ 165.4, 153.1, 145.3, 134.4, 134.0, 132.3, 129.0, 127.3, 124.1, 114.9, 56.1. **IR**: ν$_{max}$: 3318, 1669, 1533, 1401, 1255, 1035, 834, 711,

693 cm^{-1} **HRMS** (ES+) [$C_{13}H_{12}N_2O_2$ + H]: calc. 229.0977, found 229.0976. Characterization data is in accordance with prior reports.[38]
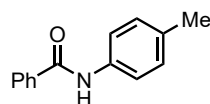
N-(4-ethoxyphenyl)benzamide (238)

The title compound was prepared according to General Procedure 3, as a brown solid (189 mg, 79%). **MP** 155 – 157 ˚C (EtOAc) **1H NMR** (500 MHz, CDCl$_3$) δ 7.86 (d, *J* = 7.4 Hz, 2H), 7.78 (s, 1H), 7.50 (dq, *J* = 15.0, 7.4 Hz, 5H), 6.89 (d, *J* = 8.9 Hz, 2H), 4.03 (q, *J* = 7.0 Hz, 2H), 1.41 (t, *J* = 7.0 Hz, 3H). **13C NMR** (126 MHz, CDCl$_3$) δ 165.7, 156.2, 135.2, 131.8, 131.0, 128.9, 127.1, 122.2, 115.0, 63.9, 15.0. **IR**: ν$_{max}$: 3269, 2361, 1639, 1508, 1298, 1233, 1115, 692 cm^{-1} **HRMS** (EI+) [$C_{15}H_{15}NO_2$]: calc. 241.1103, found 241.1103. Characterization data is in accordance with prior reports.[39]

N-(4-methoxyphenyl)benzamide (239)
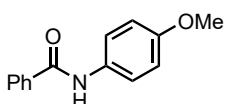
The title compound was prepared according to General Procedure 3, as a tan solid (102 mg, 45%). **MP** 144 – 146 ˚C (EtOAc) **1H NMR** (500 MHz, CDCl$_3$) δ 7.86 (d, *J* = 7.5 Hz, 2H), 7.72 (s, 1H), 7.59 – 7.51 (m, 3H), 7.49 (t, *J* = 7.4 Hz, 2H), 6.92 (d, *J* = 8.9 Hz, 2H), 3.82 (s, 3H). **13C NMR** (126 MHz, CDCl$_3$) δ 165.7, 156.8, 135.2, 131.9, 131.1, 128.9, 127.1, 122.2, 114.4, 55.7. **IR**: ν$_{max}$: 3329, 1645, 1507, 1458, 1186, 1031, 822, 692 cm^{-1} **HRMS**(ES+) [$C_{14}H_{13}NO_2$ + H]: calc. 228.1025, found 228.1024. Characterization data is in accordance with prior reports.[26]
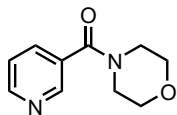
N-(*o*-tolyl)benzamide (240)

The title compound was prepared according to General Procedure 3, as a white solid (116 mg, 55%). **MP** 132 – 134 ˚C (EtOAc) **1H NMR** (500 MHz, CDCl$_3$) δ 7.97 (d, *J* = 8.0 Hz, 1H), 7.90 (d, *J* = 7.6 Hz, 2H), 7.66 (s, 1H), 7.57 (t, *J* = 7.3 Hz, 1H), 7.51 (t, *J* = 7.5 Hz, 2H), 7.32 – 7.19 (m, 3H), 7.13 (t, *J* = 7.5 Hz, 1H), 2.35 (s, 3H). **13C NMR** (126 MHz, CDCl$_3$) δ 165.6, 135.8, 135.1, 131.9, 130.6, 129.1, 128.9, 127.1, 127.0, 125.4, 123.0, 17.8. **IR**: ν$_{max}$: 3232, 1647, 1521, 1486, 1309, 909, 746, 715, 691 cm^{-1} **HRMS** (ES+)

$[C_{14}H_{13}NO + H]$: calc. 212.1075, found 212.1072. Characterization data is in accordance with prior reports.[26]

N-(2,6-dimethylphenyl)benzamide (241)

The title compound was prepared according to General Procedure 3, as white solid (63 mg, 28%). **MP** 144 – 146 ˚C (EtOAc) **^{1}H NMR** (500 MHz, CDCl$_3$) δ 7.99 – 7.87 (m, 2H), 7.58 (dd, *J* = 8.4, 6.4 Hz, 1H), 7.51 (t, *J* = 7.5 Hz, 2H), 7.38 (s, 1H), 7.18 – 7.09 (m, 3H), 2.29 (s, 6H). **^{13}C NMR** (126 MHz, CDCl$_3$) δ 166.0, 135.7, 134.7, 134.0, 132.0, 128.9, 128.5, 127.6, 127.4, 18.7. **IR**: ν$_{max}$: 3281, 1643, 1517, 1472, 1296, 1281, 1211, 764, 687, 651 cm^{-1} **HRMS** (ES+) $[C_{15}H_{15}NO + H]$: calc. 226.1232, found 226.1239. Characterization data is in accordance with prior reports.[28]

N-(6-methoxypyridin-3-yl)benzamide (242)
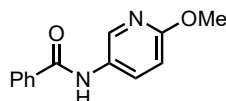
The title compound was prepared according to General Procedure 3, as a colourless crystals (25 mg, 11%). **MP** 129 – 131 ˚C (EtOAc) **^{1}H NMR** (500 MHz, CDCl$_3$) δ 8.28 (d, *J* = 2.6 Hz, 1H), 8.05 (dd, *J* = 8.9, 2.6 Hz, 1H), 7.93 (s, 1H), 7.90 – 7.80 (m, 2H), 7.59 – 7.51 (m, 1H), 7.48 (tt, *J* = 6.7, 1.4 Hz, 2H), 6.77 (d, *J* = 8.9 Hz, 1H), 3.94 (s, 3H). **^{13}C NMR** (126 MHz, CDCl$_3$) δ 166.2, 161.3, 139.0, 134.5, 133.1, 132.2, 129.0, 128.8, 127.3, 110.9, 53.9. **IR**: ν$_{max}$: 3313, 1645, 1520, 1516, 1275, 1028, 825, 718, 691, 664 cm^{-1} **HRMS** (ES+) $[C_{13}H_{12}N_2O_2 + H]$: calc. 229.0977, found 229.0977. Characterization data is in accordance with prior reports.[40]

N-(*p*-tolyl)benzamide (243)

The title compound was prepared according to General Procedure 3, as a white solid (104 mg, 49%). **MP** 141 – 143 ˚C (EtOAc) **^{1}H NMR** (500 MHz, CDCl$_3$) δ 7.86 (dd, *J* = 5.2, 3.3 Hz, 2H), 7.77 (s, 1H), 7.58 – 7.50 (m, 3H), 7.50 – 7.46 (m, 2H), 7.18 (d, *J* = 8.1 Hz, 2H), 2.34 (s, 3H). **^{13}C NMR** (126 MHz, CDCl$_3$) δ 165.8, 135.5, 135.3, 134.4, 131.9, 129.7, 128.9, 127.1, 120.4, 21.1. **IR**: ν$_{max}$: 3309, 1645, 1511, 1404, 1317, 1266, 812, 692 cm^{-1}

HRMS (ES+) [$C_{14}H_{13}NO$ + H]: calc. 212.1075, found 212.1076. Characterization data is in accordance with prior reports.[28]
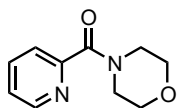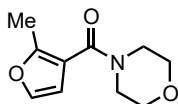
morpholino(pyridin-3-yl)methanone (256)

The title compound was prepared according to General Procedure 3, as a pale-yellow oil (88 mg, 35%). **¹H NMR** (500 MHz, CDCl₃) δ 8.78 – 8.61 (m, 2H), 7.79 (ddd, *J* = 7.8, 2.2, 1.7 Hz, 1H), 7.40 (ddd, *J* = 7.8, 4.9, 0.9 Hz, 1H), 4.05 – 3.19 (m, 7H). **¹³C NMR** (126 MHz, CDCl₃) δ 167.8, 151.0, 148.0, 135.2, 131.2, 123.6, 66.8, 48.3, 42.7. **IR**: ν_{max}: 1624, 1588, 1431, 1411, 1278, 1261, 1110, 1010, 821, 709 cm⁻¹ **HRMS** (ES+) [$C_{10}H_{12}N_2O_2$ + H]: calc. 193.0977, found 193.0972. Characterization data is in accordance with prior reports.[26]

morpholino(pyrazin-2-yl)methanone (257)
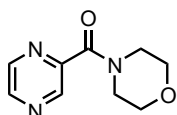
The title compound was prepared according to General Procedure 3, as a pale-yellow oil (85 mg, 44%). **¹H NMR** (500 MHz, CDCl₃) δ 8.97 (d, *J* = 1.4 Hz, 1H), 8.64 (d, *J* = 2.5 Hz, 1H), 8.53 (dd, *J* = 2.5, 1.5 Hz, 1H), 3.82 (d, *J* = 1.9 Hz, 4H), 3.69 (td, *J* = 4.2, 1.3 Hz, 4H). **¹³C NMR** (126 MHz, CDCl₃) δ 165.2, 149.0, 146.1, 145.6, 142.6, 67.1, 66.9, 47.8, 43.0. **IR**: ν_{max}: 1627, 1438, 1393, 1283, 1178, 1111, 1017, 841 cm⁻¹ **HRMS** (ES+) [$C_9H_{11}N_3O_2$ + H]: calc. 194.0930, found 194.0935. Characterization data is in accordance with prior reports.[41]

morpholino(pyridin-2-yl)methanone (258)

The title compound was prepared according to General Procedure 3, as a pale yellow crystals (67 mg, 35%). **MP** 55 – 57 ˚C (EtOAc) **¹H NMR** (500 MHz, CDCl₃) δ 8.52 (ddd, *J* = 4.8, 1.7, 0.9 Hz, 1H), 7.75 (td, *J* = 7.7, 1.7 Hz, 1H), 7.62 (dt, *J* = 7.8, 1.1 Hz, 1H), 7.30 (ddd, *J* = 7.6, 4.9, 1.2 Hz, 1H), 3.84 – 3.70 (m, 4H), 3.61 (td, *J* = 8.6, 3.8 Hz, 4H). **¹³C NMR** (126 MHz, CDCl₃) δ 167.5, 153.6, 148.3, 137.2, 124.7, 124.1, 67.0, 66.8, 47.7,

42.8. **IR**: ν_{max}: 1623, 1565, 1457, 1424, 1281, 1267, 1110, 1022, 809, 754, 730, 700, 619 cm^{-1} **HRMS** (ES+) [$C_{10}H_{12}N_2O_2$ + H]: calc. 193.0977, found 193.0975. Characterization data is in accordance with prior reports.[31]

(2-methylfuran-3-yl)(morpholino)methanone (252)

The title compound was prepared according to General Procedure 3, as a pale yellow solid (164 mg, 84%). **MP** 81 – 83 ˚C (EtOAc) **¹H NMR** (500 MHz, CDCl$_3$) δ 7.26 (d, J = 1.7 Hz, 1H), 6.33 (d, J = 2.0 Hz, 1H), 3.68 (d, J = 19.3 Hz, 8H), 2.39 (s, 3H). **¹³C NMR** (126 MHz, CDCl$_3$) δ 165.0, 153.5, 140.2, 115.0, 109.9, 66.7, 47.4, 42.3, 12.7. **IR**: ν_{max}: 1621, 1517, 1432, 1267, 1106, 1006, 835, 757, 583 cm^{-1} **HRMS** (ES+) [$C_{10}H_{13}NO_3$ + H]: calc. 196.0974, found 194.0975. Characterization data is in accordance with prior reports.[26]

morpholino(thiophen-2-yl)methanone (253)
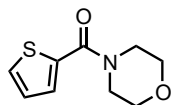
The title compound was prepared according to General Procedure 3, as a pale yellow oil (158 mg, 80%). **¹H NMR** (500 MHz, CDCl$_3$) δ 7.46 (dd, J = 5.0, 1.1 Hz, 1H), 7.29 (dd, J = 3.6, 1.1 Hz, 1H), 7.05 (dd, J = 5.0, 3.6 Hz, 1H), 3.83 – 3.65 (m, 8H). **¹³C NMR** (126 MHz, CDCl$_3$) δ 163.8, 136.7, 129.1, 129.0, 126.9, 67.0, 46.0. **IR**: ν_{max}: 1607, 1522, 1429, 1270, 1251, 1111, 999, 823, 734, 714 cm^{-1} **HRMS** (ES+) [$C_9H_{11}NO_2S$ + H]: calc. 198.0589, found 194.0590. Characterization data is in accordance with prior reports.[26]

morpholino(thiophen-3-yl)methanone (254)
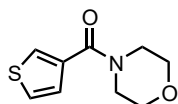
The title compound was prepared according to General Procedure 3, as a pale yellow oil (150 mg, 76%). **¹H NMR** (500 MHz, CDCl$_3$) δ 7.52 (dd, J = 3.0, 1.3 Hz, 1H), 7.35 (dd, J = 5.0, 3.0 Hz, 1H), 7.18 (dd, J = 5.0, 1.3 Hz, 1H), 3.70 (s, 8H). **¹³C NMR** (126 MHz, CDCl$_3$) δ 165.8, 135.9, 127.0, 126.7, 126.2, 66.9, 48.1, 42.9. **IR**: ν_{max}: 1616, 1522, 1428, 1273, 1250, 1110, 1024, 950, 838, 737, 582 cm^{-1} **HRMS** (ES+) [$C_9H_{11}NO_2S$ + H]: calc. 198.0589, found 194.0589. Characterization data is in accordance with prior reports.[26]
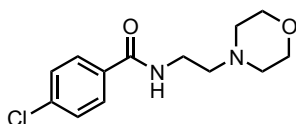
benzofuran-2-yl(morpholino)methanone (255)
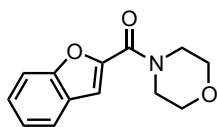
The title compound was prepared according to General Procedure 3, as a white solid (111 mg, 48%). **MP** 84 – 86 ˚C (EtOAc) **¹H NMR** (500 MHz, CDCl$_3$) δ 7.66 (ddd, J = 7.8, 1.3, 0.7 Hz, 1H), 7.52 (ddd, J = 8.4, 1.7, 0.9 Hz, 1H), 7.41 (ddd, J = 8.4, 7.2, 1.3 Hz, 1H), 7.35 (d, J = 1.0 Hz, 1H), 7.33 – 7.27 (m, 1H), 4.20 – 3.57 (m, 8H). **¹³C NMR** (126 MHz, CDCl$_3$) δ 159.8, 154.6, 148.8, 126.9, 126.7, 123.7, 122.3, 112.5, 111.9, 67.0, 47.3, 43.4. **IR**: v_{max}: 1610, 1565, 1425, 1287, 1179, 1107, 1020, 949, 837, 745 cm^{-1} **HRMS** (ES+) [C$_{13}$H$_{13}$NO$_3$ + H]: calc. 232.0974, found 232.0973. Characterization data is in accordance with prior reports.[26]

N-propylbenzamide (235)
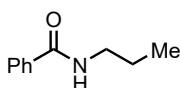
The title compound was prepared according to General Procedure 3, as colourless crystals (118 mg, 72%). **MP** 132 – 134 ˚C (EtOAc) **¹H NMR** (500 MHz, CDCl$_3$) δ 7.80 – 7.71 (m, 2H), 7.52 – 7.45 (m, 1H), 7.45 – 7.39 (m, 2H), 6.18 (s, 1H), 3.48 – 3.38 (m, 2H), 1.70 – 1.58 (m, 2H), 0.99 (t, J = 7.4 Hz, 3H). **¹³C NMR** (126 MHz, CDCl$_3$) δ 167.7, 135.0, 131.4, 128.7, 127.0, 41.9, 23.1, 11.6. **IR**: v_{max}: 3300, 2982, 1635, 1545, 1315, 1150, 694 cm^{-1} **HRMS** (Es+) [C$_{10}$H$_{13}$NO + H]: calc. 164.1075, found 164.1075. Characterization data is in accordance with prior reports.[42]

## 4-chloro-*N*-(2-morpholinoethyl)benzamide/Moclobemide (213)

The title compound was prepared according to General Procedure 3, as a white solid (246 mg, 92%). **MP** 125 – 128 ˚C (Et$_2$O) **¹H NMR** (500 MHz, CDCl$_3$) δ 7.71 (d, J = 8.5 Hz, 2H), 7.42 (d, J = 8.5 Hz, 2H), 6.73 (s, 1H), 3.79 – 3.66 (m, 4H), 3.54 (dd, J = 11.2, 5.6 Hz, 2H), 2.60 (t, J = 6.0 Hz, 2H), 2.56 – 2.43 (m, 4H). **¹³C NMR** (126 MHz, CDCl$_3$) δ 166.3, 137.7, 133.0, 128.9, 128.4, 67.0, 56.8, 53.3, 36.1. **IR**: v_{max}: 3275, 1634, 1541, 1310, 1117, 1009, 864, 727, 687, 525 cm^{-1} **HRMS** (EI+) [C$_{13}$H$_{17}$N$_2$O$_2$Cl + H]: calc. 269.1057, found 269.1062. Characterization data is in accordance with prior reports.[43]

212

N,N-diethylnicotinamide/Coramine (272)
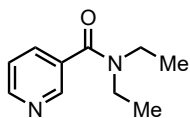
The title compound was prepared according to General Procedure 3, as a colourless oil (111 mg, 62%). **¹H NMR** (500 MHz, CDCl₃) δ 8.64 (d, *J* = 2.8 Hz, 2H), 7.73 (ddd, *J* = 7.8, 2.2, 1.7 Hz, 1H), 7.35 (ddd, *J* = 7.8, 4.9, 0.9 Hz, 1H), 3.41 (d, *J* = 144.1 Hz, 4H), 1.19 (d, *J* = 58.7 Hz, 6H). **¹³C NMR** (126 MHz, CDCl₃) δ 168.6, 150.3, 147.2, 134.6, 133.2, 123.6, 43.6, 39.7, 14.4, 13.0. **IR**: ν$_{max}$: 1622, 1588, 1431, 1411, 1289, 1100, 1026, 725, 709 cm⁻¹. **HRMS** (ES+) [C₁₀H₁₄N₂O + H] calc. 179.1184 found 179.1193. Characterization data is in accordance with prior reports.[44]

2-methyl-*N*-phenylfuran-3-carboxamide/Fenfuram (274)
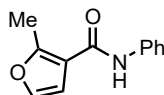
The title compound was prepared according to General Procedure 3, as white solid (139 mg, 69%). **MP** 97 – 99 ˚C (EtOAc) **¹H NMR** (500 MHz, CDCl₃) δ 7.57 (dd, *J* = 8.6, 1.0 Hz, 2H), 7.40 – 7.32 (m, 3H), 7.31 (d, *J* = 2.1 Hz, 1H), 7.13 (tt, *J* = 7.7, 1.1 Hz, 1H), 6.53 (d, *J* = 2.0 Hz, 1H), 2.64 (s, 3H). **¹³C NMR** (126 MHz, CDCl₃) δ 162.0, 158.0, 140.6, 137.8, 129.1, 124.4, 120.2, 115.8, 108.1, 13.6. **IR**: ν$_{max}$: 3316, 1640, 1597, 1517, 1442, 1327, 1226, 1098, 898, 741, 686, 667, 600, 583 cm⁻¹. **HRMS** (ES+) [C₁₂H₁₁NO₂ + H] calc. 202.0868 found 202.0875. Characterization data is in accordance with prior reports.[26]

2-(diethylamino)-*N*-(2,6-dimethylphenyl)acetamide/Lidocaine (273)
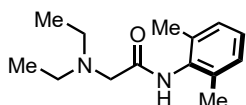
The title compound was prepared according to General Procedure 3, as a white solid (136 mg, 58%). **MP** 62 – 64 ˚C (EtOAc) **¹H NMR** (500 MHz, CDCl₃) δ 8.91 (s, 1H), 7.13 – 7.05 (m, 1H), 3.22 (s, 2H), 2.69 (q, J = 7.1 Hz, 4H), 2.23 (s, 6H), 1.14 (t, J = 7.1 Hz, 6H). **¹³C NMR** (126 MHz, CDCl₃) δ 170.4, 135.2, 134.1, 128.4, 127.2, 57.7, 49.1, 18.7, 12.8. **IR**: ν$_{max}$: 684, 704, 764, 962, 1024, 1069, 1096, 1113, 1267, 1286, 1312, 1371, 1422, 1449, 1464, 1489, 1663, 1707, 2924, 2939, 2953 cm⁻¹. **HRMS** (ES+) [C₁₄H₂₃N₂O] calc. 235.1810 found 235.1808. Characterization data is in accordance with prior reports.[45]

N-(2-morpholinoethyl)benzofuran-2-carboxamide (275)
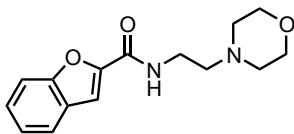
The title compound was prepared according to General Procedure 3, as a white solid (129 mg, 47%). **MP** 70 – 72 °C (EtOAc) **^{1}H NMR** (500 MHz, CDCl$_3$) δ 7.67 (ddd, *J* = 7.8, 1.3, 0.7 Hz, 1H), 7.56 – 7.50 (m, 1H), 7.47 (d, *J* = 0.9 Hz, 1H), 7.42 (ddd, *J* = 8.4, 7.2, 1.3 Hz, 1H), 7.30 (ddd, *J* = 8.1, 7.3, 1.0 Hz, 1H), 7.16 (s, 1H), 3.84 – 3.69 (m, 4H), 3.60 (dd, *J* = 11.6, 5.8 Hz, 2H), 2.64 (t, *J* = 6.0 Hz, 2H), 2.55 (s, 4H). **^{13}C NMR** (126 MHz, CDCl$_3$) δ 159.1, 154.9, 149.0, 127.8, 126.9, 123.8, 122.9, 111.9, 110.4, 67.1, 57.1, 53.5, 35.7. **IR**: v_{max}: 3312, 1647, 1516, 1446, 1294, 1119, 1010, 838, 742, 668, 632 cm^{-1}. **HRMS** (ES+) [C$_{15}$H$_{17}$N$_2$O$_3$] calc. 275.1396 found 275.1399.

Large Scale preparation of Moclobemide (213)

To two 25 mL Stainless steel milling jars (Retsch), methyl 4-chlorobenzoate (6 mmol, 1.023g), 4-(2-aminoethyl)-morpholine (5 mmol, 0.651 g), potassium *tert*-butoxide (4.25 mmol, 0.477 g) and a 12 g stainless steel ball to each jar. The jars were then placed on a Retch MM 400 mixer mill and milled at 30 Hz for 1 hour. Once the reaction was complete the reaction mixture washed from each jar with EtOAc (~5 mL) and water (~5 mL) into a separating funnel. The washings from each jar was combined in the same separating funnel. Additional EtOAc (100 mL) and water (100 mL) was then added and the aqueous extracted. The layers were separated and the aqueous phase was re-extracted with EtOAc (2 x 50 mL). The organic phases were combined and dried over magnesium sulphate and solvent removed *in vacuo*. The crude solid product was purified by flash column chromatography producing the desired product as a white solid (2.42 g, 90%).

6.4.4 General Procedure 6: The Preparation of Esters
The corresponding alcohol, triethylamine (1 equiv.), and DMAP (0.1 equiv.) were dissolved in dichloromethane (1 M) and cooled to 0 °C. Benzoyl chloride (1 equiv.) was then added slowly to this solution and the reaction was allowed to warm to room temperature and left to stir until complete by TLC (1-4 h). The reaction mixture was then transferred to a separating funnel and was partitioned with water. The organic phase was separated and then sequentially washed with water and brine. The organic phase was

then dried over magnesium sulphate and the solvent removed. The product was then purified using flash column chromatography if required.
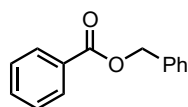
iso-propyl benzoate
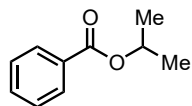
The title compound was prepared according to General Procedure 6, as a colourless oil (1.62 g, >95%). **^{1}H NMR** (500 MHz, CDCl$_3$) δ 8.04 (d, J = 7.9 Hz, 2H), 7.54 (t, J = 7.4 Hz, 1H), 7.43 (t, J = 7.6 Hz, 2H), 5.26 (hept, J = 6.2 Hz, 1H), 1.37 (d, J = 6.3 Hz, 6H). **^{13}C NMR** (126 MHz, CDCl$_3$) δ 166.2, 132.8, 131.1, 129.6, 128.4, 68.5, 22.1. **IR**: ν_{max}: 2978, 1713, 1491, 1468, 1450, 1373, 1314, 1271, 1175, 1144, 1096 cm^{-1} **HRMS** (EI+) [C$_{10}$H$_{12}$O$_2$]: calc. 164.0837, found 164.0839. Characterization data is in accordance with prior reports.[46]

phenyl benzoate
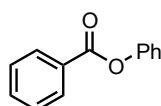
The title compound was prepared according to General Procedure 6, as a white solid (1.80 g, 91%). **MP** 56-60 ˚C (CH$_2$Cl$_2$) **^{1}H NMR** (500 MHz, CDCl$_3$) δ 8.22 (d, J = 7.8 Hz, 4H), 7.64 (t, J = 7.4 Hz, 2H), 7.52 (t, J = 7.6 Hz, 4H), 7.44 (t, J = 7.7 Hz, 4H), 7.32 – 7.25 (m, 3H), 7.24 – 7.17 (m, 4H). **^{13}C NMR** (126 MHz, CDCl$_3$) δ 165.3, 151.1, 133.7, 130.3, 129.8, 129.7, 128.7, 126.0, 121.9. **IR**: ν_{max}: 2953, 2924, 1707, 1449, 1312, 1287, 1267, 1196, 1177 cm^{-1}. **HRMS** (EI+) [C$_{13}$H$_{10}$O$_2$] calc. 198.0681, found 198.0684. Characterization data is in accordance with prior reports.[46]

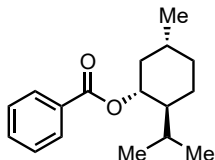### benzyl benzoate

The title compound was prepared according to General Procedure 6, as a white solid (2.02 g, 95%). **MP** 29-32 ˚C (CH$_2$Cl$_2$) **^{1}H NMR** (500 MHz, CDCl$_3$) δ 8.09 (d, J = 8.2 Hz, 2H), 7.57 (t, J = 7.4 Hz, 1H), 7.45 (dd, J = 12.4, 7.5 Hz, 4H), 7.40 (t, J = 7.4 Hz, 2H), 7.35 (t, J = 7.2 Hz, 1H), 5.38 (s, 2H). **^{13}C NMR** (126 MHz, CDCl$_3$) δ 166.6, 136.2, 133.2, 130.3, 129.8, 128.7, 128.5, 128.4, 128.3, 66.8. **IR**: ν_{max}: 3063, 3032, 2887, 1715, 1601, 1584,

1375, 1267, 1107, 1026 cm^{-1}. **HRMS** (EI+) [C$_{14}$H$_{12}$O$_2$] calc. 212.0837, found 212.0836. Characterization data is in accordance with prior reports.[47]

L-menthyl benzoate

The title compound was prepared according to General Procedure 6, as a white solid (2.15 g, 83%). **MP** 40-42 ˚C (CH$_2$Cl$_2$) **^{1}H NMR** (500 MHz, CDCl$_3$) δ 8.05 (d, J = 7.9 Hz, 2H), 7.55 (t, J = 7.4 Hz, 1H), 7.44 (t, J = 7.6 Hz, 2H), 4.94 (td, J = 10.9, 4.4 Hz, 1H), 2.13 (d, J = 12.0 Hz, 1H), 1.97 (tt, J = 9.0, 3.5 Hz, 1H), 1.73 (d, J = 11.5 Hz, 2H), 1.56 (dd, J = 16.2, 7.0 Hz, 2H), 1.20 – 1.05 (m, 2H), 0.93 (t, J = 6.0 Hz, 7H), 0.80 (d, J = 6.9 Hz, 3H). **^{13}C NMR** (126 MHz, CDCl$_3$) δ 166.3, 132.8, 131.0, 129.7, 128.4, 75.0, 47.4, 41.1, 34.5, 31.6, 26.6, 23.8, 22.2, 20.9, 16.7. **IR**: ν$_{max}$: 2953, 2940, 2924, 1707, 1449, 1312, 1287, 1267, 1177 cm^{-1}. **HRMS** (EI+) [C$_{17}$H$_{24}$O$_2$] + Na calc. 283.1674, found 283.1685. Characterization data is in accordance with prior reports.[47]

tert-butyl benzoate
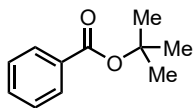
The title compound was prepared according to General Procedure 6 but substituting the alcohol with KO*t*Bu and without the presence of DMAP, as a colourless oil (1.35 g, 75%). **^{1}H NMR** (500 MHz, CDCl$_3$) δ 7.99 (d, J = 7.8 Hz, 2H), 7.52 (t, J = 7.3 Hz, 1H), 7.41 (t, J = 7.6 Hz, 2H), 1.60 (s, 9H). **^{13}C NMR** (126 MHz, CDCl$_3$) δ 165.9, 132.5, 132.2, 129.5, 128.3, 81.1, 28.3. **IR**: ν$_{max}$: 1708, 1603, 1584, 1477, 1450, 1368, 1314, 1288, 1254, 1165, 1113, 1069 cm^{-1}. **HRMS** (EI+) [C$_{11}$H$_{14}$O$_2$] calc. 178.0994, found 178.0994. Characterization data is in accordance with prior reports.[46]

methyl 3,7-dimethyloct-6-enoate
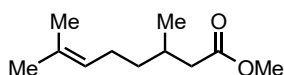
The title compounds were prepared using a method modified from the literature.[48] To a dried 100 mL round bottom flask was added CH$_2$Cl$_2$ (25 mL), citronellic acid (10 mmol), and methanol (30 mmol). This mixture was cooled to 0 ˚C and a solution of DCC in

CH$_2$Cl$_2$ (1 M, 30 mL) was added slowly. Once addition was complete the reaction mixture was allowed to rise to room temperature and stirred for a further 1 hour. Once the reaction was complete the mixture was filtered, and the filtrate collected. The filtrate was then washed with saturated sodium bicarbonate followed by brine and dried using magnesium sulfate. The solvent was removed *in vacuo* and the title compound was isolated as a colourless oil (1.25 g, 68%). **¹H NMR** (500 MHz, CDCl3) δ 5.15 – 5.03 (m, 1H), 3.66 (s, 3H), 2.32 (dd, *J* = 14.7, 5.9 Hz, 1H), 2.12 (dd, *J* = 14.7, 8.3 Hz, 1H), 2.05 – 1.88 (m, 3H), 1.68 (d, *J* = 1.1 Hz, 3H), 1.59 (t, *J* = 2.1 Hz, 3H), 1.39 – 1.16 (m, 3H), 0.94 (d, *J* = 6.7 Hz, 3H). **¹³C NMR** (126 MHz, CDCl3) δ 173.7, 131.6, 124.3, 51.4, 41.6, 36.8, 30.0, 25.7, 25.4, 19.6, 17.6. **IR**: ν$_{max}$: 1739, 1436, 1195, 1153, 1012 cm^{-1} **HRMS** (EI+) [C$_{11}$H$_{21}$O$_2$] calc. 185.1542, found 185.1536. Characterization data is in accordance with prior reports.[17]

**1-(*tert*-butyl) 2-methyl (*S*)-pyrrolidine-1,2-dicarboxylate**
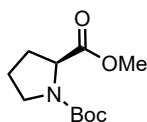
The title compound was prepared using the following procedure. L-Proline methyl ester hydrochloride (1.65 g, 10 mmol) was added to a 100 mL round bottom flask and was dissolved in CH$_2$Cl$_2$ (25 mL, 0.4 M). This solution was cooled to 0 ˚C in an ice bath and triethylamine (2.8 mL, 20 mmol) was added dropwise and the reaction was stirred for 15 minutes. Di-*tert*-butyl dicarbonate (2.4 mL, 10.5 mmol) was then added dropwise at 0 ˚C, the reaction mixture was allowed to warm to room temperature and was stirred overnight. A solution of saturated Na$_2$CO$_3$ (25 mL) was then added to the reaction mixture and stirred for 1 hour. The organic layer was then separated, and the aqueous phase was extracted with CH$_2$Cl$_2$ (20 mL), the combined organic layers were then washed with brine and dried over magnesium sulfate and the solvent removed *in vacuo* and the product was isolated as a colourless oil and used without purification. **¹H NMR** (500 MHz, CDCl3) δ 4.32 (dd, *J* = 8.6, 3.3 Hz, 0.4H), 4.21 (dd, *J* = 8.5, 4.2 Hz, 0.6H), 3.72 (s, 1H), 3.71 (s, 2H), 3.60 – 3.33 (m, 2H), 2.28 – 2.11 (m, 1H), 2.01 – 1.89 (m, 2H), 1.89 – 1.78 (m, 1H), 1.46 (s, 3.5H), 1.40 (s, 5.5H). **¹³C NMR** (126 MHz, CDCl3) δ 173.9, 173.7, 154.6, 153.9, 80.0, 79.9, 59.3, 58.9, 52.2, 52.1, 46.7, 46.5, 31.0, 30.1, 28.6, 28.4, 24.5, 23.8. **HRMS** (EI+) [C$_{11}$H$_{19}$O$_2$] calc. 197.14103, found 197.1409. [α]$_D^{25}$ = -54.1 (*c* =1.1 CH$_2$Cl$_2$) Characterization data is in accordance with prior reports.[49]

ethyl diethylglycinate
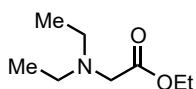
The title compound was prepared using the following procedure. Ethyl bromoacetate (1.67 g, 10 mmol), was added to dichloromethane (10 mL, 1 M) and cooled to 0 ˚C. Diethyl amine (2 mL, 20 mmol) was added dropwise, and the reaction was left to warm to room temperature. The reaction was left until complete by TLC (2 h). The reaction mixture was then diluted with dichloromethane (10 mL) and transferred to a separating funnel and partitioned with saturated NaHCO$_3$. The aqueous phase was then extracted with dichloromethane (2 x 20 mL). The combined organic phase was then extracted with brine (50 mL). The organic phase was then dried over magnesium sulphate and passed through a silica plug. The solvent was removed, and the product was isolated as a colourless oil (1.27 g, 80%). **¹H NMR** (500 MHz, CDCl$_3$) δ 4.16 (q, J = 7.1 Hz, 2H), 3.29 (s, 2H), 2.64 (q, J = 7.1 Hz, 4H), 1.26 (t, J = 7.2 Hz, 3H), 1.05 (t, J = 7.1 Hz, 6H). **¹³C NMR** (126 MHz, CDCl$_3$) δ 171.6, 60.4, 54.3, 47.8, 14.3, 12.2. **IR**: ν_{max}: 2970, 1732, 1456, 1296, 1271, 1180, 1159, 10934, 1074, 1030 cm^{-1}. **HRMS** (ES+) [C$_8$H$_{17}$NO$_2$ + H] calc. 160.1338, found 160.1331. Characterization data is in accordance with prior reports.[50]

ethyl cyclohexanecarboxylate
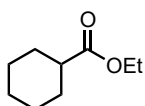
The title compound was prepared using the following procedure. Cyclohexanecarboxylic acid (1.28 g, 10 mmol) was added to a 50 mL round bottom flask and dissolved in ethanol (20 mL, 0.5 M) to this solution was added concentrated sulfuric acid (0.1 equiv, 1 mmol). This solution was the heated to reflux until the reaction was complete by TLC. The excess ethanol was then removed *in vacuo* and the residual oil dissolved in ethyl acetate. The remaining acid was quenched by the slow addition of saturated sodium bicarbonate solution. The phases were then separated, and the organic phase washed with saturated sodium bicarbonate solution and then brine. The organic phase was then dried over magnesium sulphate and solvent removed *in vacuo* to yield a colourless oil. This product was used without further purification. **¹H NMR** (500 MHz, CDCl3) δ 4.11 (q, J = 7.1 Hz, 2H), 2.27 (tt, J = 11.3, 3.6 Hz, 1H), 1.94 – 1.83 (m, 2H), 1.80 – 1.68 (m, 2H), 1.68 – 1.58 (m, 1H), 1.50 – 1.37 (m, 2H), 1.24 (t, J = 7.1 Hz, 4H). **¹³C NMR** (126 MHz, CDCl3) δ 176.3, 60.2, 43.4, 29.2, 25.9, 25.6, 14.4. Characterization data is in accordance with prior reports.[51]

6.4.5 General Procedure 7: The preparation of Ammonium Salts

The morpholine (1 equiv.) was added to a 100 mL round bottom flask and dissolved in dry Et_2O (1 M) this solution was cooled to 0 ˚C. Once cooled HCl in dioxane (4 M, 3.0 equiv.) or triflic acid (2.0 equiv.) was added slowly and after addition was complete the reaction mixture was raised to room temperature and allowed to stir for 1 hour. The mixture was then filtered, and the precipitate washed with Et_2O (5 x 20 mL). The isolated precipitate was then dried and used without further purification.

6.5   Reductive Coupling of Electron Poor Alkenes

6.5.1 Cyclic Voltammetry Study
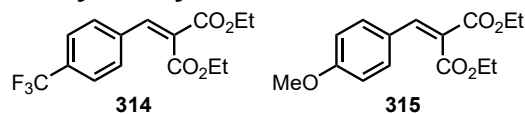
Scheme X. Substrate selection for CV analysis.
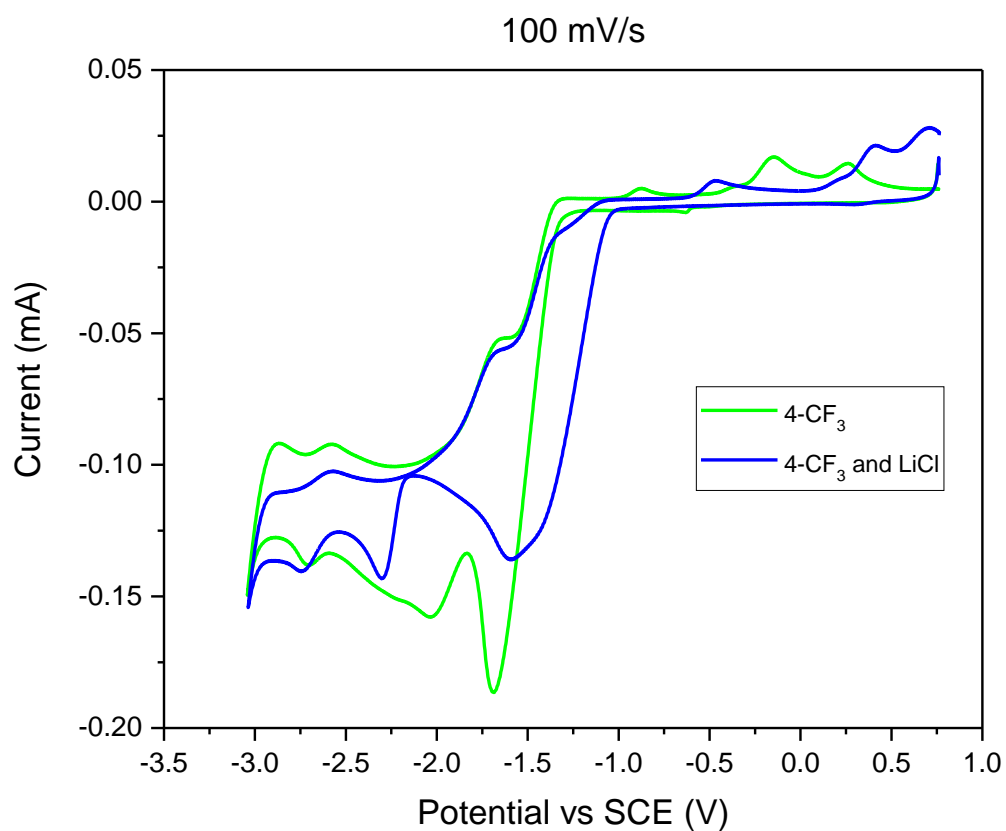
Figure X. Cyclic voltammogram of compound **314** (5 mM) in MeCN as solvent and Tetra *n*-butyl ammonium hexafluorophosphate (0.1 M) as electrolyte without LiCl (1 mM) (light green line) and with LiCl (1 mM) (dark blue line).
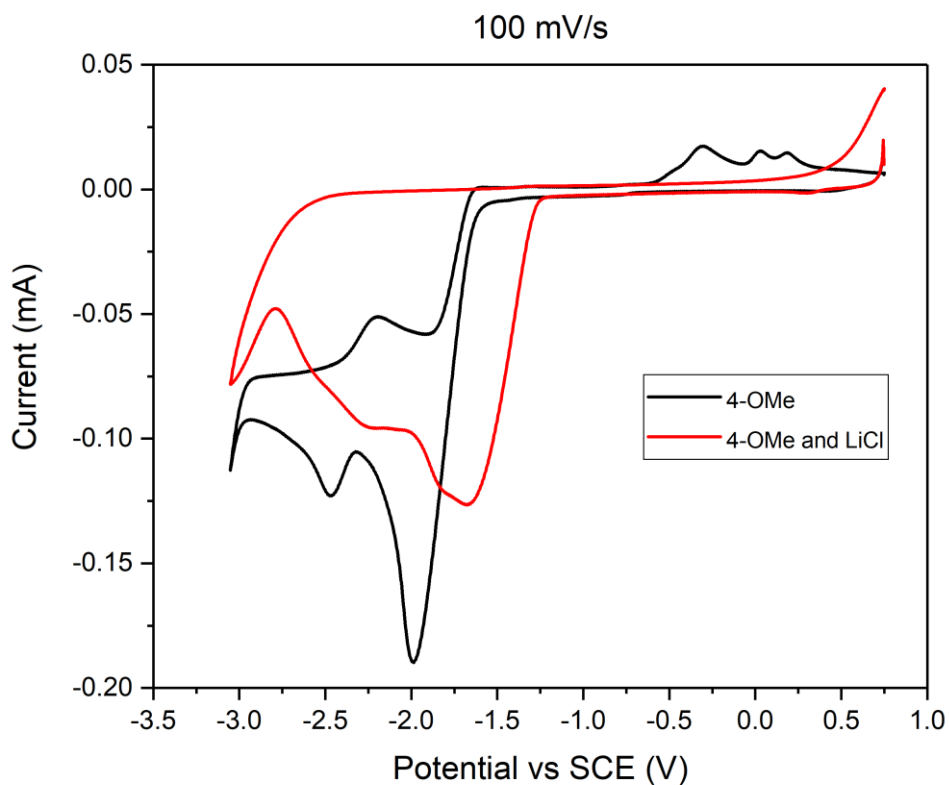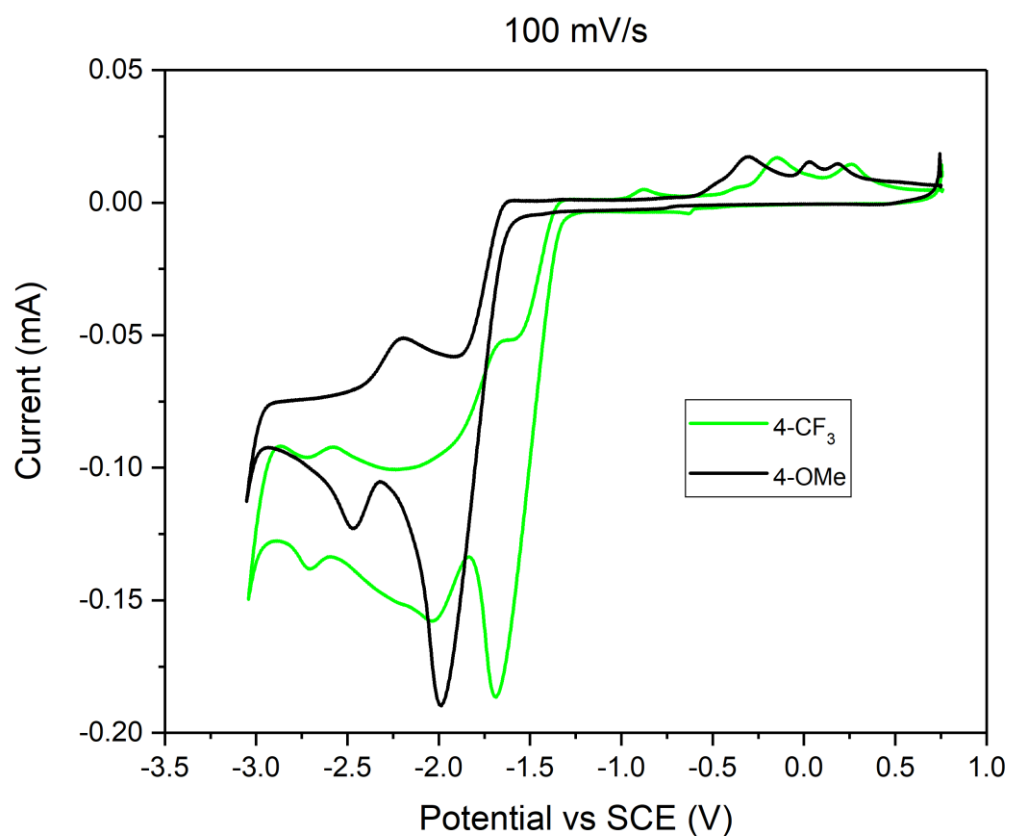
Figure X. Cyclic voltammogram of compound **315** (5 mM) in MeCN as solvent and Tetra *n*-butyl ammonium hexafluorophosphate (0.1 M) as electrolyte without LiCl (1 mM) (light black line) and with LiCl (1 mM) (red line).

Figure X. Cyclic voltammogram of compounds **314** (light green line) and **315** (black line), (5 mM) in MeCN as solvent and Tetra *n*-butyl ammonium hexafluorophosphate (0.1 M) as electrolyte.
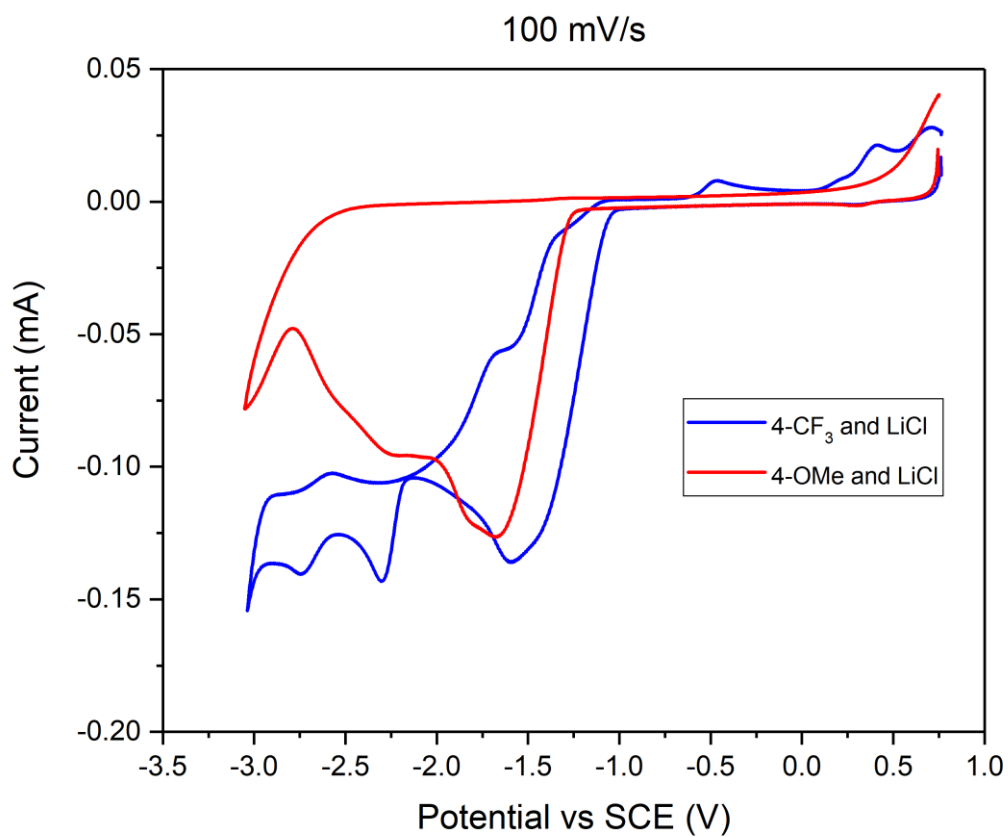
Figure X. Cyclic voltammogram of compounds**314** (dark blue line) and **315** (red line), (5 mM) in MeCN as solvent and Tetra *n*-butyl ammonium hexafluorophosphate (0.1 M) as electrolyte with LiCl (1 mM).
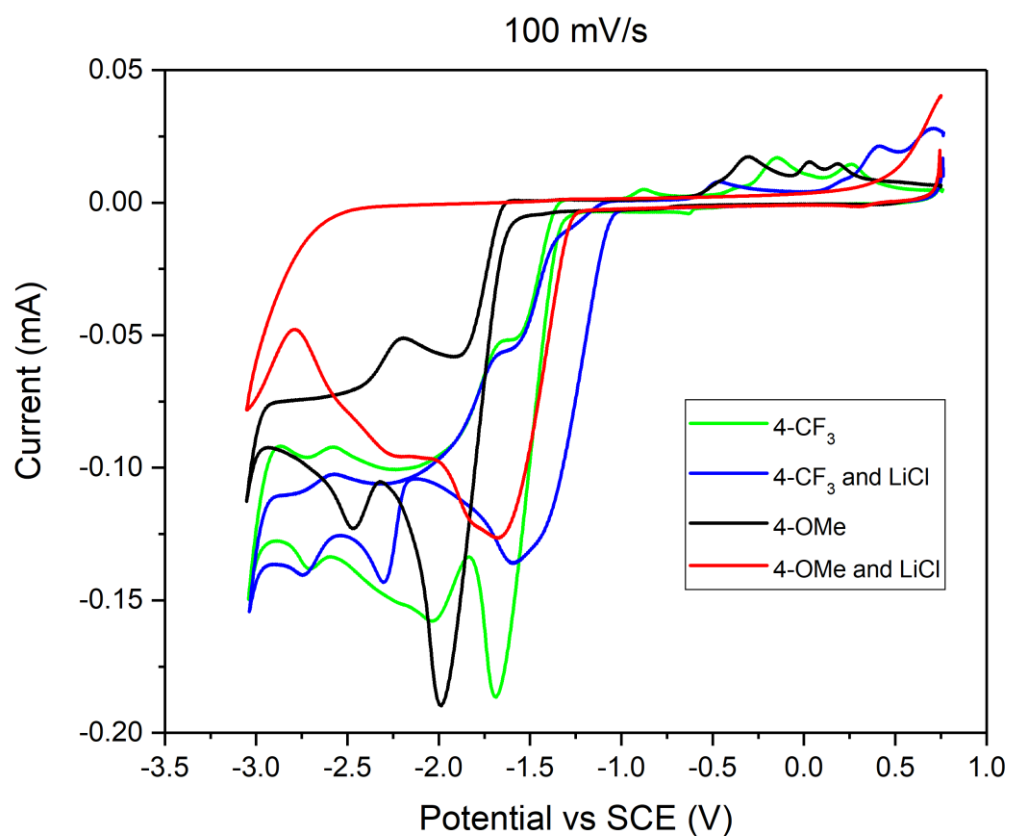
Figure X. Cyclic voltammogram of compounds with and without LiCl, **314** (light green line), **314** (dark blue line), **315** (black line), and **315** (red line), (5 mM) in MeCN as solvent and Tetra *n*-butyl ammonium hexafluorophosphate (0.1 M) as electrolyte with and without LiCl (1 mM).

Variation of conditions	Reduction potential of **314**[a]	Reduction potential of **315**[a]
With LiCl	-1.27	-1.62
Without LiCl	-1.21	-1.25
Difference	0.06	0.37

Table X. Reduction potential of a range of benzylidene malonates Vs. Fc/Fc+

$$Mn^{2+} + 2e^- \longrightarrow Mn(s) \qquad E_{1/2} = -1.185 \text{ vs SCE}$$

$$Zn^{2+} + 2e^- \longrightarrow Zn(s) \qquad E_{1/2} = -0.76 \text{ vs SCE}$$

$$Fc^+ + e^- \longrightarrow Fc(s) \qquad E_{1/2} = 0.380 \text{ vs SCE}^{[52]}$$

As the reduction potentials of the substrates were measured against Fc/Fc+ they were converted to against SCE with the following equation. This was to make them more easily comparable to that of the known value for manganese metal.

$$E_{1/2}(Substrate\ vs.SCE) = E_{1/2}(Substrate\ vs.Fc/Fc^+) - E_{1/2}(Fc/Fc^+\ vs.\ SCE)$$

Variation of conditions	Reduction potential of **314**[a]	Reduction potential of **315**[a]
With LiCl	-1.65	-2.00
Without LiCl	-1.59	-1.63
Difference	0.06 (CF3)	0.37 (OMe)

Table X. Reduction potential of a range of benzylidene malonates Vs. SCE

6.5.2 EPR Experiments

To a 14 mL stainless steel milling jar containing the milling ball (10 mm, 4.1 g) was added manganese, irregular pieces, (1.1 mmol, 60 mg), diethyl 2-(4-fluorobenzylidene)malonate (1 mmol, 266 mg), THF (2 mmol, 160 µL), and lithium chloride (1 mmol, 42 mg). The reaction mixture was milled at 30 Hz for 3 h. The resulting crude product mixture was washed with EtOAc, prior to full work-up using aqueous HCl (1 M, 25 mL) to induce separation of the product into organic and aqueous phases. The reaction mixture prior to milling resulted in the absence of an EPR spectrum, due to line broadening effects arising from the conduction properties of the Mn(0) pieces. Further confirmation of this was provided by a similar lack of observable EPR signal recorded on a solid manganese strip.
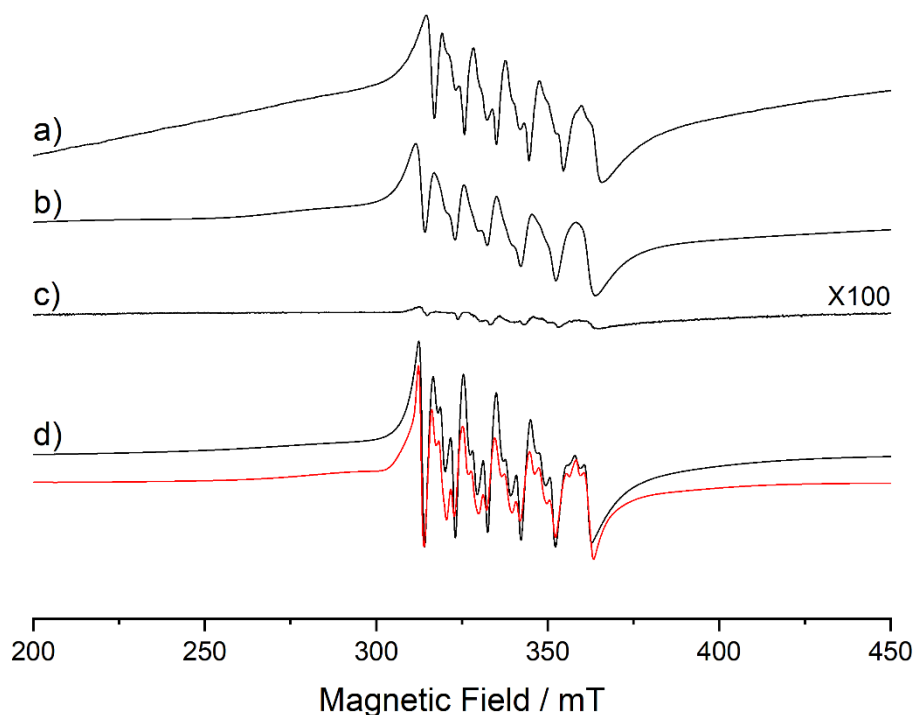
Figure X. CW X-band EPR spectra (T = 120 K) of **a)** Crude reaction mixture dissolved in ethyl acetate, **b)** aqueous layer after work-up with HCl, **c)** organic layer after work-up; **d)** Mn(OAc)$_2$ (10 mM) in a water:glycerol (50:50) solvent, and red trace showing a simulation of Mn(OAc)$_2$. A simulation of Mn(OAc)$_2$ has been included above for comparative purposes, showing the extremely similarities in spectral appearance between the crude product and its Mn(OAc)2 counterpart.

The EPR spectra of the reaction products after various treatments are presented in Figure S7. As can be seen, there is evidence of a strong EPR signal of an ethyl acetate solution of the crude reaction product (Fig S7a). The well-resolved six hyperfine lines originate from a high spin d^5 Mn(II) centre with nuclear spin value $I(^{55}Mn) = {}^5/_2$ (100 % abundance). The broad baseline effects visible on either side of the main signal originate from zero-field splitting effects, and the additional splitting superimposed on each of the six main lines arises from fine structure, both of which are typical for high-spin systems (e.g. high-spin d^5).

It is anticipated that any source of oxidised Mn generated during the course of the reaction would remain in the aqueous layer. Hence, the crude reaction product underwent a full work-up with HCl to afford separation of the organic and aqueous layers. The EPR spectrum of the aqueous layer does indeed show a strong Mn(II) signal (Fig S7b), whereas a much weaker signal is observed in the EPR spectrum of the organic layer (Fig S7c), which most likely originates from incomplete separation of the phases during work-up. Given the potential reaction pathways (involving either double electron transfer, or sequential SET processes), the most plausible identity of the oxidised manganese species involves coordination of the malonate. Hence, the spectrum of a pure sample of Mn(OAc)$_2$ is presented in Fig S7d for comparison, which closely resembles that of the crude reaction product (Fig S7a).

The dominant factor in the spin Hamiltonian parameters of high-spin systems is the zero-field interaction, arising from interaction between the multiple unpaired electrons. Spin-orbit coupling is spin-forbidden in d^5 systems (in which all 3d-orbitals are singly occupied and therefore half-filled), therefore the g-tensor is typically predominantly isotropic and close to the free-electron g-value ($g_{iso} \sim 2.0023$). Unfortunately, in the case of Mn(II) systems, electron spin delocalisation onto surrounding ligand nuclei is typically small and therefore the resulting superhyperfine coupling is typically unresolved within the linewidth of the main hyperfine features. A simulation of the Mn(OAc)$_2$ experimental spectrum is presented in Fig S7e, performed using the Easyspin toolbox within Matlab, with the following spin Hamiltonian parameters:

g_{iso} = 2.008, A = [-283.74, -265.4 -268.2] MHz, D = [-603.8, -139.4] MHz. Values are consistent with highly isotropic Mn(II) systems.[53]

In addition to following the redox process taking place at the metal centre, we performed spin trap experiments with the aim of identifying any C-based radical intermediates that could prove the multiple sequential SET pathway. EPR spectra were recorded on the

crude reaction performed in the presence of PBN spin trap, however unfortunately the data were inconclusive and are not reported here for brevity.

Diethyl 2-(4-fluorobenzylidene)malonate (308)
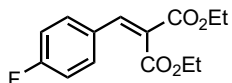
The title compound was prepared using a method modified from the literature.[54] To a 250 mL round bottom flask was added toluene (100mL, 0.5 M), diethyl malonate (50 mmol), 4-fluorobenzaldehyde (60 mmol), acetic acid (5 mmol), and pyrrolidine (5 mmol). The flask was then equipped with a Dean-Stark apparatus and vigorously refluxed for 16 h. The solvent was then removed *en vacuo* and the residual oil was dissolved in diethyl ether (100 mL) and washed with sat. bicarbonate (100 mL), water (100 mL), and brine (100 mL). The organic phase was then dried using magnesium sulphate and solvent removed *en vacuo.* The remaining volatile impurities were removed via kugelrohr distillation (120 ˚C, 80 mbar) giving the title compound as a pale-yellow oil (92%, 12.2 g). **^{1}H NMR** (500 MHz, CDCl$_3$) δ 7.68 (s, 1H), 7.49 – 7.41 (m, 2H), 7.10 – 7.02 (m, 2H), 4.34 (q, J = 7.1 Hz, 2H), 4.30 (q, J = 7.1 Hz, 2H), 1.33 (t, J = 7.1 Hz, 3H), 1.29 (t, J = 7.1 Hz, 3H). **^{13}C NMR** (126 MHz, CDCl$_3$) δ 166.7 (s), 164.2 (s), 164.0 (d, J = 252.6 Hz), 140.9 (s), 131.7 (d, J = 8.7 Hz), 129.3 (d, J = 3.4 Hz), 126.2 (s), 116.2 (d, J = 21.9 Hz), 61.9 (s), 61.8 (s), 14.3 (s), 14.1 (s). **^{19}F NMR** (376 MHz, CDCl$_3$) δ -108.7. **HRMS** (EI+) [C$_{14}$H$_{15}$O$_4$F] calc. 266.0954 found 266.0955. Characterization data is in accordance with prior reports.[55]

### 6.5.3 General Procedure 8: Synthesis of Arylidene Malonates

The arylidene malonates were prepared using a method modified from the literature.[56] A 25 ml vial equipped with a stirrer bar and 250 wt % activated 3 Å molecular sieves (beads, 3.0 – 5.0 mm) were flame dried. Aldehyde (6 mmol) and malonate (5 mmol) were added to the vial followed by dry CH$_2$Cl$_2$ (5 mL, 1.0 M). Stirring was started followed by the addition of acetic acid (0.5 mmol) and **pyrrolidine** (0.5 mmol). The mixture was stirred overnight to 4 days. The reaction mixture was filtered followed by passing through a silica plug. The product was then either used without purification or purified by column chromatography/crystallization/distillation.

Diethyl 2-(4-methoxybenzylidene)malonate (315)
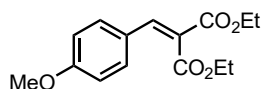
The title compound was synthesised by General Procedure 8 stirring for 4 days and purified by kugelrohr distillation (95 ˚C, <1 mbar) (49%, 0.682 g) as a colourless oil. **¹H NMR** (500 MHz, CDCl₃) δ 7.67 (s, 1H), 7.45 – 7.40 (m, 2H), 6.92 – 6.86 (m, 2H), 4.36 (q, J = 7.1 Hz, 2H), 4.29 (q, J = 7.1 Hz, 2H), 3.83 (s, 3H), 1.36 – 1.27 (m, 6H). **¹³C NMR** (126 MHz, CDCl₃) δ 167.3, 164.6, 161.7, 141.9, 131.7, 125.6, 123.8, 114.4, 61.8, 61.6, 55.5, 14.3, 14.1. **HRMS** (EI+) [C₁₅H₁₈O₅] calc. 278.1154 found 278.1153. Characterization data is in accordance with prior reports.[57]

Diethyl 2-(4-(methoxycarbonyl)benzylidene)malonate (318)
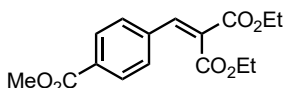
The title compound was synthesised by General Procedure 8 stirring overnight and purified by column chromatography (44%, 0.671 g) as a colourless oil. **¹H NMR** (500 MHz, CDCl₃) δ 8.04 (d, J = 7.9 Hz, 1H), 7.75 (s, 1H), 7.51 (d, J = 7.9 Hz, 1H), 4.32 (q, J = 7.1 Hz, 2H), 3.93 (s, 2H), 1.34 (t, J = 7.1 Hz, 1H), 1.27 (t, J = 7.0 Hz, 2H). **¹³C NMR** (126 MHz, CDCl₃) δ 166.5, 166.3, 163.9, 140.9, 137.4, 131.6, 130.1, 129.3, 128.5, 62.0, 52.5, 14.3, 14.0. **HRMS** (EI+) [C₁₆H₁₈O₆] calc. 306.1103 found 306.1102.

**Diethyl 2-(4-cyanobenzylidene)malonate (311)**
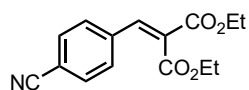
The title compound was synthesised by General Procedure 8 stirring overnight and purified by recrystallization from Et₂O and hexane (55%, 0.743 g) as a yellow solid. **MP** 69-72 ˚C. **¹H NMR** (500 MHz, CDCl₃) δ 7.71 (s, 1H), 7.69 – 7.65 (m, 2H), 7.54 (dd, J = 8.7, 0.6 Hz, 2H), 4.32 (q, J = 7.1 Hz, 4H), 4.32 (q, J = 7.1 Hz, 4H), 1.34 (t, J = 7.1 Hz, 3H), 1.27 (t, J = 7.1 Hz, 3H). **¹³C NMR** (126 MHz, CDCl₃) δ 165.9, 163.6, 139.7, 137.6, 132.6, 129.8, 129.7, 118.3, 113.8, 62.2, 62.2, 14.2, 14.0. **HRMS** (EI+) [C₁₅H₁₅NO₄] calc. 273.1001 found 273.0998. Characterization data is in accordance with prior reports. [57]

**Diethyl 2-(4-bromobenzylidene)malonate (313)**
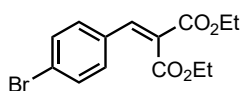
The title compound was synthesised by General Procedure 8 stirring overnight and purified by recrystallization from hexane (78%, 1.278 g) as a colourless solid. **MP** 39-41 ˚C. **^{1}H NMR** (500 MHz, CDCl$_3$) δ 7.65 (s, 1H), 7.54 – 7.47 (m, 2H), 7.34 – 7.29 (m, 2H), 4.33 (q, J = 7.1 Hz, 3H), 4.30 (q, J = 7.1 Hz, 3H), 1.33 (t, J = 7.1 Hz, 3H), 1.29 (t, J = 7.1 Hz, 3H). **^{13}C NMR** (126 MHz, CDCl$_3$) δ 166.4, 163.9, 140.7, 132.1, 131.9, 130.8, 127.0, 125.0, 61.9, 61.8, 14.1, 13.9. **HRMS** (ES+) [C$_{14}$H$_{15}$O$_4$Br + Na$^+$] calc. 349.0051 found 349.0052. Characterization data is in accordance with prior reports.[57]

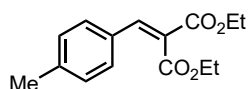**Diethyl 2-(4-chlorobenzylidene)malonate (312)**
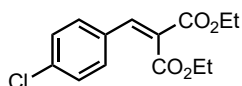
The title compound was synthesised by General Procedure 8 stirring overnight (90%, 1.29 g) as a colourless oil. **^{1}H NMR** (500 MHz, CDCl$_3$) δ 7.67 (s, 1H), 7.41 – 7.37 (m, 2H), 7.37 – 7.33 (m, 2H), 4.33 (q, J = 7.1 Hz, 3H), 4.30 (q, J = 7.1 Hz, 3H), 1.33 (t, J = 7.1 Hz, 3H), 1.29 (t, J = 7.1 Hz, 3H). **^{13}C NMR** (126 MHz, CDCl$_3$) δ 166.6, 164.1, 140.8, 136.8, 131.5, 130.8, 129.3, 127.0, 62.0, 61.9, 14.3, 14.1. **HRMS** (ES+) [C$_{14}$H$_{15}$O$_4$ + Na$^+$] calc. 305.0557 found305.0556. Characterization data is in accordance with prior reports.[57]

**Diethyl 2-(4-(trifluoromethyl)benzylidene)malonate (314)**
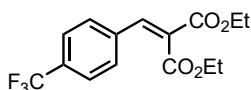
The title compound was synthesised by General Procedure 8 stirring overnight (quant., 1.58 g) as a colourless solid that went brown over time and was stored under nitrogen at 0 ˚C. **MP** 44 - 47 ˚C. **^{1}H NMR** (400 MHz, CDCl$_3$) δ 7.74 (s, 1H), 7.64 (d, J = 8.3 Hz, 1H), 7.56 (d, J = 8.3 Hz, 1H), 4.33 (q, J = 7.1 Hz, 2H), 4.32 (q, J = 7.1 Hz, 2H), 1.34 (t, J = 7.1 Hz, 1H), 1.28 (t, J = 7.1 Hz, 2H). **^{13}C NMR** (126 MHz, CDCl$_3$) δ 166.1 (s), 163.8 (s), 140.4 (s), 136.6 (s), 132.0 (q, J = 32.7 Hz), 129.6 (s, J = 17.7 Hz), 128.9 (s), 125.9 (q, J = 3.7 Hz), 123.8 (q, J = 272.3 Hz), 62.1 (s, J = 3.2 Hz), 62.1 (s), 14.2 (s, J = 29.1 Hz), 14.0 (s). **^{19}F NMR** (376 MHz, CDCl$_3$) δ -63.0 (s). **HRMS** (ES+) [C$_{15}$H$_{15}$O$_4$F$_3$ + Na$^+$] calc. 339.0820 found 339.0814. Characterization data is in accordance with prior reports. [57]

Diethyl 2-(4-methylbenzylidene)malonate (316)

The title compound was synthesised by General Procedure 8 stirring overnight and purified by recrystallization from from Et_2O and hexane (82%, 1.08 g) as a colourless solid. **MP** 41 - 43 $^{\circ}$C. **^{1}H NMR** (500 MHz, CDCl$_3$) δ 7.70 (s, 1H), 7.35 (d, J = 8.3 Hz, 1H), 7.18 (d, J = 8.1 Hz, 1H), 4.34 (q, J = 7.1 Hz, 1H), 4.30 (q, J = 7.1 Hz, 1H), 2.37 (s, 2H), 1.33 (t, J = 6.1 Hz, 1H), 1.30 (t, J = 6.1 Hz, 1H). **^{13}C NMR** (126 MHz, CDCl$_3$) δ 167.1, 164.5, 142.3, 141.3, 130.2, 129.7, 129.7, 125.3, 61.8, 61.7, 21.6, 14.3, 14.1. **HRMS** (ES+) [C$_{15}$H$_{18}$O$_4$ + Na$^+$] calc. 285.1103 found 285.1105. Characterization data is in accordance with prior reports. [57]

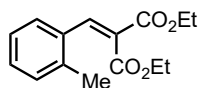**Diethyl 2-(2-fluorobenzylidene)malonate (320)**
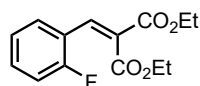
The title compound was synthesised by General Procedure 8 stirring overnight and purified by kugelrohr distillation (90 $^{\circ}$C, <1 mbar) (48%, 1.28 g) as a pale-yellow oil. **^{1}H NMR** (500 MHz, CDCl$_3$) δ 7.91 (s, 1H), 7.44 (td, J = 7.6, 1.7 Hz, 1H), 7.41 – 7.35 (m, 1H), 7.17 – 7.05 (m, 2H), 4.31 (q, J = 7.1 Hz, 2H), 4.30 (q, J = 7.1 Hz, 2H), 1.34 (t, J = 7.1 Hz, 3H), 1.26 (t, J = 7.1 Hz, 3H). **^{13}C NMR** (126 MHz, CDCl$_3$) δ 166.3 (s), 163.0 (s), 161.0 (d, J = 253.3 Hz), 135.0 (d, J = 5.2 Hz), 132.5 (d, J = 8.7 Hz), 129.5 (d, J = 2.1 Hz), 128.2 (d, J = 1.5 Hz), 124.4 (d, J = 3.7 Hz), 121.4 (d, J = 12.5 Hz), 116.1 (d, J = 21.7 Hz), 62.0 (s), 61.9 (s), 14.3 (s), 14.0 (s). **^{19}F NMR** (376 MHz, CDCl$_3$) δ -112.70. Characterization data is in accordance with prior reports.[58]

Diethyl 3-(3-fluorobenzylidene)malonate (319)
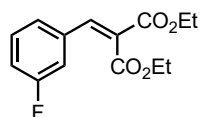
The title compound was synthesised by General Procedure 8 stirring overnight and purified by kugelrohr distillation (90 $^{\circ}$C, <1 mbar) (68%, 1.81 g) as a pale yellow oil. **^{1}H NMR** (500 MHz, CDCl$_3$) δ 7.68 (s, 1H), 7.35 (td, J = 8.0, 5.9 Hz, 1H), 7.23 (dd, J = 7.7, 0.7 Hz, 1H), 7.18 – 7.14 (m, 1H), 7.10 (tdd, J = 8.3, 2.5, 0.8 Hz, 1H), 4.34 (q, J = 7.1 Hz, 1H), 4.31 (q, J = 7.1 Hz, 1H), 1.33 (t, J = 7.1 Hz, 1H), 1.30 (t, J = 7.1 Hz, 1H). **^{13}C NMR** (126 MHz, CDCl$_3$) δ 166.4 (s), 163.9 (s), 162.8 (d, J = 247.0 Hz), 140.7 (d, J = 2.6 Hz),

135.1 (d, J = 7.9 Hz), 130.5 (d, J = 8.3 Hz), 127.7 (s), 125.5 (d, J = 3.0 Hz), 117.6 (d, J = 21.3 Hz), 115.9 (d, J = 22.5 Hz), 62.0 (s), 62.0 (s), 14.3 (s), 14.0 (s). **19F NMR** (376 MHz, CDCl$_3$) δ -112.09.

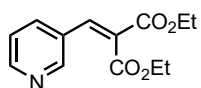### Diethyl 2-(2-methylbenzylidene)malonate (322)

The title compound was synthesised by General Procedure 8 stirring overnight and purified by kugelrohr distillation (95 ˚C, <1 mbar) (37%, 0.969 g) as a colourless oil. **1H NMR** (500 MHz, CDCl$_3$) δ 7.97 (s, 1H), 7.33 (d, J = 7.7 Hz, 1H), 7.27 (td, J = 7.5, 1.3 Hz, 1H), 7.22 – 7.18 (m, 1H), 7.18 – 7.12 (m, 1H), 4.31 (q, J = 7.1 Hz, 2H), 4.22 (q, J = 7.1 Hz, 2H), 2.38 (s, 3H), 1.34 (t, J = 7.1 Hz, 3H), 1.16 (t, J = 7.1 Hz, 3H). **13C NMR** (126 MHz, CDCl$_3$) δ 166.5, 164.2, 141.9, 137.7, 132.7, 130.5, 130.2, 127.9, 127.8, 126.1, 61.8, 61.6, 20.1, 14.3, 14.0. Characterization data is in accordance with prior reports. [574]

Diethyl 3-(3-methylbenzylidene)malonate (321)
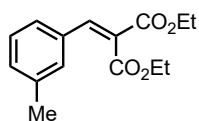
The title compound was synthesised by General Procedure 8 stirring overnight and purified by kugelrohr distillation (95 ˚C, <1 mbar) (63%, 1.65 g) as a colourless oil. **1H NMR** (500 MHz, CDCl$_3$) δ 7.71 (s, 1H), 7.30 – 7.24 (m, 3H), 7.23 – 7.18 (m, 1H), 4.34 (q, J = 7.1 Hz, 2H), 4.30 (q, J = 7.1 Hz, 2H), 2.35 (s, 3H), 1.33 (t, J = 7.1 Hz, 3H), 1.30 (t, J = 7.1 Hz, 3H). **13C NMR** (126 MHz, CDCl$_3$) δ 166.9, 164.3, 142.5, 138.6, 132.9, 131.5, 130.3, 128.8, 126.7, 126.1, 61.8, 61.8, 21.5, 14.3, 14.0.
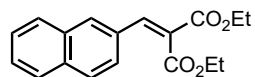
Diethyl 2-(pyridin-3-ylmethylene)malonate (317)

The title compound was synthesised by General Procedure 8 stirring overnight and purified by kugelrohr distillation (114 ˚C, <1 mbar) (54%, 0.682 g) as an orange oil. **1H NMR** (500 MHz, CDCl$_3$) δ 8.68 (d, J = 2.3 Hz, 1H), 8.61 (dd, J = 4.8, 1.6 Hz, 1H), 7.77 (dddd, J = 8.0, 2.3, 1.6, 0.6 Hz, 1H), 7.70 (s, 1H), 7.31 (dddd, J = 8.0, 4.8, 0.8, 0.4 Hz, 1H), 4.34 (q, J = 7.1 Hz, 1H), 4.32 (q, J = 7.1 Hz, 1H), 1.34 (t, J = 7.1 Hz, 1H), 1.29 (t, J = 7.1 Hz, 1H). **13C NMR** (126 MHz, CDCl$_3$) δ 166.1, 163.7, 151.2, 150.8, 138.6, 135.8,

129.1, 128.7, 123.7, 62.1, 62.1, 14.3, 14.1. **HRMS** (ES+) [$C_{13}H_{16}NO_4$] calc. 250.1079 found 250.1089.

Diethyl 2-(naphthalen-2-ylmethylene)malonate (323)
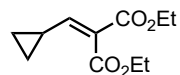

The title compound was synthesised by General Procedure 8 stirring for 2 days and purified by kugelrohr distillation (132 ˚C, <1 mbar) (59%, 0.8923 g) as a colourless oil.
^{1}H NMR (500 MHz, CDCl$_3$) δ 7.99 – 7.95 (m, 1H), 7.90 (s, 1H), 7.83 (ddd, J = 8.7, 6.6, 2.9 Hz, 1H), 7.58 – 7.45 (m, 1H), 4.38 (q, J = 7.2 Hz, 1H), 4.34 (q, J = 7.2 Hz, 1H), 1.36 (t, J = 7.1 Hz, 1H), 1.30 (t, J = 7.1 Hz, 1H). **^{13}C NMR** (126 MHz, CDCl$_3$) δ 167.0, 164.4, 142.3, 134.2, 133.2, 131.1, 130.6, 128.9, 128.7, 127.9, 127.8, 126.9, 126.5, 125.4, 61.9, 61.8, 14.3, 14.1. **HRMS** (ES+) [$C_{18}H_{18}O_4$ + Na$^+$] calc. 321.1103 found 321.1103

Diethyl 2-(naphthalen-1-ylmethylene)malonate (324)
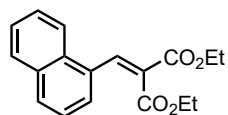
The title compound was synthesised by General Procedure 8 stirring for 2 days and purified by kugelrohr distillation (138 ˚C, <1 mbar) (67%, 1.012 g) as an orange oil. **^{1}H NMR** (500 MHz, CDCl$_3$) δ 8.47 (s, 1H), 8.00 (d, J = 8.1 Hz, 1H), 7.90 – 7.84 (m, 2H), 7.60 – 7.51 (m, 3H), 7.46 – 7.40 (m, 1H), 4.37 (q, J = 7.1 Hz, 2H), 4.16 (q, J = 7.1 Hz, 2H), 1.38 (t, J = 7.1 Hz, 3H), 1.06 (t, J = 7.1 Hz, 3H). **^{13}C NMR** (126 MHz, CDCl$_3$) δ 166.3, 164.1, 141.4, 133.5, 131.5, 131.0, 130.6, 129.4, 128.8, 127.1, 126.6, 126.5, 125.3, 124.2, 61.9, 61.6, 14.3, 13.9. **HRMS** (ES+) [$C_{18}H_{18}O_4$ + Na$^+$] calc. 321.1103 found 321.1105. Characterization data is in accordance with prior reports.[57]

Diethyl 2-(cyclopropylmethylene)malonate (326)

The title compound was synthesised by General Procedure 8 stirring for 2 days and purified by kugelrohr distillation (75 ˚C, <1 mbar) (73%, 1.55 g) as a colourless oil. **^{1}H NMR** (500 MHz, CDCl$_3$) δ 6.35 (d, J = 11.3 Hz, 1H), 4.31 (q, J = 7.1 Hz, 1H), 4.21 (q, J = 7.1 Hz, 1H), 1.96 (tdt, J = 12.4, 7.9, 4.5 Hz, 1H), 1.33 (t, J = 7.1 Hz, 2H), 1.27 (t, J = 7.1 Hz, 2H), 1.08 (qd, J = 4.9, 0.7 Hz, 1H), 0.75 (tt, J = 5.0, 2.5 Hz, 1H). **^{13}C NMR** (126 MHz, CDCl$_3$) δ 166.0, 164.5, 156.2, 125.7, 61.3, 61.2, 14.3, 14.3, 13.1, 10.0. **HRMS**

(AS+) $[C_{11}H_{16}O_4 + H]$ calc. 213.127 found 213.1120. Characterization data is in accordance with prior reports.[59]

Diethyl 2-(2,6-dimethylhept-5-en-1-ylidene)malonate (325)
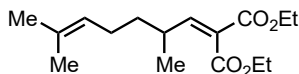
The title compound was synthesised by General Procedure 8 stirring for 2 days and purified column chromatography (77%, 1.04 g) as a colourless oil. **^{1}H NMR** (500 MHz, CDCl$_3$) δ 6.75 (d, J = 10.8 Hz, 1H), 5.03 (t, J = 7.0 Hz, 1H), 4.27 (qd, J = 7.1, 3.3 Hz, 2H), 4.22 (q, J = 7.1 Hz, 2H), 2.55 (ddd, J = 13.6, 11.0, 6.8 Hz, 1H), 1.94 (d, J = 7.5 Hz, 1H), 1.91 (d, J = 7.4 Hz, 1H), 1.65 (s, 3H), 1.56 (s, 3H), 1.44 – 1.34 (m, 2H), 1.29 (dt, J = 15.3, 7.1 Hz, 6H), 1.04 (d, J = 6.6 Hz, 3H). **^{13}C NMR** (126 MHz, CDCl$_3$) δ 165.8, 164.2, 154.3, 132.1, 127.5, 123.9, 61.3, 61.2, 36.7, 34.5, 26.0, 25.8, 19.9, 17.8, 14.3, 14.2. **HRMS** (AP+) $[C_{16}H_{27}O_4]$ calc. 283.1909 found 283.1914
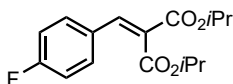
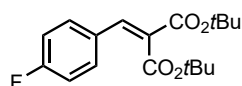## Dimethyl 2-(4-fluorobenzylidene)malonate (327)
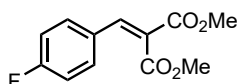
The title compound was synthesised by General Procedure 8 stirring for 2 days and purified by kugelrohr distillation (90 °C, <1 mbar) (65%, 0.771 g) as a colourless oil. **^{1}H NMR** (400 MHz, CDCl$_3$) δ 7.73 (s, 1H), 7.43 (dd, J = 8.5, 5.3 Hz, 2H), 7.08 (t, J = 8.6 Hz, 2H), 3.85 (s, 3H), 3.85 (s, 3H). **^{13}C NMR** (101 MHz, CDCl$_3$) δ 167.2 (s), 164.6 (s), 164.1 (d, J = 253.0 Hz), 141.8 (s), 131.7 (d, J = 8.7 Hz), 129.2 (d, J = 3.4 Hz), 125.4 (s), 116.3 (d, J = 21.9 Hz), 52.9 (s), 52.9 (s). **^{19}F NMR** (376 MHz, CDCl$_3$) δ -108.3. Characterization data is in accordance with prior reports.[60]
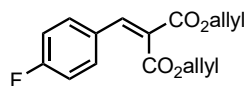
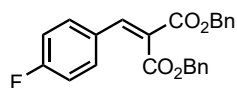## Di-*iso*-propyl 2-(4-fluorobenzylidene)malonate (328)

The title compound was synthesised by General Procedure 8 stirring for 2 days and purified by kugelrohr distillation (98 °C, <1 mbar) (57%, 0.841 g) as an orange oil. **^{1}H NMR** (400 MHz, CDCl$_3$) 7.63 (s, 3H), 7.47 (dd, J = 8.5, 5.3 Hz, 6H), 7.06 (t, J = 8.6 Hz, 6H), 5.31 – 5.20 (m, 3H), 5.20 – 5.09 (m, 3H), 1.31 (d, J = 6.4 Hz, 18H), 1.29 (d, J = 6.5 Hz, 19H). **^{13}C NMR** (101 MHz, CDCl$_3$) δ 166.3 (s), 164.0 (d, J = 252.3 Hz), 163.8 (s), 140.2 (s), 131.7 (d, J = 8.6 Hz), 129.4 (d, J = 3.3 Hz), 127.0 (s), 116.1 (d, J = 21.8 Hz), 69.5 (s), 21.9 (s), 21.7 (s). **^{19}F NMR** (376 MHz, CDCl$_3$) δ -108.9.

234

Di-*tert*-butyl 2-(4-fluorobenzylidene)malonate (329)

The title compound was synthesised by General Procedure 8 stirring for 2 days and purified by kugelrohr distillation (105 ˚C, <1 mbar) (42%, 0.676 g) as a yellow oil. **¹H NMR** (500 MHz, CDCl₃) δ 7.53 – 7.47 (m, 3H), 7.08 – 7.01 (m, 2H), 1.53 (s, 9H), 1.52 (s, 9H). **¹³C NMR** (126 MHz, CDCl₃) δ 166.0 (s), 163.8 (d, J = 251.6 Hz), 163.6 (s), 138.7 (s), 131.6 (d, J = 8.5 Hz), 129.7 (d, J = 3.4 Hz), 129.1 (d, J = 2.0 Hz), 115.9 (d, J = 21.8 Hz), 82.6 (s), 82.3 (s), 28.2 (s), 28.0 (s). **¹⁹F NMR** (376 MHz, CDCl₃) δ -109.6.
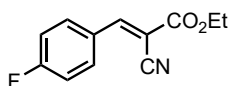
Diallyl 2-(4-fluorobenzylidene)malonate (331)

The title compound was synthesised by General Procedure 8 stirring for 2 days and purified by kugelrohr distillation (95 ˚C, <1 mbar) (65%, 0.944 g) as a colourless oil. **¹H NMR** (400 MHz, CDCl₃) δ 7.73 (s, 1H), 7.46 (dd, J = 8.5, 5.3 Hz, 2H), 7.07 (t, J = 8.6 Hz, 2H), 5.94 (tddd, J = 16.3, 11.9, 10.4, 5.7 Hz, 2H), 5.42 – 5.31 (m, 2H), 5.31 – 5.22 (m, 2H), 4.76 (ddt, J = 7.9, 5.6, 1.4 Hz, 4H). **¹³C NMR** (101 MHz, CDCl₃) δ 166.2 (s), 164.1 (d, J = 252.9 Hz), 163.8 (s), 141.8 (s), 131.9 (d, J = 8.7 Hz), 131.7 (s), 131.3 (s), 129.1 (d, J = 3.4 Hz), 125.6 (d, J = 2.0 Hz), 119.6 (s), 118.7 (s), 116.2 (d, J = 21.9 Hz), 66.5 (s), 66.3 (s). **¹⁹F NMR** (376 MHz, CDCl₃) δ -108.3.

**Dibenzyl 2-(4-fluorobenzylidene)malonate (330)**

The title compound was synthesised by General Procedure 8 stirring for 2 days and purified by kugelrohr distillation (136 ˚C, <1 mbar) (70%, 1.37 g) as a yellow oil. **¹H NMR** (400 MHz, CDCl₃) δ 7.63 (s, 1H), 7.39 – 7.11 (m, 13H), 6.81 (t, J = 8.6 Hz, 2H), 5.20 (s, 2H), 5.18 (s, 2H). **¹³C NMR** (101 MHz, CDCl₃) δ 166.3 (s), 164.0 (d, J = 252.8 Hz), 163.9 (s), 142.0 (s), 135.6 (s), 134.9 (s), 131.8 (d, J = 8.7 Hz), 129.1 (s), 129.0 (d, J = 3.2 Hz), 128.7 (s), 128.5 (s), 128.2 (s), 125.5 (s), 125.5 (s, J = 2.0 Hz), 116.1 (d, J = 21.9 Hz), 67.8 (s), 67.4 (s). **¹⁹F NMR** (376 MHz, CDCl₃) δ -108.3.

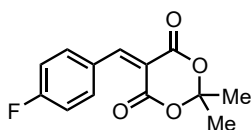## Ethyl (E)-2-cyano-3-(4-fluorophenyl)acrylate (332)

The title compound was synthesised by General Procedure 8 stirring for 1 days and purified by recrystallization in ethanol (90%, 0.996 g) as a yellow solid. **MP** 94 - 97 ˚C. **¹H NMR** (500 MHz, CDCl₃) δ 8.21 (s, 1H), 8.07 – 7.99 (m, 1H), 7.22 – 7.16 (m, 1H), 4.39 (q, J = 7.1 Hz, 1H), 1.40 (t, J = 7.1 Hz, 2H). **¹³C NMR** (126 MHz, CDCl₃) δ 165.6 (d, J = 257.6 Hz), 162.6 (s), 153.7 (s), 133.7 (d, J = 9.2 Hz), 128.0 (d, J = 3.3 Hz), 116.9 (d, J = 22.1 Hz), 115.6 (s), 102.7 (d, J = 2.4 Hz), 63.0 (s), 14.3 (s). **¹⁹F NMR** (376 MHz, None) δ -104.8.

5-(4-Fluorobenzylidene)-1,3-dimethylpyrimidine-2,4,6(1*H*,3*H*,5*H*)-trione (334)
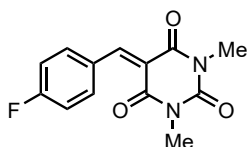

The title compound was synthesised by General Procedure 8 stirring for 1 days and purified by recrystallization in ethanol (95%, 1.245 g) as a yellow solid. **MP** 161 - 164 ˚C. **¹H NMR** (500 MHz, CDCl₃) δ 8.52 (s, 1H), 8.23 – 8.14 (m, 2H), 7.20 – 7.11 (m, 2H), 3.42 (s, 3H), 3.38 (s, 3H). **¹³C NMR** (126 MHz, CDCl₃) δ 165.6 (d, J = 257.7 Hz), 162.7 (s), 160.7 (s), 158.0 (s), 151.3 (s), 136.9 (d, J = 9.3 Hz), 129.0 (d, J = 3.1 Hz), 117.1 (d, J = 1.7 Hz), 115.8 (d, J = 21.8 Hz), 29.3 (s), 28.6 (s). **¹⁹F NMR** (471 MHz, CDCl₃) δ -103.3. Characterization data is in accordance with prior reports.[59]

5-(4-Fluorobenzylidene)-2,2-dimethyl-1,3-dioxane-4,6-dione (335)

The title compound was synthesised by General Procedure 8 stirring for 2 days and purified by recrystallization from diethyl ether and petroleum ether (98%, 1.225 g) as a white solid. **MP** 135 - 137 ˚C. **¹H NMR** (500 MHz, CDCl₃) δ 8.39 (s, 1H), 8.17 (dd, J = 8.1, 5.7 Hz, 2H), 7.17 (t, J = 8.3 Hz, 2H), 1.80 (s, 6H). **¹³C NMR** (126 MHz, CDCl₃) δ 165.8 (d, J = 258.9 Hz), 163.3 (s), 159.9 (s), 156.7 (s), 136.9 (d, J = 9.5 Hz), 128.1 (d, J = 3.3 Hz), 116.2 (d, J = 21.9 Hz), 114.2 (d, J = 1.8 Hz), 104.6 (s), 27.6 (s). **¹⁹F NMR** (376 MHz, CDCl₃) δ -101.9.

Ethyl 2-oxo-2*H*-chromene-3-carboxylate (336)
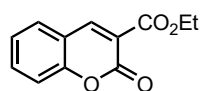
The title compound was prepared using a method modified from the literature.[61] To a flame dried 25 mL microwave vial was added salicylaldehyde (1.2 g, 10 mmol) and diethylmalonate (2.2 g, 14 mmol), the vial was then sealed and put under nitrogen. Ethanol (5 mL ,2 M) that had been dried over 3 Å molecular sieves was then added followed by piperidine (0.125 mL, 1 mmol) and acetic acid (0.050 mL 1 mmol). The vial was then heated to 125 ˚C for 3 hours. After which the reaction was cooled to 0 ˚C and water (10 mL) was added. This mixture was then filtered and washed with water ethanol (1:1) solution. The remaining solid was recrystalized from the minimum amount of boiling water:ethanol (3:1). This gave the title compound as a white solid (82%, 1.89 g). **MP** 61 - 65 ˚C. **^{1}H NMR** (500 MHz, CDCl$_3$) δ 8.52 (s, 1H), 7.68 – 7.58 (m, 2H), 7.39 – 7.30 (m, 2H), 4.42 (q, *J* = 7.1 Hz, 2H), 1.41 (t, *J* = 7.1 Hz, 3H). **^{13}C NMR** (126 MHz, CDCl$_3$) δ 163.2, 156.9, 155.3, 148.7, 134.5, 129.6, 125.0, 118.5, 118.0, 117.0, 62.1, 14.4. **HRMS** (ES+) [C$_{12}$H$_{10}$O$_4$ + Na$^+$] calc. 241.477 found 241.079

2-benzylidenemalononitrile (333)
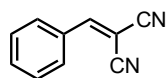
The title compound was prepared using a method modified from the literature.[62] To a 25 mL round bottom flask was added, benzaldehyde (1.061 g, 10 mmol), malononitrile (0.661 g, 10 mmol), piperidine (0.099 mL, 1 mmol), and ethanol (10 mL). The mixture was stirred at room temperature overnight. The solvent was removed under reduced pressure, dichloromethane (50 mL) and HCl (0.1 M, 50mL) were added and the mixture transferred to a separating funnel. The layers were separated and the aqueous layer further extracted with dichloromethane (2 x 50 mL). The combined organic phase was dried (MgSO$_4$), filtered and the solvent removed under reduced pressure. The residue was then recrystallized from boiling water:ethanol (3:1) to yield the product as yellow crystals (0.941 g, 6.11 mmol, 61%). **MP** 80 - 81 °C. **^{1}H NMR** (500 MHz; CDCl$_3$): δ 7.91 (d, *J* = 7.8 Hz, 2H), 7.78 (s, 1H), 7.65-7.62 (m, 1H), 7.55 (t, *J* = 7.6 Hz, 2H). **^{13}C NMR** (126 MHz; CDCl$_3$): δ 160.0, 134.8, 131.1, 130.9, 129.8, 113.8, 112.7, 83.1. Thanks to Joseph L. Howard for this result.

Ethyl 3-phenylpropiolate (344)
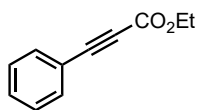
The title compound was prepared using a method modified from the literature.[63] To an oven-dried flask was added potassium carbonate (2.073 g, 15 mmol) and the flask flushed with nitrogen. Ethyl propiolate (0.507 mL, 5 mmol), iodobenzene (0.839 mL, 7.5 mmol) and dry THF (40 mL) were added and stirred. To this mixture was added $Pd(PPh_3)_2Cl_2$ (0.070 g, 0.1 mmol) and CuI (0.018 g, 0.1 mmol) and the flask flushed with nitrogen. The mixture was heated to reflux, stirred for 22 hours, cooled and filtered through cotton wool into a separating funnel. Dichloromethane (50 mL) and water (50 mL) were added, the layers separated and the aqueous layer further extracted with dichloromethane (2 x 50 mL). The combined organic phase was washed (brine), dried ($MgSO_4$), filtered and the solvent removed under reduced pressure. The product was purified by flash column chromatography and the product obtained as a yellow oil (0.325 g, 1.87 mmol, 37%). **¹H NMR** (500 MHz; CDCl₃): δ 7.59 (d, J = 8.0 Hz, 2H), 7.46-7.43 (m, 1H), 7.37 (t, J = 7.6 Hz, 2H), 4.32-4.28 (m, 2H), 1.36 (t, J = 7.1 Hz, 3H). **¹³C NMR** (126 MHz; CDCl₃): δ 154.2, 133.1, 130.7, 128.7, 119.8, 86.2, 80.8, 62.3, 14.3. Thanks to Joseph L. Howard for this result.

Diethyl 2-(4-fluorobenzyl)malonate (351)
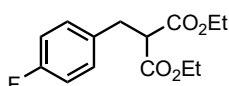
The title compound was prepared using a method modified from the literature.[64] To a flame dried 10 mL microwave vial was added sodium hydride (60% suspension in mineral oil) (42 mg, 1.05 mmol) and the vial placed under nitrogen. Dry THF (5 mL, 0.2 M) was then added and the vial was cooled to 0 ˚C. Diethyl malonate (0.160 mL, 1.05 mmol) was then added dropwise and the mixture was stirred for 15 mins followed by the addition of 4-fluorobenzyl bromide (0.125 mL, 1 mmol). The vial was then heated to 75 ˚C for 1 hour. Water (2 mL) was then added and the solvent was removed *en vacuo* and the remaining oil was dissolved in diethyl ether 20 mL and washed with water (20 mL). The water layer was then extracted twice more with diethyl ether and the combined organic phases were dried over magnesium sulphate. The solvent was then removed *en vacuo* this oil was then purified using flash column chromatography (hexane:ethyl acetate). The title compound was isolated as a colourless oil (52.6 mg, 20%). **¹H NMR** (500 MHz, CDCl₃) δ 7.17 (dd, J = 8.3, 5.4 Hz, 1H), 6.96 (t, J = 8.7 Hz, 1H), 4.25 − 4.06

(m, 2H), 3.60 (td, J = 7.9, 1.1 Hz, 1H), 3.18 (d, J = 7.9 Hz, 1H), 1.30 – 1.11 (m, 3H). **^{13}C NMR** (126 MHz, CDCl$_3$) δ 168.9 (s), 161.9 (d, J = 244.8 Hz), 133.7 (d, J = 3.3 Hz), 130.5 (d, J = 8.0 Hz), 115.5 (d, J = 21.3 Hz), 61.7 (s), 54.1 (s), 54.1 (s), 34.0 (s), 14.2 (s). **^{19}F NMR** (471 MHz, CDCl$_3$) δ -116.3. **HRMS** (ES+) [C$_{14}$H$_{17}$O$_4$F + Na$^+$] calc. 291.1009 found 291.1016.

Methyl 4-formylbenzoate
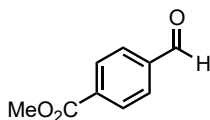
The title compound was prepared using the following procedure. To an oven dried 100 mL round bottom flask that had been placed under nitrogen was added, 4-carboxybenzaldehyde (2.25 g, 15 mmol), imidazole (2.04 g, 30 mmol), DMAP (0.366 g, 3 mmol), CH$_2$Cl$_2$ (30 mL, 0.5 M) and methanol (2 mL, 45 mmol). This solution was then cooled to 0 ˚C. A solution containing DCC (1 M, 17 mL) in CH$_2$Cl$_2$ was prepared in a dried flask. This DCC solution was then added dropwise to the cooled reaction flask after which it was left to increase to room temperature and continued to stir for a further 3 hours. The reaction mixture was then filtered, and the filtrate collected. The filtrate was then washed with 0.5 M HCl (30 mL), saturated NaHCO$_3$ (30 mL), and brine (30 mL). The organic phase was then dried over magnesium sulfate and solvent removed *en vacuo*. This gave the title compound as a white solid and was used without further purification (quant., 2.62 g). **MP** 50 - 52 ˚C. **^{1}H NMR** 10.10 (s, 1H), 8.20 (d, J = 7.6 Hz, 2H), 7.95 (d, J = 7.6 Hz, 2H), 3.96 (s, 3H). **^{13}C NMR** (126 MHz, CDCl$_3$) δ 191.8, 166.2, 139.3, 135.2, 130.3, 129.7, 52.7.

### 6.5.4 General Procedure 9: Synthesis of malonates

The title compounds were prepared using a method modified from the literature.[65] To a dried 100 mL round bottom flask was added diethyl ether (25 mL), malonic acid (10 mmol), and desired alcohol coupling partner (30 mmol). This mixture was cooled to 0 ˚C and a solution of DCC in diethyl ether (1 M, 30 mL) was added slowly. Once addition was complete the reaction mixture was allowed to rise to room temperature and stirred for a further 1 hour. Once the reaction was complete the mixture was filtered and the filtrate collected. The filtrate was then washed with saturated sodium bicarbonate followed by brine and dried using magnesium sulphate. The solvent was removed *en vacuo* and the title compound was used without further purification or purified by flash column chromatography.
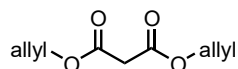
Di-*iso*-propyl malonate
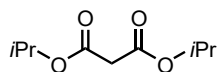
The title compound was prepared by General Procedure 9 (93%, 1.72 g) as a colourless oil. **¹H NMR** (500 MHz, CDCl₃) δ 5.05 (hept, J = 6.3 Hz, 1H), 3.29 (s, 1H), 1.25 (d, J = 6.3 Hz, 6H). **¹³C NMR** (126 MHz, CDCl₃) δ 166.4, 69.1, 42.5, 21.8.

Di-*tert*-butyl malonate
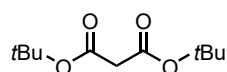
The title compound was prepared by General Procedure 9 exchanging diethyl ether as solvent for acetonitrile (97%, 2.10 g) as a yellow oil. **¹H NMR** (500 MHz, CDCl₃) δ 3.18 (s, 2H), 1.47 (s, 18H). **¹³C NMR** (126 MHz, CDCl₃) δ 166.3, 81.8, 44.5, 28.1.

Diallyl malonate

The title compound was prepared by General Procedure 9 (93%, 1.76 g) as a colourless oil. **¹H NMR** (500 MHz, CDCl₃) δ 5.91 (ddt, J = 17.2, 10.4, 5.8 Hz, 1H), 5.34 (ddd, J = 17.2, 3.0, 1.5 Hz, 1H), 5.26 (ddd, J = 10.4, 1.3 Hz, 1H), 4.65 (ddd, 2H), 3.44 (s, 1H). **¹³C NMR** (126 MHz, CDCl₃) δ 166.2, 131.6, 119.0, 66.2, 41.6.

6.5.5 General Procedure 10: Reductive Dimerization of Alkenes

To a 14 mL stainless steel milling jar (Insolido Technologies) containing a stainless steel milling ball (4.1 g) was added manganese, irregular pieces, (1.1 mmol, 60 mg), the appropriate arylidene malonate (1 mmol), THF (2 mmol, 160 μL), and lithium chloride (1 mmol, 42 mg). The reaction mixture was then milled at 30 Hz for 3 h. The mixture was then washed into a flask with EtOAc, HCl (1 M, 25 mL) was added and the mixture stirred for ten minutes and the organic phase was separated, washed with brine and dried with magnesium sulphate. This crude mixture was then purified using flash column chromatography. If the diastereomers of the product could not be separated the columned material was then further purified using recycling preparative HPLC.

6.5.6   General Procedure 11: Reductive Dimerization of Alkenes in solution

If required, manganese of the appropriate form (275 mg) was placed in a 14 mL stainless steel milling jar containing one milling ball (10 mm, 4.1 g) and milled at 30 Hz for 5 mins.

To a 5 mL vial containing a magnetic stirrer bar was added manganese, (0.55 mmol, 30 mg) diethyl 2-(4-fluorobenzylidene)malonate (0.5 mmol, 133 mg), lithium chloride (0.5 mmol, 21 mg), and THF (2 mL, 0.25 M). The reaction mixture was left to stir and upon completion trifluorotoluene (0.167 mmol, 21 µL) was added as an internal standard followed by aq. HCl (1.5 mL, 1 M) and EtOAc (1.5 mL). The biphasic mixture was left to stir until the remaining manganese had been quenched and effervescing had ceased. The organic phase was then analysed by ^{19}F NMR spectroscopy.

Tetraethyl 2,3-bis(4-fluorophenyl)butane-1,1,4,4-tetracarboxylate (310)
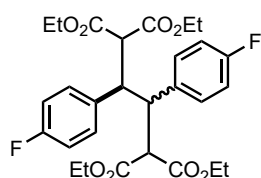
The title compound was prepared by General Procedure 10 as a mixture of diastereomers (88%, 3:2, 235 mg) as a white solid. The anti diastereomer was separated by column chromatography and the syn diastereomer was separated by recycling preparative HPLC using 80:20 hexane:EtOAc. **MP** 144 - 145 °C. **Anti ^{1}H NMR** (500 MHz, CDCl$_3$) δ 7.32 – 7.27 (m, 1H), 6.96 (t, J = 8.6 Hz, 1H), 4.07 (dd, J = 5.6, 2.0 Hz, 1H), 3.95 (ddq, J = 14.6, 7.4, 3.6 Hz, 1H), 3.86 (q, J = 7.1 Hz, 1H), 3.58 (dd, J = 5.6, 2.1 Hz, 1H), 1.11 (t, J = 7.1 Hz, 1H), 0.97 (t, J = 7.1 Hz, 2H). **Anti ^{13}C NMR** (126 MHz, CDCl$_3$) δ 168.3 (s), 167.7 (s), 162.3 (d, J = 246.6 Hz), 133.8 (d, J = 3.3 Hz), 131.9 (d, J = 7.9 Hz), 115.1 (d, J = 21.2 Hz), 61.7 (s), 61.4 (s), 55.5 (s), 47.9 (s), 14.0 (s), 13.8 (s). **Anti ^{19}F NMR** (376 MHz, CDCl$_3$) δ -114.4. . **IR**: ν_{max}: 1749, 1722, 1219, 1157, 1106 cm^{-1} **Anti HRMS** (AP+) [C$_{28}$H$_{33}$F$_2$O$_8$] calc. 535.2143 found 535.2144

Syn ^{1}H NMR (400 MHz, CDCl$_3$) δ 6.88 (br s, 4H), 4.49 – 4.29 (m, 2H), 3.90 – 3.72 (m, 3H), 3.65 (q, J = 1.7 Hz, 1H), 1.41 (t, J = 7.1 Hz, 3H), 0.85 (t, J = 7.1 Hz, 3H). **Syn ^{13}C NMR** (126 MHz, CDCl$_3$) δ 167.9 (s), 167.1 (s), 162.3 (d, J = 246.7 Hz), 131.6 (d, J = 3.3 Hz), 114.8 (d, J = 18.7 Hz), 62.3 (s), 61.5 (s), 55.7 (s), 45.9 (s), 14.3 (s), 13.7 (s). **Syn ^{19}F NMR** (376 MHz, CDCl$_3$) δ -114.6 (s). **Syn HRMS** (ES+) [C$_{28}$H$_{32}$O$_8$F$_2$ + Na$^+$] calc. 557.1963 found 557.1943

Tetraethyl 2,3-diphenylbutane-1,1,4,4-tetracarboxylate (297)
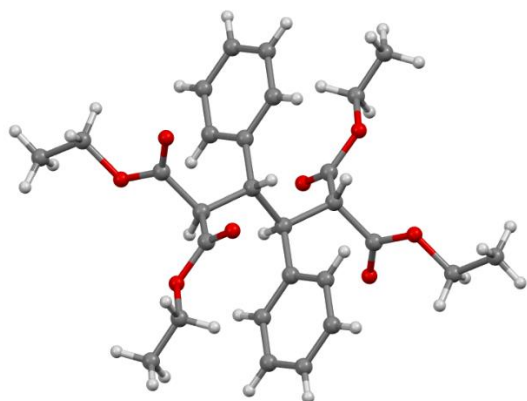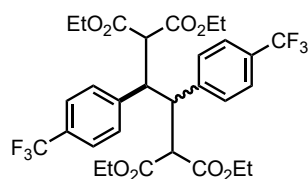
EtO$_2$C, CO$_2$Et

EtO$_2$C, CO$_2$Et
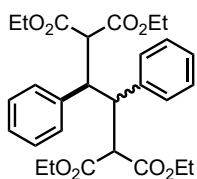
The title compound was prepared by General Procedure 10 as a mixture of diastereomers (56%, 3:5, 140 mg) as a white solid. The diastereomers were separated by preparatory TLC, 5 runs at 80:20 hexane:EtOAc. **MP** 89 - 90 ˚C. **Anti ^{1}H NMR** (500 MHz, CDCl$_3$) δ 7.37 – 7.07 (m, 16H), 4.09 (dd, J = 6.0, 2.2 Hz, 3H), 3.98 – 3.85 (m, 6H), 3.81 (qd, J = 7.1, 1.0 Hz, 6H), 3.67 (dd, J = 6.0, 2.2 Hz, 3H), 1.10 (t, J = 7.1 Hz, 9H), 0.91 (t, J = 7.1 Hz, 9H). **Anti ^{13}C NMR** (500 MHz, CDCl$_3$) δ 7.4 – 7.1 (m, 16H), 4.1 (dd, J = 6.0, 2.2 Hz, 3H), 4.0 – 3.9 (m, 6H), 3.8 (qd, J = 7.1, 1.0 Hz, 6H), 3.7 (dd, J = 6.0, 2.2 Hz, 3H), 1.1 (t, J = 7.1 Hz, 9H), 0.9 (t, J = 7.1 Hz, 9H). **IR**: ν$_{max}$: 1759, 1736, 1203, 1165 cm^{-1} **Anti HRMS** (AP+) [C$_{28}$H$_{35}$O$_8$] calc. 499.2332 found 499.2309

Syn ^{1}H NMR (500 MHz, CDCl$_3$) δ 9.94 (s, enol 1H), 7.79 (d, J = 8.0 Hz, enol 2H), 7.48 (d, J = 8.1 Hz, enol 2H), 7.35 – 7.27 (m, 7H), 7.19 (m, 7H), 4.84 (d, J = 12.1 Hz, enol 1H), 4.50 – 4.31 (m, 4H), 4.02 (m, 2H), 3.91 (s, 1H), 3.88 (s, 1H), 3.84 – 3.69 (m, 6H), 1.42 (t, J = 7.1 Hz, 6H), 1.04 (t, J = 7.1 Hz, enol 6H), 1.02 (t, J = 7.1 Hz, enol 6H), 0.79 (t, J = 7.1 Hz, 6H). **Syn ^{13}C NMR** (126 MHz, CDCl$_3$) δ 191.8 (enol), 168.1, 167.5 (enol), 167.4 (enol), 167.4, 148.6 (enol), 140.3 (enol), 136.0, 135.3 (enol), 130.3, 129.0, 128.6, 128.0, 127.7, 127.7, 127.5, 127.5 (enol), 62.2, 61.9 (enol), 61.8 (enol), 61.3, 57.2 (enol), 55.7, 51.3 (enol), 46.6, 14.3, 14.0 (enol), 13.9 (enol), 13.6. **Syn HRMS** (AP+) [C$_{28}$H$_{35}$O$_8$] calc. 499.2332 found 499.2322

Single crystal X-Ray diffraction structure of anti:

CCDC reference. 2142859 contains the supplementary crystal data for this structure.

Tetraethyl (2,3-bis(4-(trifluoromethyl)phenyl)butane-1,1,4,4-tetracarboxylate (345)

The title compound was prepared by General Procedure 10 as a mixture of diastereomers (58%, 6:5, 368 mg) as a white solid. The diastereomers were separated by column chromatography. **MP** 186 – 188 ˚C. **Anti ¹H NMR** (500 MHz, CDCl₃) δ 7.55 (d, J = 8.1 Hz, 2H), 7.44 (d, J = 8.1 Hz, 2H), 4.20 (dd, J = 5.6, 2.2 Hz, 1H), 3.99 – 3.90 (m, 2H), 3.86 (qd, J = 7.1, 2.8 Hz, 2H), 3.60 (dd, J = 5.6, 2.2 Hz, 1H), 1.10 (t, J = 7.1 Hz, 3H), 0.94 (t, J = 7.1 Hz, 3H). **Anti ¹³C NMR** (126 MHz, CDCl₃) δ 167.9 (s), 167.2 (s), 130.5 (s), 130.0 (q, J = 32.5 Hz), 128.6 (s), 127.8 (q), 125.1 (q, J = 3.6 Hz), 61.8 (s), 61.4 (s), 55.1 (s), 47.9 (s), 13.8 (s), 13.6 (s). **Anti ¹⁹F NMR** (471 MHz, CDCl₃) δ -62.7. **IR**: v_{max}: 2970, 1740, 1716, 1325, 1126 cm⁻¹ **Anti HRMS** (ES+) [$C_{28}H_{35}O_8$] calc. 499.2332 found 499.2309

MP 100 – 102 ˚C. **Syn ¹H NMR** (500 MHz, CDCl₃) δ 7.61 – 7.35 (br, m, 1H), 6.83 (br, s, 1H), 4.51 – 4.34 (m, 1H), 3.99 (q, J = 1.9 Hz, 1H), 3.89 – 3.74 (m, 1H), 3.70 (q, J = 1.8 Hz, 1H), 1.42 (t, J = 7.1 Hz, 1H), 0.84 (t, J = 7.1 Hz, 1H). **Syn ¹³C NMR** (126 MHz, CDCl₃) δ 167.6 (s), 166.8 (s), 140.1 (s), 130.7 (s), 130.2 (q, J = 32.6 Hz), 124.9 (s), 124.1 (q, J = 272.1 Hz), 62.6 (s), 61.7 (s), 55.3 (s), 46.3 (s), 14.3 (s), 13.6 (s). **Syn ¹⁹F NMR** (471 MHz, CDCl₃) δ -62.6. **IR**: v_{max}: 2980, 1749, 1722, 1323, 1118, 1068 cm⁻¹ **Syn HRMS** (ES+) [$C_{30}H_{32}O_8F_6$ + Na⁺] calc. 657.1899 found 657.1899

Tetraethyl 2,3-di-*p*-tolylbutane-1,1,4,4-tetracarboxylate (347)
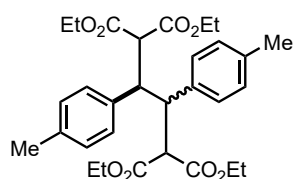
The title compound was prepared by General Procedure 10 as a mixture of diastereomers (85%, 3:2, 223 mg) as a white solid. The diastereomers were separated by column chromatography. **MP** 92 – 94 ˚C. **Anti ¹H NMR** (500 MHz, CDCl₃) δ 7.17 (d, J = 8.1 Hz, 1H), 7.08 – 7.03 (m, 1H), 4.07 – 4.00 (m, 1H), 3.96 – 3.78 (m, 2H), 3.69 – 3.60 (m, 1H), 2.29 (s, 2H), 1.10 (t, J = 7.1 Hz, 2H), 0.94 (t, J = 7.1 Hz, 2H). **Anti ¹³C NMR** (126 MHz, CDCl₃) δ 168.6, 167.9, 137.0, 135.2, 130.1, 128.8, 61.5, 61.1, 56.0, 48.4,

21.2, 13.9, 13.8. **IR**: ν_{max}: 1751, 1722, 1251, 1146 cm^{-1} **Anti HRMS** (ES+) [C$_{30}$H$_{38}$O$_8$ + Na$^+$] calc. 549.2464 found 549.2466

Syn MP 62 – 64 °C. **^{1}H NMR** (500 MHz, CDCl$_3$) δ 6.96 (s, 1H), 4.52 – 4.27 (m, 1H), 3.93 – 3.58 (m, 1H), 2.29 (s, 1H), 1.41 (t, J = 7.1 Hz, 1H), 0.81 (t, J = 7.1 Hz, 1H). **Syn ^{13}C NMR** (126 MHz, CDCl$_3$) δ 168.2, 167.5, 137.0, 132.9, 130.3, 128.4, 62.0, 61.2, 55.8, 46.1, 21.2, 14.3, 13.7. **IR**: ν_{max}: 1740, 1721, 1228, 1143, 1034 cm^{-1} **Syn HRMS** (ES+) [C$_{30}$H$_{38}$O$_8$ + Na$^+$] calc. 549.2464 found 549.2465
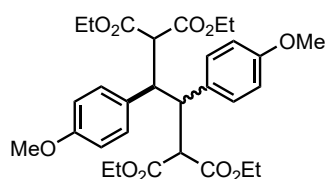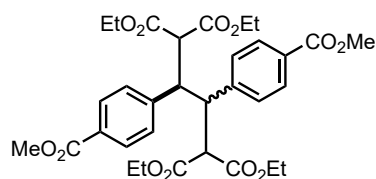
Tetraethyl 2,3-bis(4-methoxyphenyl)butane-1,1,4,4-tetracarboxylate (348)

The title compound was prepared by General Procedure 10 as a mixture of diastereomers (85%, 3:1, 237 mg) as a white solid. The anti-diastereomer was separated by recycling preparative HPLC using 80:20 hexane:EtOAc. **Anti ^{1}H NMR** (500 MHz, CDCl$_3$) δ 7.21 (d, J = 8.7 Hz, 1H), 6.79 (d, J = 8.8 Hz, 1H), 4.01 (dd, J = 5.6, 2.2 Hz, 1H), 3.97 – 3.81 (m, 2H), 3.78 (s, 2H), 3.61 (dd, J = 5.6, 2.2 Hz, 1H), 1.11 (t, J = 7.1 Hz, 2H), 0.97 (t, J = 7.1 Hz, 2H). **Anti ^{13}C NMR** (126 MHz, CDCl$_3$) δ 168.6, 168.0, 158.9, 131.4, 130.3, 113.5, 61.5, 61.2, 55.9, 55.3, 48.2, 14.0, 13.9. **Anti HRMS** (ES+) [C$_{30}$H$_{38}$O$_{10}$ + Na$^+$] calc. 581.2363 found 581.2379

Mixed ^{1}H NMR (500 MHz, CDCl$_3$) δ 6.71 (s, 4H), 4.47 – 4.30 (m, 1H), 3.96 – 3.89 (m, 2H), 3.78 (s, 1H), 1.41 (t, J = 7.1 Hz, 1H), 0.84 (t, J = 7.1 Hz, 1H). **Mixed ^{13}C NMR** ^{13}C NMR (126 MHz, CDCl$_3$) δ 168.62, 168.16, 167.99, 167.49, 158.92, 158.89, 131.40, 131.35, 130.28, 127.95, 113.49, 113.05, 62.08, 61.50, 61.26, 61.14, 55.93, 55.89, 55.32, 55.30, 48.14, 45.93, 14.32, 13.98, 13.88, 13.76.

Tetraethyl 2,3-bis(4-(methoxycarbonyl)phenyl)butane-1,1,4,4-tetracarboxylate (349)
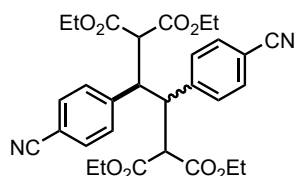

The title compound was prepared by General Procedure 10 as a mixture of diastereomers (85%, 17:10, 522 mg) as a white solid. The anti-diastereomer was

separated by column chromatography. **MP** 156 – 158 ˚C. **Anti** ^{1}**H NMR** (500 MHz, CDCl$_3$) δ 7.91 (d, J = 8.5 Hz, 1H), 7.29 (d, J = 8.5 Hz, 1H), 4.15 (dd, J = 6.2, 2.1 Hz, 1H), 3.96 (q, J = 7.1 Hz, 1H), 3.88 (s, 1H), 3.80 (q, J = 7.1 Hz, 1H), 3.61 (dd, J = 6.2, 2.2 Hz, 1H), 1.11 (t, J = 7.1 Hz, 1H), 0.89 (t, J = 7.1 Hz, 2H).**Anti** ^{13}**C NMR** (126 MHz, CDCl$_3$) δ 168.1, 167.4, 166.9, 143.4, 130.2, 129.6, 129.5, 61.9, 61.5, 55.1, 52.3, 48.2, 14.0, 13.8. **IR**: ν$_{max}$: 1744, 1728, 1718, 1265, 1118 cm^{-1} **Anti HRMS** (AP+) [C$_{32}$H$_{39}$O$_{12}$] calc. 615.2442 found 615.2441

Mixed ^{1}**H NMR** (500 MHz, CDCl$_3$) δ 7.84 (s, 16H), 7.04 (t, J = 83.0 Hz, 10H), 4.51 – 4.30 (m, 11H), 4.04 – 3.94 (m, 8H), 3.90 (d, J = 8.7 Hz, 20H), 3.84 – 3.75 (m, 11H), 3.73 (dt, J = 4.4, 1.7 Hz, 7H), 1.42 (t, J = 7.1 Hz, 16H), 0.83 (t, J = 7.1 Hz, 17H). **Mixed** ^{13}**C NMR** (126 MHz, CDCl$_3$) δ 167.61, 166.75, 166.73, 141.20, 129.49, 129.41, 129.02, 62.34, 61.46, 55.15, 52.18, 46.35, 14.17, 13.61.
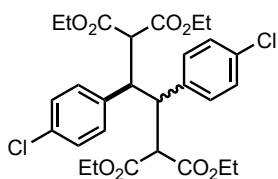
Tetraethyl bis(4-cyanophenyl)butane-1,1,4,4-tetracarboxylate (346)

The title compound was prepared by General Procedure 10 as a mixture of diastereomers (88%, 5:4, 242 mg) as a white solid. The diastereomers were separated by column chromatography. **MP** 204 – 207 ˚C. **Anti** ^{1}**H NMR** (500 MHz, CDCl$_3$) δ 7.59 (d, J = 8.5 Hz, 1H), 7.42 (d, J = 8.5 Hz, 1H), 4.19 (dd, J = 5.5, 2.1 Hz, 1H), 4.00 (qd, J = 7.1, 2.0 Hz, 1H), 3.89 (q, J = 7.1 Hz, 1H), 3.54 (dd, J = 5.5, 2.2 Hz, 1H), 1.13 (t, J = 7.1 Hz, 1H), 0.98 (t, J = 7.1 Hz, 1H). **Anti** ^{13}**C NMR** (126 MHz, CDCl$_3$) δ 167.8, 167.2, 143.3, 132.1, 131.0, 118.5, 112.0, 62.1, 61.8, 54.7, 47.9, 14.0, 13.9. **IR**: ν$_{max}$: 2226, 1748, 1717, 1310, 1146 cm^{-1} **Anti HRMS** (ES+) [C$_{30}$H$_{31}$N$_2$O$_8$] calc. 547.2080 found 547.2079

Syn MP 104 – 106 ˚C. ^{1}**H NMR** (500 MHz, CDCl$_3$) δ 7.50 (br, s, 1H), 6.81 (br, s, 1H), 4.56 – 4.27 (m, 1H), 3.96 (q, J = 1.9 Hz, 1H), 3.90 – 3.76 (m, 1H), 3.68 (q, J = 1.8 Hz, 1H), 1.41 (t, J = 7.1 Hz, 1H), 0.89 (t, J = 7.1 Hz, 1H). **Syn** ^{13}**C NMR** (126 MHz, CDCl$_3$) δ 167.4, 166.5, 141.5, 131.8, 130.6 (br), 118.4, 112.0, 62.8, 61.9, 55.0, 46.5, 14.2, 13.8. **IR**: ν$_{max}$: 2224, 1757, 1736, 1204, 1165 cm^{-1} **Syn HRMS** (ES+) [C$_{30}$H$_{31}$N$_2$O$_8$] calc. 547.2080 found 547.2078

Tetraethyl 2,3-bis(4-chlorophenyl)butane-1,1,4,4-tetracarboxylate (350)

The title compound was prepared by General Procedure 10 as a mixture of diastereomers (82%, 13:10, 231 mg) as a white solid. The anti-diastereomer was separated by column chromatography and the syn diastereomer was separated using recycling preparative HPLC using 80:20 hexane:EtOAc. **MP** 170 - 173 °C. **Anti ^{1}H NMR** (500 MHz, CDCl$_3$) δ 7.25 – 7.19 (m, 1H), 4.05 (dd, J = 5.7, 2.2 Hz, 1H), 4.02 – 3.91 (m, 1H), 3.87 (qt, J = 4.8, 2.5 Hz, 1H), 3.58 (dd, J = 5.7, 2.2 Hz, 1H), 1.13 (t, J = 7.1 Hz, 1H), 0.98 (t, J = 7.1 Hz, 1H). **Anti ^{13}C NMR** (126 MHz, CDCl$_3$) δ 168.2, 167.6, 136.6, 133.7, 131.6, 128.5, 61.8, 61.5, 55.3, 47.9, 29.9, 14.0, 13.8. **IR**: ν_{max}: 1746, 1719, 1308, 1171, 1152, 1011 cm^{-1} **Anti HRMS** (ES+) [C$_{28}$H$_{32}$O$_8$Cl$_2$ + Na$^+$] calc. 589.1372 found 583.1376

Syn ^{1}H NMR (500 MHz, CDCl$_3$) δ 7.17 (s, 1H), 4.46 – 4.32 (m, 1H), 3.90 – 3.75 (m, 2H), 3.64 (d, J = 11.9 Hz, 1H), 1.41 (t, J = 7.1 Hz, 2H), 0.87 (t, J = 7.1 Hz, 2H). **Syn ^{13}C NMR** (126 MHz, CDCl$_3$) δ 167.8, 167.0, 134.4, 133.7, 128.1, 62.4, 61.6, 55.5, 45.9, 14.3, 13.8. **Syn HRMS** (ES+) [C$_{28}$H$_{32}$O$_8$Cl$_2$ + Na$^+$] calc. 589.1372 found 583.1376
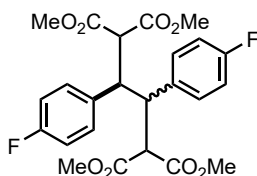
Tetramethyl 2,3-bis(4-fluorophenyl)butane-1,1,4,4-tetracarboxylate (337)
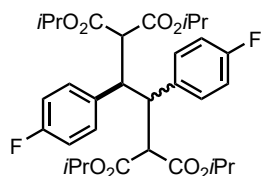

The title compound was prepared by General Procedure 10 as a mixture of diastereomers (62%, 3:2, 149 mg) as a white solid. The diastereomers were separated by column chromatography. **MP** 161 – 162 °C. **Anti ^{1}H NMR** (500 MHz, CDCl$_3$) δ 7.32 – 7.27 (m, 1H), 6.99 (t, J = 8.7 Hz, 1H), 4.09 (dd, J = 5.1, 2.3 Hz, 1H), 3.60 (dd, J = 5.1, 2.3 Hz, 1H), 3.48 (s, 1H), 3.41 (s, 1H). **Anti ^{13}C NMR** (126 MHz, CDCl$_3$) δ 168.71 (s), 168.14 (s), 162.43 (d, J = 246.9 Hz), 133.64 (d, J = 3.4 Hz), 131.80 (d, J = 6.7 Hz), 115.43 (d, J = 21.2 Hz), 55.47 (s), 52.75 (s), 52.47 (s), 47.96 (s).j **Anti ^{19}F NMR** (471 MHz, CDCl$_3$) δ -114.2 (s). **IR**: ν_{max}: 1747, 1504, 1433, 1258, 1157 cm^{-1} **Anti HRMS** (ES+) [C$_{24}$H$_{24}$F$_2$O$_8$ + Na$^+$] calc. 501.1337 found 501.1334

Syn MP 107 – 108 °C ^{1}H NMR (500 MHz, CDCl$_3$) δ 6.88 (s, 1H), 3.94 (s, 1H), 3.80 (q, J = 1.6 Hz, 1H), 3.72 (q, J = 1.5 Hz, 1H), 3.35 (s, 1H). **Syn ^{13}C NMR** (126 MHz, CDCl$_3$) δ

168.2 (s), 167.5 (s), 162.3 (d, J = 247.0 Hz), 131.3 (d, J = 3.3 Hz), 114.9 (d, J = 21.6 Hz), 55.4 (s), 53.4 (s), 52.6 (s), 46.1 (s). **IR**: ν_{max}: 1755, 1734, 1508, 1258, 1229, 1153 cm^{-1} **Syn** **^{19}F NMR** (471 MHz, CDCl$_3$) δ -114.3 (s). **Syn HRMS** (ES+) [C$_{24}$H$_{24}$F$_2$O$_8$ + Na$^+$] calc. 501.1337 found 501.1331

Tetraisopropyl 2,3-bis(4-fluorophenyl)butane-1,1,4,4-tetracarboxylate (338)

The title compound was prepared by General Procedure 10 as a mixture of diastereomers (51%, 1:1,126 mg) as a white solid. The anti-diastereomer was separated by column chromatography and the syn diastereomer was separated using recycling preparative HPLC using 80:20 hexane:EtOAc. **MP** 167 – 170 °C. **Anti ^{1}H NMR** (500 MHz, CDCl$_3$) δ 7.22 – 7.16 (m, 3H), 6.87 (t, J = 8.7 Hz, 2H), 4.77 (hept, J = 6.3 Hz, 1H), 4.66 (hept, J = 6.3 Hz, 1H), 4.04 – 3.89 (m, 1H), 3.46 (dd, J = 5.8, 2.2 Hz, 1H), 1.07 (d, J = 6.3 Hz, 3H), 0.95 (d, J = 6.3 Hz, 3H), 0.92 (d, J = 6.3 Hz, 3H), 0.86 (d, J = 6.3 Hz, 3H). **Anti ^{13}C NMR** (126 MHz, CDCl$_3$) δ 167.96 (s), 167.30 (s), 162.26 (d, J = 246.1 Hz), 134.07 (d, J = 3.3 Hz), 132.01 (s), 115.03 (d, J = 21.1 Hz), 69.30 (s), 68.79 (s), 55.50 (s), 47.72 (s), 21.60 (s), 21.49 (s), 21.44 (s), 21.30 (s). **Anti ^{19}F NMR** (471 MHz, CDCl$_3$) δ -115.16. **IR**: ν_{max}: 1740, 1717, 1506, 1296, 1159, 1123 cm^{-1} **Anti HRMS** (AP+) [C$_{32}$H$_{41}$F$_2$O$_8$] calc. 591.2769 found 591.2776.

Syn ^{1}H NMR (500 MHz, CDCl$_3$) δ 6.88 (s, br, 1H), 1.42 (d, J = 6.3 Hz, 1H), 1.36 (d, J = 6.3 Hz, 1H), 0.90 (d, J = 6.3 Hz, 1H), 0.83 (d, J = 6.2 Hz, 1H). **Syn ^{13}C NMR** (126 MHz, CDCl$_3$) δ 167.42 (s), 166.73 (s), 162.22 (d, J = 246.4 Hz), 131.98 (d, J = 3.3 Hz), 114.70 (d, J = 18.2 Hz), 69.86 (s), 68.92 (s), 55.93 (s), 45.49 (s), 21.94 (s), 21.69 (s), 21.34 (s), 21.16 (s). **Syn ^{19}F NMR** (471 MHz, CDCl$_3$) δ -114.83. **Syn HRMS** (AP+) [C$_{32}$H$_{41}$F$_2$O$_8$] calc. 591.2769 found 591.2776.
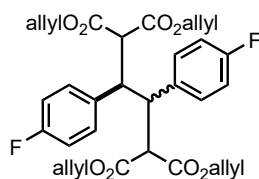
Tetraallyl 2,3-bis(4-fluorophenyl)butane-1,1,4,4-tetracarboxylate (339)

The title compound was prepared by General Procedure 10 as a mixture of diastereomers (77%, 5:3, 151 mg) as a white solid. The anti-diastereomer was separated by column chromatography. **MP** 90 – 92 °C. **Anti ^{1}H NMR** (500 MHz, CDCl$_3$) δ 7.29 (dd, J = 8.7, 5.3 Hz, 1H), 6.96 (t, J = 8.7 Hz, 1H), 5.72 (ddt, J = 17.2, 10.4, 5.8 Hz, 1H), 5.64 – 5.53 (m, 1H), 5.19 (ddq, J = 10.0, 7.1, 1.4 Hz, 1H), 5.15 – 5.08 (m, 1H), 4.41 – 4.23 (m, 2H), 4.11 (dd, J = 5.3, 2.2 Hz, 1H), 3.64 (dd, J = 5.3, 2.2 Hz, 1H). **Anti ^{13}C NMR** (126 MHz, CDCl$_3$) δ 167.8 (s), 167.2 (s), 162.4 (d, J = 246.8 Hz), 133.5 (d, J = 3.3 Hz), 131.9 (s), 131.9 (s), 131.3 (d, J = 10.7 Hz), 119.0 (s), 119.0 (s), 115.3 (d, J = 21.2 Hz), 66.3 (s), 66.0 (s), 55.5 (s), 47.9 (s). **Anti ^{19}F NMR** (376 MHz, CDCl$_3$) δ -114.4. **IR**: ν$_{max}$: 1746, 1722, 1504, 1219, 1167, 1126 cm^{-1} **Anti HRMS** (AP+) [C$_{32}$H$_{33}$F$_2$O$_8$] calc. 583.2134 found 583.2151

Mixed ^{1}H NMR (500 MHz, CDCl$_3$) δ 6.87 (s, 3H), 6.03 (ddt, J = 17.1, 10.5, 5.8 Hz, 1H), 5.51 – 5.37 (m, 2H), 5.32 (ddd, J = 10.5, 2.4, 1.1 Hz, 1H), 5.08 – 4.96 (m, 2H), 4.93 – 4.81 (m, 1H), 4.77 (ddt, J = 13.1, 5.9, 1.3 Hz, 1H), 4.27 – 4.15 (m, 2H), 3.89 (t, J = 6.7 Hz, 1H), 3.72 (t, J = 6.7 Hz, 1H). **Mixed ^{13}C NMR** (126 MHz, CDCl$_3$) δ 167.41 (s), 166.66 (s), 162.30 (d, J = 246.9 Hz), 131.57 (s), 131.38 (d, J = 3.4 Hz), 131.15 (s), 119.44 (s), 118.96 (s), 118.95 (d, J = 6.8 Hz), 114.88 (d, J = 20.9 Hz), 66.79 (s), 66.13 (s), 55.60 (s), 45.89 (s). **Mixed ^{19}F NMR** (376 MHz, CDCl$_3$) δ -114.4.

Diethyl 2,5-dicyano-3,4-bis(4-fluorophenyl)hexanedioate (340)
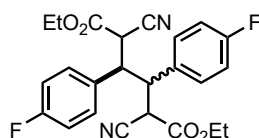
The title compound was prepared by General Procedure 10 as a single diastereomers (55%, 121 mg) as a white solid. **MP** 173 – 176 °C. **^{1}H NMR** (500 MHz, CDCl$_3$) δ 7.60 (s, 1H), 7.16 (t, J = 8.4 Hz, 1H), 4.10 – 3.91 (m, 2H), 3.49 (dd, J = 2.4, 1.8 Hz, 1H), 1.04 (t, J = 7.1 Hz, 2H). **^{13}C NMR** (126 MHz, CDCl$_3$) δ 164.2 (s), 163.2 (d, J = 249.7 Hz), 130.2 (d, J = 3.4 Hz), 116.8 (d, J = 21.8 Hz), 114.6 (s), 63.1 (s), 47.3 (s), 42.3 (s), 13.8 (s). **^{19}F NMR** (376 MHz, CDCl$_3$) δ -111.3. **IR**: ν$_{max}$: 2232, 1749, 1510, 1269, 1228 1167 cm^{-1} **HRMS** (AP+) [C$_{24}$H$_{23}$N$_2$F$_2$O$_4$] calc. 441.1626 found 441.1626.

## 6.6 Generation of Organomanganese Halides *via* Ball Milling

6.6.1 General Procedure 12: One-pot Organomanganese Generation

To a 14 mL stainless-steel milling jar (Insolido Technologies) containing a stainless steel milling ball (4.1 g) was added manganese, irregular pieces, (1.0 mmol, 55 mg), conjugate electrophile (0.5 mmol), pro-nucleophile (0.5 mmol) THF (1.0 mmol, 81 µL), and lithium chloride (0.5 mmol, 21 mg). The reaction mixture was then milled at 30 Hz for 3 h. The mixture was then washed into a flask with Et_2O and HCl (1 M, 25 mL) was added, and the mixture stirred for ten minutes, and the organic phase was separated, washed with brine and dried with magnesium sulphate. This crude mixture was then purified using flash column chromatography.

6.6.2 General Procedure 13: One-pot Organomanganese Generation and Copper Catalysed Conjugate Addition

To a 14 mL stainless-steel milling jar (Insolido Technologies) containing a stainless-steel milling ball (4.1 g) was added manganese, irregular pieces, (1.0 mmol, 55 mg), 2-cyclohexen-1-one (0.5 mmol, 48 µL), 4-fluorobenzyl bromide (0.625 mmol, 78 µL) *i*PrOH (0.75 mmol, 35 µL), lithium bromide (0.5 mmol, 43 mg) copper(I) iodide (0.1 mmol, 19 mg). The reaction mixture was then milled at 30 Hz for 3 h. The mixture was then washed into a flask with Et_2O and HCl (1 M, 25 mL) was added, and the mixture stirred for ten minutes, and the organic phase was separated, washed with brine and dried with magnesium sulphate. This crude mixture was then purified using flash column chromatography.

3-benzylcyclohexan-1-one (392)
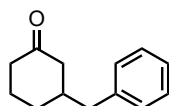
The title compound was synthesised by General Procedure 12 as a colourless oil (8%, 7.6 mg). **^{1}H NMR** (500 MHz, $CDCl_3$) δ 7.37 – 7.25 (m, 2H), 7.24 – 7.17 (m, 1H), 7.16 – 7.08 (m, 2H), 2.72 – 2.54 (m, 2H), 2.49 – 2.31 (m, 2H), 2.31 – 2.20 (m, 1H), 2.05 (dddd, J = 13.8, 7.6, 4.6, 2.5 Hz, 3H), 1.88 (d, J = 14.7 Hz, 1H), 1.62 (dtdd, J = 13.5, 12.3, 4.8, 3.6 Hz, 1H), 1.45 – 1.32 (m, 1H). **^{13}C NMR** (126 MHz, $CDCl_3$) δ 211.8, 139.6, 129.3, 128.5, 126.4, 48.0, 43.2, 41.6, 41.0, 31.1, 25.3. Characterization data is in accordance with prior reports.[66]

3-(4-fluorobenzyl)cyclohexan-1-one (394)
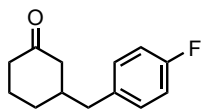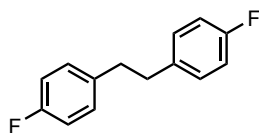

The title compound was synthesised by General Procedure 13 as a colourless oil (48%, 50 mg). **¹H NMR** (500 MHz, CDCl₃) δ 7.07 (dd, *J* = 8.3, 5.6 Hz, 2H), 6.97 (t, *J* = 8.7 Hz, 2H), 2.68 – 2.53 (m, 2H), 2.36 (dd, *J* = 9.8, 7.8 Hz, 2H), 2.32 – 2.19 (m, 1H), 2.10 – 1.96 (m, 3H), 1.86 (d, *J* = 13.7 Hz, 1H), 1.71 – 1.59 (m, 1H), 1.36 (td, *J* = 13.8, 3.8 Hz, 1H). **¹⁹F NMR** (376 MHz, CDCl₃) δ -117.11. **¹³C NMR** (126 MHz, CDCl₃) δ 211.6 (s), 161.7 (d, J = 244.2 Hz), 135.2 (d, J = 3.1 Hz), 130.6 (d, J = 7.8 Hz), 115.3 (d, J = 21.2 Hz), 47.9 (s), 42.2 (s), 41.5 (s), 41.1 (s), 31.0 (s), 25.2 (s). Characterization data is in accordance with prior reports.[67]

1,2-bis(4-fluorophenyl)ethane (395)

The title compound was synthesised by General Procedure 13 as a white solid (12%, 8 mg). **¹H NMR** (500 MHz, CDCl₃) δ 7.12 – 7.01 (m, 2H), 7.00 – 6.91 (m, 2H), 2.86 (s, 2H). **¹⁹F NMR** (376 MHz, CDCl₃) δ -117.47. **¹³C NMR** (126 MHz, CDCl₃) δ 161.5 (d, J = 243.6 Hz), 137.1 (d, J = 3.2 Hz), 130.0 (d, J = 7.8 Hz), 115.2 (d, J = 21.1 Hz), 37.3 (s). Characterization data is in accordance with prior reports.[68]

6.7 Bibliography

1. X.-B. Lan, Y. Li, Y.-F. Li, D.-S. Shen, Z. Ke and F.-S. Liu, *J. Org. Chem.*, 2017, **82**, 2914-2925.
2. S. S. Murthy Bandaru, S. Bhilare, N. Chrysochos, V. Gayakhe, I. Trentin, C. Schulzke and A. R. Kapdi, *Org. Lett.*, 2018, **20**, 473-476.
3. A. Winkler, K. Brandhorst, M. Freytag, P. G. Jones and M. Tamm, *Organometallics*, 2016, **35**, 1160-1169.
4. B. Lü, P. Li, C. Fu, L. Xue, Z. Lin and S. Ma, *Adv. Synth. Catal.*, 2011, **353**, 100-112.
5. T. Shimasaki, M. Tobisu and N. Chatani, *Angew. Chem. Int. Ed.*, 2010, **122**, 2991-2994.
6. X. Qian, Z. Yu, A. Auffrant and C. Gosmini, *Chem. Eur. J.*, 2013, **19**, 6225-6229.
7. J. P. Wolfe and S. L. Buchwald, *J. Am. Chem. Soc.*, 1997, **119**, 6054-6058.
8. I. Geukens, J. Fransaer and D. E. De Vos, *ChemCatChem*, 2011, **3**, 1431-1434.
9. P. Y. S. Lam, S. Deudon, K. M. Averill, R. Li, M. Y. He, P. Deshong and C. G. Clark, *J. Am. Chem. Soc.*, 2000, **122**, 7600-7601.
10. M. Quadri, C. Stokes, A. Gulsevin, A. C. J. Felts, K. A. Abboud, R. L. Papke and N. A. Horenstein, *J. Med. Chem.*, 2017, **60**, 7928-7934.
11. T. J. Barker and E. R. Jarvo, *J. Am. Chem. Soc.*, 2009, **131**, 15598-15599.
12. N. Girard, J.-P. Hurvois, C. Moinet and L. Toupet, *Eur. J. Org. Chem.*, 2005, **2005**, 2269-2280.
13. T. Tu, W. Fang and J. Jiang, *Chem. Commun.*, 2011, **47**, 12358-12360.
14. J. F. Franz, W. B. Kraus and K. Zeitler, *Chem. Commun.*, 2015, **51**, 8280-8283.
15. S. Zhou, Z. Yang, X. Chen, Y. Li, L. Zhang, H. Fang, W. Wang, X. Zhu and S. Wang, *J. Org. Chem.*, 2015, **80**, 6323-6328.
16. P. Horrillo-Martínez, K. C. Hultzsch, A. Gil and V. Branchadell, *Eur. J. Org. Chem.*, 2007, **2007**, 3311-3325.
17. J.-A. García-López, M. Çetin and M. F. Greaney, *Angew. Chem. Int. Ed.*, 2015, **54**, 2156-2159.
18. H. Wang, Y. Mao, L. Jiang, T. Chen, H. He and G. Liu, *Synthesis*, 2015, **47**, 1387-1389.
19. L. R. Mills, L. M. Barrera Arbelaez and S. A. L. Rousseaux, *J. Am. Chem. Soc.*, 2017, **139**, 11357-11360.
20. M. D. Lawlor, T. W. Lee and R. L. Danheiser, *J. Org. Chem.*, 2000, **65**, 4375-4384.
21. Matthew, T. D. Newton, Y. Zhao, B. K. Collins, C. H. Hendon and M. D. Pluth, *Chem. Sci.*, 2019, **10**, 1773-1779.
22. N. Park, K. Park, M. Jang and S. Lee, *J. Org. Chem.*, 2011, **76**, 4371-4378.
23. B. Bang-Andersen, T. Ruhland, M. Jørgensen, G. Smith, K. Frederiksen, K. G. Jensen, H. Zhong, S. M. Nielsen, S. Hogg, A. Mørk and T. B. Stensbøl, *J. Med. Chem.*, 2011, **54**, 3206-3221.
24. V. P. Reddy, K. Swapna, A. V. Kumar and K. R. Rao, *J. Org. Chem.*, 2009, **74**, 3189-3191.
25. T. Ben Halima, J. Masson-Makdissi and S. G. Newman, *Angew. Chem. Int. Ed.*, 2018, **57**, 12925-12929.
26. T. Wang, L. Yuan, Z. Zhao, A. Shao, M. Gao, Y. Huang, F. Xiong, H. Zhang and J. Zhao, *Green Chem.*, 2015, **17**, 2741-2744.
27. M. M. Rahman, G. Li and M. Szostak, *J. Org. Chem.*, 2019, **84**, 12091-12100.
28. W. Zhang and J. M. Ready, *Angew. Chem. Int. Ed.*, 2014, **53**, 8980-8984.
29. C. G. Kokotos, C. Baskakis and G. Kokotos, *J. Org. Chem.*, 2008, **73**, 8623-8626.
30. J. McNulty, R. Vemula, V. Krishnamoorthy and A. Robertson, *Tetrahedron*, 2012, **68**, 5415-5421.

31. J. A. Forni, N. Micic, T. U. Connell, G. Weragoda and A. Polyzos, *Angew. Chem. Int. Ed.*, 2020, **59**, 18646-18654.
32. D. Ameen and T. J. Snape, *Eur. J. Org. Chem.*, 2014, **2014**, 1925-1934.
33. G. Li, C.-L. Ji, X. Hong and M. Szostak, *J. Am. Chem. Soc.*, 2019, **141**, 11161-11172.
34. F. D. King and S. Caddick, *Org. Biomol. Chem.*, 2011, **9**, 4361.
35. Y.-L. Zheng and S. G. Newman, *ACS Catalysis*, 2019, **9**, 4426-4433.
36. K. L. Manasa, Y. Tangella, N. H. Krishna and M. Alvala, *Beilstein J. Org. Chem.*, 2019, **15**, 1864-1871.
37. W. Harnying, J.-M. Neudörfl and A. Berkessel, *Org. Lett.*, 2020, **22**, 386-390.
38. C. C. D. Wybon, C. Mensch, K. Hollanders, C. Gadais, W. A. Herrebout, S. Ballet and B. U. W. Maes, *ACS Catalysis*, 2018, **8**, 203-218.
39. S. Ueda and H. Nagasawa, *J. Org. Chem.*, 2009, **74**, 4272-4277.
40. C. W. Cheung, J.-A. Ma and X. Hu, *J. Am. Chem. Soc.*, 2018, **140**, 6789-6792.
41. R. M. Patel and N. P. Argade, *Org. Lett.*, 2013, **15**, 14-17.
42. S. Tan, F. Li, S. Park and S. Kim, *Org. Chem. Front.*, 2019, **6**, 3854-3858.
43. V. Kumar and S. J. Connon, *Chem. Commun.*, 2017, **53**, 10212-10215.
44. S. Tortoioli, L. Bannwart and S. Abele, *Synthesis*, 2016, **48**, 2069-2078.
45. D. E. Fitzpatrick, T. Maujean, A. C. Evans and S. V. Ley, *Angew. Chem. Int. Ed.*, 2018, **57**, 15128-15132.
46. H. Yu, J. Wang, Z. Wu, Q. Zhao, D. Dan, S. Han, J. Tang and Y. Wei, *Green Chem.*, 2019, **21**, 4550-4554.
47. C. Zhang, G. Zhang, S. Luo, C. Wang and H. Li, *Org. Biomol. Chem.*, 2018, **16**, 8467-8471.
48. R. Shelkov, M. Nahmany and A. Melman, *J. Org. Chem.*, 2002, **67**, 8975-8982.
49. K. M. Ruíz-Pérez, B. Quiroz-García and M. Hernández-Rodríguez, *Eur. J. Org. Chem.*, 2018, **2018**, 5763-5772.
50. D. Kang, J. H. Ko, J. Choi, K. Cho, S. M. Lee, H. J. Kim, Y.-J. Ko, K. H. Park and S. U. Son, *Chem. Commun.*, 2017, **53**, 2598-2601.
51. X. Zhang, C. Shen, C. Xia, X. Tian and L. He, *Green Chem.*, 2018, **20**, 5533-5539.
52. R. Francke and R. D. Little, *Chem. Soc. Rev.*, 2014, **43**, 2492-2521.
53. a) T. A. Stich, S. Lahiri, G. Yeagle, M. Dicus, M. Brynda, A. Gunn, C. Aznar, V. J. Derose and R. D. Britt, *Appl. Magn. Reson.*, 2007, **31**, 321-341; b) C. Duboc, M.-N. Collomb and F. Neese, *Appl. Magn. Reson.*, 2010, **37**, 229-245; c) K. Keller, M. Zalibera, M. Qi, V. Koch, J. Wegner, H. Hintz, A. Godt, G. Jeschke, A. Savitsky and M. Yulikov, *PCCP*, 2016, **18**, 25120-25135.
54. S. Hajra, S. M. Aziz and R. Maji, *RSC Adv.*, 2013, **3**, 10185-10188.
55. J. Wang, Y. Zhou, L. Zhang, Z. Li, X. Chen and H. Liu, *Org. Lett.*, 2013, **15**, 1508-1511.
56. R. C. Betori, B. R. McDonald and K. A. Scheidt, *Chem. Sci.*, 2019, **10**, 3353-3359.
57. A. Kazia, R. Melngaile, A. Mishnev and J. Veliks, *Org. Biomol. Chem.*, 2020, **18**, 1384-1388.
58. S. Ghosh and C. K. Jana, *Org. Biomol. Chem.*, 2019, **17**, 10153-10157.
59. E. Fillion, A. Kavoosi, K. Nguyen and C. Ieritano, *Chem. Commun.*, 2016, **52**, 12813-12816.
60. Y. Matsumoto, D. Nakatake, R. Yazaki and T. Ohshima, *Chem. Eur. J.*, 2018, **24**, 6062-6066.
61. Z. Zhang, Z.-W. Bai, Y. Ling, L.-Q. He, P. Huang, H.-X. Gu and R.-F. Hu, *Med. Chem. Res.*, 2018, **27**, 1198-1205.
62. J.-R. Xin, J.-T. Guo, D. Vigliaturo, Y.-H. He and Z. Guan, *Tetrahedron*, 2017, **73**, 4627-4633.
63. J. Li, J. Zhang, H. Tan and D. Z. Wang, *Org. Lett.*, 2015, **17**, 2522-2525.

64. S. Herold, D. Bafaluy and K. Muñiz, *Green Chem.*, 2018, **20**, 3191-3196.
65. R. Shelkov, M. Nahmany and A. Melman, *The Journal of Organic Chemistry*, 2002, **67**, 8975-8982.
66. Y. J. Kim and D. Y. Kim, *Org. Lett.*, 2019, **21**, 1021-1025.
67. M. D. Rathnayake and J. D. Weaver, *Org. Lett.*, 2021, **23**, 2036-2041.
68. K. Sato, Y. Inoue, T. Mori, A. Sakaue, A. Tarui, M. Omote, I. Kumadaki and A. Ando, *Org. Lett.*, 2014, **16**, 3756-3759.

Appendix 1   N-Heterocyclic Carbene Acyl Anion Organocatalysis by Ball-Milling

N-Heterocyclic Carbene Acyl Anion Organocatalysis by Ball-Milling

William I. Nicholson, Alex C. Seastram, Saqib A. Iqbal, Benjamin G. Reed-Berendt, Louis C. Morrill, and Duncan L. Browne, *ChemSusChem,* 2020, **13**, 131–135.

Although this work is not presented with this PhD thesis a significant portion was contributed by the author.